SYNTHETIC, STRUCTURAL AND SPATIAL STUDIES OF RHENIUM COMPOUNDS

By

YI WEI, M. Sc.

A Thesis

Submitted to the School of Graduate Studies

in Partial Fulfilment of the Requirements

for the Degree

Doctor of Philosophy

McMaster University

DOCTOR OF PHILOSOPHY (1994) McMASTER UNIVERSITY

(Chemistry) Hamilton, Ontario

TITLE: **Synthetic, Structural and Spatial Studies of Rhenium Compounds**

AUTHOR: Yi Wei, B. Sc. (Beijing Normal University)

M. Sc. (Beijing Normal University)

SUPERVISOR: Professor C. J. L. Lock

NUMBER OF PAGES: xx, 270

ABSTRACT

A new concept, Virtual Radii, is introduced to define the non-bonding interactions of ligating atoms in the coordination sphere of six coordinated transition metal compounds. The interactions of structural parameters in the coordination sphere and their chemical consequences are discussed within the bounds of a systematic study. Virtual Radii and Solid Angle Factors were extracted for six coordinated rhenium compounds with the use of the Cambridge Structural Database, recent publications, and structures determined in this study.

Thirteen structures were determined to answer chemical questions as well as to provide additional data for the spatial studies. The questions were: i. What was the real structure of the compound formulated as $K[Re_2O_2H(CO)_8]$ by Hieber and Schuster? ii. Is the cyanide ion bonded to the rhenium atom through the nitrogen atom in the compound "$K_2[ReN(NC)_4]\cdot H_2O$" as proposed in the literature? iii. Is it possible to synthesize some new neutral or monocationic rhenium or technetium species with ligands that contain pyrazole?

Reactions of $Re(CO)_5Cl$ and KOH under various conditions produced several products. The structures of five of them, $KRe_3(CO)_9(OMe)_4$ (3A), $Re_4(CO)_{12}(OH)_2(OEt)_2\cdot 2EtOH$ (3B), $Re_4(CO)_{12}(OH)_4\cdot 8H_2O$ (3C), $KRe_2(CO)_6(OH)_3\cdot 2H_2O$

(3D), $KRe_3(CO)_9(OH)_4$ (3E), were determined by single-crystal X-ray diffraction methods. The structure of 3D clarified question (i).

X-ray crystal structure determination of $(AsPh_4)_2[ReN(CN)_4(H_2O)]\cdot 5H_2O$ (4B) indirectly answered question (ii) and showed that the literature was wrong.

As part of the basic research on the development of new radiopharmaceuticals, new compounds with pyrazole-containing ligands, $ReO(HBPz_3)(NCS)_2$ (5A), $ReO(HBPz_3)(PzOCMe_2)\cdot ReO_4$ (5B), $ReOCl_2(PPh_3)(PzOCMe_2)$ (5C), $ReOCl_2(PPh_3)(PzOCHMe)\cdot 0.5CHOCHO$ (5D), $Re_2O_3Cl_2(PPh_3)_2(Pz)_2\cdot CHCl_3$ (5E), $Re_2O_3Cl_2(3,5\text{-}Me_2\text{-}Pz)_2(3,5\text{-}Me_2\text{-}HPz)_2$ (5F) were prepared and characterized. The investigations were extended to new compounds $[ReOCl_2(PPh_3)L]\cdot 2H_2O$ (5G) and $[TcOL_2(HL)]TcO_4$ (5H), where HL was 4-hydroxymethyl-1,5-dimethyl-imidazole. The X-ray crystal structures of all compounds, except 5A, were determined.

ACKNOWLEDGEMENTS

I thank Professor Colin J. L. Lock, for his guidance, encouragement and continued support throughout the years. The "Champagne Molecule" will remain a happy episode in my scientific talk about the "designed condensation reaction of pyrazole and acetone".

I also thank the members of my supervisory committee Drs. I. David Brown and Gary J. Schrobilgen for their valuable contributions and support.

Special thanks to Dr. Jim Britten for his generous help in X-ray crystallography. I would also like to acknowledge Dr. Helen Howard-Lock for help with the I.R. spectral assignments, Dr. Richard W. Smith for obtaining the mass spectra, and Dr. Donald Hughes for acquiring the COSY ^{1}H NMR spectrum.

I thank Dr. Alan Guest for his patience in reading and correcting the drafts of this thesis.

To our group members, Drs. Russell Bell, Zhixian Wang, Hosen Alarabi, and the future Drs. Daren LeBlanc, Theresa Fauconnier, John Valliant, Byron DeLaBarre, your help and friendship are much appreciated.

I would also like to thank all of my friends in China and Canada. Your care and help made my work more meaningful.

Financial assistance in the form of Scholarships and Teaching Assistantships from the Department of Chemistry, McMaster University, and an Ontario Graduate Scholarship (1994) from the Education Council of Ontario, are gratefully acknowledged.

ABBREVIATIONS

Symbol	Word
Å	angstrom, 10^{-10} meters
BL	bond length
°C	degrees Celsius
COSY	correlated spectroscopy
CSD	Cambridge Structural Database
deg., °	degree
Et	ethyl, C_2H_5
FA	fan angle
g	gram
Hpz	pyrazole
im	imidazole
IR	infrared
K	Kelvin
max	maximum
M	molar
Me	methyl, CH_3
min	minimum

mL	millilitres
mm	millimetre
mmol	millimole
NMR	nuclear magnetic resonance
Ph	phenyl
ppm	parts per million
PPh_3	triphenyl phosphine
pz	pyrazolyl
pz'	pyrazolyl derivative
R	radius
SI	shape index
SAF	solid angle factor
SSAF	sum of solid angle factors
σ	standard deviation
VR	virtual radii, or virtual radius

TABLE OF CONTENTS

CHAPTER 1.

INTRODUCTION

CHAPTER 2.

EXPERIMENTAL METHODS

CHAPTER 3

RHENIUM(I) CARBONYL COMPOUNDS

CHAPTER 4

SYNTHESIS AND CHARACTERIZATION OF TWO NITRIDORHENIUM(V) CYANIDE COMPOUNDS

CHAPTER 5

SYNTHESIS AND CHARACTERIZATION OF RHENIUM AND TECHNETIUM COMPOUNDS WITH PYRAZOLYL LIGANDS

CHAPTER 7

APPLICATIONS OF THE SOLID ANGLE MODEL

LIST OF TABLES

Appendix Tables

LIST OF FIGURES

Appendix Figures

CHAPTER 1.

INTRODUCTION

1.1 The Opening Question

Crystallography has given us the ability to visualize the world at the atomic level and has thus shaped the way we look at chemistry. Almost all the significant advances in rhenium chemistry have depended on the determination of structures of compounds by single-crystal X-ray diffraction. Up to 1993, 1593 entries of rhenium compounds were collected in the Cambridge Structural Database (CSD) [1]. Table 1.1 shows that, for the past 30 years, there has been an enormous growth in the number of structures of new rhenium compounds determined each year.

Examinations of the structures of simple binary compounds ReO_2 [2], ReO_3 [3], $ReCl_4$ [4], and $ReCl_5$ [5] showed that there was one common feature among their structures. Obviously, each of them has a different ratio of metal and ligand atoms, and there are three different oxidation states. Not obviously, they have one thing in common, i.e., the rhenium atoms are all six coordinated by sharing ligating atoms in the structures of these compounds.

Their charges are stoichiometrically well balanced. So a question is "Why do the rhenium atoms share ligating atoms to obtain distorted octahedral coordination?" The answer is "The coordination space around each rhenium needs be filled." If they did not

share their ligands there would be vacancies in the coordination space, and if there were other ligands (such as water) available to the metal, then something different from what was expected would be produced.

Table 1.1 The Number of Coordination and Organometallic Compounds of Rhenium Collected in Cambridge Structural Database Each Year

Year	1991	1990	1989	1988	1987	1986	1985
Number	207	191	135	134	159	84	95
Year	1984	1983	1982	1981	1980	1979	1978
Number	94	53	72	42	30	38	28
Year	1977	1976	1975	1974	1973	1972	1971
Number	32	20	20	14	5	8	6
Year	1970	1969	1968	1967	1966	1965	1964
Number	5	6	9	6	5	3	1

Even though these compounds are fairly simple, they reveal one important feature shown by all molecules that exist in a three-dimensional space. If a metal compound is to be prepared, the spatial requirements of the metal ion need to be considered. This led us to an examination of the three-dimensional coordination space, and the parameters that describe it.

In classical mathematics, the coordination space is a three-dimensional space with

a limit of 4π radians in terms of solid angle. This limit requires that only an appropriate degree of occupancy of the coordination space is adapted by a stable structure. Overcrowding or undercrowding leads to unstable structures. To measure the solid angle occupied by a ligating atom, the size of the ligating atoms and the bond lengths need to be known.

1.2 The Scope of This Thesis

This thesis addresses applications of structural data to rhenium chemistry which profit from the maturity of the techniques of crystal structure determination. To make any generalization, it is better to use a collection of rhenium compound structures, rather than individual structures. Systematic studies are not only surveys of the literature, but enquire into the quantitative relationship between molecular connectivity (bond lengths and angles) and the atomic properties (size of the coordination atoms). Metal-ligand bonding is a particularly important field of study for practical transition metal chemistry since ligands provide a powerful and subtle means of controlling reactivity, and other properties of the metal such as its ability to act as a catalyst.

This systematic study was made possible by the availability of a large number of rhenium structures from CSD and recent publications. In addition to the structure information obtained from the CSD and recent publications, 12 structures of rhenium compounds were determined in this work. In choosing the compounds for the structural studies, an attempt was made to answer some structural questions that existed in the literature, or to characterize some new compounds that had potential applications. The

three areas that were studied were: (i) rhenium carbonyl compounds produced by the reaction between $Re(CO)_5Cl$ and KOH, (ii) rhenium nitrido-cyanide compounds, (iii) rhenium compounds that contained the hydridotris(1-pyrazolyl)borate or pyrazole ligand.

The incentive for parts (i) and (ii) was to examine some problems in previous research by others. This work was extended, when new compounds were synthesized. Studies of parts (i) and (ii) are presented in Chapters 3 and 4, respectively. The incentive for part (iii) was to prepare some neutral (zero charge) or monocationic compounds which were lipophilic and therefore have the potential to be used in nuclear medicine. Again, new and unusual compounds were prepared. Studies of part (iii) are presented in Chapter 5. The major experimental methods which are common for these three chapters are described in Chapter 2.

Space considerations have been recognised as important in chemistry since van't Hoff and Le Bel introduced the concept of the tetrahedral carbon atom. Molecular structure, non-bonded interactions, space requirements of electron-pairs, and stereochemical selection are all related to spatial properties.

In a complex molecule, there are two types of interactions. One is the bonding interactions between the central metal and the ligands. Another is the non-bonding interactions between the ligands. The non-bonding interactions are determined by the geometrical features of the ligands, such as shape and size characterized by their van der Waals radii. When the size of the ligand or the coordination number is large, or the bonding interactions are weak, the non-bonding interactions may play a dominant role.

Tolman [6] used the two dimensional cone angle as a measure of the size of the

phosphine ligands. The concepts of the non-circular cone angle [7] have been proposed for phosphine ligands. The three dimensional solid angle model was introduced by Li [8]. The solid angle model [8] differs from the cone angle models [6, 7] in that, the solid angle has one more dimension than the cone angle, so that the solid angle is more relevant to a description of the spatial properties of a ligand. In addition, the solid angle can be used to study any ligand or ligating atom rather than only phosphine ligands. So the solid angle model [8] was used in this study.

The solid angle model used the conventional van der Waals radii [9] to describe the sizes of ligating atoms. Nine years ago, it was modified by "normalizing" the conventional van der Waals radii [9] to examine the steric effects in technetium complexes [10, 11]. The method of normalization [10, 11] was not quite pertinent, but the conclusions that the conventional van der Waals radii [9] can not be universally and simply used and the proper values should be obtained for specific problems, are still valid, and these ideas are carried on in this study.

A new and better method is introduced in this thesis to define the size of the non-bonding interactions of ligating atoms in six coordinated metal compounds. In Chapter 6, procedures and computer programs have been established to calculate the intramolecular non-bonding **virtual radii** for ligating atoms in the coordination sphere. The new name, **Virtual Radii** (VR), has been coined to differentiate this set of radii from all the other ones. The **virtual radii** has a formularized definition and the VR values are extracted from real structural data.

The aim of Chapter 6 is to answer the question "What is a typical intramolecular

non-bonding distance?" and "Can a typical coordination environment around the central metal atom be reconstructed with properties extracted from a large set of the molecular structures?" Positive answers to these questions would allow the building of realistic structural models for molecular species in cases where direct observation of the geometry is either impractical or impossible. Reliable standard geometries are invaluable as starting points for molecular design or for predicting reaction pathways.

By exploring a database of all the relevant structural data of rhenium compounds, the corresponding bond type or functional group in a wide range of environments can be examined. This allows for some estimate of the environmental effects on the changes of molecular parameters under study, as well as experimental uncertainties. Thus both the mean value of a parameter and its variability are important pieces of information and both need to be considered in the discussion of suitability of the 'typical' dimensions for a structural unit.

Steric effects have been studied quantitatively in terms of Fan Angle, Solid Angle Factor, the Sum of Solid Angle Factors [8], and statistical analyses have been conducted in Chapter 6. This kind of systematic study for rhenium compounds has not been undertaken before. It should be useful as an overview or for purpose of comparison, or in the design of new rhenium compounds.

In Chapter 6, tables of average bond lengths, **Virtual Radii**, and other quantities used in this study have been compiled to describe the spatial properties for rhenium compounds with use of the structural data so far available. These compilations are a summary of a large body of structural information of rhenium compounds and therefore

summarize a large body of rhenium chemistry.

In Chapter 7, the applications of the Solid Angle Model for three groups of rhenium compounds studied in this thesis are discussed, to demonstrate what kind of insight this model can provide into their structures.

1.3 Rhenium Chemistry

The discovery of rhenium was first claimed by Noddack, Tacke, and Berg in 1925. Since then it has been found that rhenium forms an extensive series of compounds covering the widest range of formal oxidation states from Re(-1) through (+7) and coordination numbers 4 through 9. Rhenium has played an important part in the history of chemistry: for example, the dinuclear anion, $[Re_2Cl_8]^{2-}$, was the first stable chemical species shown to possess a quadruple bond [12], the discovery of $Re_3Cl_{12}^{3-}$ sparked the renaissance of cluster chemistry [13], and Cp_2ReH was the first example of a non-carbonyl-containing metal hydride [14]. The hydrido complex anions MH_9^{2-} [15] are unique for Re and Tc, and the chemistry of hydrido complexes is extensive for Re.

In addition to the well known carbonyl compounds, $Re_2(CO)_{10}$ [16] and $Re(CO)_5Cl$ [17], rhenium forms many metal cluster carbonyls and mixed ligand-carbonyl species. Another important class of compounds is that of oxorhenium(V) with phosphine ligands, of the type $ReOX_3(PR_3)_2$. Among them, $ReOCl_3(PPh_3)_2$ is the most widely used starting material to make new rhenium compounds [18]. The structures studied in this thesis are related to these two categories of compounds. Extensive reviews of the chemistry of rhenium are available [19].

CHAPTER 2.

EXPERIMENTAL METHODS

2.1 Preparation

In this thesis, preparation apparatus and methods used are all conventional. A vacuum line was used for the preparation of compounds studied in Chapter 3. The compounds, $ReO(HBPz_3)Cl_2$ [20] and $ReOCl_3(PPh_3)_2$ [21], were prepared by the methods described in the literature. Pyrazole and 3,5-dimethylpyrazole were purchased from Lancaster Research Chemicals Company and used without further purification. 4-hydoxymethyl-1,5-dimethylimidazole was synthesized and supplied by Dr. Zhixian Wang, Department of Chemistry, McMaster University. Details of the individual preparations are included in the appropriate Chapters 3, 4, or 5.

2.2 X-Ray Crystallography

Whenever possible, a single crystal X-ray structure determination was made to determine the unambiguous three-dimensional arrangement of atoms within a crystal and the composition of the compound. Since single crystal X-ray crystallography was used as

a major tool to study compounds in this study, a brief description of the theory is presented here. Details of the theory and the operations can be found in standard text books [22] and manuals [23].

2.2.1 Crystal Selection and Mounting

Transparent crystals with well defined faces that showed sharp and uniform extinctions under the polarizing microscope, were used for X-ray studies. The preferred crystal size was generally 0.05 to 0.2 mm to ensure that the entire crystal is bathed in the monochromatic portion of the X-ray beam.

Crystals were usually glued to the end of a glass fibre with epoxy resin. Crystals found to undergo rapid decomposition through loss of solvent were sealed in 0.2 mm (inner diameter) Lindemann capillaries with a drop of the mother liquor. For $[Re(CO)_3(OH)]_4 \cdot 8H_2O$ (3C) the crystal was bathed in nujol and sealed in a Lindemann capillary. The advantages of nujol are that it is not as volatile as other common solvents, so it provides enough time for the crystal to be manipulated under the microscope. It is also fairly viscous and this helps to immobilize the crystal in the capillary if the surface of the crystal is covered with nujol. This is a benefit since one does not want the crystal moving around in the capillary.

2.2.2 The Orientation Matrix

The orientation matrix of the crystal on the diffractometer in terms of four angles, θ, ω, ϕ, and χ, was determined automatically. A number of strong reflections (usually 25

reflections with $I > 10\sigma(I)$) were randomly searched and automatically centred. The refined parameters were used to generate vectors indexed for an arbitrary cell. By examination of the vector lengths and the cosines of the angles between pairs of vectors the unit cell vectors were identified. The centred reflections were then reindexed according to these cell vectors and refined in a least-squares calculation to generate the orientation matrix.

2.2.3 Data Collection

With use of this orientation matrix a set of intensities was measured for the appropriate symmetry determined quadrant or hemisphere. Generally, measurements were made up to 2θ values of 45-50° and for ranges of h. k and l determined by the ratio of (cell dimension)/λ.

Crystal cell dimensions were obtained from a least-squares fit of χ, ϕ and 2θ for 25 strong reflections in the appropriate range of 2θ recorded on a Siemens R3m/V diffractometer with graphite monochromated AgKα radiation (λ=0.56086Å) (some times at low temperature by use of liquid nitrogen), or Siemens P4 diffractometer with graphite monochromated MoKα radiation (λ = 0.71073 Å) at room temperature. Intensities were measured with a 2θ-θ scan, with scan rates from 1.50 to 14.55° min^{-1} in ϖ. The scan range was from +1° to -1° in 2θ (or in ϖ) on each side of Kα and background counts were made on each side of the peak for 25% of the peak scan time. The intensity of a reflection, I, and its estimated standard deviation are given by:

$$I = (N_t - N_l - N_r)(R_s)/\Delta\omega$$

$$\sigma(I) = (N_t + N_l + N_r)^{1/2}(R_s)/\Delta\omega$$

where N_t is the total number of counts, N_l and N_r are the left and right background counts, R_s is the scanning rate and $\Delta\omega$ is the range scanned in ω ($\Delta\omega = 1°$).

Three standard reflections were measured every 97 reflections to check the stability of crystal and the instrument, and scaling was applied. A series of ψ-scan measurements of intensities of selected reflections was made for all crystals to allow an absorption correction to be made. A set of up to 11 moderately intense reflections were selected representing the span of 2θ measured, and having values of $\chi = 90\pm25°$ or $\chi = 270\pm25°$. For each reflection in 2θ, the intensity of the reflection was monitored every 10° as the crystal was rotated a full 360° about the scattering vector (which under these conditions was close to the ϕ-axis of the diffractometer). The crystal size was accurately measured. An empirical absorption correction was applied with the use of the program XEMP in SHELXTL-PC.

2.2.4 Data Corrections

The intensity measured for the hkl reflection is related to the square of the structure factor, F_{hkl}, by $I_{hkl} = L*P*F_{hkl}^2/(A'*t^2)$, where L is the Lorentz factor, P is the polarization term, A' is the absorption factor and t is the scale factor. The Lorentz factor takes into account the time during which the lattice point (of finite size) passes from the outer to the inner edge of the sphere of reflection. $L = 1/\sin 2\theta$.

The polarization term, P, arises because the electric vector components of waves are reflected to different extents, resulting in the partial polarization of the incident beam.

This loss of intensity arises because the component of the wave electric vector parallel to the diffracting plane is reflected by an amount dependent only upon the plane's electron density whereas the efficiency of the reflection of the electric vector perpendicular to the reflection plane decreases with $\cos^2 2\theta$.

As the X-ray beam passes through the crystal some of its energy is absorbed by the atoms present. $A' = V/(\int \exp(\mu x) dV)$, where V is the crystal volume, x is the distance travelled by the beam through the crystal, and μ is the linear absorption coefficient. A summation is taken over all atoms present in the crystal, so $\mu = \Sigma \mu_a$ (cm^{-1}). Values for μ_a's are tabulated in the International Tables of X-ray Crystallography, Vol. III, Table 3.2.2B [24]. Calculations were done for the unit cell, than scaled by the crystal dimensions.

The total absorption factor, A', comprises an analytical factor, A'_θ, and an empirical term, A'_ψ, $A' = A'_\theta * A'_\psi$. The A'_θ correction is applied to spherical and cylindrical crystals based on the values of 2θ and μR. Here R is the crystal radius. These values are tabulated in the International Tables of X-ray Crystallography, Vol. II, Table 5.3.5B [25]. The A'_ψ correction is applied with the use of the ψ-scan data collection as described above. For each reflection a A'_ψ correction curve can be constructed and by interpolation a correction can be applied to each reflection in the data set. The A'_θ corrections are made with R values determined by use of the ψ-scan calculations.

The scale factor, t, depends on the beam intensity, crystal size and other constants and is determined with the use of a Wilson plot [26] from the given cell contents.

2.2.5 DIFABS Correction

The program DIFABS [27] was often found to give a better result for absorption corrections, however. The DIFABS method works from the premise that the manifestation of systematic errors caused by absorption, unlike most other sources of systematic error, will not be evenly distributed through reciprocal space, but will be localized. A Fourier series in the polar angles of the incident and diffracted beam paths is used to model an absorption surface for the difference between the observed and calculated structure factors. A knowledge of crystal dimensions or the linear absorption coefficient is not required, and the method does not necessitate the measurement of azimuthal scans or any extra data beyond the unique set.

In the DIFABS correction, the observed structure-factor amplitudes, $F_{o,j}$ are modified by the following empirical correction: $F_{m,j} = kF_{o,j}A_{p,s}$, where k is an overall scale factor obtained from the least-squares refinement, and $F_{m,j}$ are the modified values for $F_{o,j}$. The absorption coefficient, $A_{p,s}$, is represented by a Fourier series: $A_{p,s} = \Sigma_n\Sigma_m P_{n,m}[\sin(n\varphi_p + m\mu_p) + \sin(n\varphi_s + m\mu_s)] + Q_{n,m}[\cos(n\varphi_p + m\mu_p) + \cos(n\varphi_s + m\mu_s)]$, where φ_p, μ_p, φ_s and μ_s are the spherical polar angles defining the incident and diffracted beams, respectively. $P_{n,m}$ and $Q_{n,m}$ are Fourier coefficients whose values are obtained by minimizing the sum of the squares of the residuals, $R_j = (|\,|F_{c,j}| - |F_{o,j}|\,|)\omega_j$, where ω_j is a suitable weighting function. A DIFABS correction was used for all of the data sets in this work.

2.2.6 Anomalous Dispersion

Scattering curves were taken from the International Tables for Crystallography

[28] and anomalous dispersion corrections were applied [29]. The normal scattering factors, f_o's are calculated assuming that the bound electrons can be approximated as free electrons. The errors resulting from this approximation become quite significant as the wavelength of the radiation approaches the absorption edge of the atom (i.e. the atomic number of the atom approaches that of the element used to generate the X-ray). This effect is shown by scattered waves with a phase difference other than π radians. The corrected scattering factors are given by, $f_o anom = f_o + \Delta f' + i\Delta f''$, where f_o is the normal scattering factor and $\Delta f'$ and $\Delta f''$ represent the real and imaginary (amplitude and phase) correction term, respectively.

2.2.7 Temperature Factors

Atoms in a crystal generally have some degree of thermal motion. To correct for this a modified scattering factor, $f_{j,2\theta}' = f_{j,2\theta}\exp(-T_j)$, is employed. The anisotropic temperature factor is expressed as

$$T_j = 2\pi^2(U_{11}h^2\mathbf{a}^{*2} + U_{22}k^2\mathbf{b}^{*2} + U_{33}l^2\mathbf{c}^{*2} + 2U_{12}hk\mathbf{a}^*\mathbf{b}^*\cos\gamma + 2U_{13}hl\mathbf{a}^*\mathbf{c}^*\cos\beta + 2U_{23}kl\mathbf{b}^*\mathbf{c}^*\cos\alpha)$$

where U_{ij} is a tensor representing the mean square amplitude of vibration along the principal axis of an ellipsoid for $i = j$, or the orientation of the ellipsoid for $i \neq j$. In some cases thermal motion is expressed by an isotropic temperature factor, $T_{iso} = 2\pi^2U(2\sin\theta/\lambda)^2$, where U is related to the root mean square amplitude of the atomic vibration.

2.2.8 Secondary Extinction Corrections

The assumption that the intensity of the incident beam is constant throughout the crystal is incorrect for strong, low angle reflections, as the beam incident on the deeper planes is substantially reduced by upper plane scattering. The correction for secondary extinction is applied as, $F_c = F_{hkl} (1 - gF_{hkl}^2/\sin\theta)$, where g is a variable parameter with a value in the range of 10^{-3}.

2.2.9 Solving a Structure

The relationship between the measured intensities of reflections and the three-dimensional arrangement of atoms in a crystal is

$$I_{hkl} = L*P*F_{hkl}^2/(A'*t^2)$$

$$F_{hkl} = \Sigma f_{j,2\theta} \exp(2\pi i(hx_j + ky_j + lz_j))$$

The solution of a crystal structure hinges on obtaining a reasonably accurate set of amplitudes and phases of the structure factors.

2.2.10 The Direct Method

This approach generates a trial structure by assigning phases directly to the structure factor amplitudes, and assumes that the electron density is positive throughout the crystal (thus constraining phases to result in positive electron density) and that the intensities do contain some phasing information.

For centrosymmetric structures Friedel's law , $I_{hkl} = I_{-h,-k,-l}$, holds whether or not anomalous dispersion effects are present because of the centre of symmetry. The phase

angle is restricted to be either 0 or π radians. Therefore one need only determine the sign (+/-) of the structure factor.

Following the approach by Zachariasen [30] three strong reflections are selected from the data set and phases assigned with origin parity shift considerations. Further phase assignments, relative to the triad basis set, are made with use of structure factor equality relationships of the space group and the probability equations of Sayre [31].

In practice the moduli of normalized structure factors, E_{hkl}, are used in place of F_{hkl}.

$$E_{hkl}^2 = |F_{hkl}|^2/[i\Sigma N_{nj}^2] = |F_{hkl}|^2/[\varepsilon\Sigma N_{fj}^2]$$

F_{hkl} values are modulated (via the point charge model) to remove the fall off in f_a with 2θ and are relative to the average value for reflections in that area of $\sin\theta/\lambda$. The factor ε takes into account that, depending upon the space group, certain classes of reflections will have intensities higher than those for the general reflections.

2.2.11 The Patterson-Heavy Atom Method

The Patterson Method [32] allows one to determine the position of heavy atoms in the structure independently of the phasing. A Fourier transformation of F_o^2 is made to map interatomic vectors, (u, v, w).

$$P(u,v,w) = V_c^{-1}\Sigma_h\Sigma_k\Sigma_l F_o^2 \cos 2\pi(hu + kv + lw)$$

Here V_c is the crystal volume and u,v,w are the fractional coordinates of the real space cell. This expression can be regarded as a convolution of the electron density at all points, p1 = (x,y,z) with all other points, p2 = (x+u, y+v, z+w) in the unit cell. For every

interatomic distance, (u,v,w), thus obtained, a peak will appear in the Patterson map at (u,v,w) with a peak height roughly proportional to the product of the atomic numbers, Z_1Z_2. Therefore, the peaks resulting from interatomic vectors between heavy atoms will dominate the Patterson map. The heavy atom position can then be calculated based upon the symmetry relationships between the atoms.

2.2.12 Refinement of the Structure

Once a starting model is obtained, the difference Fourier synthesis is calculated from coefficients of ΔF, $\Delta F = F_o - F_c$, which represents a point by point subtraction of the F_c Fourier from the F_o Fourier calculated with the same phases. Such a difference map will contain peaks of electron density representing atoms absent in the trial structure and deep valleys indicating improperly placed atoms. An improved trial structure comprising refined atoms from a previous trial structure that are judged acceptable, and new atoms identified in the difference map, is constructed. This new trial structure is subjected to further least-squares refinements until no significant peaks of electron density remain in the difference map. The refinement is usually terminated when the ratio of the (maximum shift)/(average e.s.d) of the parameters being refined is less than 0.1 and the R-factor is acceptable.

All of the structures in this work were solved by direct methods or Patterson methods with use of Siemens SHELXTL PLUS (PC Version) program. After the Fourier map revealed all non-hydrogen atoms, hydrogen atoms were located or placed in calculated positions and were not refined. Full-matrix least-squares refinement minimized

$\Sigma w(|F_o|-|F_c|)^2$ with use of all data. The R factor, weighting scheme w, weighted R_w, and goodness-of-fit, s, are defined by the following expressions:

$$R = \Sigma(|F_o| - |F_c|)/\Sigma|F_o|$$

$$w^{-1} = \sigma_o^2 + g|F_o|^2$$

$$R_w = (\Sigma w(|F_o| - |F_c|)^2)^{1/2}/(\Sigma w(|F_o|)^2)^{1/2}$$

$$s = (\Sigma w(|F_o| - |F_c|)^2/(m-n))^{1/2}$$

where σ_o is the estimated standard deviation (e.s.d.) in F_o from counting statistics, g is a variable parameter with a value in the range of 10^{-3}, m is the total number of reflections and n is the number of parameters used in the refinement. Equivalent isotropic U is defined as one third of the trace of the orthogonalized U_{ij} tensor.

Tables of bond lengths and angles, and an thermal ellipsoid probability diagram for each structure are shown in the text. Tables of crystallographic data, atom coordinates and thermal parameters are found in appendices. Tables of hydrogen atom positional parameters and isotropic temperature factors, the anisotropic temperature factors, and the observed and calculated structure factors for each structure, are deposited on magnetic disks.

Since good quality single crystals which diffract well cannot always be prepared, other supplementary techniques were also used to characterize compounds of interest.

2.3 Infrared and Ultraviolet-Visible Spectroscopy

When a pure sample was prepared, infrared spectroscopy was always used to detect the presence or absence of certain group frequencies to identify whether the desired

or a different compound was made.

Samples were prepared as KBr disks (1-5%) and infrared spectra were recorded on a Perkin-Elmer 283 spectrometer in the range of 4000-300 cm^{-1} (typical acquisition parameters: scan time 12 minutes, baseline transmission 60%-90%, expansion 1, response 1) and a BIO-RAD FTS-40 spectrometer in the range of 4000-400 cm^{-1} (typical acquisition parameters: number of scans 16, resolution 4) and were calibrated against polystyrene film absorptions. The theory of infrared spectroscopy can be found in N. B. Colthup, *et al.* [36], and K. Nakamoto [37].

Ultraviolet-visible spectroscopy was used to give a quantitative description of the compound color in solution if there was still enough sample available. Ultraviolet spectra were recorded on a Hewlett Packard 8451A Diode Array Spectrophotometer with samples as solutions in quartz cells (1 cm).

2.4 Nuclear Magnetic Resonance Spectroscopy

When the expected compound has protons in its composition, proton NMR is often used to determine the confirmation of the molecule in solution.

^1H NMR spectra were recorded as d_6-acetone or $CDCl_3$ solutions with a deuterium lock on a Bruker AC-200 spectrometer operating at 200.133 MHz and equipped with a 4.70 Tesla cryomagnet and an Aspect 3000 computer, or on a Bruker AM-500 spectrometer operating at 500.138 MHz and equipped with a 11.745 Tesla cryomagnet and an Aspect 3000 computer. Acquisition parameters are specified for each compound in Chapters 3 and 5.

One ^1H COSY two-dimensional NMR spectrum for compound 5B was acquired under the experimental conditions specified in Chapter 5. For a detailed survey of traditional aspects of experimental NMR spectroscopy, see: M. L. Martin, *et al* [34]. For knowledges of modern NMR techniques, see: A. E. Derome [33].

2.5 Mass Spectometry

Mass spectrometry was often found helpful in identifying the composition of the compound, since it gives the exact molecular weight, the characteristic isotopic distribution, and the fragment masses of the compound. Sometimes it could also reveal the exchange mechanism as in the study of compound 5B in Chapter 5.

FAB+ (Fast Atom Bombardment) mass spectra were obtained by use of a VG ZAB-E mass spectrometer equipped with a standard saddle-field gun (Ion Tech Ltd., Middlesex, U. K.) that produced a beam of xenon atoms at 8 keV and 1 mA. Samples were applied to the FAB target as solutions in chloroform or acetone. The matrix used was 3-nitrobenzyl alcohol. All spectra were taken in the positive ion mode.

DEI (direct electron ionization) mass spectra were recorded on a VG ZAB-E mass spectrometer (70 eV). A practical book on mass spectrometry was written by Davis *et al.* [35].

CHAPTER 3

RHENIUM(I) CARBONYL COMPOUNDS

3.1 Introduction

Hieber and Schuster [38] studied the reaction of $Re(CO)_5Cl$ and KOH in H_2O and ethanol. The proposed formulation of the product as $K[Re_2O_2H(CO)_8]$ was based on indirect evidence: analysis suggested a 1K:2Re:8C ratio, the oxidation state of rhenium was +1, and the compound was ionic as shown by its conductivity in acetone solution. The presence and the position of the hydrogen atom was a matter of controversy. Was it associated with one or both of the bridging oxygen atoms, or did it exist as a bridging hydride (Re-H-Re) group?

A few years later, the structure determination of "$K[Re_2O_2H(CO)_8]$" was undertaken at this university [39], but the structure did not refine satisfactorily because, as it was later discovered, the space group C2 was incorrect.

This work has demonstrated that the reaction is not as simple as was previously believed. Several new compounds, $KRe_3(CO)_9(OMe)_4$ (**3A**), $Re_4(CO)_{12}(OH)_2(OEt)_2 \cdot 2EtOH$ (**3B**), $Re_4(CO)_{12}(OH)_4 \cdot 8H_2O$ (**3C**), $KRe_2(CO)_6(OH)_3 \cdot 2H_2O$ (**3D**), $KRe_3(CO)_9(OH)_4$ (**3E**), were produced, and their structures were determined by X-ray crystallography. The correct space group of the dimer (**3D**) was found to be C2/m, and the molecular formula was found to be $KRe_2(CO)_6(OH)_3 \cdot 2H_2O$.

3.2 Preparations

3.2.1 Preparation of $K[Re_3(\mu_2\text{-}OCH_3)_3(\mu_3\text{-}OCH_3)(CO)_9]$ (3A)

Chloropentacarbonylrhenium(I) (452 mg, 1.25 mmol) and KOH (91 mg, 1.62 mmol) in methanol (1.7 mL) were sealed into an evacuated Carius tube and heated at 70-80°C for three days (>72 hours). After the tube was cooled and opened, precipitated potassium chloride was separated by filtration and washed twice with methanol (5 mL). The solutions were combined and evaporated to give a white solid. The infrared spectra of the solid obtained from the solution contained more peaks than the spectrum reported for the intended compound, "$K[Re_2O_2H(CO)_8]$" [38]. So the solid was extracted with diethylether. The residue was dissolved in acetone and then a few drops of water added, and fairly stable colourless single crystals of **3A** were obtained by slow evaporation of the solution at room temperature. IR for **3A** (cm^{-1}, KBr disk): 2991 w, 2965 w, 2950 m, 2929 m, 2892 m, 2823 m, 2032 s, 2015 vs, 2009 vs, 1938 vs, 1923 vs, 1904 vs, 1886 vs, 1875 vs, 1849 vs, 1458 m, 1451 m, 1441 m, 1157 w, 1035 m(b), 1018 m(b), 991 m, 663 m, 643 w, 555 m, 535 m(b), 520-505 m(b), 489 s, 440 m(b), 380 m, 335 w. ^1H NMR (in d_6-acetone, ppm): 4.53 (s, 3H), 4.25 (s, 9H).

3.2.2 Preparation of $[Re_4(CO)_{12}(OH)_2(EtO)_2]\cdot 2EtOH$ (3B)

Chloropentacarbonylrhenium(I) (101 mg, 0.279 mmol) and KOH (58 mg, 1.04 mmol) in ethanol (2.2 mL) were sealed into an evacuated Carius tube and heated at 70-80°C for three days (>72 hours). The solution was dried in open air and the product was extracted with diethylether. The solid obtained from the ether layer was dissolved in ethanol and a few drops of water; colorless thin plate shaped crystals of **3B** were obtained

by slow evaporation of the solution at room temperature. IR for **3B** (cm^{-1}, KBr disk): 3660 w, 3653 w, 3641 w, 3627 w, 3592 m, 3576 w, 3556 w, 3440 w(b), 2986 w, 2925 m, 2855 w, 2028 vs, 1992 w, 1967 w, 1942 m, 1927 vs, 1925 vs, 1924 vs, 1918 s, 1911 m, 1895 w, 1889 w, 1611 m, 1451 m, 1442 w, 1039 w, 983 m, 875 w, 829 w, 662 m, 646 w, 552 m, 507 m, 477 m, 440 m.

3.2.3 Preparation of $[Re(CO)_3(OH)]_4 \cdot 8H_2O$ (3C)

Chloropentacarbonylrhenium(I) (335 mg, 0.926 mmol) and KOH (69 mg, 1.24 mmol) in water (1.7 mL) were sealed into an evacuated Carius tube and heated at 70-80°C for 67 hours. Tetrahedron shaped colorless crystals of $[Re(CO)_3(OH)]_4 \cdot 8H_2O$ were obtained. The crystals rapidly became white and translucent when they were removed from the solution. The crystals were very soluble in EtOH or acetone but not in water. IR for **3C** (cm^{-1}, KBr disk): 3577 vs, 3423 s(b), 3220 s(b), 2551 w, 2430 w, 2032 vs, 1927 vs, 1913 vs, 1898 vs, 1637 m, 1511 w, 982 m, 914 w, 662 m, 645 m, 544 m, 510 m, 503 m, 463 m, 435 m. ^1H NMR (in d_6-acetone, ppm): 6.75 (s, 4H), 3.05 (s, 16H).

3.2.4 Preparation of $KRe_2(CO)_6(OH)_3 \cdot 2H_2O$ (3D) and $KRe_3(CO)_9(OH)_4$ (3E)

Chloropentacarbonylrhenium(I) (150 mg, 0.415 mmol) and KOH (70 mg, 1.25 mmol) in 1.8 mL 95% EtOH, or chloropentacarbonylrhenium(I) (152 mg, 0.420 mmol) and KOH (53 mg, 0.946 mmol) in 2.0 mL 90% MeOH, were sealed in an evacuated Carius tube and heated at 70-80°C for 16-17 hours. The 95% EtOH solution was yellow, and the MeOH/H_2O solution was a pale yellow. Slightly orange-colored diamond shaped crystals of $KRe_3(CO)_9(OH)_4$ were obtained by slow evaporation of acetone/water solutions of the products. A few days later, colorless needle-shaped crystals of

$KRe_2(CO)_6(OH)_3{\cdot}2H_2O$ were obtained from the same solutions. IR for **3D** (cm^{-1}, KBr disk): 3596 s, 3564 s, 3442-3207 s(b), 2926 s, 2854 m, 2364 w, 2018 vs, 2011 vs, 1913 vs, 1894 vs, 1870 vs, 1846 vs, 1653 s, 1195 w, 1150 w, 1019 m, 883 m, 811 w, 698 w, 662 m, 641 s, 544 m, 526 s, 467 s, 436 m, 420 m. IR for **3E** (cm^{-1}, KBr disk): 3610 vs, 3564 s, 2034 vs, 2018 vs, 2011 vs, 1920 vs, 1906 vs, 1884 vs, 1155 w, 1032 w, 883 vs, 824 m, 699 m, 662 m, 644 m, 545 m, 524 m, 516 m, 467 s, 447 m, 362 w.

3.3 Spectroscopic Measurements

The infrared spectroscopic data for compounds **3A**, **3B**, **3C**, **3D**, and **3E** are shown in the appropriate preparation sections. A comparison of the IR spectra of these compounds are shown in Fig. 3.1.

The ^1H NMR spectra of **3A** were recorded as D_6-acetone solutions with a deuterium lock on a Bruker AC-200 spectrometer or on a Bruker AM-500 spectrometer. The AC-200 spectra were obtained in 88 scans at a spectral width of 2.5 kHz (16K, 0.305 Hz/data point, 3.277 s acquisition time) and on the AM-500 in 8 scans at a spectral width of 5kHz (32K, 0.305 Hz/data point, 1.638 s acquisition time). To attempt to detect any hydride hydrogen atoms, ^1H spectra were run on the AM-500 in 464 scans at a spectral width of 14.7 kHz (64K, 0.449 Hz/data point, 1.114 s acquisition time). ^1H NMR spectra of **3C** were recorded as D_6-acetone solutions with a deuterium lock on a Bruker AC-200 spectrometer in 16 scans at a spectral width of 2.4 kHz (16K, 0.293 Hz/data point, 3.408 s acquisition time). ^1H NMR results are shown in the appropriate preparation sections.

3.4 X-ray Structural Determinations

Crystallographic details for **3A**, **3B**, **3C**, **3D** and **3E** are summarized in the appendix Table 3.1. All the structures were solved by direct methods with use of the SHELXTL-PC [23] software package, except for the structure of **3E**. **3E** was first solved by direct methods with the use of NRCVAX [40] software package. The solution was finally found by refining the 5th possible model provided by NRCVAX. After the structure of **3E** was known, it was found that the correct solution was obtained from SHELXTL-PC in the second possible model. SHELXTL-PC usually works well, but it was unfortunate that the first choice automatically made by the programs of SHELXTL-PC for the solution of **3E** was incorrect.

The atom coordinates and temperature factors for compounds **3A**, **3B**, **3C**, **3D**, and **3E** are listed in the appendix Table **3A.2**, **3B.2**, **3C.2**, **3D.2**, and **3E.2**, respectively. The structures of **3A**, **3B**, **3C**, **3D**, and **3E** are shown in Figure **3A.1**, **3B.1**, **3C.1**, **3D.1**, and **3E.1**, respectively. Their bond lengths and angles are listed in Table **3A.1**, **3B.1**, **3C.1**, **3D.1**, and **3E.1**, respectively.

3.5 Results and Discussion

3.5.1 Preparation

The preparation of some of the above compounds seems to be almost accidental, therefore some rationale and more details are provided below. It was found that reaction time, solvent, and recrystallization methods are the factors which govern what is the final product.

To remove oxygen from the reaction mixture, the Carius tube, which contained the mixture of reactants and solvent was placed in liquid nitrogen, after the solvent froze, the system was evacuated and the tube was then sealed. Usually, when the reactants were mixed and sealed into the Carius tube, bubbles were seen evolving from the surface of solid $Re(CO)_5Cl$ immediately and for several (3-6) hours later. The solution became yellow or slightly yellow. There were some white solids (KCl or K_2CO_3) and a small amount of black solid (which may be ReO_2 from impurities in the starting material) precipitated at the bottom.

3.5.1.1 Reaction Time

Several initial trials did not produce any crystals. In further trials, the reaction time was extended from two days to three days in the hope that the reaction was complete. When the tube was cooled to room temperature and the seal was broken, a explosive sound was heard, indicating that the gas pressure inside the tube was greater than 1 atm. at room temperature. Considering that the tube had been evacuated before it was sealed, this meant that a lot of gas had been generated during the reaction.

In contrast, when the reaction was stopped after 16-17 hours, no explosive sound was heard when the seal was broken. This indicated that less gas was generated in these reactions than in the ones which were heated for a longer time. This is consistent in that the formation of the trimer or tetramer requires a further loss of CO from the starting compound or the dimer.

3.5.1.2 The Solvent

Encouraged by the success of the separation and characterization of **3A**, it was decided that the solvent used for the reaction was worthy of investigation. Therefore ethanol or water were used as solvents instead of MeOH and the reactions were repeated under essentially the same conditions, in the hope that salts similar to $K[Re_3(\mu_2\text{-}OEt)_3(\mu_3\text{-}OEt)(CO)_9]$ or $K[Re_3(\mu_2\text{-}OH)_3(\mu_3\text{-}OH)(CO)_9]$ could be formed. With the use of ethanol, the tetramer **3B** was isolated. With the use of water, some $KReO_4$ was obtained along with the tetramer **3C**.

A careful comparison of the IR spectrum of the initial white powder obtained from the MeOH reaction, from which pure trimer, **3A**, had been separated, with the IR spectra of the pure compounds indicated that other compounds were present. The use of pure water eliminated the possibility of the formation of **3A**. But the use of MeOH in the reaction could generate some water. Therefore, in MeOH the reaction could lead to the formation of the tetramer **3C** and the trimer **3E** after three days of heating.

When the reactions were conducted in 95% EtOH, or a solution with MeOH:H_2O = 9:1, but the heating was discontinued after they had been maintained at 70-80°C for 16-17 hours, the dimer **3D** and the trimer **3E** were obtained.

3.5.1.3 Recrystallizations

The possibility of forming different compounds in the same tube made recrystallization an essential method to obtain pure samples. The recrystallizations were conducted in the following way. First, the solid was dissolved in the appropriate amount

of acetone or ethanol, then, water drops were added trying to ensure that the solution remained clear. If too much water was added, a white suspension appeared, and addition of more acetone or ethanol did not cause resolution. In such cases, a yellow oil was often found at the bottom of the container rather than crystals. However, if no water was added, a white coating was often found on the walls of the vial when the solution dried and no crystals were obtained. Crystals of **3A** were formed in a solution of acetone and water. Crystals of **3B** were found floating on the surface of a solution of ethanol and water. Sometime crystals of $KReO_4$, $Re(CO)_5Cl$, or $Re_2(CO)_{10}$ were formed. Slow evaporation at room temperature was achieved by opening a small hole (0.3-0.5 cm in diameter) in the cap of the vial, and ethanol was used rather than acetone as it has a higher boiling point than acetone.

In summary, it was found that higher polymerization was facilitated by a longer heating time, and that the solvent may be involved in the final product.

3.5.2 The Structural Studies

From the reactions between $Re(CO)_5Cl$ and KOH under different conditions, five different compounds were separated and characterized. These compounds include one dimer, **3D**, two trimers, **3A** and **3E**, and two tetramers, **3B** and **3C**. The two tetramers have cubane type of structures. The two trimers have pseudo-cubane structures where a K^+ ion occupies one corner of the cubane. The dimer has two $[Re(CO)_3]^+$ units bridged by three OH^- groups. From the dimer to the trimer and tetramer, it is clear that the basic construction unit is $[Re(CO)_3]^+$, and a number of such units are connected by bridging

OH^- or OMe^-, OEt^- groups depending on their degrees of polymerization. The coordination of each Re atom in all structures was distorted octahedral.

Table 3A.1. Bond Lengths (Å) and Angles (°) for $K[Re_3(OCH_3)_4(CO)_9]$ (3A)

Note: Bond lengths and angles are taken in sequence round the structure. Thus i' is i+2 for i equals 1 and i-1 for i equals 2 or 3.

i=	1	2	3
Re(i)-O(i)	2.153 (8)	2.144 (8)	2.136 (7)
Re(i)-O(i')	2.162 (8)	2.148 (7)	2.168 (8)
Re(i)-O(4)	2.190 (8)	2.184 (8)	2.175 (8)
Re(i)-C(i1)	1.89 (1)	1.89 (1)	1.89 (1)
Re(i)-C(i2)	1.93 (1)	1.90 (2)	1.91 (1)
Re(i)-C(i3)	1.88 (1)	1.92 (1)	1.87 (1)
O(i1)-C(i1)	1.16 (1)	1.17 (2)	1.16 (2)
O(i2)-C(i2)	1.14 (2)	1.17 (2)	1.14 (2)
O(i3)-C(i3)	1.15 (2)	1.14 (2)	1.18 (2)
O(1)-C(1)	1.41 (2)	1.42 (2)	1.44 (2)
O(4)-C(4)	1.48 (2)		
O(i)-Re(i)-O(i')	79.3 (3)	80.4 (3)	79.8 (3)
O(i)-Re(i)-O(4)	74.9 (3)	74.8 (3)	74.8 (3)
O(i')-Re(i)-O(4)	74.0 (3)	75.1 (3)	74.5 (3)
O(i)-Re(i)-C(i1)	99.0 (4)	100.7 (5)	97.1 (4)

O(i)-Re(i)-C(i2)	172.2 (5)	172.5 (4)	171.1 (4)
O(i)-Re(i)-C(i3)	95.8 (5)	93.3 (5)	96.7 (4)
O(i')-Re(i)-C(i1)	101.5 (4)	97.5 (4)	101.1 (5)
O(i')-Re(i)-C(i2)	93.9 (5)	94.5 (5)	94.2 (4)
O(i')-Re(i)-C(i3)	169.7 (4)	171.6 (5)	172.2 (5)
O(4)-Re(i)-C(i1)	172.9 (4)	171.7 (4)	171.2 (4)
O(4)-Re(i)-C(i2)	99.7 (4)	98.6 (4)	97.4 (4)
O(4)-Re(i)-C(i3)	96.0 (4)	98.0 (5)	97.9 (5)
C(i1)-Re(i)-C(i2)	86.0 (5)	85.5 (6)	90.4 (5)
C(i1)-Re(i)-C(i3)	88.1 (5)	89.1 (6)	86.2 (6)
C(i2)-Re(i)-C(i3)	90.3 (6)	91.1 (6)	88.5 (5)
Re(i)-O(i)-Re(i')	104.9 (3)	105.1 (3)	105.4 (3)
Re(i)-O(i)-C(i)	116.4 (7)	117.3 (7)	116.9 (7)
Re(i')-O(i)-C(i)	117.1 (7)	117.5 (7)	117.3 (7)
Re(i)-O(4)-Re(i')	102.5 (3)	103.1 (3)	103.5 (3)
Re(i)-O(4)-C(4)	114.5 (7)	116.2 (7)	115.2 (7)
Re(i)-C(i1)-O(i1)	178 (1)	177 (1)	176 (1)
Re(i)-C(i2)-O(i2)	178 (1)	178 (1)	177 (1)
Re(i)-C(i3)-O(i3)	176 (1)	179 (1)	178 (1)
K-O(1)	2.790 (1)	K-O(2)	2.766 (8)
K-O(3)	2.791 (9)	K-O(13A)	2.91 (1)
K-O(22A)	2.87 (1)	K-O(32A)	2.78 (1)
K-O(33A)	2.75 (1)		
O(1)-K-O(2)	59.8 (2)	O(1)-K-O(3)	59.1 (2)
O(1)-K-O(13A)	133.8 (3)	O(1)-K-O(22A)	150.2 (3)

O(1)-K-O(32A)	84.5 (3)	O(1)-K-O(33A)	82.5 (3)
O(2)-K-O(3)	59.6 (2)	O(2)-K-O(13A)	85.7 (3)
O(2)-K-O(22A)	119.5 (3)	O(2)-K-O(32A)	135.3 (3)
O(2)-K-O(33A)	92.5 (3)	O(3)-K-O(13A)	130.0 (3)
O(3)-K-O(22A)	93.8 (3)	O(3)-K-O(32A)	79.9 (3)
O(3)-K-O(33A)	139.9 (3)	O(13A)-K-O(22A)	72.0 (3)
O(13A)-K-O(32A)	138.2 (3)	O(13A)-K-O(33A)	68.3 (3)
O(22A)-K-O(32A)	78.2 (3)	O(22A)-K-O(33A)	126.1 (3)
O(32A)-K-O(33A)	109.8 (3)		

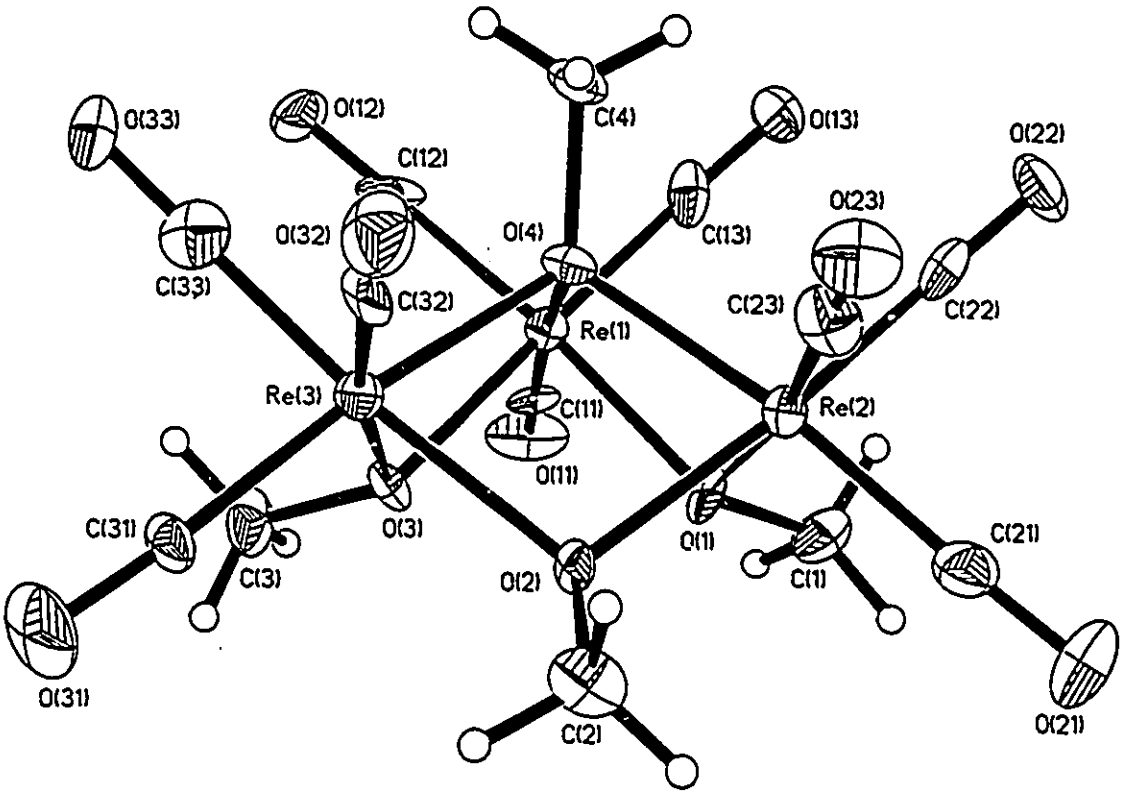

Fig. 3A.1 Structure of $K[Re_3(\mu_2\text{-}OCH_3)_3(\mu_3\text{-}OCH_3)(CO)_9]$ (3A) Anion

Table 3B.1. Bond Lengths (Å) and Bond Angles (°)

for $[Re_4(CO)_{12}(OH)_2(EtO)_2]$·2EtOH (3B)

Re(1)-O(1)	2.145 (8)	Re(1)-O(2)	2.192 (8)
Re(1)-C(11)	1.91 (2)	Re(1)-C(12)	1.90 (2)
Re(1)-C(13)	1.93 (2)	Re(1)-O(2a)	2.196 (8)
Re(2)-O(1)	2.202 (9)	Re(2)-O(2)	2.195 (8)
Re(2)-C(21)	1.95 (2)	Re(2)-C(22)	1.89 (2)
Re(2)-C(23)	1.91 (1)	Re(2)-O(1a)	2.193 (8)
O(1)-Re(2a)	2.193 (8)	O(2)-C(40)	1.43 (2)
O(2)-C(40')	1.43 (3)	O(2)-Re(1a)	2.196 (8)
C(11)-O(11)	1.13 (2)	C(12)-O(12)	1.17 (2)
C(13)-O(13)	1.10 (2)	C(21)-O(21)	1.11 (2)
C(22)-O(22)	1.11 (2)	C(23)-O(23)	1.15 (2)
O(10)-C(10)	1.35 (3)	C(10)-C(20)	1.29 (5)
C(30)-C(40)	1.52 (5)	C(30)-C(40')	1.52 (4)
C(40)-C(40')	0.78 (4)		

O(1)-Re(1)-O(2)	75.3(3)	O(1)-Re(1)-C(11)	96.3(5)
O(2)-Re(1)-C(11)	169.8(5)	O(1)-Re(1)-C(12)	174.0(5)
O(2)-Re(1)-C(12)	100.0(5)	C(11)-Re(1)-C(12)	88.0(7)
O(1)-Re(1)-C(13)	99.1(6)	O(2)-Re(1)-C(13)	99.6(5)
C(11)-Re(1)-C(13)	87.4(7)	C(12)-Re(1)-C(13)	85.2(7)

O(1)-Re(1)-O(2a)	75.0(3)	O(2)-Re(1)-O(2a)	73.2(3)
C(11)-Re(1)-O(2a)	99.2(5)	C(12)-Re(1)-O(2a)	100.3(5)
C(13)-Re(1)-O(2a)	171.5(5)	O(1)-Re(2)-O(2)	74.1(3)
O(1)-Re(2)-C(21)	171.2(5)	O(2)-Re(2)-C(21)	98.4(6)
O(1)-Re(2)-C(22)	100.6(5)	O(2)-Re(2)-C(22)	173.6(5)
C(21)-Re(2)-C(22)	86.6(7)	O(1)-Re(2)-C(23)	99.4(5)
O(2)-Re(2)-C(23)	97.5(5)	C(21)-Re(2)-C(23)	86.0(6)
C(22)-Re(2)-C(23)	86.8(7)	O(1)-Re(2)-O(1a)	72.8(4)
O(2)-Re(2)-O(1a)	74.1(3)	C(21)-Re(2)-O(1a)	101.0(5)
C(22)-Re(2)-O(1a)	101.2(5)	C(23)-Re(2)-O(1a)	169.7(5)
Re(1)-O(1)-Re(2)	103.4(4)	Re(1)-O(1)-Re(2a)	104.0(3)
Re(2)-O(1)-Re(2a)	105.5(4)	Re(1)-O(2)-Re(2)	102.1(3)
Re(1)-O(2)-C(40)	106(2)	Re(2)-O(2)-C(40)	142(2)
Re(1)-O(2)-C(40')	112(1)	Re(2)-O(2)-C(40')	114(1)
C(20)-O(2)-C(40')	32(2)	Re(1)-O(2)-Re(1a)	105.8(3)
Re(2)-O(2)-Re(1a)	102.3(3)	C(40)-O(2)-Re(1a)	93(2)
C(40')-O(2)-Re(1a)	119(1)	Re(1)-C(11)-O(11)	175(2)
Re(1)-C(12)-O(12)	174(1)	Re(1)-C(13)-O(13)	178(2)
Re(2)-C(21)-O(21)	179(2)	Re(2)-C(22)-O(22)	179(2)
Re(2)-C(23)-O(23)	178(2)	O(10)-C(10)-C(20)	133(3)
O(2)-C(40)-C(30)	143(3)	O(2)-C(40')-C(30)	143(2)

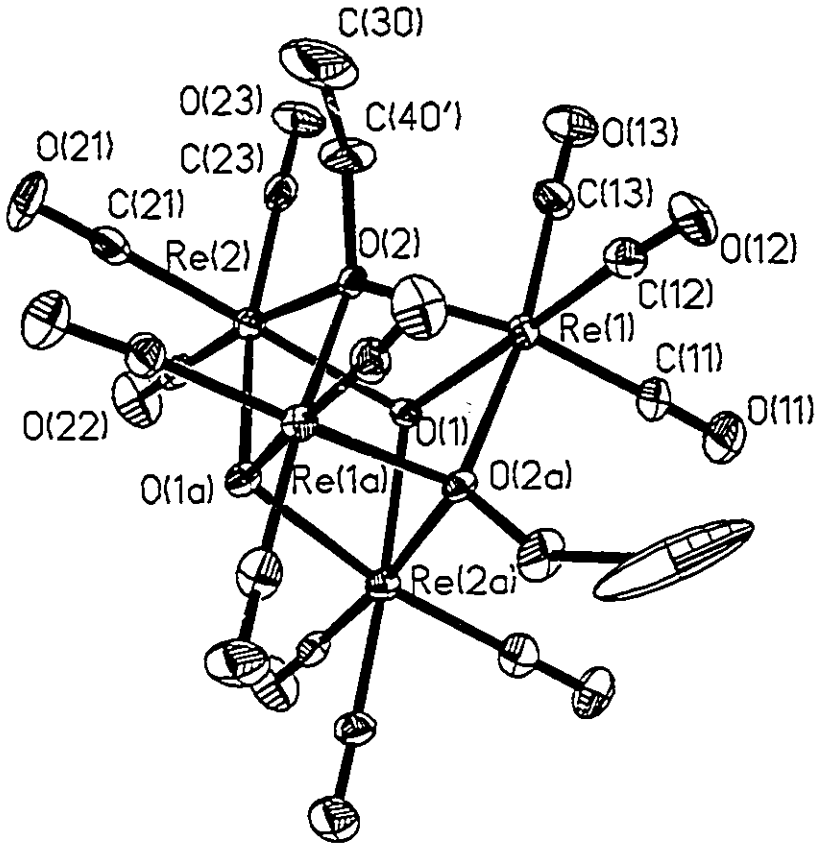

Fig. 3B.1 Structure of $[Re_4(CO)_{12}(OH)_2(EtO)_2]\cdot 2EtOH$ (3B), EtOH Molecules and Hydrogen Atoms were Omitted for Clarity

Table 3C.1. Bond Lengths (Å) and Bond Angles (°)

for $[Re(CO)_3(OH)]_4 \cdot 8H_2O$ (3C)

Re-C(1)	1.903 (8)	Re-C(2)	1.896 (8)
Re-C(3)	1.903 (7)	Re-O(4)	2.188 (6)
Re-O(4a)	2.160 (6)	Re-O(4b)	2.169 (5)
C(1)-O(1)	1.16 (1)	C(2)-O(2)	1.17 (1)
C(3)-O(3)	1.166 (9)	O(4)-Rea	2.160 (6)
O(4)-Reb	2.169 (5)		

C(1)-Re-C(2)	86.7(3)	C(1)-Re-C(3)	86.4(4)
C(2)-Re-C(3)	88.6(5)	C(1)-Re-O(4)	170.5(3)
C(2)-Re-O(4)	100.0(3)	C(3)-Re-O(4)	100.4(3)
C(1)-Re-O(4a)	98.1(3)	C(2)-Re-O(4a)	172.0(4)
C(3)-Re-O(4a)	98.0(3)	O(4)-Re-O(4a)	74.5(2)
C(1)-Re-O(4b)	99.9(4)	C(2)-Re-O(4b)	100.0(4)
C(3)-Re-O(4b)	169.5(3)	O(4)-Re-O(4b)	72.4(2)
O(4a)-Re-O(4b)	73.0(2)	Re-C(1)-O(1)	178(1)
Re-C(2)-O(2)	178.7(7)	Re-C(3)-O(3)	176.4(7)
Re-O(4)-Rea	102.3(2)	Re-O(4)-Reb	105.0(2)
Rea-O(4)-Reb	106.0(2)		

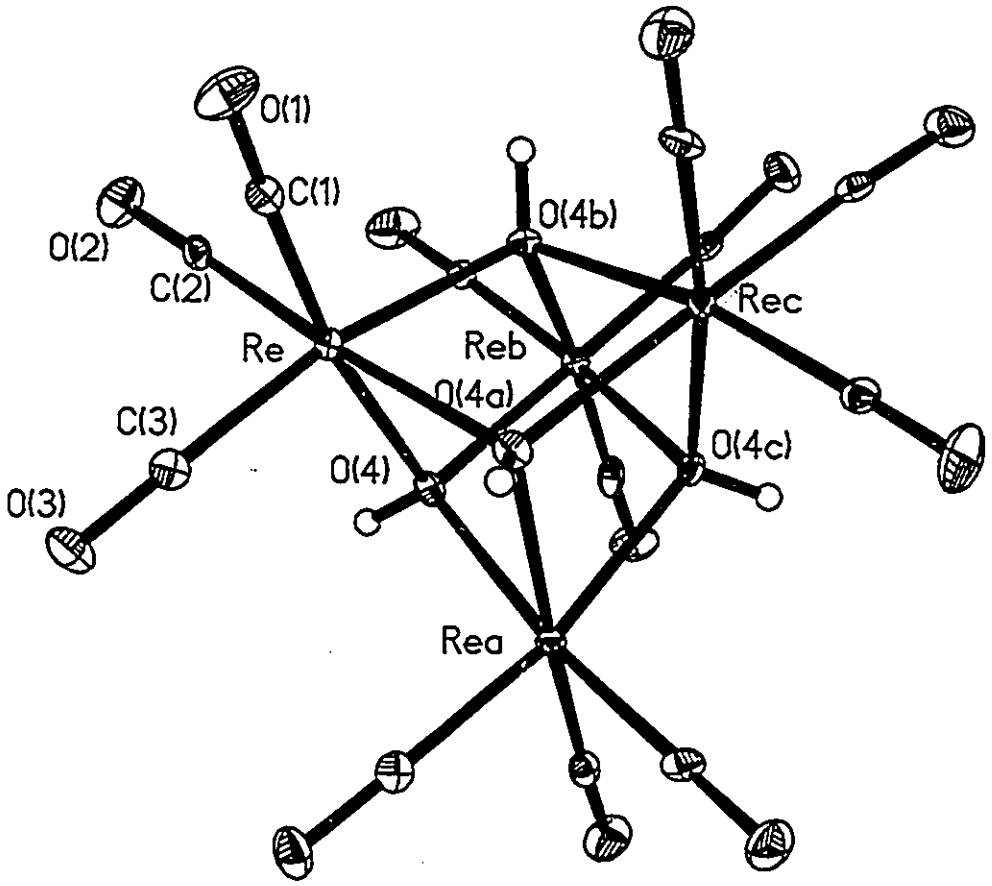

Fig. 3C.1. Structure of $[Re(CO)_3(OH)]_4 \cdot 8H_2O$ (3C) (Water was Omitted)

Table 3D.1. Bond Lengths (Å) and Bond Angles (°)

for $KRe_2(CO)_6(OH)_3 2H_2O$ (3D)

Re(1)-O(2)	2.16 (1)	Re(1)-C(1a)	1.89 (1)
Re(1)-C(1b)	1.92 (1)	Re(1)-O(1c)	2.157 (6)
Re(1)-C(1aa)	1.89 (1)	Re(1)-O(1)	2.157 (6)
Re(2)-O(1)	2.164 (6)	Re(2)-C(2aa)	1.91 (1)
Re(2)-O(2)	2.15 (1)	Re(2)-C(2a)	1.91 (1)
Re(2)-C(2b)	1.87 (2)	Re(2)-O(1c)	2.164 (6)
Re(3)-O(3)	2.137 (6)	Re(3)-O(4)	2.16 (1)
Re(3)-C(3a)	1.902 (9)	Re(3)-C(3b)	1.84 (1)
Re(3)-O(3c)	2.137 (6)	Re(3)-C(3aa)	1.902 (9)
Re(4)-O(3)	2.156 (7)	Re(4)-O(4)	2.191 (9)
Re(4)-C(4a)	1.89 (1)	Re(4)-C(4b)	1.90 (1)
Re(4)-O(3c)	2.156 (7)	Re(4)-C(4aa)	1.89 (1)
C(1a)-O(1a)	1.17 (1)	C(2b)-O(2b)	1.18 (2)
C(1b)-O(1b)	1.14 (2)	C(2a)-O(2a)	1.14 (1)
C(3a)-O(3a)	1.15 (1)	C(3b)-O(3b)	1.20 (2)
C(4a)-O(4a)	1.17 (1)	C(4b)-O(4b)	1.16 (2)

O(2b)-K(1)	3.008 (8)	K(1)-O(1aa)	2.755 (7)
K(1)-O(2aa)	2.750 (7)	K(1)-O(3ba)	2.937 (7)
K(1)-O(4aa)	2.755 (8)	K(1)-O(4ba)	2.931 (7)
O(3a)-K(1)	2.847 (7)	O(11)-O(11a)	0.94 (3)
O(22)-O(33)	1.12 (2)		

O(1)-Re(1)-O(2)	72.6(3)	C(1)-Re(1)-C(1b)	101.4(4)
O(1)-Re(1)-C(1a)	98.5(3)	O(2)-Re(1)-C(1a)	98.2(3)
O(2)-Re(1)-C(1b)	172.2(5)	C(1a)-Re(1)-C(1b)	87.5(4)
O(2)-Re(1)-O(1c)	72.6(3)	C(1a)-Re(1)-O(1c)	170.0(3)
C(1b)-Re(1)-O(1c)	101.4(4)	O(1)-Re(1)-O(1c)	75.4(3)
O(1)-Re(1)-C(1aa)	170.0(3)	O(2)-Re(1)-C(1aa)	98.2(3)
C(1a)-Re(1)-C(1aa)	86.4(6)	C(1b)-Re(1)-C(1aa)	87.5(4)
O(1a)-Re(1)-C(1aa)	98.5(3)	O(1)-Re(2)-O(2)	72.7(3)
O(1)-Re(2)-C(2a)	98.8(4)	C(2a)-Re(2)-C(2b)	87.7(4)
O(2)-Re(2)-C(2a)	97.9(4)	O(1)-Re(2)-C(2aa)	169.9(4)
O(1)-Re(2)-C(2b)	101.3(4)	O(2)-Re(2)-C(2b)	172.3(5)
O(1)-Re(2)-O(1c)	75.1(3)	O(2)-Re(2)-O(1c)	72.7(3)
C(2a)-Re(2)-O(1c)	169.9(4)	C(2b)-Re(2)-O(1c)	101.3(4)
O(2)-Re(2)-C(2aa)	97.9(4)	C(2a)-Re(2)-C(2aa)	86.1(6)
C(2b)-Re(2)-C(2aa)	87.7(4)	O(1a)-Re(2)-C(2aa)	98.8(4)
O(3)-Re(3)-O(4)	74.9(3)	O(3)-Re(3)-O(3c)	72.8(3)

O(3)-Re(3)-C(3a)	99.9(3)	O(4)-Re(3)-C(3a)	96.5(3)
O(3)-Re(3)-C(3b)	98.1(4)	O(4)-Re(3)-C(3aa)	96.5(3)
O(4)-Re(3)-C(3b)	171.1(5)	C(3a)-Re(3)-C(3b)	89.9(4)
O(4)-Re(3)-O(3c)	74.9(3)	C(3a)-Re(3)-O(3c)	169.8(3)
C(3b)-Re(3)-O(3c)	98.1(4)	O(3)-Re(3)-C(3aa)	169.8(3)
C(3a)-Re(3)-C(3aa)	86.3(6)	C(3b)-Re(3)-C(3aa)	89.9(4)
O(3c)-Re(3)-C(3aa)	99.9(3)	O(3)-Re(4)-O(4)	73.8(3)
O(3)-Re(4)-C(4a)	100.4(4)	O(3)-Re(4)-C(4aa)	169.2(3)
O(4)-Re(4)-C(4a)	97.0(3)	C(4a)-Re(4)-C(4b)	88.6(4)
O(3)-Re(4)-C(4b)	100.0(4)	O(4)-Re(4)-C(4b)	172.3(5)
O(3)-Re(4)-O(3c)	72.0(3)	O(4)-Re(4)-O(3c)	73.8(3)
C(4a)-Re(4)-O(3c)	169.2(3)	C(4b)-Re(4)-O(3c)	100.0(4)
O(4)-Re(4)-C(4aa)	97.0(3)	C(4a)-Re(4)-C(4aa)	86.1(6)
C(4b)-Re(4)-C(4aa)	88.6(4)	O(3c)-Re(4)-C(4aa)	100.4(4)
Re(1)-O(1)-Re(2)	92.5(2)	Re(1)-O(2)-Re(2)	92.7(3)
Re(3)-O(3)-Re(4)	92.9(2)	Re(3)-O(4)-Re(4)	91.3(3)
Re(1)-C(1a)-O(1a)	178.9(5)	Re(2)-C(2b)-O(2b)	178(1)
Re(1)-C(1b)-O(1b)	179.2(8)	Re(2)-C(2a)-O(2a)	179.2(6)
Re(3)-C(3a)-O(3a)	176.8(7)	Re(3)-C(3b)-O(3b)	179(1)
Re(4)-C(4a)-O(4a)	176.8(8)	Re(4)-C(4b)-O(4b)	179.4(7)

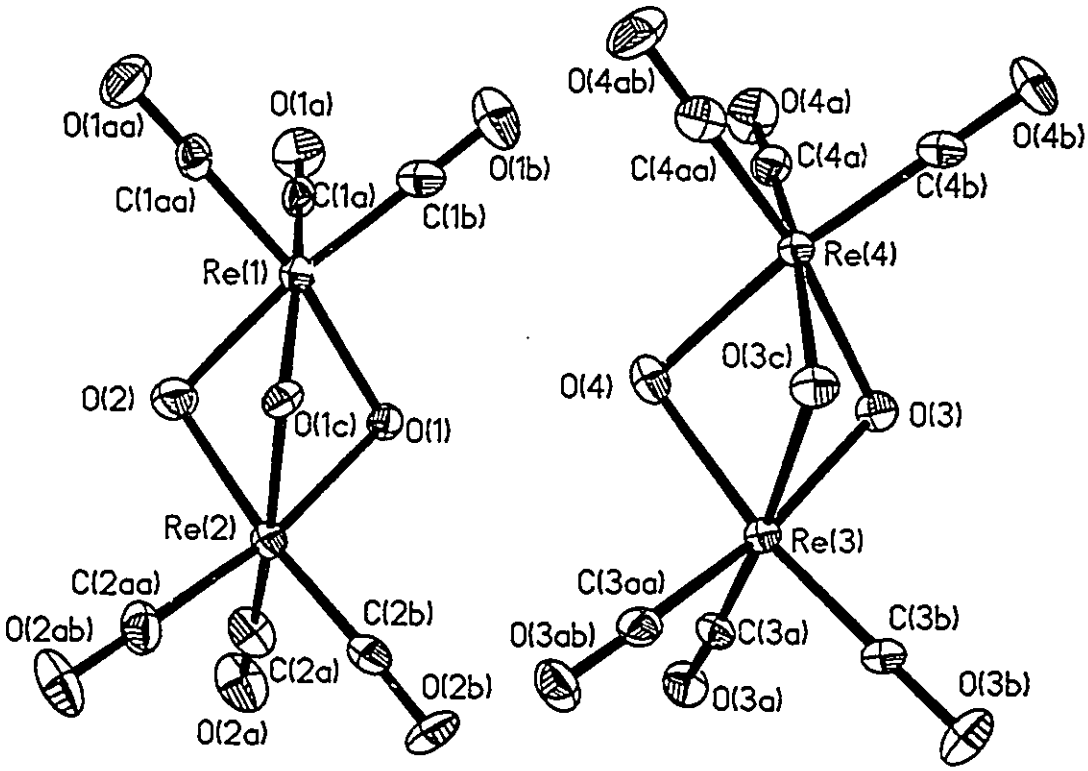

Fig. 3D.1. Structure of $KRe_2(CO)_6(OH)_3 2H_2O$ (3D) Anions

Table 3E.1 Bond Lengths (Å) and Bond Angles (°) for $KRe_3(CO)_9(OH)_4$ (3E)

Re-O(4)	2.205 (5)	Re-C(2)	1.88 (1)
Re-C(1)	1.89 (1)	Re-C(3)	1.89 (1)
Re-O(5a)	2.161 (8)	Re-O(5)	2.178 (8)
O(5)-Rea	2.161 (8)	O(4)-Rea	2.205 (5)
O(4)-Reb	2.205 (5)	O(3)-C(3)	1.19 (2)
C(2)-O(2)	1.19 (2)	C(1)-O(1)	1.148 (2)
K(2)-O(5)	2.362 (8)	K(2)-O(5a)	2.362 (8)
K(2)-O(5b)	2.362 (8)	K(2)-O(5c)	2.362 (8)
K(2)-O(5d)	2.362 (8)	K(2)-O(5e)	2.362 (8)
O(5)-Re-O(4)	74.1(3)	O(5)-Re-C(1)	96.9(5)
O(5)-Re-C(2)	173.4(5)	O(4)-Re-C(2)	100.6(4)
O(4)-Re-C(1)	98.1(5)	C(2)-Re-C(1)	87.7(6)
O(4)-Re-C(3)	171.6(5)	C(2)-Re-C(3)	86.1(6)
C(1)-Re-C(3)	87.2(6)	O(5)-Re-C(3)	98.8(5)
O(5)-Re-O(5a)	79.0(4)	O(4)-Re-O(5a)	74.5(3)
C(2)-Re-O(5a)	95.8(5)	C(1)-Re-O(5a)	172.2(5)
C(3)-Re-O(5a)	99.9(5)	Re-O(5)-K(2)	102.0(3)
Re-O(5)-Rea	105.6(3)	K(2)-O(5)-Rea	102.5(3)
Re-O(4)-Rea	103.2(4)	Re-O(4)-Reb	103.2(4)
Rea-O(4)-Reb	103.2(4)	Re-C(2)-O(2)	176(1)
Re-C(1)-O(1)	174(1)	Re-C(3)-O(3)	177(1)
O(5)-K(2)-O(5d)	180.0(1)	O(5)-K(2)-O(5b)	71.5(3)

O(5)-K(2)-O(5a)	71.5(3)	O(5)-K(2)-O(5e)	108.5(3)
O(5)-K(2)-O(5c)	108.5(3)	O(5d)-K(2)-O(5e)	71.5(3)
O(5b)-K(2)-O(5e)	108.5(3)	O(5c)-K(2)-O(5e)	71.5(3)
O(5a)-K(2)-O(5e)	180.0(1)	O(5d)-K(2)-O(5a)	108.5(3)
O(5b)-K(2)-O(5a)	71.5(3)	O(5c)-K(2)-O(5a)	108.5(3)
O(5d)-K(2)-O(5c)	71.5(3)	O(5b)-K(2)-O(5c)	180.0(1)
O(5d)-K(2)-O(5b)	108.5(3)		

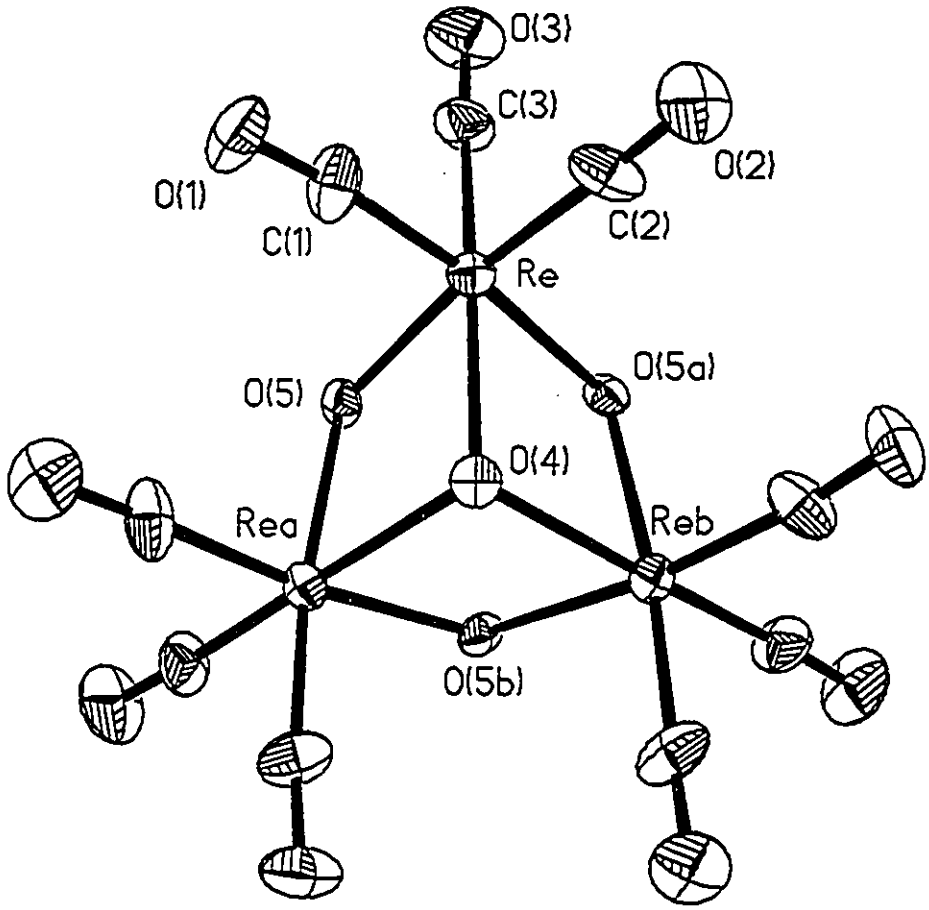

Fig. 3E.1. Structure of $KRe_3(CO)_9(OH)_4$ (3E) Anion

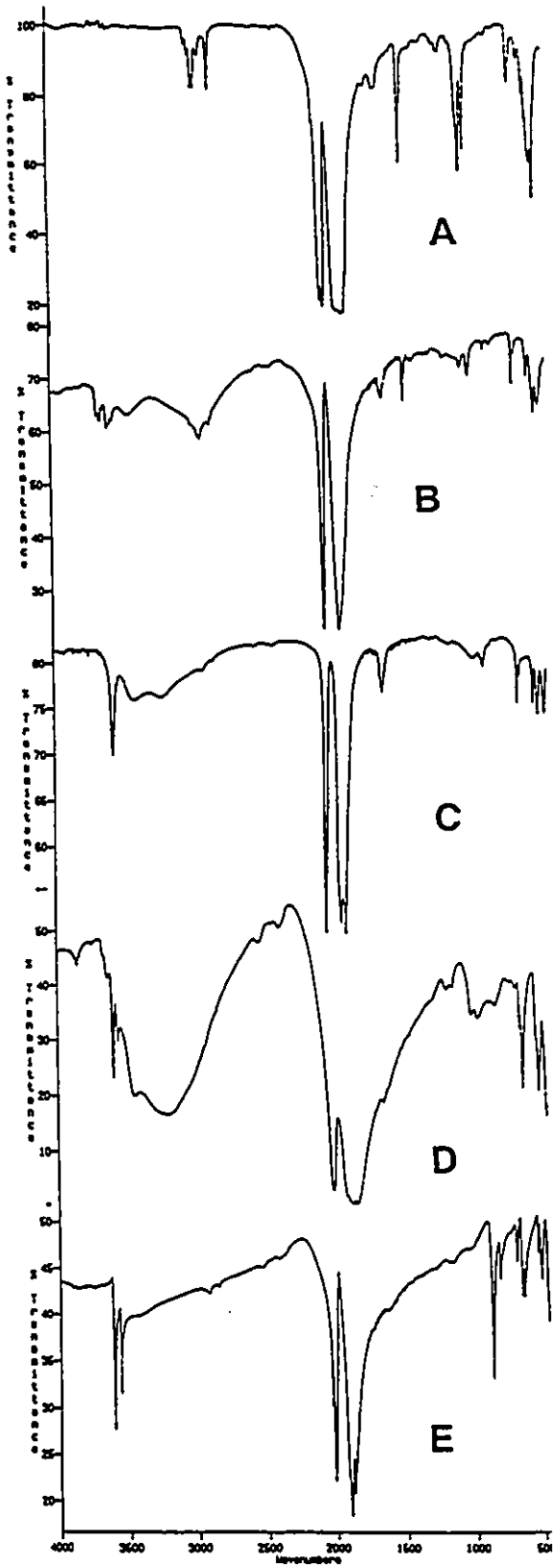

Fig. 3.1. Comparison of I R Spectra of 3A, 3B, 3C, 3D and 3E.

3.5.2.1 Structures of the Two Tetramers $[Re_4(CO)_{12}(OH)_2(EtO)_2]\cdot 2EtOH$ (3B) and $[Re(CO)_3(OH)]_4\cdot 8H_2O$ (3C)

There was a two fold axis in the molecule of **3B**. There was disorder in the bridging ethoxy group and the lattice ethanol molecule. The disorder was caused by lack of enough constraints around the carbon atoms. The final structure of **3B** was obtained by a constrained refinement of the bridging ethoxy group with O(2)-C(40) and O(2)-C(40') fixed at 1.43(3) Å, C(40)-C(30) and C(40')-C(30) fixed at 1.52(5) Å, and the sum of the occupancy factors of C(40) and C(40') fixed at 1 (0.35 + 0.65). The O(10a)...O(1) distance is 2.646 Å, and the hydrogen bond length of O(1)...H(10a) is 1.83 Å.

The molecule of **3C** had tetrahedral symmetry, and the lattice water molecules in **3C** were well refined. Crystals of **3C** were found to be very unstable. They rapidly turned translucent on loss of lattice water when they were removed from the mother liquor. A special technique was used to mount the crystal of **3C**, as described in chapter 2, and the data were collected at low temperature (173(3) K).

Compound **3B** and **3C** belong to the family of compounds with the general formula $[ML_3X]_4$ (e.g. $[Re(CO)_3F]_4.4H_2O$ [41], $[Re(CO)_3(SMe)]_4$ [42]). A comparison of the geometries of some rhenium carbonyl structures is provided in Table 3.2.

It has been reported that the reaction of $M(CO)_5Cl$ (where M = Mn or Re) with a thiol (RSH) leads to the formation of the corresponding $[M_2(CO)_8(\mu_2\text{-}SR)_2]$ compound, and further loss of CO from the molecules yields the cubane clusters $[M_4(CO)_{12}(\mu_3\text{-}SR)_4]$. IR [43] and X-ray studies of $[Re_4(CO)_{12}(\mu_3\text{-}SMe)_4]$ [42] show that these tetramers have regular tetrahedral structures and do not contain direct metal-metal bonding interactions.

The dimension ranges are 3.85-3.96 Å for Re---Re, 3.05-3.17 Å for S---S, 2.48 -2.52 Å for Re-S; 100.7-104.1° for Re-S-Re; and 75.8-77.9° for S-Re-S.

Table 3.2. The Average Geometry of Some Rhenium Carbonyl Structures

	Re-Re(Å)	Re-C(Å)	C-Re-C(°)
$[Re(CO)_3F]_4.4H_2O$	3.469(3)	1.893(7)	86.6(4)
$[Re(CO)_3(SMe)]_4$	3.898(3)	1.87(5)	89.8(2)
3A	3.418(1)	1.898(6)	88.4(3)
3B	3.443(1)	1.916(7)	86.7(3)
3C	3.434(1)	1.901(5)	87.2(2)
3D	3.116(1)	1.891(3)	87.7(1)
3E	3.456(1)	1.887(8)	87.0(3)
$[Re(CO)_3(OH)]_4 \cdot 2C_6H_6$	3.480(2)	1.88(2)	--

Tetrakis(tricarbonyl-μ_3-hydroxo-rhenium), $[Re(CO)_3(OH)]_4$ was first reported by M. Herberhold and co-workers to be formed by photolysis of $Re_2(CO)_{10}$ in aqueous ether [44], or by the reaction of either $Re_2(CO)_{10}$ or $Re(CO)_5Cl$ with water at 200°C [45]. But they did not specify whether the compound was solvated and did not determine the structure of their compound. The structure of $[Re(CO)_3(OH)]_4 \cdot 2C_6H_6$ (3A') was determined [46] by Nuber and co-workers. Formation of interwoven 2-dimensional

networks by the spontaneous strict self-assembly of $[M(CO)_3(OH)]_4$ (M = Mn, Re) and complementary angular spacer molecules was studied recently by Zaworotko and his co-workers [47]. It is interesting that $[Re(CO)_3(OH)]_4$ can be cocrystallized with solvents of very different polarity, from water (3A) through dipyridine and methanol ($[Re(CO)_3(OH)]_4 \cdot 2dipy \cdot 2MeOH$, dipy = 4,4'-dipyridine) [47] to benzene (3A'). This feature was used to prepare supramolecular 2-dimensional or 3-dimensional compounds by Zaworotko and co-workers [47].

3.5.2.2 The Structures of the Two Trimers $K[Re_3(OCH_3)_4(CO)_9]$ (3A) and $KRe_3(CO)_9(OH)_4$ (3E)

In 3E or 3A, the three rhenium atoms form an equilateral (3E) or a near equilateral triangle (3A), with one hydroxide or methoxide group bridging all three rhenium atoms on one side of the Re_3 plane, while the other three hydroxide or methoxide groups, which are on the other side of the Re_3 plane, each bridge two rhenium atoms. Each rhenium atom has six ligating atoms that form a rough octahedron, with three hydroxide or methoxide groups in a facial arrangement and the other positions filled by three carbonyl ligands.

Although trimeric systems with hydride bridges [48], or hydride and alkoxy bridges [49], carboxylate bridges [50], tin bridges [51], or only thiol bridges [52] are well known, units of the type $M_3(\mu_3\text{-}L)(\mu_2\text{-}L')_3(L'')_9$ are relatively rare in rhenium chemistry and are almost exclusively restricted to Re(I) systems, where L=OR, L' is H and L" is CO [53]. Complexes with $M_3(OR)_4$ and $M_4(OR)_4$ cores are much more common in

Mo(IV) and W(IV) chemistry [54]. In all these systems, however, there are metal-metal bonds connecting the three metal atoms. This is not the case in the compounds **3A**, **3B**, **3C**, **3D**, or **3E**; the Re...Re distances (3.411(1), 3.424(1), 3.419(1) Å in **3A**; 3.499(1), 3.413(1), 3.418(1) Å in **3B**; 3.457(1), 3.388(1), 3.457(1) Å in **3C**; 3.121(1), 3.111(1) Å in **3D**; 3.456(1) Å in **3E**) are far too long for Re-Re bonding.

Each rhenium atom is a conventional Re(I) d^6 system in a strong pseudo-octahedral field. For **3A**, the local symmetry is roughly C_s; the overall symmetry of the anion is roughly C_{3v}, with O(4) on the C_3 axis. Angular distortion from an ideal octahedron is quite substantial. Although C-Re-C angles are close to 90° (ave. 88.4(7)°, range 85.5(6)-91.1(6)° in **3A**), the O-Re-O angles are substantially less. The μ_2-O-Re-μ_3-O angles (74.7(2)°, range 74.0(3)-75.1(3)° in **3A**) are significantly less than the μ_2-O-Re-μ_2-O angles (79.8(3)°, range 79.3(3)°-80.4(3)° in **3A**).

The Re-C bonds (ave. 1.898(6)Å, range 1.87(1) - 1.93(1)Å in **3A**) are shorter than in $Re(CO)_6^+$ or systems where CO groups are trans to other CO groups (range 1.987(6)-2.018(7)Å in **3A**) [55]. They are typical of distances where the CO group is trans to a ligand which is not a good π-acceptor (range 1.86(5) - 1.929(7)Å). Two Re-C bonds do differ significantly (Re(1)-C(12) and Re(3)-C(33) differ by 3.1σ in **3A**), but there is no obvious correlation of Re-C distances with trans-Re-O distances. Carbonyl bond lengths (ave. 1.16(1)Å, range 1.14(1) - 1.18(2)Å in **3A**) do not differ significantly. The Re-O bonds fall into two groups, related to the μ_2- and μ_3-hydroxides or methoxides: Although few of the individual bond pairs are significantly different, the average of the μ_2-O-Re distances (2.152(5) Å in **3A**) is significantly different from the average μ_3-O-Re distance

(2.183(4)Å in 3A). Similar differences are reflected in the O-C bond lengths for the methoxide groups. Although, individually, μ_2-O-C distances hardly differ significantly from the μ_3-O-C distance (1.48(2)Å in 3A), the average value (1.424(8)Å in 3A) is significantly shorter.

The potassium ion in 3A is surrounded by an irregular array of seven oxygen atoms; three from μ_2-methoxy groups and four from carbonyl groups. The structure of the technetium analogue of 3A, $Na[Tc_3(CO)_9(OMe)_4]$, was reported recently [56], and its dimensions are quite close to 3A.

3.5.2.3 The Structure of the Dimer $KRe_2(CO)_6(OH)_3{\cdot}2H_2O$ (3D)

There were two independent molecules, which had a plane of symmetry, in the structural model of 3D. The correct space group of 3D was C2/m. In Jayadevan's Ph.D. thesis [39], the space group chosen was C2, and a plane of symmetry was missed. A cell transformation of the parameters of Jayadevan's crystal (28.27(1) Å, 10.380(3) Å, 12.463(5) Å, 130.6(1)°) by a matrix (1 0 2, 0 -1 0 , 0 0 1) gives the correct unit cell (22.438 Å, 10.380 Å, 12.463 Å, 106.9°), which is very close to that found in this study (22.538(5) Å, 10.328(3) Å, 12.458(3) Å, 106.68(2)°). The addition of a plane of symmetry had removed inherent singularities associated with refining the structure in a space group of unnecessarily low symmetry [57].

The Re-Re distances were 3.121(1) and 3.111(1) Å in 3D. There was only one potassium ion in the model which occupied a general position. All water molecules were disordered. O(11) and O(11A) were related by mirror symmetry. The O(22) and O(33)

sites could not be occupied at the same time since they were only 1.12(2) Å from each other. Refinement of the occupancy gave values of 0.5 for each site. O(44) had a full occupancy factor but a large temperature factor.

Three alkoxy analogues of **3D** have been reported. They were $NEt_4[Re_2(CO)_6(\mu\text{-}OMe)_x(\mu\text{-}OEt)_y]$ (x + y = 3) (Re···Re 3.086(3) Å) [58], $[Re_2(CO)_6(\mu\text{-}OMe)(\mu\text{-}OEt)_2]^-$ (Re···Re 3.117(2) Å) [59], and $NMe_4[Re_2(CO)_6(\mu\text{-}OMe)_3]$ (Re···Re 3.113(9) Å) [60]. There was disorder in the first two structures and the Re···Re distances were in agreement with those of **3D**.

3.5.3 Spectroscopic Studies

The ^1H NMR spectrum of compound **3A** showed the presence of two types of protons occurring at 4.53 ppm and 4.25 ppm, with the intensities of the integrated peaks approaching a 1:3 ratio. This is in accord with the IR spectra and the structure of the anion. No other signals were detected in the ^1H NMR spectrum to -20 ppm. The ^1H NMR spectrum of compound **3C** showed the presence of two types of protons that occurred at 6.75 ppm and 3.05 ppm. The intensities of the integrated peaks had a ratio of almost 1:4. This is again in accord with the IR spectra and the structure of the anion. Not enough sample was available to obtain a useful NMR study of **3B**, **3D** or **3E**.

Nine bands were observed in the carbonyl region of the IR spectrum for **3A**. Each independent rhenium atom is the centre of a $ML_3(CO)_3$ system, where L is not a π-acceptor, and therefore the CO stretching vibrations would be expected to occur at relatively low wave-numbers compared to that of free CO at 2155 cm^{-1} [61]. The X-ray

crystal structure of 3A indicates there are three CO groups trans to the μ_3-OCH_3 groups and six trans to the μ_2-OCH_3 groups. An examination of the carbonyl region of the IR spectrum of 3A shows two groups of bands centred at about 2020 and 1900 cm^{-1}. It is postulated that the μ_3-OCH_3 group has a weaker interaction with the carbonyl group trans to it than the two μ_2-OCH_3 groups have with the CO groups trans to them. Therefore the bands at about 2020 cm^{-1} arise from the carbonyl groups trans to μ_3-OCH_3 and the 1900 cm^{-1} bands arise from the carbonyls trans to μ_2-OCH_3.

In the carbonyl region of the IR spectra, six very strong bands were observed for 3D and 3E, which demonstrated a higher symmetry than 3A (See Fig. 3A.1, 3D.1, 3E.1). Similarly only four very strong bands were observed in the carbonyl region for 3C, which had the highest symmetry of the five compounds (see Fig. 3C.1). Eleven bands were observed in the carbonyl region for 3B, which had the lowest symmetry (see Fig. 3B.1). In general, this study shows that the bands in the carbonyl region are very sensitive to the overall symmetry of the compound, and each of the above five compounds has a distinctive IR spectrum, as shown in Fig. 3.1.

3.6 Summary and Suggested Future Work

A mystery in the early literature of the rhenium carbonyl compounds has remained for about 40 years, since Hieber, the pioneer worker in this area, and his co-worker Schuster proposed the possible structure of the dimer "$K[Re_2(CO)_8O_2H]$" [38]. Their proposal stimulated Jayadevan's investigation which was conducted about 30 years ago [39]. Considering the techniques they employed in those days, Hieber and Schuster's

analysis was not too bad. Their elemental composition of 1K:2Re:8C:10O:1H is not too far from the one obtained in this study by X-ray diffraction method 1K:2Re:6C:11O:7H. Jayadevan had obtained crystals of the dimer and collected X-ray diffraction data of the crystal, but unfortunately chose the wrong space group, C2 instead of C2/m. The wrong space group introduced severe ambiguity in the determination of the structure, and the results were not publishable.

In an attempt to study the structure of the dinuclear complex "$K[Re_2(CO)_8O_2H]$", the reactions between $Re(CO)_5Cl$ and KOH under different conditions were reinvestigated. Five different compounds, the dimer $KRe_2(CO)_6(OH)_3 \cdot 2H_2O$ (**3D**), two trimers, $K[Re_3(CO)_9(OMe)_4]$ (**3A**) and $KRe_3(CO)_9(OH)_4$ (**3E**), and two tetramers, $Re_4(CO)_{12}(OH)_4 \cdot 8H_2O$ (**3C**) and $Re_4(CO)_{12}(OH)_2(OEt)_2 \cdot 2EtOH$ (**3B**) were obtained. This study resolved the mystery about the dimer and also resulted in the discovery of some related new compounds. The dimer has two $[Re(CO)_3]^+$ units bridged by three OH^- groups. There is no hydride in the compound.

From the dimer, to trimer and tetramer, a number of the basic construction units $[Re(CO)_3]^+$ are connected by bridging OH^-, or OMe^-, OEt^- groups. The studies for the series with OH^- bridging groups, from dimer to tetramer, is now completed, but for the series with OMe^- or OEt^- bridging groups, there are still opportunities in this area to prepare and isolate some new species.

CHAPTER 4

SYNTHESIS AND CHARACTERIZATION OF TWO NITRIDORHENIUM(V) CYANIDE COMPOUNDS

4.1 Introduction

Nitrido-complexes of transition metals, especially molybdenum, have been intensively investigated in attempts to develop models of the intermediate step of N_2-assimilation [62]. Nitrido-complexes of rhenium were explored in the early 1960s [63]. One unreliable structure determination of "$K_2[ReN(NC)_4]\cdot H_2O$" was reported by Davies *et al.* [64].

The reported C≡N and Re≡N bond distances differed significantly from values usually found and the cyanide ligands were coordinated through the nitrogen atoms rather than the carbon atoms. No further information has been published, but in a personal communication to Rouschias [65], Johnson admitted that there were difficulties in the refinement, and opined that only the Re...Re separation was known with any certainty.

The intent of this work was to clarify the above ambiguity by use of modern techniques in X-ray crystal data collection and computation. Investigations were extended to the closely related compound, $(AsPh_4)_2[ReN(CN)_4(H_2O)]\cdot 5H_2O$. Part of this study has been published [66]. More results are presented in this Chapter.

4.2 Preparation

4.2.1 $K_2[ReN(CN)_4]\cdot H_2O$ (4A)

$ReNCl_2(PPh_3)_2$ was prepared according the method of Chatt *et al.* [67] and converted to $K_2[ReN(CN)_4]\cdot H_2O$, **4A**, by reaction with excess potassium cyanide in methanol [68]. IR (cm^{-1}, KBr disk): 3653 (vs, H_2O), 3571 (vs, H_2O), 3445 m, 2143 m, 2120 (vs, C≡N), 2080 m, 1608 s, 997 vs, 968 vs, 914 m, 484 m, 440 m, 407 vs, 384 s, 348 m, 334 m.

Crystals of **4A** suitable for X-ray studies were grown from an aqueous solution with excess KCN by slow evaporation at room temperature over solid KOH in a water pump evacuated desiccator. Crystals of **4A** were red, tiny, thin plates.

4.2.2 $(AsPh_4)_2[ReN(CN)_4(H_2O)]\cdot 5H_2O$ (4B)

$(AsPh_4)_2[ReN(CN)_4(H_2O)]\cdot 5H_2O$, **4B**, was prepared by mixing an aqueous solution of $AsPh_4Cl$ (232 mg, 0.554 mmol, in 10 mL water) and **4A** (111 mg, 0.227 mmol, in 10 mL water). IR (cm^{-1}, KBr disk): 3656 (vs, H_2O), 3456-3415 s(b), 3155 w, 3079 m, 3057 m, 2658 w, 2129 w, 2110 (vs, C≡N), 2069 w, 1912 w, 1830 w, 1636 m, 1576 m, 1482 s, 1499 vs, 1406 m, 1342 m, 1314 m, 1281 w, 1186 m, 1165 m, 1107 m, 1082 vs, 1021 m, 997 vs, 986 m, 925 w, 852 w, 774 vs, 689 vs, 669 m, 613 m, 478 s, 468 vs, 460 s, 405 s, 396 s, 355 vs.

Bright yellow crystals of **4B** were obtained by recrystallization from a dilute aqueous solution of **4B** at room temperature. Crystals of **4B** were stable in the capped vial, but decomposed slowly in air, especially under X-ray irradiation, by loss of water of crystallization, to become a powder.

4.3 Physical Measurements

Infrared spectroscopic data of **4A** and **4B** are shown in the appropriate preparation section. The density of **4B** was measured by the suspension method in a carbon tetrachloride/cyclohexane mixture.

4.4 X-ray Structural Determinations

For compound **4A** four data sets were collected, but none of them gave satisfactory results. The details are addressed in the discussion section.

For compound **4B** crystallographic data were collected on a Siemens R3m/V diffractometer, with use of graphite-monochromated Ag $K\alpha$ radiation (λ=0.56086 Å at 167 (2) K). Crystallographic details of **4B** are summarized in the appendix Table **4B**.2. Bond lengths and angles of **4B** are shown in Table **4B**.1. Atomic positional parameters and U_{eq} of **4B** are given in the appendix Table **4B**.3. The structure for the anion of **4B** is shown in Fig. **4B**.1.

4.5 Results and Discussion

4.5.1 Preparations

The aqueous solutions of **4A** and **4B** were both bright yellow, but the crystals of **4A** were red and crystals of **4B** were yellow. It was found that good crystals of **4A** were fairly hard to grow as mentioned by R.H. Fenn and co-workers [69], while large high quality crystals of **4B** were not that hard to grow.

Table 4B.1

Selected Bond Lengths (Å) and Bond Angles (°) for

$(AsPh_4)_2[ReN(CN)_4(H_2O)]\cdot 5H_2O$ (4B)

Re-O	2.463 (3)	Re-C(1)	2.102 (4)
Re-C(2)	2.108 (5)	Re-C(3)	2.096 (4)
Re-C(4)	2.114 (5)	Re-N(5)	1.655 (4)
As(2)-C(1D)	1.897 (5)	As(2)-C(1E)	1.904 (5)
As(2)-C(1F)	1.923 (5)	As(2)-C(1G)	1.913 (4)
As(1)-C(1A)	1.908 (5)	As(1)-C(1B)	1.893 (5)
As(1)-C(1C)	1.916 (5)	As(1)-C(1H)	1.914 (4)
C(1)-N(1)	1.149 (6)	C(2)-N(2)	1.149 (7)
C(3)-N(3)	1.150 (6)	C(4)-N(4)	1.149 (7)

O-Re-C(1)	79.2(2)	O-Re-C(2)	81.3(2)
C(1)-Re-C(2)	92.0(2)	O-Re-C(3)	83.6(2)
C(1)-Re-C(3)	162.7(2)	C(2)-Re-C(3)	83.4(2)
O-Re-C(4)	80.0(2)	C(1)-Re-C(4)	89.0(2)
C(2)-Re-C(4)	160.8(2)	C(3)-Re-C(4)	90.0(2)
O-Re-N(5)	177.7(1)	C(1)-Re-N(5)	98.7(2)
C(2)-Re-N(5)	99.7(2)	C(3)-Re-N(5)	98.5(2)
C(4)-Re-N(5)	99.1(2)	Re-C(1)-N(1)	178.7(4)
Re-C(2)-N(2)	172.0(4)	Re-C(3)-N(3)	175.5(4)
Re-C(4)-N(4)	179.6(5)	C(1D)-As(2)-C(1E)	109.4(2)
C(1D)-As(2)-C(1F)	110.5(2)	C(1E)-As(2)-C(1F)	108.6(2)
C(1D)-As(2)-C(1G)	108.4(2)	C(1E)-As(2)-C(1G)	111.5(2)

C(1F)-As(2)-C(1G)	108.4(2)	C(1A)-As(1)-C(1B)	106.4(2)
C(1A)-As(1)-C(1C)	112.0(2)	C(1B)-As(1)-C(1C)	108.0(2)
C(1A)-As(1)-C(1H)	110.8(2)	C(1B)-As(1)-C(1H)	109.5(2)
C(1C)-As(1)-C(1H)	110.0(2)	As(1)-C(1A)-C(2A)	121.6(4)
As(1)-C(1A)-C(6A)	116.5(4)		

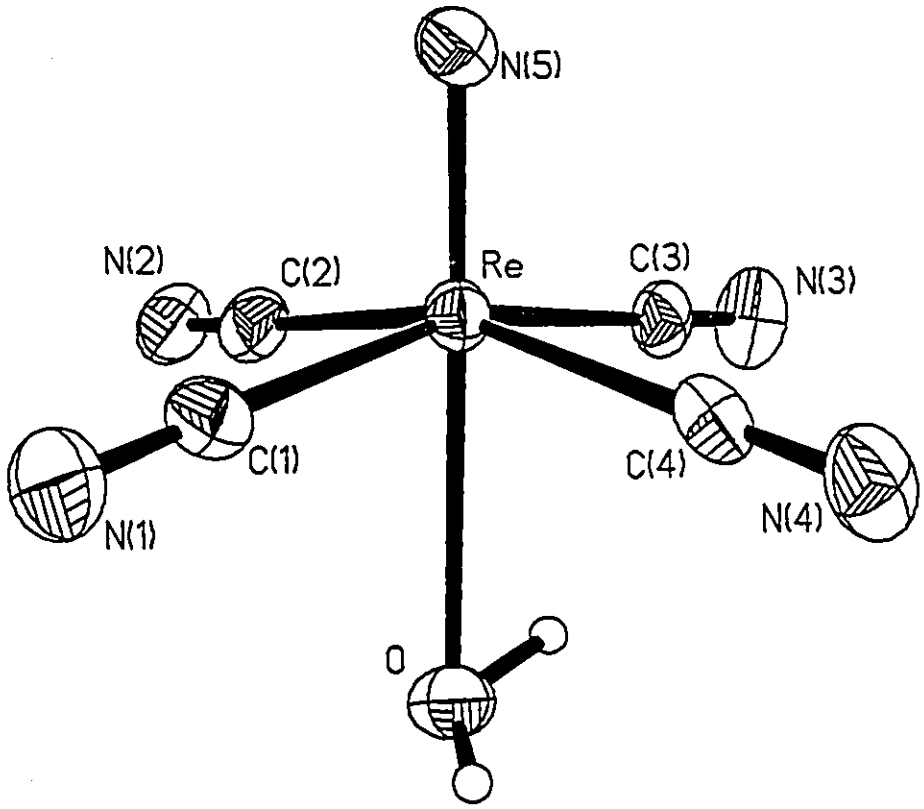

Fig. 4B.1 Structure of $(AsPh_4)_2[ReN(CN)_4(H_2O)]\cdot 5H_2O$ (4B) Anion

4.5.2 Data Collection and Refinement

For **4A**, efforts were made to collect the data sets in the 'body centred' cell. The first data set of **4A**, which could be solved and refined to an R value of about 15% in the space group Imm2, was obtained with Mo radiation. The scan speed, which was chosen with new software, was too fast, and the experiment was aborted. The structure solution for the second data set, again obtained with Mo radiation on a tiny crystal, showed ghost peaks along the Re≡N direction in the electron density difference map. It was considered that these peaks might be caused by an absorption problem, so silver radiation was used to measure the third data set in the hope that the absorption could be reduced. The same problems were encountered again, however. It was then recognised that either the molecules packed in two opposite oriented chains in the cell, or the crystal chosen was twinned. Another tiny crystal was chosen to obtain a fourth data set with Mo radiation in a 'body centred cell' to check if the crystal was twined. Same problems were encountered again. It was concluded that a complete data set in a primitive cell should be collected in the future for **4A** rather than struggle with a probably incomplete data set obtained for a 'body centred cell'. The choice of the cell was made by the program after the very first 25 strong reflections (usually $\rangle 10\sigma(I)$) were randomly searched and the cell dimensions decided. The cell determined in this way does not necessarily mean that the structure belongs to the crystal class, however. Unfortunately, weak reflections, which can distinguish between a true and an approximate centre, were not collected adequately in our initial trials because the heavy atom sits at a nearly body centred position and the average appearance of the two molecules of opposite direction makes the cell look like

body centred. The refinement proved difficult with the 'body centred' data set. Not only was it impossible to refine the structure below a residual of 10%, but also 'disorder' or 'bend' of cyanide ligand was observed, same as Davies *et al.* [64].

If the average electron numbers in two oppositely oriented molecules along each chain was considered, about 73.9% of the electron density of the two anions in two different orientations was near the body centred position, and only 26.1% of the electron gave information about the primitive cell. For the Tc analogue in the same situation, 65.7% of the electron density favoured the body centred cell and 34.3% of the electron density favoured the primitive cell. Thus it might have proved easier to solve the structure for the Tc analogue than for Re compound. A recent paper [70] on [Cs(18-crown-6)][$TcNCl_4$] indeed showed that the infinite chains were not necessarily packed in the same orientation.

For **4B**, in order to confirm that the cyanide groups were bound through the carbon atoms an alternative series of refinements was undertaken in which the carbon atoms of the cyanide groups were given nitrogen scattering factors and *vice versa*. The residuals were R = 6.1% and wR = 3.4%. In addition U_{eq} was higher for the carbon atoms (C(1N), 0.052; C(2N), 0.054; C(3N), 0.051, C(4N), 0.056) whereas those for the nitrogen atoms were reduced (N(1C), 0.023; N(2C), 0.018; N(3C), 0.020; N(4C), 0.024). All of these results were consistent with the original refinement being the correct solution.

4.5.3 The Vibrational Spectroscopic Studies

For **4A**, the sharp bands at 3653 and 3571 cm^{-1} were typical for the non-bonded lattice water. The strong doublet at 997 and 968 cm^{-1} could be rationalized as the

asymmetric and symmetric stretching of the N-Re≡N bonds, which was consistent with an infinite N-Re≡N-Re≡N... chain structure. For **4B**, the broad O-H bands suggest more than one lattice water molecule is present. The strong band at 1082 cm^{-1} can be assigned to $\nu_{Re\equiv N}$ [74, 85, 86]. So IR spectra show that **4A** and **4B** have different structures.

It has been observed that the CN stretching wave numbers (cm^{-1}) of the cyano compounds were ca. 100(cm^{-1}) higher than that of their isocyano isomers [71]:

	$(Me)_3M$-CN	$(Me)_3M$-NC	
M=Si	2198	2095	(gas phase)
M=Ge	2182	2090	($CHCl_3$ solution)

Table 4.1 Comparison of the C≡N Stretching Wavenumber of $K_2[ReN(CN)_4]\cdot H_2O$ with Other Compounds

$K_3ReO_2(CN)_4$	2121s (Lock [72])
$K_3TcO_2(CN)_4$	2120s (Davison [73])
$K_2[ReN(CN)_4]\cdot H_2O$	2120s (Johnson, 1969)
	2120s (this work)
$(AsPh_4)_2[ReN(CN)_4(H_2O)]\cdot 5H_2O$	2110s (this work)
$(AsPh_4)_2[TcN(CN)_4(H_2O)]\cdot 5H_2O$	2112s (Baldas, [74])

A detailed analysis of the vibrational spectra of $K_3ReO_2(CN)_4$, $K_3ReO_2(^{13}CN)_4$ and

$K_3Re^{18}O^{16}O(CN)_4$ [72], and other structurally well characterized compounds that contained Re-C≡N bonds also provided evidence of a complex with cyanide ligands coordinated through the carbon atoms. A comparison of reported CN stretching wave numbers with IR data of this work, suggested that the C≡N bond lengths of **4A** would be comparable to other compounds and the coordination mode of cyanide ligands in **4A** would be the same as in other compounds. This was confirmed by the refinement of **4B** stated above and structures discussed below.

4.6 Comparison of the Related Structures

4.6.1 $(AsPh_4)_2[TcN(CN)_4(H_2O)]\cdot 5H_2O$ vs $(AsPh_4)_2[ReN(CN)_4(H_2O)]\cdot 5H_2O$

The results observed for $(AsPh_4)_2[ReN(CN)_4(H_2O)]\cdot 5H_2O$ (**4B**) in this work were very similar to those observed for isomorphous bis[tetraphenylarsonium] aquonitridotetracyanotechnetate(V) pentahydrate [74] by Baldas *et al.* The cells were oriented differently; the cell reported here was related to that of the technetium compound by the matrix 0 0 1/0 -1 0/1 0 0. In addition there is an origin shift. The cell for the rhenium compound was 2.9% smaller than that for the technetium compound, and reflected a decrease of about 1% in each axis. The cell is smaller because the data were measured at 165 (2) K instead of 298 K, since bond lengths and angles are generally very similar in the two compounds. The non-bonding interactions between ligating atoms in the coordination spheres of these two compounds are compared in Chapter 7.

Table 4.2 Comparison of the Re≡N Bond Lengths in Some Rhenium Nitrido-complexes (Å)

	Re≡N	Ref.
$ReNCl_4$	1.58(4)	[77]
$ReNCl_2(PPh_3)_2$	1.603(9)	[78]
$ReNCl_2(PEt_2Ph)_3$	1.78(1)	[79]
$ReNCl_2(PMe_2Ph)_3$	1.660(8)	[80]
$(AsPh_4)[ReNCl_4]$	1.62(1)	[81]
$(AsPh_4)[ReNBr_4]$	1.62(1)	[82]
$(AsPh_4)_2[ReN(NCS)_5]$	1.66(1)	[83]
$ReN(S_2CNEt_2)_2$	1.656(6)	[84]
$Cs_2Na[ReN(N_3)(CN)_4]$	1.65(2)	[85]
$(PPh_4)_3[ReN(CN)_5]\cdot 7H_2O$	1.68(1)	[86]
$(AsPh_4)_2[ReN(CN)_4(H_2O)]\cdot 5H_2O$	1.655(4)	this work

4.6.2 The Re≡N Bond

$ReNCl_4$ was prepared by the reaction of $ReCl_5$ with NCl_3. Its structure, which was solved in space group I1, and had chains of $ReNCl_4$ units, linked by alternating Re≡N-Re bonds (Re≡N 1.58(4) Å, Re-N 2.48(4) Å, Re-Cl_{av} 2.27(2) Å). $[ReNCl_3(POCl_3)]_4.2POCL_3$ [75] was reported to have eight membered Re_4N_4 rings with alternating Re≡N-Re units, but no structural details were available. The terminal nitrido ligand was sufficiently basic

to coordinate to Lewis acids, as in the reaction of $ReNCl_2(PMe_2Ph)_3$ with $MoCl_4(NCMe)_2$ to give the bridged nitrido complex $(PhMe_2P)_3Cl_2ReNMoCl_4(CNMe)$ [76]. Most of the Re≡N bond lengths were around 1.65 Å.

4.6.3 The Re-C≡N Bond

The X-ray crystal structure of $K_4Re(CN)_7.2H_2O$ showed that this complex contained a pentagonal bipyramidal anion, with $r(Re\text{-}C_{ax}) = 2.077(3)$ Å and $r(Re\text{-}C_{eq}) = 2.095(5)$ Å, $r(C\equiv N) = 1.161(5)$ Å. The structure of $K_3ReO_2(CN)_4$ has been determined by both X-ray [87] and neutron diffraction [69] and shown to contain cyanide rather than isocyanide ligand. A recent study on the structure of $NEt_4[ReO(H_2O)(CN)_4]\cdot 2H_2O$ revealed its anion had a distorted octahedral geometry with the Re atom displaced by 0.30Å out of the plane formed by the 4 C atoms of the cyano ligands, towards the oxo ligand. The structure of $[Pt(NH_3)_4]_2Re_2O_3(CN)_8$ and its vibrational spectrum, and recent studies on the structure of $K_3Na[Re_2O_3(CN)_8]\cdot 2H_2O$, $(PPh_4)_3[ReN(CN)_5]\cdot 7H_2O$, and $Cs_2Na[ReN(N_3)(CN)_4]$ were also in agreement with a cyanide compound.

In contrast to these reported structures, the structure of "$K_2[ReN(NC)_4](H_2O)$" [64] was reported to have the C≡N bond distance 1.31 Å, that was significantly longer than the usual 1.13-1.16 Å for cyanide complexes, and the Re≡N bond 1.53 Å, which was shorter than those in other compounds. It was reported that the cyanide ligands were coordinated through the nitrogen atoms. The structure was not reliable, however. The 300 diffraction data collected with use of Cu-Kα radiation, were used without absorption correction, and were estimated visually. Therefore, the data were not sufficient or precise

enough to say that the cyanide ligands were bound through the carbon atoms.

Table 4.3 Comparison of the Re-C and C≡N Bond Lengths in Some Rhenium Cyanide-complexes (Å)

	Re-C	C≡N	Ref.
$K_4Re(CN)_7 \cdot 2H_2O$	2.077(3), 2.095(5)	1.161(5)	[88]
$K_3ReO_2(CN)_4$	2.139(3), 2.130(3)	1.155(5)	[69]
$K_3ReO_2(CN)_4$	2.115(7), 2.132(6)	1.156(8)	[87]
$[Pt(NH_3)_4]_2Re_2O_3(CN)_8$	2.124(7), 2.115(7)	1.134(9)	[89]
$K_3Na[Re_2O_3(CN)_6] \cdot 2H_2O$	2.119(8)	1.136(12)	[90]
$Et_4[ReO(H_2O)(CN)_4] \cdot 2H_2O$	2.11(1)	1.14(1)	[91]
$Cs_2Na[ReN(N_3)(CN)_4]$	2.11(1)	1.13(2)	[85]
$(PPh_4)_3[ReN(CN)_5] \cdot 7H_2O$	2.12(1)	1.13(2)	[86]
$(AsPh_4)_2[ReN(CN)_4(H_2O)] \cdot 5H_2O$	2.105(5)	1.149(6)	this work

The results of this work revealed a possible difference in space group. Indirect evidence obtained from the IR spectroscopy and the comparison with related compounds showed that the cyanide ligands in $K_2[ReN(CN)_4] \cdot H_2O$ were carbon-bound. All the compounds, $(AsPh_4)_2[ReN(CN)_4(H_2O)] \cdot 5H_2O$, which was isomporphous with the technetium analogue, $(PPh_4)_3[ReN(CN)_5] \cdot 7H_2O$ and $Cs_2Na[ReN(N_3)(CN)_4]$, contained carbon-bound cyanide groups. All the above evidence suggested that the work by Davies

et al. [64] was incorrect.

The cell parameters of $K_2[ReN(CN)_4]\cdot H_2O$ obtained in this study were: a 15.175(1) Å, b 8.122(1) Å, c 4.003(1) Å (Mo-Kα radiation); or a 15.136(3) Å, b 8.153(2) Å, c 4.008(1) Å (Ag-Kα radiation), which are very close to those reported (15.27 Å, 8.16 Å, 3.97 Å, Cu-Kα radiation) [64]. The chain structure was also found in this study, and since the Re...Re chain was along the shortest axis, the Re...Re separation was about 4.003 to 4.008 Å.

Although it has not been shown directly that the cyanide group in $K_2[ReN(CN)_4]\cdot H_2O$ is bound to the rhenium atom through the carbon atom, the other evidence suggests this is so. Thus we are not far from a final clarification of this stubborn problem.

4.7 Summary and Suggested Future Work

When the automatic cell search routines of the diffractometer were applied to a crystal with pseudosymmetry, that caused all the reflections of odd l to be much weaker than those of even l, it is possible that the procedure could fail to find any of the weak l reflections by a rapid search. The consequence would be a cell axis (c in this case) with half its true length, loss of half the intensity data, and conversion of the pseudosymmetry into a required symmetry in the resulting model. In the case of $K_2[ReN(CN)_4]\cdot H_2O$ (**4A**), there seems no compulsive reason to orient all of the "...N≡Re...N≡Re..." chain in the same direction along c axis (which is required by a body centred lattice). Half of the chains may be arranged in the opposite direction as "...Re≡N...Re≡N..." along the c axis.

This problem should be studied if it is possible to obtain better quality crystals of this compound in the future. The determination of structure of this compound was not a trivial problem, as shown by the mistakes of previous researchers. One useful tool to avoid mistakes, perhaps, is the willingness to accept the possibility that first choice made by the machine may be wrong.

Other precautions which may increase the possibility of conquering this problem include: (1) try to grow larger good quality crystals; (2) use much slower scan speeds; (3) collect the data in a primitive cell, rather than a body centred cell; (4) use a more intense X-ray source; (5) maintain the crystal at near liquid nitrogen temperature in the data collecting process. These practices will increase the signal to noise ratio, increase crystal stability in the X-ray beam to ensure that the same material is present for the entire data collection, and reduce those structural ambiguities associated with atomic motion.

CHAPTER 5

SYNTHESIS AND CHARACTERIZATION OF RHENIUM AND TECHNETIUM COMPOUNDS WITH PYRAZOLYL LIGANDS

5.1 Introduction

Technetium (^{99m}Tc, γ, 140Kev, $t_{\frac{1}{2}}$ = 6h) radiopharmaceuticals are widely used in diagnostic nuclear medicine around the world. For therapeutic purposes, the β^- emitting nuclides ^{186}Re ($t_{\frac{1}{2}}$ = 90h) and ^{188}Re ($t_{\frac{1}{2}}$ = 17h) are optimal candidates [92]. Many important biochemicals and drugs are predominantly lipophilic, so the investigation of lipophilic technetium or rhenium complexes is of major interest.

Complexes that contain the pyrazolyl ligand (Pz') have proved to be lipophilic. Several biochemical model complexes that contain the hydridotris(1-pyrazolyl)borato ligand have been studied. For example, the O_2 binding and activation model compound $(HBPz'_3)Co(O_2)$ [93], the O_2 binding compound that models haemocyanin (copper protein), $[(HBPz'_3)Cu]_2(O_2)$ [94], the model compound for the binuclear iron centre of hemerythin, $[(HBPz_3)Fe(O_2CMe)]_2(O)$ [95], the model compound for the O_2 binding sites of non-heme iron proteins $(HBPz'_3)Fe(OBz)(NCMe)$ [96], and the zinc enzyme carbonic anhydrase model compound $(HBPz'_3)Zn(OH)$ [97], have been studied in recent years.

As part of this research on the development of new radiopharmaceuticals, new oxorhenate(V) compounds with pyrazole-containing ligands, $ReO(HBPz_3)(NCS)_2$ **(5A)**, $ReO(HBPz_3)(PzOCMe_2)\cdot ReO_4$ **(5B)**, $ReOCl_2(PPh_3)(PzOCMe_2)$ **(5C)**, $ReOCl_2(PPh_3)(PzOCHMe)\cdot 0.5CHOCHO$ **(5D)**, $Re_2O_3Cl_2(PPh_3)_2(Pz)_2\cdot CHCl_3$ **(5E)**, $Re_2O_3Cl_2(3,5\text{-}Me_2\text{-}Pz)_2(3,5\text{-}Me_2\text{-}HPz)_2$ **(5F)** were prepared and characterized. The investigations were also extended to the new oxorhenate(V) compound $[ReOCl_2(PPh_3)L]\cdot 2H_2O$ **(5G)**, and a technetium compound, $[TcOL_2(HL)]TcO_4$ **(5H)**, where HL is an imidazole derivative, 4-hydroxymethyl-1,5-dimethyl-imidazole ($4\text{-}HOCH_2\text{-}1,5\text{-}Me_2\text{-}Im$).

5.2 Preparations

5.2.1 $ReO(HBPz_3)(NCS)_2$ (5A)

A mixture of $ReO(HBPz_3)Cl_2$ (200 mg, 0.414 mmol, in 40 mL acetone) and KNCS (81 mg, 0.834 mmol, in 1 mL water) was stirred at room temperature under N_2 for one day, until the colour of the solution changed from blue to green. The white precipitate of KCl was filtered off. The remaining solution was evaporated to obtain the product **5A** (190 mg, in 85% yield). Green crystals of **5A** were obtained by recrystallization from hot toluene, as rectangular plates. Mass spectrum (DEI): m/e = 532 ($[ReO(HBPz_3)(NCS)_2]^+$), 474 ($[ReO(HBPz_3)(NCS)]^+$), 406 ($[ReO(HBPz_2)(NCS)]^+$). Electronic spectra in acetone, λ_{max1} = 726 nm, ε=1.7X10^2 L mol^{-1} cm^{-1}, λ_{max2} = 366 nm, ε=1.3X10^3 L mol^{-1} cm^{-1}. ^{1}H NMR (acetone-d_6, ppm): 8.38 (d, 2H, $^3J_{HH}$ = 2.4 Hz), 8.35 (d, 1H, $^3J_{HH}$ = 2.4 Hz), 7.86 (d, 2H, $^3J_{HH}$ = 2.2 Hz), 7.69 (d, 1H, $^3J_{HH}$ = 2.2 Hz), 6.83 (t, 2H, $^3J_{HH}$ = 2.5 Hz), 6.32 (t,

1H, $^3J_{HH}$ = 2.3 Hz). IR (cm^{-1}, KBr disk): 3141 w, 3117 m, 2525 (m, B-H); 2059 (vs, C=N), 2025 (vs, C=N), 1505 m, 1444 w, 1417 m, 1405 vs, 1389 m, 1314 s, 1309 s, 1213 s, 1189 m, 1182 m, 1126 m, 1120 m, 1079 m, 1054 vs, 999 m, 982 (vs Re=O), 916 w, 813 m, 790 m, 768 vs, 721 w, 709 m, 671 w, 648 m, 645 m, 615 s, 612 s, 466 m, 456 m, 373 m, 355 m, 329 m, 321 m.

5.2.2 $[ReO(HBPz_3)(Pz\text{-}(CO)Me_2)][ReO_4]$ (5B)

A mixture of $ReO(HBPz_3)Cl_2$ (216 mg, 0.447 mmol, in 40 mL acetone) and AgF (227 mg, 1.789 mmol, in 1 mL water) was stirred in a 80 mL plastic bottle at room temperature for three days. A silver mirror was seen on the wall of the bottle. The precipitated AgCl was filtered off. The remaining solution was evaporated to obtain the product, **5B** (160 mg, in 90% yield). Violet, shiny crystals of **5B** were obtained by slow evaporation of a solution in acetone:toluene = 3:1, V:V. Mass spectrum (FAB): m/e = 541 ($[ReO(HBPz_3)(Pz\text{-}(CO)Me_2)]^+$), 483 ($[ReO(HBPz_3)(Pz)]^+$), 415 ($[ReO(HBPz_3)]^+$). Electronic spectra in acetone, λ_{max1}=426 nm, ε=2.9X10^2 L mol^{-1} cm^{-1}, λ_{max2} = 326 nm, ε=7.6X10^2 L mol^{-1} cm^{-1}. ^{1}H NMR (acetone-d_6, ppm): 9.26 (d, 1H, $^3J_{HH}$ = 2.6 Hz), 8.66 (d, 1H, $^3J_{HH}$ = 2.4 Hz), 8.59 (d, 1H, $^3J_{HH}$ = 2.4 Hz), 8.49 (d, 2H, $^3J_{HH}$ = 2.6 Hz), 8.33 (d, 1H, $^3J_{HH}$ = 2.6 Hz), 7.81 (d, 1H, $^3J_{HH}$ = 2.4 Hz), 7.36 (t, 1H, $^3J_{HH}$ = 2.6 Hz), 6.85 (t, 1H, $^3J_{HH}$ = 2.4 Hz), 6.77 (t, 1H, $^3J_{HH}$ = 2.4 Hz), 6.43 (d, 1H, $^3J_{HH}$ = 2.2 Hz), 6.05 (t, 1H, $^3J_{HH}$ = 2.3 Hz), 2.39 (s, 3H), 1.90 (s, 3H). IR (cm^{-1}, KBr disk): 3459 vs(b), 3419 vs(b), 3139-3117-3089 vs(b), 2994 m, 2927 m, 2552 m, 2529 m, 1660 w, 1637 w, 1623 w, 1509 m, 1504 m, 1443 m, 1437 w, 1410 vs, 1391 s, 1386 s, 1374 m, 1328 m, 1312 s, 1239 m, 1221 s, 1214 s, 1191 m, 1180 m, 1164 vs, 1129 s, 1118 vs, 1109 s, 1084 vs, 1057 vs, 1041 s, 998

m, 987 (vs, Re=O); 970, 932, 920, 912 (all vs, ReO_4^-); 855 m, 803 m, 784 vs, 743 w, 725 w, 716 s, 689 w, 674 w, 649 m, 624 m, 613 s, 558 m, 522 m, 450 w, 477 w, 458 w, 314 s, 300 s.

5.2.3 $ReOCl_2(PPh_3)(pz\text{-}COMe_2)$ (5C)

Pyrazole (25 mg, 0.37 mmol) was added to 155 mg (0.19 mmol) $ReOCl_3(PPh_3)_2$ in acetone (30 mL) in a 100 mL round flask under nitrogen and stirred at room temperature overnight. All the material dissolved and a green solution was obtained which gradually turned dark blue. The solution was allowed to evaporate slowly at room temperature for two days. Diamond shaped dark blue crystals of 5C were obtained (100 mg, in 80% yield). The crystals are soluble in acetone and chloroform. Mass spectrum (FAB): m/e = 660 ($[ReOCl_2(PPh_3)(pz\text{-}COMe_2)]^+$), 625 ($[ReOCl(PPh_3)(pz\text{-}COMe_2)]^+$), 605 ($[ReOCl_2(PPh_3)(Hpz)]^+$), 567 ($[ReOCl(PPh_3)(pz)]^+$). ^1H NMR ($CDCl_3$, ppm): 7.49-7.35 (complex, 15H), 7.08 (d, 1H, $^3J_{HH}$ = 1.7 Hz), 7.01 (d, 1H, $^3J_{HH}$ = 2.5 Hz), 6.55 (t, 1H, $^3J_{HH}$ = 2.4 Hz), 1.63 (s, 3H), 0.88 (s, 3H). IR (cm^{-1}, KBr disk): 3447 s), 3136 w, 3127 s, 3117 s, 3080 w, 3077 w, 3066 w, 3055 w, 3046 w, 2996 w, 2989 w, 2983 w, 2932 w, 1611 w, 1508 w, 1483 w, 1435 vs, 1404 s, 1388 s, 1368 s, 1350 s, 1259 vs, 1215 s, 1207 s, 1195 vs, 1157 s, 1098 vs, 1077 s, 1012 vs, 999 s, 973 w, 954 (vs, Re=O); 925 s, 891 w, 863 vs, 845 w, 770 vs, 761 vs, 744 vs, 709 s, 698 vs, 688 s, 666 s, 648 s, 616 s, 555 s, 529 vs, 521 s, 510 vs, 500 s, 429 s, 335 s.

5.2.4 $ReOCl_2(PPh_3)(pz\text{-}COHMe)\cdot 0.5CHOCHO$ (5D)

Pyrazole (45 mg, 0.66 mmol) was added to 137 mg (0.16 mmol) $ReOCl_3(PPh_3)_2$ in acetaldehyde (36 mL) in a 100 mL round flask under nitrogen and stirred at room

temperature for six hours. The solution turned blue in 10 minutes, and all the material dissolved. The solution was allowed to evaporate slowly at room temperature for two days. Plate shaped violet-blue crystals were obtained (70 mg, in 60% yield). The crystals of **5D** are soluble in acetone and chloroform. ^{1}H NMR (acetone-d_6, ppm): 7.52-7.38 (complex, 15H), 7.34 (d, 1H, $^3J_{HH}$ = 2.6 Hz), 7.13 (d, 1H, $^3J_{HH}$ = 2.3 Hz), 6.56 (t, 1H, $^3J_{HH}$ = 2.4 Hz), 5.13-5.01 (complex, 1H), 1.34 (d, 1H, $^3J_{HH}$ = 5.6 Hz), 1.18 (d, 1H, $^3J_{HH}$ = 5.2 Hz), 1.01 (d, 1H, $^3J_{HH}$ = 5.6 Hz). IR (cm^{-1}, KBr disk): 3418 s, 3119 s, 3053 w, 2981 w, 2934 w, 1725 (s, C=O); 1482 w, 1435 vs, 1414 s, 1403 s, 1387 s, 1370 s, 1349 s, 1258 vs, 1210 s, 1186 vs, 1152 s, 1098 vs, 1075 s, 1014 vs, 998 s, 982 (vs, Re=O); 928 s, 924 s, 863 w, 749 vs, 746 vs, 711 vs, 695 vs, 661 s, 620 s, 617 s, 553 s, 531 vs, 506 s, 450 s.

5.2.5 $[ReOCl(PPh_3)]_2(\mu\text{-}O)(\mu\text{-}pz)_2 \cdot CHCl_3$ (5E)

Two methods were found to work equally well in the production of **5E**. (a) 28 mg (0.41 mmol) of pyrazole were added to 85 mg (0.10 mmol) $ReOCl_3(PPh_3)_2$ in CS_2 (30 mL) and THF (1 mL) in a 100 mL round flask under nitrogen and stirred at room temperature overnight. A dark green solution was generated in about 1 hour. The solution was allowed to evaporate at room temperature to give a green solid. The solid was recrystallized from a 1:1 (v/v) mixture of MeOH and $CHCl_3$ to give green, needle shaped crystals of **5E** (53 mg, in about 80% yield).

(b) 36 mg (0.53 mmol) of pyrazole were added to 110 mg (0.13 mmol) of $ReOCl_3(PPh_3)_2$ in 30 mL of MeCOEt and the same procedures and gave 60 mg of **5E** (70% yield). The green solid was very soluble in $CHCl_3$ and less soluble in MeOH. Mass

spectrum (FAB): m/e = 1150 ([{$ReOCl(PPh_3)$}$_2$(μ-O)(μ-pz)$_2$]$^+$), 1085 ([{$ReOCl(PPh_3)$}$_2$(μ-OH)(μ-Hpz)]$^+$), 888 ([{$ReOCl$}$_2$(PPh_3)(μ-O)(pz)$_2$]$^+$), 567 ([$ReOCl(PPh_3)$(pz)]$^+$), 551 ([$ReCl(PPh_3)$(pz)]$^+$). Mass spectrum (DEI): m/e = 1150, 888, 820 ([{$ReOCl$}$_2$(PPh_3)(μ-O)(pz)]$^+$). ^{1}H NMR ($CDCl_3$, ppm): 7.40-7.15 (complex, 32H), 6.68 (s, 2H), 6.65 (s, 2H). IR (cm^{-1}, KBr disk): 3420 s(b), 3054 m, 2930 w, 1620 w(b), 1483 s, 1435 vs, 1386 s, 1334 w, 1315 w, 1288 m, 1261 m, 1188 m, 1166 m, 1125 m, 1097 s, 1074 m, 1055 vs, 1028 m, 999 m, 961 (vs Re=O), 957 (vs Re=O), 805 m(b), 765 m, 744 vs, 708 s, 692 vs, 670 m, 636 s, 623 vs, 615 vs, 531 s, 525 vs, 509 s, 498 s, 430 m(b), 313 m.

5.2.6 [ReOCl(3,5-Me_2-HPz)]$_2$(μ-O)(μ-3,5-Me_2-Pz)$_2$ (5F)

3,5-dimethyl-pyrazole (150 mg, 1.56 mmol) was added to (123 mg, 0.148 mmol) $ReOCl_3(PPh_3)_2$ in acetonitrile (30 mL) in a 100 mL round flask under nitrogen and stirred at reflux temperature for two hours. All the material dissolved and a dark green solution was obtained. The solution was allowed to evaporate slowly at room temperature for two days to dryness. Chloroform was added to extract the solid sample and give a clear green solution. Plate shaped green crystals were obtained on slow evaporation (40 mg, in 60% yield). The crystals are soluble in acetone and chloroform. Mass spectrum (DEI): m/e = 872 ([{$ReOCl$}$_2$(μ-O)(3,5-Me_2-Pz)$_4$]$^+$), 838 ([{ReO}$_2$Cl(3,5-Me_2-HPz)$_2$(μ-O)(3,5-Me_2-Pz)$_2$]$^+$), 777 ([{$ReOCl$}$_2$(3,5-Me_2-Pz)$_3$(μ-O)]$^+$), 742 ([{ReO}$_2$Cl(3,5-Me_2-Pz)$_3$(μ-O)]$^+$), 682 ([{$ReOCl$}$_2$(3,5-Me_2-Pz)$_2$(μ-O)]$^+$), 611 ([{ReO}$_2$(3,5-Me_2-Pz)$_2$(μ-O)]$^+$). ^{1}H NMR ($CDCl_3$, ppm): 9.89 (s, 2H), 6.01 (s, 2H), 5.82 (s, 2H), 2.79 (s, 6H), 2.70 (s, 6H), 2.42 (s, 6H), 2.28 (s, 6H). IR (cm^{-1}, KBr disk): 3296 (vs, broad, N-H), 3146 w, 3114 w, 2964 w, 2927 m, 2856 w, 1569 s, 1531 s, 1475 m, 1437 m, 1415 s, 1381 m, 1374 m, 1348 m, 1291 s,

1180 m, 1152 s, 1118 w, 1053 s, 1028 m, 986 m, 958 (vs, Re=O), 837 w, 818 w, 795 m, 782 m, 766 w, 760 w, 749 m, 720 m, 694 m, 669 s, 653 s, 634 vs, 609 vs, 591 s, 543 s, 504 m, 490 m, 446 m, 300 s.

5.2.7 $ReOCl_2(PPh_3)(4\text{-}CH_2O\text{-}1,5\text{-}Me_2\text{-}Im)\cdot 2H_2O$ (5G)

$ReOCl_3(PPh_3)_2$ (96 mg, 116 mmol) was mixed with 4-hydoxymethyl-1,5-dimethyl-Imidazole (27 mg 0.214 mmol) in chloroform (30 mL) in a 100 mL round flask under nitrogen and stirred at room temperature for two hours. All the material dissolved in ten minutes, and a dark blue solution was obtained. The solution was allowed to evaporate slowly at room temperature for two days to dryness. Chloroform (20 mL) was added to dissolve the solid sample and then 10 mL cyclohexane was added to the top of the solution. Needle shaped tiny blue crystals were obtained (73 mg, in about 80% yield). Some of the crystals were redissolved in chloroform and a few drops of water to obtain big plate shaped crystals, which were used for the X-ray study. Electronic spectra in acetone, λ_{max1} = 566 nm, $\varepsilon = 5.2X10^1$ L mol^{-1} cm^{-1}, λ_{max2} = 330 nm, $\varepsilon = 1.0X10^3$ L mol^{-1} cm^{-1}. ^1H NMR (acetone-d_6, ppm): 7.69-7.48 (complex, 15H), 7.15 (s, 1H), 4.24 (d, 1H, $^2J_{HH}$ = 16.0 Hz), 4.12 (d, 1H, $^2J_{HH}$ = 16.7 Hz), 3.76 (s, 3H), 1.92 (s, 3H). IR (cm^{-1}, KBr disk): 3342 m(b), 3141 w, 3119 w, 3055 m, 3029 w, 2979 m, 2921 w, 2885 w, 2846 m, 2804 w, 2755 w, 1630 m, 1586 w, 1572 w, 1562 w, 1523 s, 1483 s, 1449 m, 1436 s, 1389 w, 1379 w, 1342 w, 1316 w, 1281 w, 1231 m, 1189 m, 11[illegible] s, 1143 w, 1113 m, 1095 s, 1063 m, 1045 s, 1022 m, 998 m, 981 w, 948 (vs, Re=O), 909 w, 846 w, 788 m, 751 s, 745 s, 709 s, 695 s, 664 m, 625 m, 545 s, 531 s, 512 vs, 496 m, 453 w, 441 w, 417 w, 320 m.

5.2.8 $[TcO(4\text{-}OCH_2\text{-}1,5\text{-}Me_2\text{-}Im)_2(4\text{-}HOCH_2\text{-}1,5\text{-}Me_2\text{-}Im)]TcO_4$ (5H)

A mixture of 40 mg of $[(n\text{-}Bu)_4N][TcOCl_4]$ (0.08 mmol) and 41 mg of 4-hydoxymethyl-1,5-dimethyl-Imidazole (0.328 mmol) of acetone (15 mL) was stirred at room temperature. The solution turned green in 20 minutes. The solvent was allowed to evaporate at room temperature to dryness. Plate shaped green crystals were obtained (21 mg, in 80% yield) from recrystallization in EtOH. Mass spectrum (ES): m/e = 365 $[TcO(4\text{-}OCH_2\text{-}1,5\text{-}Me_2\text{-}Im)_2]^+$. ^1H NMR ($CDCl_3$, ppm): 8.08 (s, 1H), 7.92 (s, 1H), 7.53 (s, 1H), 5.75 (d, 2H, $^2J_{HH}$ = 6.64 Hz), 5.66 (t, 1H, $^2J_{HH}$ = 6.97 Hz), 4.55 (d of d, 2H, $^2J_{HH}$ = 6.87 Hz, $^3J_{HH}$ = 2.63 Hz), 4.27 (d, 2H, $^2J_{HH}$ = 4.49 Hz), 3.87 (s, 3H), 3.71 (s, 3H), 3.63 (s, 3H), 2.28 (s, 3H), 2.26 (s, 3H), 2.17 (s, 3H). IR (cm^{-1}, KBr disk): 3268 (s, broad, OH), 3139 m, 3130 m, 3110 s, 3014 w, 2965 m, 2920 m, 2881 m, 2840 s, 1620 s(b), 1519 vs, 1484 s, 1451 vs, 1433 s, 1419 s, 1390 m, 1377 m, 1343 m, 1335 s, 1226 s(b), 1207 m, 1167 vs, 1151 vs, 1118 s, 1081 m, 1069 m, 1057 vs, 1022 vs, 1002 vs, 980 m, 927 (vs, Tc=O), 910, 904, 896, 885 (all vs, TcO_4^-), 832 m, 818 w, 796 s, 766 m, 760 m, 744 s, 691 w, 673 w, 667 m, 642 s, 633 s, 602 w, 566 vs, 536 s, 495 vs, 438 m, 425 m, 411 w.

5.3 Spectroscopic Measurements

Mass spectrometric data, electronic spectroscopic data, NMR and IR spectroscopic data are listed in the appropriate preparation section for compounds **5A** to **5H.**

The ^1H NMR spectrum of **5A** was obtained for an acetone-d_6 solution of **5A** on an AC-200 in 128 scans at a spectral width of 2.5 kHz (16K, 0.305 Hz/data point, 3.277

s acquisition time). The ^{1}H NMR spectrum of **5B** was obtained for an acetone-d_6 solution of **5B** on an AC-200 in 32 scans at a spectral width of 2.4kHz (16K, 0.293 Hz/data point, 3.408s acquisition time). The ^{1}H NMR spectrum of **5C** was obtained for a $CDCl_3$ solution of **5C** on an AC-200 in 128 scans at a spectral width of 2.4 kHz (16K, 0.293 Hz/data point, 3.408 s acquisition time). The ^{1}H NMR spectrum of **5D** was obtained for an acetone-d_6 solution of **5D** on an AC-200 in 32 scans at a spectral width of 2.4kHz (16K, 0.293 Hz/data point, 3.408s acquisition time). The ^{1}H NMR spectrum of **5E** was obtained for a $CDCl_3$ solution of **5E** on an AC-200 in 256 scans at a spectral width of 2.4 kHz (16K, 0.293 Hz/data point, 3.408 s acquisition time). The ^{1}H NMR spectrum of **5F** was obtained for a $CDCl_3$ solution of **5F** on an AC-200 in 128 scans at a spectral width of 2.4 kHz (16K, 0.293 Hz/data point, 3.408 s acquisition time). The ^{1}H NMR spectrum of **5G** was obtained for an acetone-d_6 solution of **5G** on an AC-200 in 128 scans at a spectral width of 2.4kHz (16K, 0.293 Hz/data point, 3.408s acquisition time). The ^{1}H NMR spectrum of **5H** was obtained for a $CDCl_3$ solution of **5H** on an AC-200 in 256 scans at a spectral width of 2.4 kHz (16K, 0.293 Hz/data point, 3.408 s acquisition time). All chemical shifts are expressed in ppm downfield from TMS.

The proton COSY 2-D NMR spectrum of **5B** was recorded in the absolute value mode by use of the pulse sequence 90°-t_1-90°-ACQ on a Bruker AM-500 spectrometer (500.135 MHz, 5 mm dual frequency ^{1}H - ^{13}C probe) and the same sample of **5B** used for the 1-D spectrum. The spectrum was acquired over the aromatic region at a spectral width of 2.841 kHz in 16 scans for each of the 256 FIDs that contained 2K data points in F2. The ^{1}H 90° pulse width was 18.6 μs. A 2.0 s relaxation delay was employed

between acquisitions. Zero-filling in F1 produced a 1K X 1K data matrix with a digital resolution of 2.774 Hz/data point in both dimensions. For the 2-D Fourier transformation a sine-bell squared window function was applied to both dimensions. The transformed data were then symmetrized.

5.4 X-ray Structure Determinations

Crystallographic details for **5B**, **5C**, **5D**, **5E**, **5F**, **5G** and **5H** are summarized in the Appendix Table 5.1. Atom coordinates and temperature factors for compounds **5B**, **5C**, **5D**, **5E**, **5F**, **5G** and **5H** are listed in the Appendix Table **5B**.2, **5C**.2, **5D**.2, **5E**.2, **5F**.2, **5G**.2 and **5H**.2, respectively. Bond lengths and angles for compounds **5B**, **5C**, **5D**, **5E**, **5F**, **5G** and **5H** are listed in Table **5B**.1, **5C**.1, **5D**.1, **5E**.1, **5F**.1, **5G**.1 and **5H**.1 respectively. Structures for compound **5B**, **5C**, **5D**, **5E**, **5F**, **5G** and **5H** are shown in Figure **5B**.1, **5C**.1, **5D**.1, **5E**.1, **5F**.1, **5G**.1 and **5H**.1, respectively. Anisotropic thermal parameters, structure factors, and hydrogen positions for compounds **5B**, **5C**, **5D**, **5E**, **5F**, **5G** and **5H** were deposited on magnetic disks. There were disorders in the ReO_4^- anion of **5B**. The final refinement was obtained by a constraint of Re(2)-O(n) = 1.70(3) (n = 1, 2, 3, 4) and a tetrahedral geometry for ReO_4^-. Since **5B** had a chiral space group, $P2_12_12_1$, the absolute structure of **5B** was also obtained by comparing the refinement results for the two mirror models (R 6.27%, wR 5.82%, *vs* R 6.27%, wR 5.69%).

In the structure of **5D**, one solvate molecule of CHOCHO was shared by two $ReOCl_2(PPh_3)$(pz-COHMe) units. The temperature factors of the solvate CHOCHO were higher than others because of less constraint in the lattice. C(7) also had a much higher

temperature factor, that indicated large thermal motion.

There were also disorders in the lattice solvate $CHCl_3$ of **5E**. The structure of **5E** was refined with the constraint of C(1)-Cl(n) and C(2)-Cl(nA) = 1.72(1) Å (n = 3, 4, 5) in solvate $CHCl_3$, and the sum of occupancy factors of related atoms was fixed at 1 (0.5217 + 0.4783).

Table 5B.1.

Bond Lengths (Å) and Bond Angles (°)

for $[ReO(HBPz_3)(Pz\text{-}(CO)Me_2)][ReO_4]$ (5B)

Re(1)-O	1.68 (1)	Re(1)-N(1A)	2.12 (2)
Re(1)-N(1B)	2.09 (2)	Re(1)-N(1C)	2.25 (2)
Re(1)-O(1D)	1.91 (1)	Re(1)-N(1D)	2.07 (2)
B-N(2A)	1.55 (3)	B-N(2B)	1.53 (3)
B-N(2C)	1.48 (3)	N(1A)-N(2A)	1.37 (2)
N(1A)-C(5A)	1.36 (3)	N(2A)-C(3A)	1.35 (3)
C(3A)-C(4A)	1.30 (4)	C(4A)-C(5A)	1.39 (4)
N(1B)-N(2B)	1.36 (2)	N(1B)-C(5B)	1.35 (2)
N(2B)-C(3B)	1.39 (2)	C(3B)-C(4B)	1.34 (3)
C(4B)-C(5B)	1.38 (3)	N(1C)-N(2C)	1.35 (2)
N(1C)-C(5C)	1.37 (3)	N(2C)-C(3C)	1.31 (3)
C(3C)-C(4C)	1.36 (3)	C(4C)-C(5C)	1.34 (3)

O(1D)-C(6D)	1.41 (2)	N(1D)-N(2D)	1.33 (2)
N(1D)-C(5D)	1.33 (3)	N(2D)-C(3D)	1.33 (3)
N(2D)-C(6D)	1.52 (3)	C(3D)-C(4D)	1.42 (3)
C(4D)-C(5D)	1.31 (4)	C(6D)-C(7D)	1.46 (3)
C(6D)-C(8D)	1.51 (3)	Re(2)-O(1)	1.73 (3)
Re(2)-O(2)	1.72 (2)	Re(2)-O(3)	1.69 (2)
Re(2)-O(4)	1.66 (3)		

O-Re(1)-N(1A)	89.2(6)	O-Re(1)-N(1B)	96.3(6)
N(1A)-Re(1)-N(1B)	89.0(6)	O-Re(1)-N(1C)	163.6(6)
N(1A)-Re(1)-N(1C)	74.5(6)	N(1B)-Re(1)-N(1C)	81.8(6)
O-Re(1)-O(1D)	107.4(6)	N(1A)-Re(1)-O(1D)	163.3(6)
N(1B)-Re(1)-O(1D)	87.4(6)	N(1C)-Re(1)-O(1D)	88.8(5)
O-Re(1)-N(1D)	102.0(7)	N(1A)-Re(1)-N(1D)	99.7(6)
N(1B)-Re(1)-N(1D)	159.8(6)	N(1C)-Re(1)-N(1D)	83.0(6)
O(1D)-Re(1)-N(1D)	79.0(6)	N(2A)-B-N(2B)	105(2)
N(2A)-B-N(2C)	106(2)	N(2B)-B-N(2C)	109(2)
Re(1)-N(1A)-N(2A)	120(1)	Re(1)-N(1A)-C(5A)	131(2)
N(2A)-N(1A)-C(5A)	109(2)	B-N(2A)-N(1A)	122(2)
B-N(2A)-C(3A)	132(2)	N(1A)-N(2A)-C(3A)	105(2)
N(2A)-C(3A)-C(4A)	113(2)	C(3A)-C(4A)-C(5A)	106(2)
N(1A)-C(5A)-C(4A)	108(2)	Re(1)-N(1B)-N(2B)	122(1)

Re(1)-N(1B)-C(5B)	129(1)	N(2B)-N(1B)-C(5B)	110(2)
B-N(2B)-N(1B)	121(2)	B-N(2B)-C(3B)	130(2)
N(1B)-N(2B)-C(3B)	107(2)	N(2B)-C(3B)-C(4B)	108(2)
C(3B)-C(4B)-C(5B)	109(2)	N(1B)-C(5B)-C(4B)	107(2)
Re(1)-N(1C)-N(2C)	120(1)	Re(1)-N(1C)-C(5C)	131(1)
N(2C)-N(1C)-C(5C)	107(2)	B-N(2C)-N(1C)	121(2)
B-N(2C)-C(3C)	133(2)	N(1C)-N(2C)-C(3C)	106(2)
N(2C)-C(3C)-C(4C)	113(2)	C(3C)-C(4C)-C(5C)	104(2)
N(1C)-C(5C)-C(4C)	110(2)	Re(1)-O(1D)-C(6D)	121(1)
Re(1)-N(1D)-N(2D)	113(1)	Re(1)-N(1D)-C(5D)	141(2)
N(2D)-N(1D)-C(5D)	106(2)	N(1D)-N(2D)-C(3D)	112(2)
N(1D)-N(2D)-C(6D)	118(2)	C(3D)-N(2D)-C(6D)	129(2)
N(2D)-C(3D)-C(4D)	104(2)	C(3D)-C(4D)-C(5D)	107(2)
N(1D)-C(5D)-C(4D)	111(2)	O(1D)-C(6D)-N(2D)	104(2)
O(1D)-C(6D)-C(7D)	109(2)	N(2D)-C(6D)-C(7D)	111(2)
O(1D)-C(6D)-C(8D)	109(2)	N(2D)-C(6D)-C(8D)	106(2)
C(7D)-C(6D)-C(8D)	117(2)	O(1)-Re(2)-O(2)	107(1)
O(1)-Re(2)-O(3)	107(2)	O(2)-Re(2)-O(3)	108.3(8)
O(1)-Re(2)-O(4)	111(2)	O(2)-Re(2)-O(4)	110(1)
O(3)-Re(2)-O(4)	113(1)		

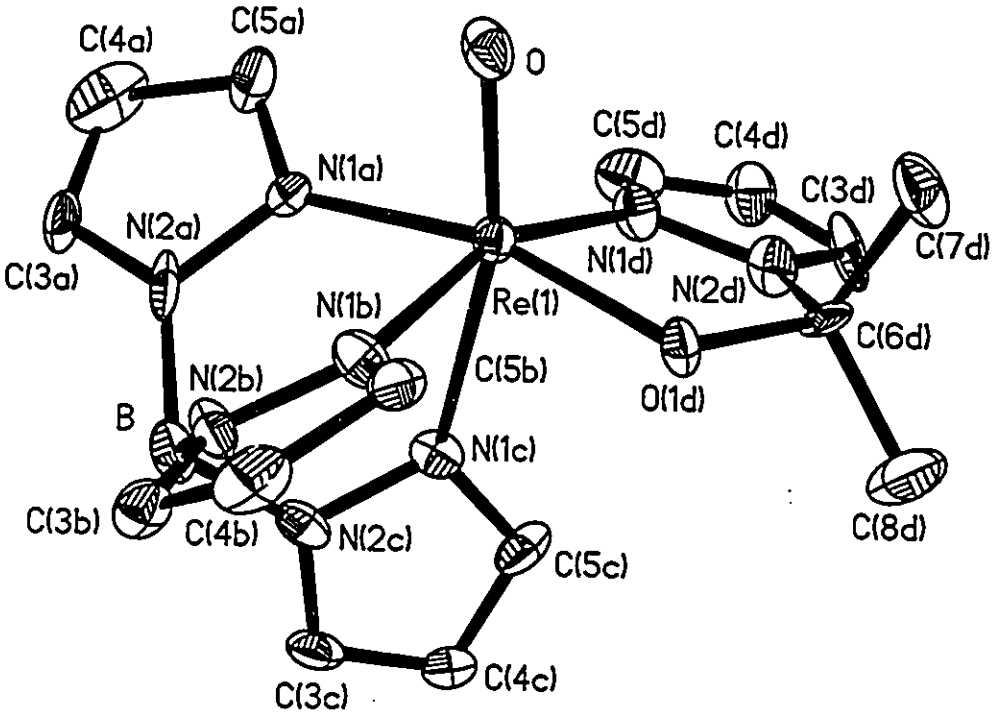

Fig. 5B.1 The Structure of $[ReO(HBPz_3)(Pz\text{-}(CO)Me_2)][ReO_4]$ (5B) Cation, Hydrogen Atoms are Omitted for Clarity

Table 5C.1. Bond Lengths (Å) and Bond Angles (°)

for $ReOCl_2(PPh_3)(pz\text{-}COMe_2)$ (5C)

Re-O(1)	1.696 (3)	Re-Cl(1)	2.432 (2)
Re-Cl(2)	2.342 (2)	Re-P	2.478 (1)
Re-O(2)	1.935 (3)	Re-N(1)	2.132 (5)
P-C(1A)	1.824 (5)	P-C(1B)	1.834 (6)
P-C(1C)	1.820 (5)	O(2)-C(6)	1.409 (7)
N(1)-N(2)	1.344 (6)	N(1)-C(5D)	1.335 (6)
N(2)-C(3D)	1.347 (8)	N(2)-C(6)	1.490 (6)
C(3D)-C(4D)	1.368 (8)	C(4D)-C(5D)	1.37 (1)
C(6)-C(7)	1.533 (8)	C(6)-C(8)	1.527 (9)
C(1A)-C(2A)	1.393 (9)	C(1A)-C(6A)	1.38 (1)
C(2A)-C(3A)	1.40 (1)	C(3A)-C(4A)	1.34 (2)
C(4A)-C(5A)	1.35 (1)	C(5A)-C(6A)	1.392 (9)
C(1B)-C(2B)	1.375 (8)	C(1B)-C(6B)	1.368 (8)
C(2B)-C(3B)	1.39 (1)	C(3B)-C(4B)	1.369 (8)
C(4B)-C(5B)	1.36 (1)	C(5B)-C(6B)	1.39 (1)
C(1C)-C(2C)	1.374 (7)	C(1C)-C(6C)	1.384 (7)
C(2C)-C(3C)	1.375 (8)	C(3C)-C(4C)	1.377 (9)
C(4C)-C(5C)	1.380 (9)	C(5C)-C(6C)	1.383 (8)

O(1)-Re-Cl(1)	93.8(1)	O(1)-Re-Cl(2)	105.9(1)
Cl(1)-Re-Cl(2)	88.4(1)	O(1)-Re-P	86.4(1)
Cl(1)-Re-P	176.2(1)	Cl(2)-Re-P	87.9(1)

O(1)-Re-O(2)	162.2(2)	Cl(1)-Re-O(2)	89.7(1)
Cl(2)-Re-O(2)	91.6(1)	P-Re-O(2)	91.3(1)
O(1)-Re-N(1)	87.7(2)	Cl(1)-Re-N(1)	88.9(1)
Cl(2)-Re-N(1)	166.3(1)	P-Re-N(1)	94.8(1)
O(2)-Re-N(1)	74.9(1)	Re-P-C(1A)	113.1(2)
Re-P-C(1B)	110.9(2)	C(1A)-P-C(1B)	105.1(3)
Re-P-C(1C)	117.3(2)	C(1A)-P-C(1C)	105.0(2)
C(1B)-P-C(1C)	104.4(3)	Re-O(2)-C(6)	127.3(3)
Re-N(1)-N(2)	115.0(3)	Re-N(1)-C(5D)	137.7(4)
N(2)-N(1)-C(5D)	107.4(5)	N(1)-N(2)-C(3D)	109.2(4)
N(1)-N(2)-C(6)	117.5(4)	C(3D)-N(2)-C(6)	132.7(5)
N(2)-C(3D)-C(4D)	107.8(6)	C(3D)-C(4D)-C(5D)	106.1(5)
N(1)-C(5D)-C(4D)	109.5(5)	O(2)-C(6)-N(2)	104.3(4)
O(2)-C(6)-C(7)	110.6(5)	N(2)-C(6)-C(7)	108.0(5)
O(2)-C(6)-C(8)	110.6(5)	N(2)-C(6)-C(8)	110.0(4)
C(7)-C(6)-C(8)	112.9(5)	P-C(1A)-C(2A)	122.5(5)
P-C(1A)-C(6A)	119.4(4)	C(2A)-C(1A)-C(6A)	118.1(5)
C(1A)-C(2A)-C(3A)	119.2(8)	C(2A)-C(3A)-C(4A)	121.6(8)
C(3A)-C(4A)-C(5A)	119.9(7)	C(4A)-C(5A)-C(6A)	120.5(9)
C(1A)-C(6A)-C(5A)	120.6(7)	P-C(1B)-C(2B)	121.3(4)
P-C(1B)-C(6B)	118.9(5)	C(2B)-C(1B)-C(6B)	119.8(6)
C(1B)-C(2B)-C(3B)	120.2(5)	C(2B)-C(3B)-C(4B)	119.4(6)
C(3B)-C(4B)-C(5B)	120.2(6)	C(4B)-C(5B)-C(6B)	120.5(6)
C(1B)-C(6B)-C(5B)	119.8(6)	P-C(1C)-C(2C)	121.0(4)
P-C(1C)-C(6C)	119.7(4)	C(2C)-C(1C)-C(6C)	119.2(5)

C(1C)-C(2C)-C(3C)	120.5(5)	C(2C)-C(3C)-C(4C)	120.3(5)
C(3C)-C(4C)-C(5C)	119.9(6)	C(4C)-C(5C)-C(6C)	119.4(6)
C(1C)-C(6C)-C(5C)	120.7(5)		

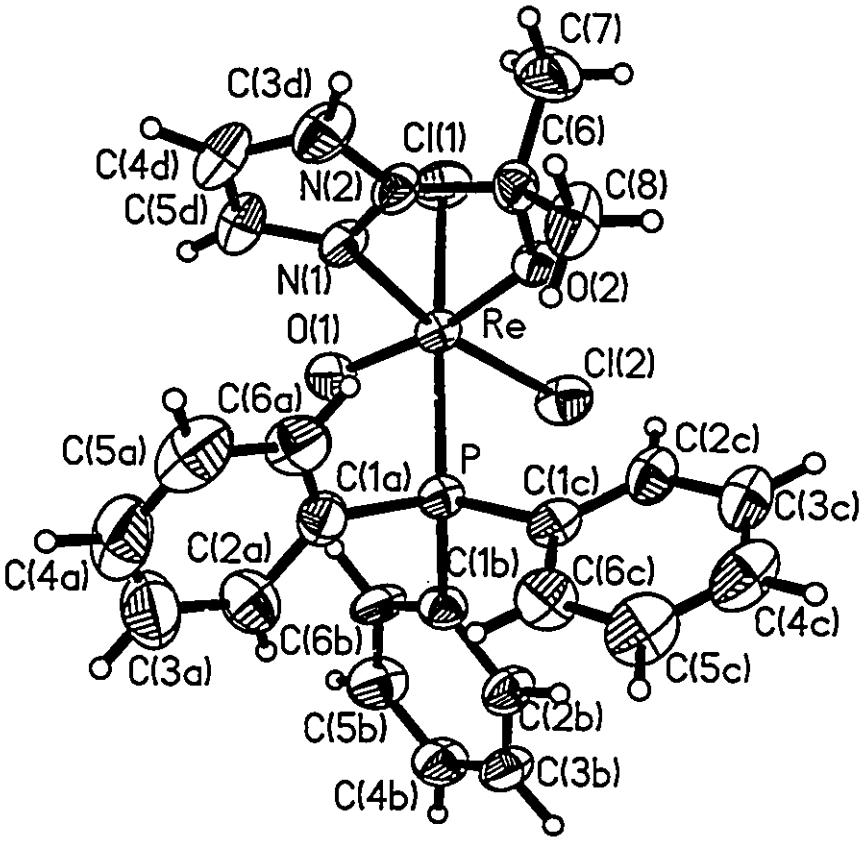

Fig. 5C.1. Structure of $ReOCl_2(PPh_3)(pz\text{-}COMe_2)$ (5C)

Table 5D.1. Bond Lengths (Å) and Bond Angles (°)

for $ReOCl_2(PPh_3)(pz\text{-}COHMe)\cdot 0.5CHOCHO$ (5D)

Re-Cl(1)	2.336 (3)	Re-Cl(2)	2.418 (4)
Re-P	2.462 (3)	Re-O(1)	1.66 (1)
Re-O(2)	1.931 (8)	Re-N(2)	2.16 (1)
P-C(11)	1.83 (1)	P-C(21)	1.82 (1)
P-C(31)	1.84 (1)	O(2)-C(6)	1.40 (2)
N(2)-N(1)	1.28 (2)	N(2)-C(3)	1.35 (2)
N(1)-C(5)	1.36 (2)	N(1)-C(6)	1.50 (2)
C(3)-C(4)	1.41 (3)	C(4)-C(5)	1.28 (3)
C(6)-C(7)	1.43 (3)	C(11)-C(12)	1.42 (2)
C(11)-C(16)	1.40 (2)	C(12)-C(13)	1.40 (2)
C(13)-C(14)	1.40 (3)	C(14)-C(15)	1.34 (2)
C(15)-C(16)	1.38 (2)	C(21)-C(22)	1.39 (2)
C(21)-C(26)	1.39 (2)	C(22)-C(23)	1.41 (2)
C(23)-C(24)	1.38 (2)	C(24)-C(25)	1.39 (2)
C(25)-C(26)	1.39 (2)	C(31)-C(32)	1.40 (2)
C(31)-C(36)	1.34 (2)	C(32)-C(33)	1.41 (2)
C(33)-C(34)	1.35 (3)	C(34)-C(35)	1.36 (3)
C(35)-C(36)	1.42 (2)	C(41)-O(41)	1.30 (5)
C(41)-C(41A)	1.53 (8)		

Cl(1)-Re-Cl(2)	89.0(1)	Cl(1)-Re-P	88.7(1)
Cl(2)-Re-P	168.6(1)	Cl(1)-Re-O(1)	100.9(4)

Cl(2)-Re-O(1)	97.0(3)	P-Re-O(1)	94.3(3)
Cl(1)-Re-O(2)	97.2(2)	Cl(2)-Re-O(2)	87.2(2)
P-Re-O(2)	82.0(2)	O(1)-Re-O(2)	161.5(4)
Cl(1)-Re-N(2)	169.2(3)	Cl(2)-Re-N(2)	85.9(3)
P-Re-N(2)	94.5(3)	O(1)-Re-N(2)	89.2(5)
O(2)-Re-N(2)	73.1(4)	Re-P-C(11)	112.5(4)
Re-P-C(21)	114.1(4)	C(11)-P-C(21)	104.7(6)
Re-P-C(31)	112.4(4)	C(11)-P-C(31)	105.8(6)
C(21)-P-C(31)	106.6(5)	Re-O(2)-C(6)	126.7(9)
Re-N(2)-N(1)	115.7(8)	Re-N(2)-C(3)	136(1)
N(1)-N(2)-C(3)	108(1)	N(2)-N(1)-C(5)	110(1)
N(2)-N(1)-C(6)	118(1)	C(5)-N(1)-C(6)	132(1)
N(2)-C(3)-C(4)	107(2)	C(3)-C(4)-C(5)	106(2)
N(1)-C(5)-C(4)	109(2)	O(2)-C(6)-N(1)	104(1)
O(2)-C(6)-C(7)	119(2)	N(1)-C(6)-C(7)	119(2)
P-C(11)-C(12)	116.9(9)	P-C(11)-C(16)	123(1)
C(12)-C(11)-C(16)	120(1)	C(11)-C(12)-C(13)	117(1)
C(12)-C(13)-C(14)	121(2)	C(13)-C(14)-C(15)	122(2)
C(14)-C(15)-C(16)	119(1)	C(11)-C(16)-C(15)	121(1)
P-C(21)-C(22)	120.5(9)	P-C(21)-C(26)	118.3(9)
C(22)-C(21)-C(26)	121(1)	C(21)-C(22)-C(23)	118(1)
C(22)-C(23)-C(24)	121(1)	C(23)-C(24)-C(25)	121(1)
C(24)-C(25)-C(26)	119(1)	C(21)-C(26)-C(25)	121(1)
P-C(31)-C(32)	120(1)	P-C(31)-C(36)	119(1)
C(32)-C(31)-C(36)	122(1)	C(31)-C(32)-C(33)	119(2)

C(32)-C(33)-C(34)	120(2)	C(33)-C(34)-C(35)	121(2)
C(34)-C(35)-C(36)	121(2)	C(31)-C(36)-C(35)	118(1)
O(41)-C(41)-C(41A)	96(4)		

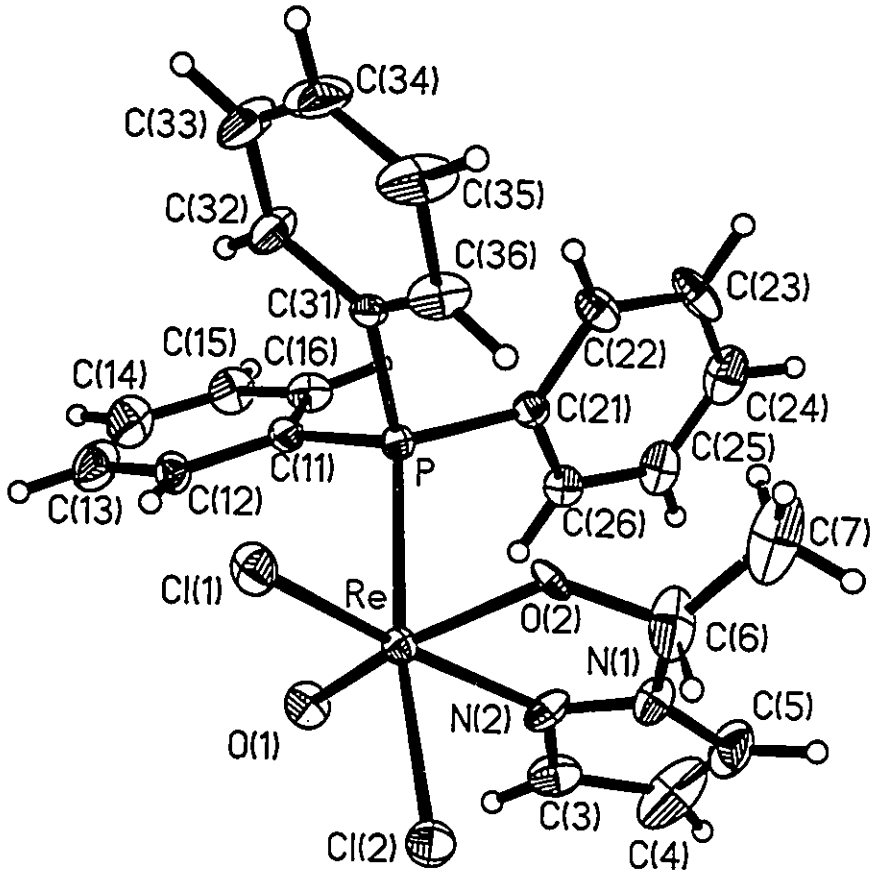

Fig. 5D.1. Structure of $ReOCl_2(PPh_3)(pz\text{-}COHMe)\cdot 0.5CHOCHO$ (5D)

(Solvent Molecule is Omitted)

Table 5E.1. Bond Lengths (Å) and Bond Angles (°)

for $[ReOCl(PPh_3)]_2(\mu\text{-}O)(\mu\text{-}pz)_2 \cdot CHCl_3$ (5E)

Re(1)-P(1)	2.451 (2)	Re(1)-Cl(1)	2.375 (2)
Re(1)-O(1)	1.694 (4)	Re(1)-O(3)	1.936 (3)
Re(1)-N(2G)	2.129 (5)	Re(1)-N(2H)	2.067 (5)
Re(2)-P(2)	2.467 (1)	Re(2)-Cl(2)	2.355 (2)
Re(2)-O(2)	1.696 (4)	Re(2)-O(3)	1.938 (3)
Re(2)-N(1G)	2.090 (4)	Re(2)-N(1H)	2.140 (5)
P(1)-C(1A)	1.814 (5)	P(1)-C(1B)	1.821 (6)
P(1)-C(1C)	1.820 (7)	P(2)-C(1D)	1.836 (5)
P(2)-C(1E)	1.818 (6)	P(2)-C(1F)	1.805 (7)
N(1G)-N(2G)	1.371 (6)	N(1G)-C(5G)	1.333 (8)
N(2G)-C(3G)	1.334 (7)	N(1H)-N(2H)	1.388 (6)
N(1H)-C(5H)	1.334 (8)	N(2H)-C(3H)	1.341 (9)
C(1A)-C(2A)	1.371 (9)	C(1A)-C(6A)	1.391 (9)
C(2A)-C(3A)	1.379 (9)	C(3A)-C(4A)	1.38 (1)
C(4A)-C(5A)	1.34 (1)	C(5A)-C(6A)	1.38 (1)
C(1B)-C(2B)	1.384 (8)	C(1B)-C(6B)	1.393 (7)

C(2B)-C(3B)	1.385 (8)	C(3B)-C(4B)	1.391 (9)
C(4B)-C(5B)	1.371 (9)	C(5B)-C(6B)	1.378 (9)
C(1C)-C(2C)	1.381 (7)	C(1C)-C(6C)	1.383 (9)
C(2C)-C(3C)	1.39 (1)	C(3C)-C(4C)	1.35 (1)
C(4C)-C(5C)	1.386 (9)	C(5C)-C(6C)	1.38 (1)
C(1D)-C(2D)	1.38 (1)	C(1D)-C(6D)	1.370 (9)
C(2D)-C(3D)	1.363 (9)	C(3D)-C(4D)	1.37 (1)
C(4D)-C(5D)	1.38 (1)	C(5D)-C(6D)	1.385 (8)
C(1E)-C(2E)	1.397 (8)	C(1E)-C(6E)	1.365 (9)
C(2E)-C(3E)	1.38 (1)	C(3E)-C(4E)	1.35 (1)
C(4E)-C(5E)	1.394 (9)	C(5E)-C(6E)	1.405 (9)
C(1F)-C(2F)	1.372 (9)	C(1F)-C(6F)	1.417 (9)
C(2F)-C(3F)	1.40 (1)	C(3F)-C(4F)	1.36 (1)
C(4F)-C(5F)	1.38 (1)	C(5F)-C(6F)	1.38 (1)
C(3G)-C(4G)	1.38 (1)	C(4G)-C(5G)	1.367 (8)
C(3H)-C(4H)	1.36 (1)	C(4H)-C(5H)	1.38 (1)
C(1)-C(2)	0.40 (2)	C(1)-Cl(4)	1.72 (1)
C(1)-Cl(3)	1.721 (9)	C(1)-Cl(5)	1.72 (2)
C(2)-Cl(4A)	1.72 (1)	C(2)-Cl(3A)	1.72 (2)
C(2)-Cl(5A)	1.72 (2)		

P(1)-Re(1)-Cl(1)	90.9(1)	P(1)-Re(1)-O(1)	94.4(2)
Cl(1)-Re(1)-O(1)	98.1(2)	P(1)-Re(1)-O(3)	84.1(1)
Cl(1)-Re(1)-O(3)	100.0(1)	O(1)-Re(1)-O(3)	161.9(2)
P(1)-Re(1)-N(2G)	94.8(1)	Cl(1)-Re(1)-N(2G)	174.2(1)
O(1)-Re(1)-N(2G)	82.7(2)	O(3)-Re(1)-N(2G)	79.4(2)
P(1)-Re(1)-N(2H)	163.4(1)	Cl(1)-Re(1)-N(2H)	87.7(2)
O(1)-Re(1)-N(2H)	102.2(2)	O(3)-Re(1)-N(2H)	79.9(2)
N(2G)-Re(1)-N(2H)	86.5(2)	P(2)-Re(2)-Cl(2)	92.8(1)
P(2)-Re(2)-O(2)	93.5(1)	Cl(2)-Re(2)-O(2)	98.7(2)
P(2)-Re(2)-O(3)	86.0(1)	Cl(2)-Re(2)-O(3)	100.0(1)
O(2)-Re(2)-O(3)	161.3(2)	P(2)-Re(2)-N(1G)	165.5(1)
Cl(2)-Re(2)-N(1G)	85.9(1)	O(2)-Re(2)-N(1G)	101.0(2)
O(3)-Re(2)-N(1G)	80.0(2)	P(2)-Re(2)-N(1H)	93.5(1)
Cl(2)-Re(2)-N(1H)	173.2(1)	O(2)-Re(2)-N(1H)	83.3(2)
O(3)-Re(2)-N(1H)	78.1(2)	N(1G)-Re(2)-N(1H)	87.4(2)
Re(1)-P(1)-C(1A)	113.4(2)	Re(1)-P(1)-C(1B)	114.3(2)
C(1A)-P(1)-C(1B)	102.3(2)	Re(1)-P(1)-C(1C)	113.9(2)
C(1A)-P(1)-C(1C)	106.9(3)	C(1B)-P(1)-C(1C)	105.0(3)
Re(2)-P(2)-C(1D)	116.2(2)	Re(2)-P(2)-C(1E)	116.2(2)
C(1D)-P(2)-C(1E)	101.8(2)	Re(2)-P(2)-C(1F)	109.8(2)

C(1D)-P(2)-C(1F)	106.0(3)	C(1E)-P(2)-C(1F)	105.8(3)
Re(1)-O(3)-Re(2)	124.9(2)	Re(2)-N(1G)-N(2G)	118.1(4)
Re(2)-N(1G)-C(5G)	133.2(4)	N(2G)-N(1G)-C(5G)	108.5(4)
Re(1)-N(2G)-N(1G)	120.0(3)	Re(1)-N(2G)-C(3G)	133.0(4)
N(1G)-N(2G)-C(3G)	106.9(5)	Re(2)-N(1H)-N(2H)	119.7(3)
Re(2)-N(1H)-C(5H)	133.6(4)	N(2H)-N(1H)-C(5H)	106.6(5)
Re(1)-N(2H)-N(1H)	118.4(4)	Re(1)-N(2H)-C(3H)	134.9(4)
N(1H)-N(2H)-C(3H)	106.7(5)	P(1)-C(1A)-C(2A)	122.2(5)
P(1)-C(1A)-C(6A)	118.8(5)	C(2A)-C(1A)-C(6A)	118.6(5)
C(1A)-C(2A)-C(3A)	121.2(7)	C(2A)-C(3A)-C(4A)	119.3(8)
C(3A)-C(4A)-C(5A)	119.9(7)	C(4A)-C(5A)-C(6A)	121.5(8)
C(1A)-C(6A)-C(5A)	119.5(7)	P(1)-C(1B)-C(2B)	121.7(4)
P(1)-C(1B)-C(6B)	118.7(4)	C(2B)-C(1B)-C(6B)	119.5(5)
C(1B)-C(2B)-C(3B)	120.6(5)	C(2B)-C(3B)-C(4B)	119.5(6)
C(3B)-C(4B)-C(5B)	119.7(6)	C(4B)-C(5B)-C(6B)	121.3(6)
C(1B)-C(6B)-C(5B)	119.5(5)	P(1)-C(1C)-C(2C)	121.7(5)
P(1)-C(1C)-C(6C)	119.4(4)	C(2C)-C(1C)-C(6C)	118.7(6)
C(1C)-C(2C)-C(3C)	120.2(6)	C(2C)-C(3C)-C(4C)	120.0(6)
C(3C)-C(4C)-C(5C)	121.0(8)	C(4C)-C(5C)-C(6C)	118.9(7)
C(1C)-C(6C)-C(5C)	121.2(5)	P(2)-C(1D)-C(2D)	119.7(5)

P(2)-C(1D)-C(6D)	120.9(5)	C(2D)-C(1D)-C(6D)	119.0(5)
C(1D)-C(2D)-C(3D)	120.4(7)	C(2D)-C(3D)-C(4D)	120.7(8)
C(3D)-C(4D)-C(5D)	119.8(6)	C(4D)-C(5D)-C(6D)	119.2(6)
C(1D)-C(6D)-C(5D)	120.9(7)	P(2)-C(1E)-C(2E)	119.2(5)
P(2)-C(1E)-C(6E)	122.7(4)	C(2E)-C(1E)-C(6E)	118.1(5)
C(1E)-C(2E)-C(3E)	120.8(7)	C(2E)-C(3E)-C(4E)	120.4(6)
C(3E)-C(4E)-C(5E)	120.9(6)	C(4E)-C(5E)-C(6E)	117.9(7)
C(1E)-C(6E)-C(5E)	121.9(5)	P(2)-C(1F)-C(2F)	123.3(5)
P(2)-C(1F)-C(6F)	118.0(5)	C(2F)-C(1F)-C(6F)	118.2(7)
C(1F)-C(2F)-C(3F)	120.4(7)	C(2F)-C(3F)-C(4F)	121.0(8)
C(3F)-C(4F)-C(5F)	120(1)	C(4F)-C(5F)-C(6F)	120.5(7)
C(1F)-C(6F)-C(5F)	120.2(6)	N(2G)-C(3G)-C(4G)	110.0(5)
C(3G)-C(4G)-C(5G)	105.0(6)	N(1G)-C(5G)-C(4G)	109.6(6)
N(2H)-C(3H)-C(4H)	111.3(6)	C(3H)-C(4H)-C(5H)	104.2(7)
N(1H)-C(5H)-C(4H)	111.1(6)	Cl(4)-C(1)-Cl(3)	109.9(6)
Cl(4)-C(1)-Cl(5)	109.9(7)	Cl(3)-C(1)-Cl(5)	109.9(8)
Cl(3A)-C(2)-Cl(4A)	109.8(7)	Cl(4A)-C(2)-Cl(5A)	109.9(8)
Cl(3A)-C(2)-Cl(5A)	109.8(9)		

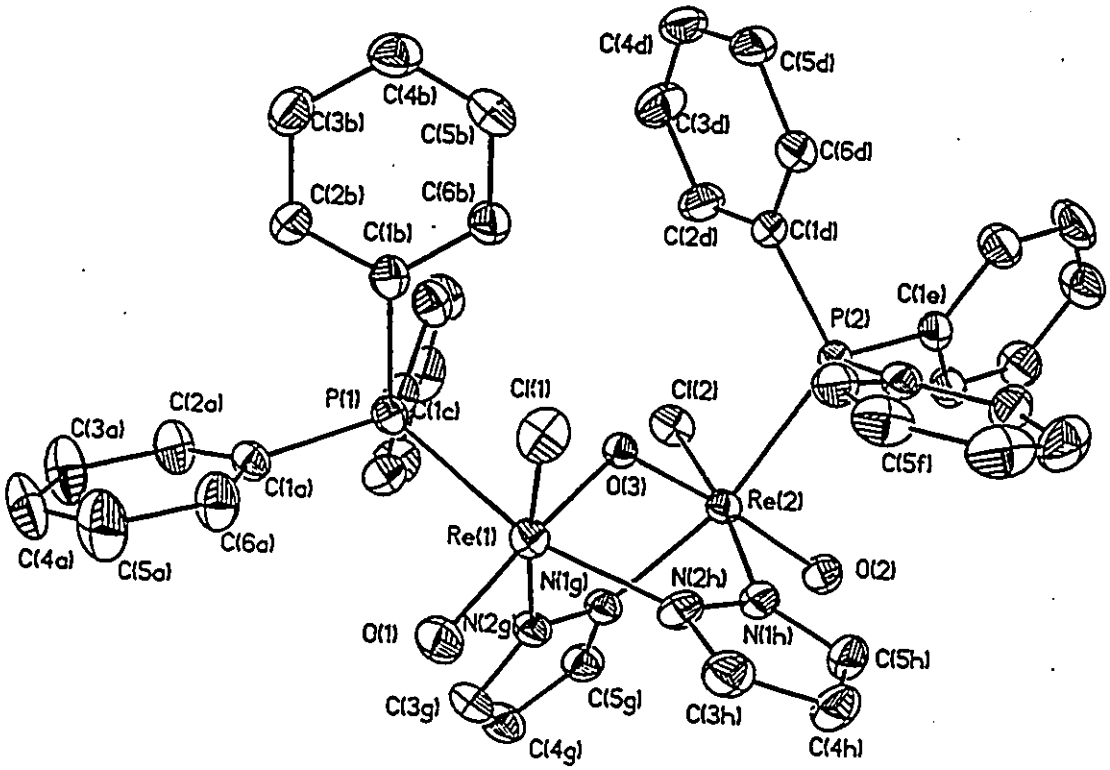

Fig. 5E.1 Structure of $[ReOCl(PPh_3)]_2(\mu\text{-}O)(\mu\text{-}pz)_2 \cdot CHCl_3$ (5E)

($CHCl_3$ Molecule is Omitted)

Table 5F.1. Bond Lengths (Å) and Bond Angles (°)

for $[ReOCl(3,5\text{-}Me_2\text{-}HPz)]_2(\mu\text{-}O)(\mu\text{-}3,5\text{-}Me_2\text{-}Pz)_2$ (5F)

Re(1)-Cl(1)	2.387 (4)	Re(1)-O(12)	1.92 (1)
Re(1)-O(1)	1.70 (1)	Re(1)-N(1A)	2.12 (2)
Re(1)-N(1B)	2.11 (1)	Re(1)-N(1C)	2.08 (2)
Re(2)-Cl(2)	2.396 (6)	Re(2)-O(12)	1.95 (1)
Re(2)-O(2)	1.65 (1)	Re(2)-N(2B)	2.05 (1)
Re(2)-N(2C)	2.12 (2)	Re(2)-N(1D)	2.11 (1)
N(1A)-N(2A)	1.35 (2)	N(1A)-C(5A)	1.36 (3)
N(2A)-C(3A)	1.40 (3)	C(3A)-C(4A)	1.36 (4)
C(3A)-C(6A)	1.49 (4)	C(4A)-C(5A)	1.36 (4)
C(5A)-C(7A)	1.41 (4)	N(1B)-N(2B)	1.32 (2)
N(1B)-C(5B)	1.44 (2)	N(2B)-C(3B)	1.39 (2)
C(3B)-C(4B)	1.33 (2)	C(3B)-C(6B)	1.56 (3)
C(4B)-C(5B)	1.41 (3)	C(5B)-C(7B)	1.49 (3)
N(1C)-N(2C)	1.40 (2)	N(1C)-C(5C)	1.37 (3)
N(2C)-C(3C)	1.28 (2)	C(3C)-C(4C)	1.38 (3)
C(3C)-C(6C)	1.53 (3)	C(4C)-C(5C)	1.39 (3)
C(5C)-C(7C)	1.50 (3)	N(1D)-N(2D)	1.34 (2)
N(1D)-C(5D)	1.32 (2)	N(2D)-C(3D)	1.35 (2)
C(3D)-C(4D)	1.39 (3)	C(3D)-C(6D)	1.50 (3)
C(4D)-C(5D)	1.39 (2)	C(5D)-C(7D)	1.46 (3)
Re(3)-Cl(3)	2.367 (6)	Re(3)-O(34)	1.966 (8)
Re(3)-O(3)	1.676 (9)	Re(3)-N(1E)	2.10 (2)

Re(3)-N(1F)	2.17 (1)	Re(3)-N(1G)	2.08 (1)
Re(4)-Cl(4)	2.369 (4)	Re(4)-O(34)	1.87 (1)
Re(4)-O(4)	1.68 (1)	Re(4)-N(2F)	2.10 (1)
Re(4)-N(2G)	2.13 (1)	Re(4)-N(1H)	2.10 (1)
N(1E)-N(2E)	1.37 (2)	N(1E)-C(5E)	1.35 (3)
N(2E)-C(3E)	1.32 (3)	C(3E)-C(4E)	1.41 (3)
C(3E)-C(6E)	1.50 (3)	C(4E)-C(5E)	1.38 (3)
C(5E)-C(7E)	1.49 (2)	N(1F)-N(2F)	1.37 (2)
N(1F)-C(5F)	1.32 (2)	N(2F)-C(3F)	1.31 (3)
C(3F)-C(4F)	1.36 (3)	C(3F)-C(6F)	1.52 (3)
C(4F)-C(5F)	1.38 (3)	C(5F)-C(7F)	1.46 (2)
N(1G)-N(2G)	1.42 (2)	N(1G)-C(5G)	1.34 (2)
N(2G)-C(3G)	1.29 (2)	C(3G)-C(4G)	1.41 (2)
C(3G)-C(6G)	1.51 (2)	C(4G)-C(5G)	1.37 (3)
C(5G)-C(7G)	1.54 (2)	N(1H)-N(2H)	1.38 (2)
N(1H)-C(5H)	1.31 (2)	N(2H)-C(3H)	1.39 (2)
C(3H)-C(4H)	1.42 (3)	C(3H)-C(6H)	1.48 (3)
C(4H)-C(5H)	1.34 (3)	C(5H)-C(7H)	1.53 (3)

Cl(1)-Re(1)-O(12)	88.4(3)	Cl(1)-Re(1)-O(1)	101.6(4)
O(12)-Re(1)-O(1)	169.3(5)	Cl(1)-Re(1)-N(1A)	87.0(4)
O(12)-Re(1)-N(1A)	84.2(5)	O(1)-Re(1)-N(1A)	100.0(6)
Cl(1)-Re(1)-N(1B)	168.9(3)	O(12)-Re(1)-N(1B)	80.5(4)
O(1)-Re(1)-N(1B)	89.5(5)	N(1A)-Re(1)-N(1B)	91.7(6)
Cl(1)-Re(1)-N(1C)	89.3(4)	O(12)-Re(1)-N(1C)	80.7(5)

O(1)-Re(1)-N(1C)	95.4(6)	N(1A)-Re(1)-N(1C)	164.6(5)
N(1B)-Re(1)-N(1C)	89.1(5)	Cl(2)-Re(2)-O(12)	90.3(4)
Cl(2)-Re(2)-O(2)	102.7(5)	O(12)-Re(2)-O(2)	166.8(6)
Cl(2)-Re(2)-N(2B)	87.3(5)	O(12)-Re(2)-N(2B)	81.2(4)
O(2)-Re(2)-N(2B)	96.8(5)	Cl(2)-Re(2)-N(2C)	169.6(4)
O(12)-Re(2)-N(2C)	79.4(5)	O(2)-Re(2)-N(2C)	87.7(6)
N(2B)-Re(2)-N(2C)	92.3(5)	Cl(2)-Re(2)-N(1D)	90.9(4)
O(12)-Re(2)-N(1D)	83.1(5)	O(2)-Re(2)-N(1D)	98.9(5)
N(2B)-Re(2)-N(1D)	164.1(5)	N(2C)-Re(2)-N(1D)	86.7(5)
Re(1)-O(12)-Re(2)	121.0(5)	Re(1)-N(1A)-N(2A)	116(1)
Re(1)-N(1A)-C(5A)	136(2)	N(2A)-N(1A)-C(5A)	108(2)
N(1A)-N(2A)-C(3A)	109(2)	N(2A)-C(3A)-C(4A)	106(2)
N(2A)-C(3A)-C(6A)	118(2)	C(4A)-C(3A)-C(6A)	136(3)
C(3A)-C(4A)-C(5A)	110(3)	N(1A)-C(5A)-C(4A)	107(2)
N(1A)-C(5A)-C(7A)	120(2)	C(4A)-C(5A)-C(7A)	133(2)
Re(1)-N(1B)-N(2B)	118.9(8)	Re(1)-N(1B)-C(5B)	131(1)
N(2B)-N(1B)-C(5B)	109(1)	Re(2)-N(2B)-N(1B)	120.0(9)
Re(2)-N(2B)-C(3B)	132(1)	N(1B)-N(2B)-C(3B)	108(1)
N(2B)-C(3B)-C(4B)	111(2)	N(2B)-C(3B)-C(6B)	122(1)
C(4B)-C(3B)-C(6B)	127(2)	C(3B)-C(4B)-C(5B)	107(1)
N(1B)-C(5B)-C(4B)	105(1)	N(1B)-C(5B)-C(7B)	121(2)
C(4B)-C(5B)-C(7B)	134(1)	Re(1)-N(1C)-N(2C)	120(1)
Re(1)-N(1C)-C(5C)	132(1)	N(2C)-N(1C)-C(5C)	107(2)
Re(2)-N(2C)-N(1C)	116(1)	Re(2)-N(2C)-C(3C)	136(1)
N(1C)-N(2C)-C(3C)	108(2)	N(2C)-C(3C)-C(4C)	111(2)

N(2C)-C(3C)-C(6C)	123(2)	C(4C)-C(3C)-C(6C)	126(2)
C(3C)-C(4C)-C(5C)	106(2)	N(1C)-C(5C)-C(4C)	107(2)
N(1C)-C(5C)-C(7C)	123(2)	C(4C)-C(5C)-C(7C)	130(2)
Re(2)-N(1D)-N(2D)	117(1)	Re(2)-N(1D)-C(5D)	136(1)
N(2D)-N(1D)-C(5D)	107(1)	N(1D)-N(2D)-C(3D)	113(1)
N(2D)-C(3D)-C(4D)	104(1)	N(2D)-C(3D)-C(6D)	122(2)
C(4D)-C(3D)-C(6D)	133(2)	C(3D)-C(4D)-C(5D)	107(2)
N(1D)-C(5D)-C(4D)	109(2)	N(1D)-C(5D)-C(7D)	121(1)
C(4D)-C(5D)-C(7D)	130(2)	Cl(3)-Re(3)-O(34)	91.0(3)
Cl(3)-Re(3)-O(3)	100.3(5)	O(34)-Re(3)-O(3)	168.1(5)
Cl(3)-Re(3)-N(1E)	88.9(4)	O(34)-Re(3)-N(1E)	82.6(5)
O(3)-Re(3)-N(1E)	101.1(6)	Cl(3)-Re(3)-N(1F)	169.7(3)
O(34)-Re(3)-N(1F)	78.9(4)	O(3)-Re(3)-N(1F)	89.9(5)
N(1E)-Re(3)-N(1F)	87.7(6)	Cl(3)-Re(3)-N(1G)	89.1(4)
O(34)-Re(3)-N(1G)	80.5(4)	O(3)-Re(3)-N(1G)	96.0(5)
N(1E)-Re(3)-N(1G)	162.9(4)	N(1F)-Re(3)-N(1G)	91.2(5)
Cl(4)-Re(4)-O(34)	88.0(3)	Cl(4)-Re(4)-O(4)	103.3(4)
O(34)-Re(4)-O(4)	168.0(4)	Cl(4)-Re(4)-N(2F)	87.3(3)
O(34)-Re(4)-N(2F)	82.0(5)	O(4)-Re(4)-N(2F)	94.3(6)
Cl(4)-Re(4)-N(2G)	168.7(4)	O(34)-Re(4)-N(2G)	80.7(5)
O(4)-Re(4)-N(2G)	87.9(5)	N(2F)-Re(4)-N(2G)	91.5(5)
Cl(4)-Re(4)-N(1H)	89.8(4)	O(34)-Re(4)-N(1H)	85.7(5)
O(4)-Re(4)-N(1H)	98.2(5)	N(2F)-Re(4)-N(1H)	167.5(5)
N(2G)-Re(4)-N(1H)	88.9(5)	Re(3)-O(34)-Re(4)	123.1(5)
Re(3)-N(1E)-N(2E)	120(1)	Re(3)-N(1E)-C(5E)	135(1)

N(2E)-N(1E)-C(5E)	105(2)	N(1E)-N(2E)-C(3E)	112(2)
N(2E)-C(3E)-C(4E)	108(2)	N(2E)-C(3E)-C(6E)	121(2)
C(4E)-C(3E)-C(6E)	132(2)	C(3E)-C(4E)-C(5E)	105(2)
N(1E)-C(5E)-C(4E)	111(2)	N(1E)-C(5E)-C(7E)	122(2)
C(4E)-C(5E)-C(7E)	128(2)	Re(3)-N(1F)-N(2F)	118(1)
Re(3)-N(1F)-C(5F)	131(1)	N(2F)-N(1F)-C(5F)	110(1)
Re(4)-N(2F)-N(1F)	118(1)	Re(4)-N(2F)-C(3F)	136(1)
N(1F)-N(2F)-C(3F)	106(1)	N(2F)-C(3F)-C(4F)	110(2)
N(2F)-C(3F)-C(6F)	121(2)	C(4F)-C(3F)-C(6F)	128(2)
C(3F)-C(4F)-C(5F)	107(2)	N(1F)-C(5F)-C(4F)	106(2)
N(1F)-C(5F)-C(7F)	127(2)	C(4F)-C(5F)-C(7F)	127(2)
Re(3)-N(1G)-N(2G)	118.2(9)	Re(3)-N(1G)-C(5G)	134(1)
N(2G)-N(1G)-C(5G)	107(1)	Re(4)-N(2G)-N(1G)	117(1)
Re(4)-N(2G)-C(3G)	136(1)	N(1G)-N(2G)-C(3G)	106(1)
N(2G)-C(3G)-C(4G)	112(2)	N(2G)-C(3G)-C(6G)	123(1)
C(4G)-C(3G)-C(6G)	125(2)	C(3G)-C(4G)-C(5G)	104(2)
N(1G)-C(5G)-C(4G)	110(2)	N(1G)-C(5G)-C(7G)	122(2)
C(4G)-C(5G)-C(7G)	128(2)	Re(4)-N(1H)-N(2H)	120.9(8)
Re(4)-N(1H)-C(5H)	137(1)	N(2H)-N(1H)-C(5H)	102(1)
N(1H)-N(2H)-C(3H)	115(1)	N(2H)-C(3H)-C(4H)	100(2)
N(2H)-C(3H)-C(6H)	124(2)	C(4H)-C(3H)-C(6H)	136(2)
C(3H)-C(4H)-C(5H)	108(2)	N(1H)-C(5H)-C(4H)	115(2)
N(1H)-C(5H)-C(7H)	117(2)	C(4H)-C(5H)-C(7H)	128(2)

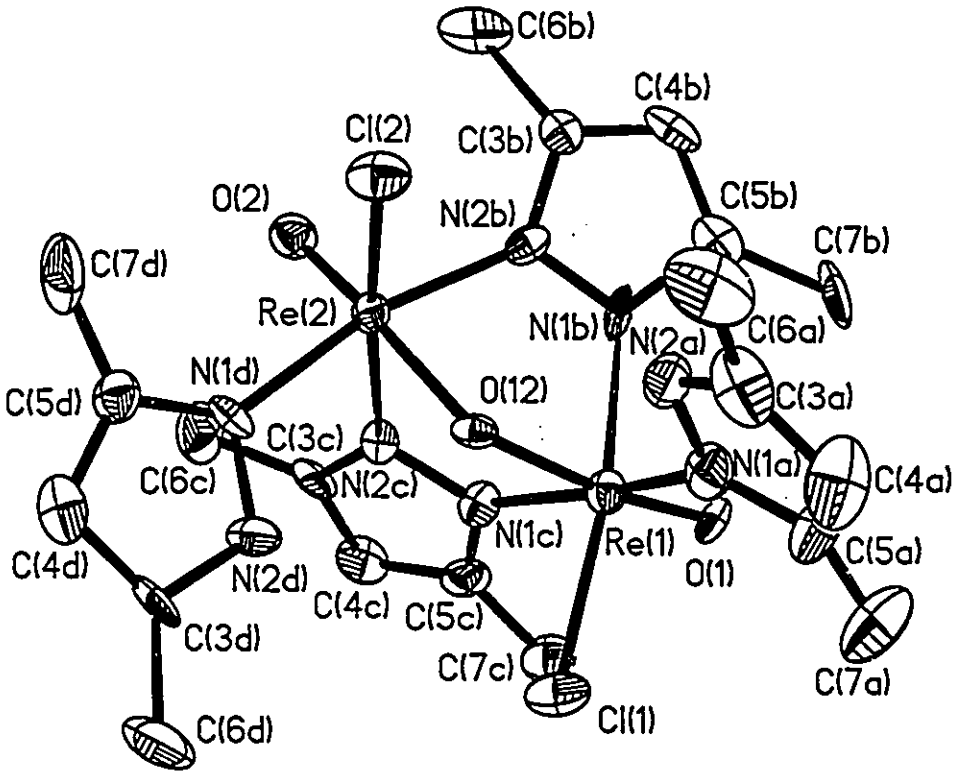

Fig. 5F.1.1 The Structure of $[ReOCl(3,5\text{-}Me_2\text{-}HPz)]_2(\mu\text{-}O)(\mu\text{-}3,5\text{-}Me_2\text{-}Pz)_2$ (5F), One of the Two Independent Molecules

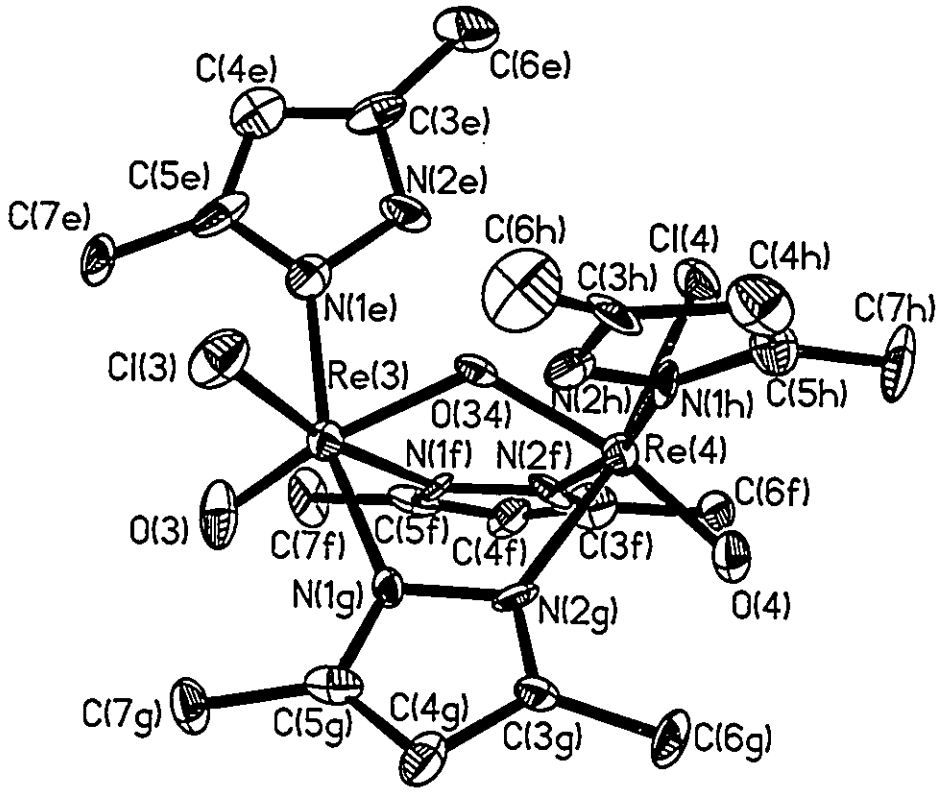

Fig. 5F.1.2 The Structure of $[ReOCl(3,5\text{-}Me_2\text{-}HPz)]_2(\mu\text{-}O)(\mu\text{-}3,5\text{-}Me_2\text{-}Pz)_2$ (5F), One of the Two Independent Molecules

Table 5G.1. Bond Lengths (Å) and Bond Angles (°)

for $ReOCl_2(PPh_3)(4\text{-}CH_2O\text{-}1,5\text{-}Me_2\text{-}Im)\cdot 2H_2O$ (5G)

Re-Cl(1)	2.410 (6)	Re-Cl(2)	2.360 (6)
Re-P	2.454 (6)	Re-O(1)	1.70 (1)
Re-O(2)	1.92 (1)	Re-N(3A)	2.15 (2)
P-C(1B)	1.82 (2)	P-C(1C)	1.85 (2)
P-C(1D)	1.83 (3)	O(2)-C(6)	1.40 (3)
N(1A)-C(2A)	1.32 (3)	N(1A)-C(5A)	1.38 (3)
N(1A)-C(8)	1.43 (3)	C(2A)-N(3A)	1.31 (3)
N(3A)-C(4A)	1.34 (3)	C(4A)-C(5A)	1.36 (3)
C(4A)-C(6)	1.50 (3)	C(5A)-C(7)	1.50 (4)
C(1B)-C(2B)	1.45 (3)	C(1B)-C(6B)	1.30 (4)
C(2B)-C(3B)	1.38 (4)	C(3B)-C(4B)	1.35 (4)
C(4B)-C(5B)	1.39 (5)	C(5B)-C(6B)	1.39 (4)
C(1C)-C(2C)	1.39 (4)	C(1C)-C(6C)	1.43 (4)
C(2C)-C(3C)	1.38 (5)	C(3C)-C(4C)	1.33 (5)
C(4C)-C(5C)	1.35 (4)	C(5C)-C(6C)	1.50 (5)
C(1D)-C(2D)	1.35 (4)	C(1D)-C(6D)	1.42 (3)
C(2D)-C(3D)	1.41 (4)	C(3D)-C(4D)	1.32 (4)
C(4D)-C(5D)	1.37 (4)	C(5D)-C(6D)	1.42 (4)
O(3)-O(4)	1.01 (6)	O(6)-O(7)	0.91 (6)
C(1)-Re-Cl(2)	88.3(2)	Cl(1)-Re-P	176.6(2)
Cl(2)-Re-P	92.0(2)	Cl(1)-Re-O(1)	95.3(5)

Cl(2)-Re-O(1)	103.6(5)	P-Re-O(1)	88.0(5)
Cl(1)-Re-O(2)	89.8(4)	Cl(2)-Re-O(2)	91.8(4)
P-Re-O(2)	86.8(4)	O(1)-Re-O(2)	163.9(6)
Cl(1)-Re-N(3A)	87.1(5)	Cl(2)-Re-N(3A)	167.3(5)
P-Re-N(3A)	91.9(5)	O(1)-Re-N(3A)	88.6(7)
O(2)-Re-N(3A)	76.3(6)	Re-P-C(1B)	113.4(8)
Re-P-C(1C)	114.2(8)	C(1B)-P-C(1C)	104(1)
Re-P-C(1D)	111.9(8)	C(1B)-P-C(1D)	107(1)
C(1C)-P-C(1D)	106(1)	Re-O(2)-C(6)	124(1)
C(2A)-N(1A)-C(5A)	110(2)	C(2A)-N(1A)-C(8)	123(2)
C(5A)-N(1A)-C(8)	126(2)	N(1A)-C(2A)-N(3A)	107(2)
Re-N(3A)-C(2A)	134(2)	Re-N(3A)-C(4A)	116(2)
C(2A)-N(3A)-C(4A)	110(2)	N(3A)-C(4A)-C(5A)	109(2)
N(3A)-C(4A)-C(6)	114(2)	C(5A)-C(4A)-C(6)	137(2)
N(1A)-C(5A)-C(4A)	104(2)	N(1A)-C(5A)-C(7)	126(2)
C(4A)-C(5A)-C(7)	131(2)	O(2)-C(6)-C(4A)	110(2)
P-C(1B)-C(2B)	120(2)	P-C(1B)-C(6B)	127(2)
C(2B)-C(1B)-C(6B)	113(2)	C(1B)-C(2B)-C(3B)	124(2)
C(2B)-C(3B)-C(4B)	117(3)	C(3B)-C(4B)-C(5B)	122(3)
C(4B)-C(5B)-C(6B)	116(3)	C(1B)-C(6B)-C(5B)	127(3)
P-C(1C)-C(2C)	131(2)	P-C(1C)-C(6C)	115(2)
C(2C)-C(1C)-C(6C)	114(3)	C(1C)-C(2C)-C(3C)	129(3)
C(2C)-C(3C)-C(4C)	113(3)	C(3C)-C(4C)-C(5C)	127(3)
C(4C)-C(5C)-C(6C)	117(3)	C(1C)-C(6C)-C(5C)	118(2)
P-C(1D)-C(2D)	121(2)	P-C(1D)-C(6D)	120(2)

C(2D)-C(1D)-C(6D)	118(2)	C(1D)-C(2D)-C(3D)	123(2)
C(2D)-C(3D)-C(4D)	121(3)	C(3D)-C(4D)-C(5D)	118(3)
C(4D)-C(5D)-C(6D)	125(3)	C(1D)-C(6D)-C(5D)	116(2)

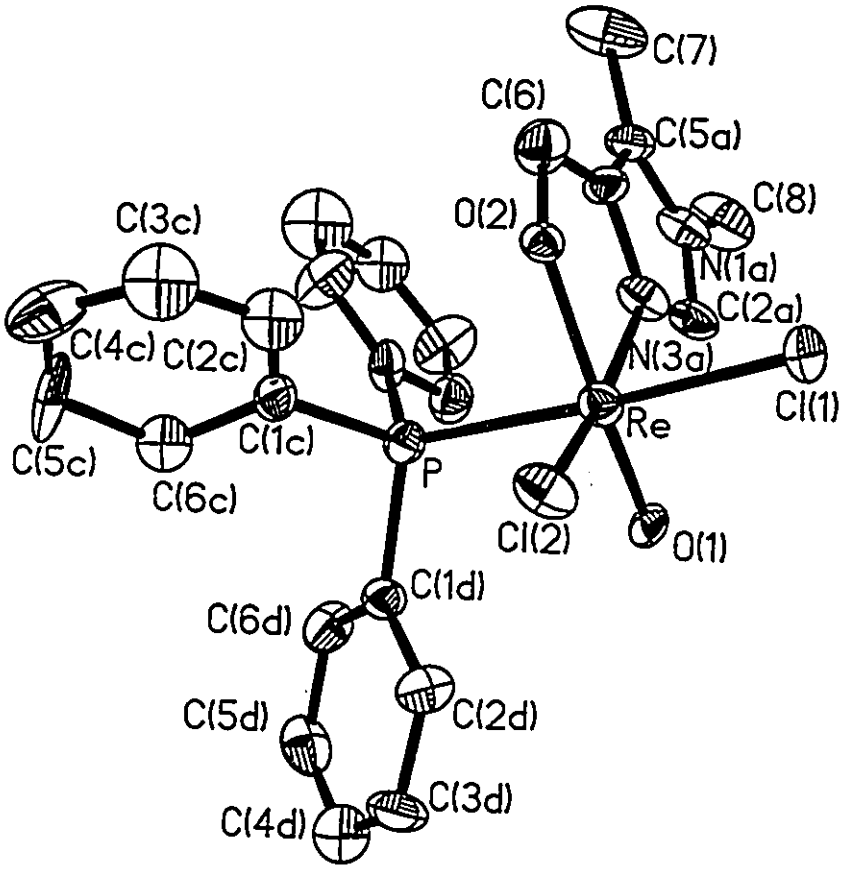

Fig. 5G.1. Structure of $ReOCl_2(PPh_3)(4\text{-}CH_2O\text{-}1,5\text{-}Me_2\text{-}Im)\cdot 2H_2O$ (5G)

(Solvent Molecules and Hydrogen Atoms are Omitted for Clarity)

Table 5H.1. Bond Lengths (Å) and Bond Angles (°)

for [TcO(4-OCH_2-1,5-Me_2-Im)$_2$(4-$HOCH_2$-1,5-Me_2-Im)]TcO_4 (5H)

Tc(1)-O	1.708 (8)	Tc(1)-N(3A)	2.161 (7)
Tc(1)-O(6A)	1.945 (7)	Tc(1)-N(3B)	2.111 (9)
Tc(1)-O(6B)	1.940 (6)	Tc(1)-N(3C)	2.120 (8)
N(1A)-C(2A)	1.36 (1)	N(1A)-C(5A)	1.38 (1)
N(1A)-C(8A)	1.46 (1)	C(2A)-N(3A)	1.33 (1)
N(3A)-C(4A)	1.36 (1)	C(4A)-C(5A)	1.34 (1)
C(4A)-C(6A)	1.49 (1)	C(5A)-C(7A)	1.51 (1)
C(6A)-O(6A)	1.43 (1)	N(1B)-C(2B)	1.33 (1)
N(1B)-C(5B)	1.40 (1)	N(1B)-C(8B)	1.46 (1)
C(2B)-N(3B)	1.30 (1)	N(3B)-C(4B)	1.40 (1)
C(4B)-C(5B)	1.35 (2)	C(4B)-C(6B)	1.47 (1)
C(5B)-C(7B)	1.50 (2)	C(6B)-O(6B)	1.46 (1)
N(1C)-C(2C)	1.33 (1)	N(1C)-C(5C)	1.42 (1)
N(1C)-C(8C)	1.46 (2)	C(2C)-N(3C)	1.35 (1)
N(3C)-C(4C)	1.41 (1)	C(4C)-C(5C)	1.35 (2)
C(4C)-C(6C)	1.50 (2)	C(5C)-C(7C)	1.49 (1)
C(6C)-O(6C)	1.43 (1)	Tc(2)-O(21)	1.70 (1)
Tc(2)-O(22)	1.707 (8)	Tc(2)-O(23)	1.69 (1)
Tc(2)-O(24)	1.68 (1)		
O-Tc(1)-N(3A)	86.1(3)	O-Tc(1)-O(6A)	161.5(3)
N(3A)-Tc(1)-O(6A)	75.5(3)	O-Tc(1)-N(3B)	92.2(4)
N(3A)-Tc(1)-N(3B)	96.7(3)	O(6A)-Tc(1)-N(3B)	87.8(3)

O-Tc(1)-O(6B)	109.0(3)	N(3A)-Tc(1)-O(6B)	164.7(3)
O(6A)-Tc(1)-O(6B)	89.3(3)	N(3B)-Tc(1)-O(6B)	80.9(3)
O-Tc(1)-N(3C)	93.6(4)	N(3A)-Tc(1)-N(3C)	90.6(3)
O(6A)-Tc(1)-N(3C)	88.9(3)	N(3B)-Tc(1)-N(3C)	171.0(3)
O(6B)-Tc(1)-N(3C)	90.7(3)	C(2A)-N(1A)-C(5A)	109.0(8)
C(2A)-N(1A)-C(8A)	123(1)	C(5A)-N(1A)-C(8A)	127.6(9)
N(1A)-C(2A)-N(3A)	108(1)	Tc(1)-N(3A)-C(2A)	136.4(7)
Tc(1)-N(3A)-C(4A)	116.2(6)	C(2A)-N(3A)-C(4A)	107.4(8)
N(3A)-C(4A)-C(5A)	110.8(9)	N(3A)-C(4A)-C(6A)	115.1(7)
C(5A)-C(4A)-C(6A)	134(1)	N(1A)-C(5A)-C(4A)	105.1(8)
N(1A)-C(5A)-C(7A)	121.8(8)	C(4A)-C(5A)-C(7A)	133(1)
C(4A)-C(6A)-O(6A)	108.3(8)	Tc(1)-O(6A)-C(6A)	124.6(6)
C(2B)-N(1B)-C(5B)	106.4(8)	C(2B)-N(1B)-C(8B)	127.3(8)
C(5B)-N(1B)-C(8B)	126.2(9)	N(1B)-C(2B)-N(3B)	113.2(8)
Tc(1)-N(3B)-C(2B)	141.6(7)	Tc(1)-N(3B)-C(4B)	111.6(6)
C(2B)-N(3B)-C(4B)	105.1(8)	N(3B)-C(4B)-C(5B)	109.6(7)
N(3B)-C(4B)-C(6B)	116.6(9)	C(5B)-C(4B)-C(6B)	133.8(9)
N(1B)-C(5B)-C(4B)	105.7(8)	N(1B)-C(5B)-C(7B)	123(1)
C(4B)-C(5B)-C(7B)	130.9(8)	C(4B)-C(6B)-O(6B)	110.3(8)
Tc(1)-O(6B)-C(6B)	117.8(5)	C(2C)-N(1C)-C(5C)	108.6(9)
C(2C)-N(1C)-C(8C)	125.9(7)	C(5C)-N(1C)-C(8C)	125.3(8)
N(1C)-C(2C)-N(3C)	110.7(8)	Tc(1)-N(3C)-C(2C)	126.1(6)
Tc(1)-N(3C)-C(4C)	128.4(7)	C(2C)-N(3C)-C(4C)	105.5(8)
N(3C)-C(4C)-C(5C)	110.1(8)	N(3C)-C(4C)-C(6C)	124.2(9)
C(5C)-C(4C)-C(6C)	125.6(9)	N(1C)-C(5C)-C(4C)	105.1(8)

N(1C)-C(5C)-C(7C)	123(1)	C(4C)-C(5C)-C(7C)	131.6(9)
C(4C)-C(6C)-O(6C)	114(1)	O(21)-Tc(2)-O(22)	109.4(5)
O(21)-Tc(2)-O(23)	107.2(5)	O(22)-Tc(2)-O(23)	110.4(5)
O(21)-Tc(2)-O(24)	109.6(6)	O(22)-Tc(2)-O(24)	109.4(5)
O(23)-Tc(2)-O(24)	110.7(7)		

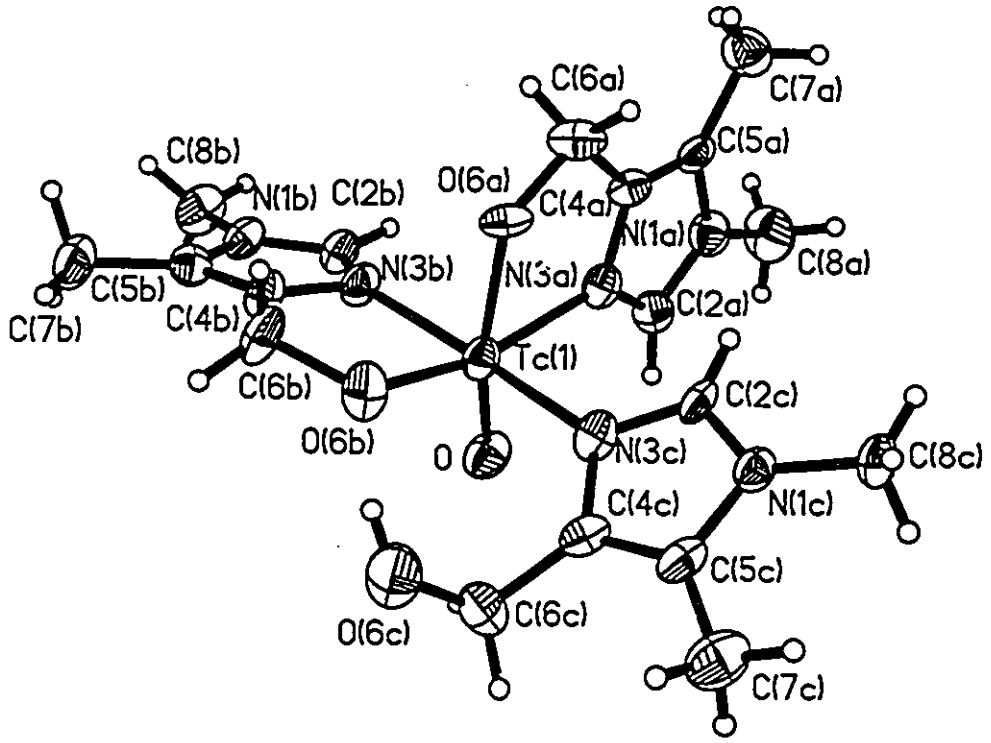

Fig. 5H.1 The Structure of

$[TcO(4\text{-}OCH_2\text{-}1,5\text{-}Me_2\text{-}Im)_2(4\text{-}HOCH_2\text{-}1,5\text{-}Me_2\text{-}Im)]TcO_4$ (5H) Cation

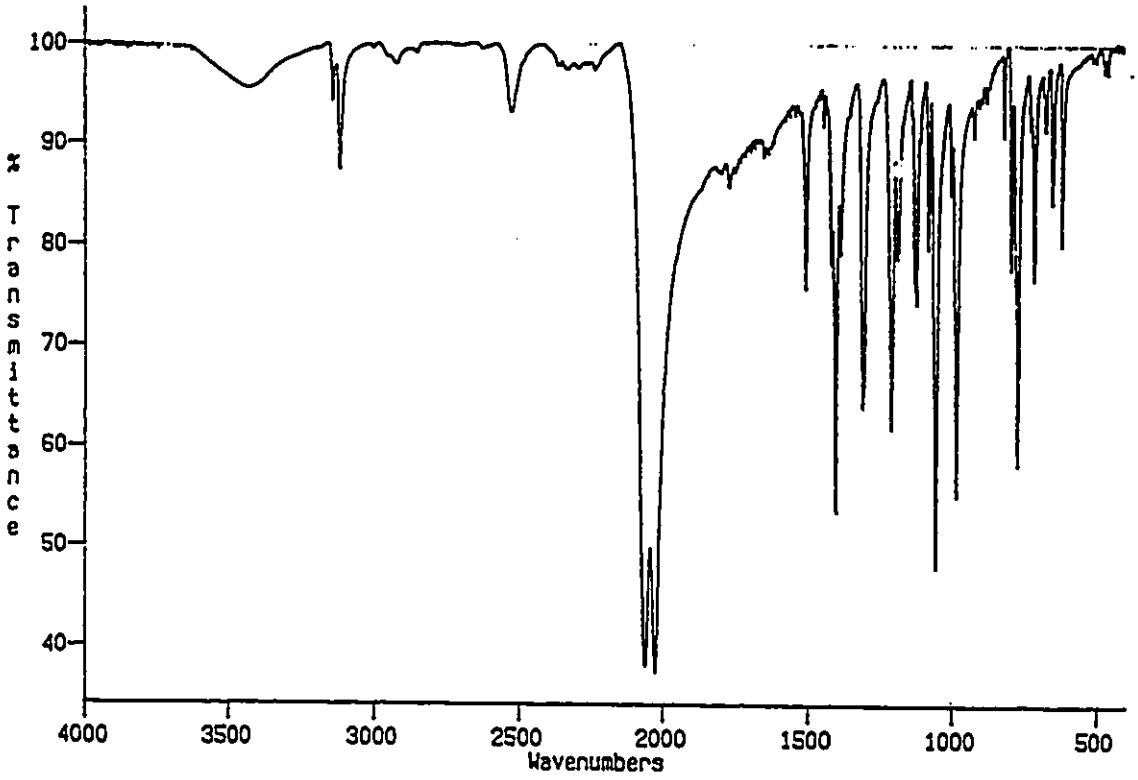

Fig. 5A.1 I R Spectrum of $ReO(HBpz_3)(NCS)_2$ (5A)

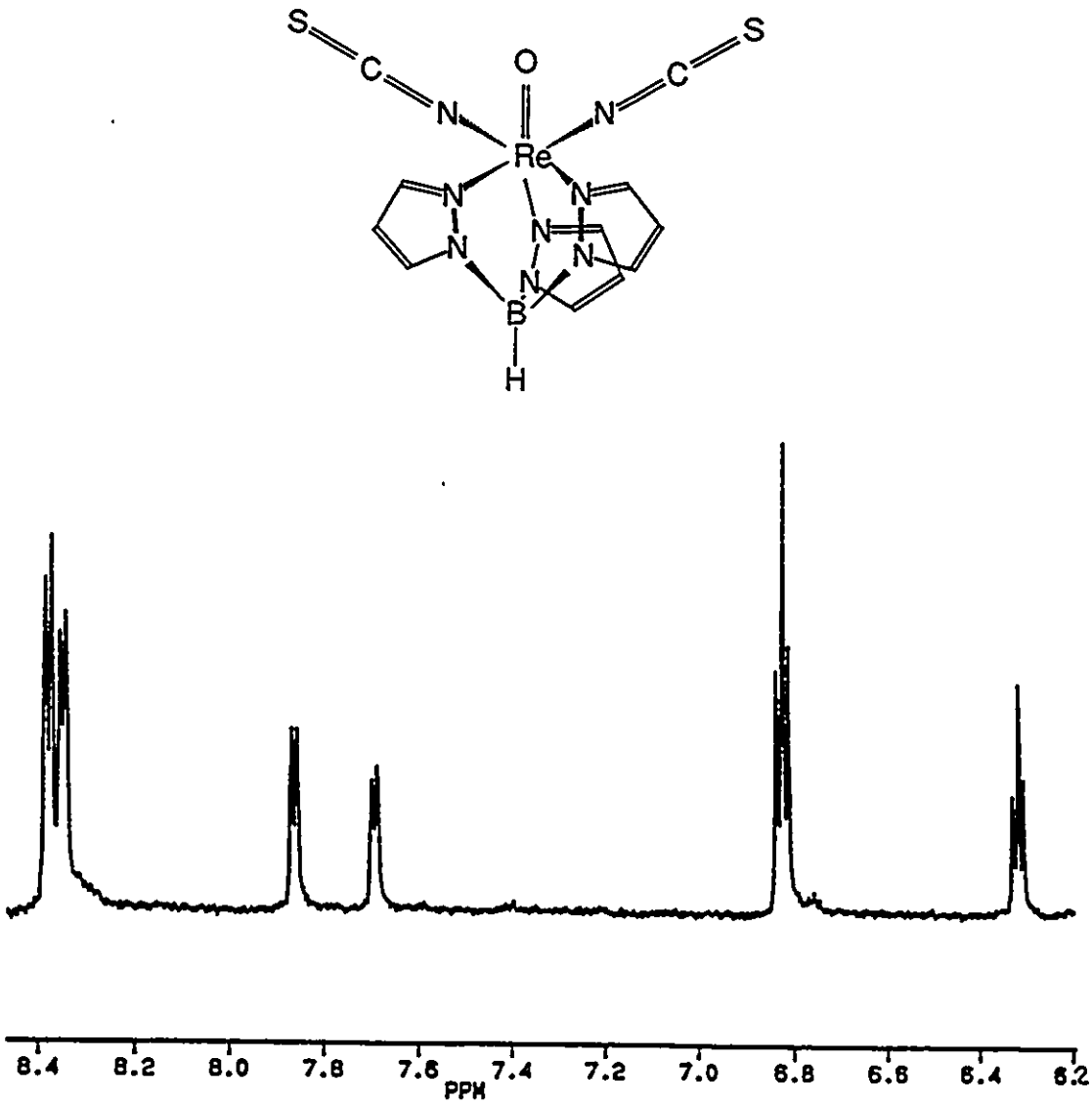

Fig. 5A.2 ^{1}H NMR Spectrum of $ReO(HBpz_2)(NCS)_2$ (5A) in D_6-Acetone

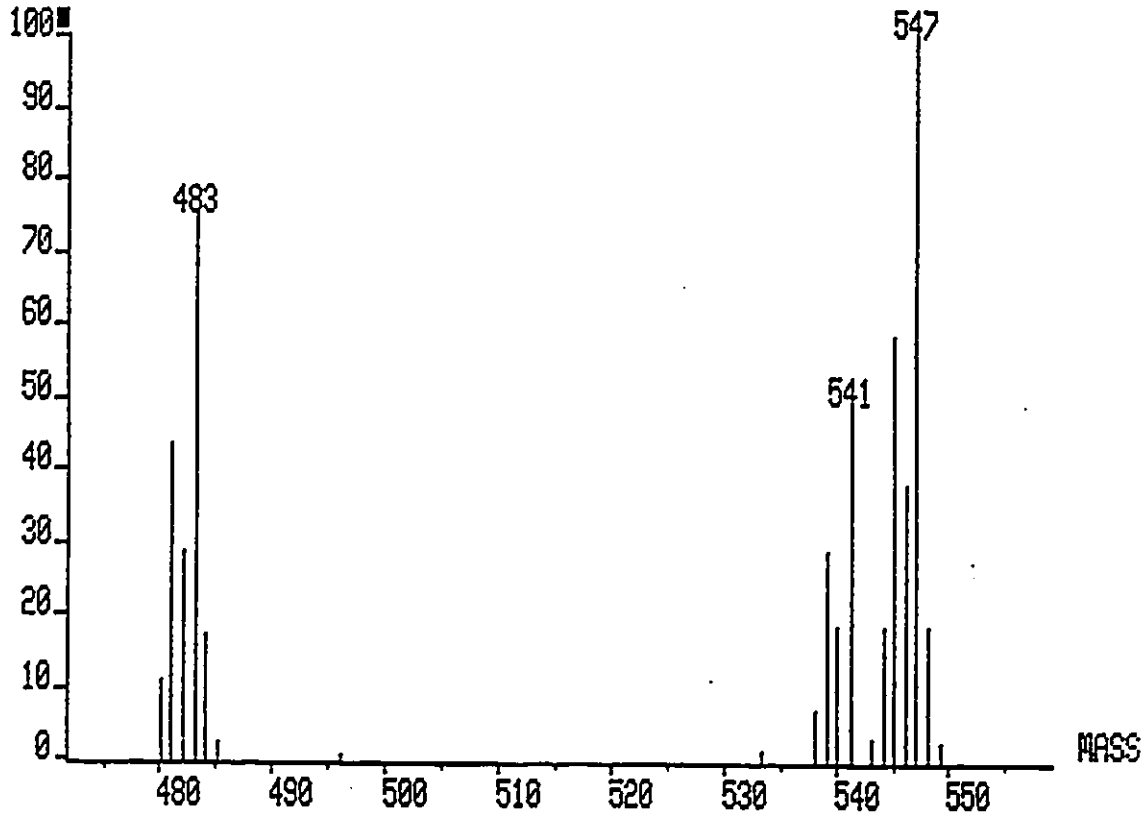

Fig. 5B.2 High Mass Region Of the Mass Spectrum of

$ReO(HBpz_3)(pz\text{-}CO(CH_3)_2]^+$ and $ReO(HBpz_3)(pz\text{-}CO(CD_3)_2]^+$

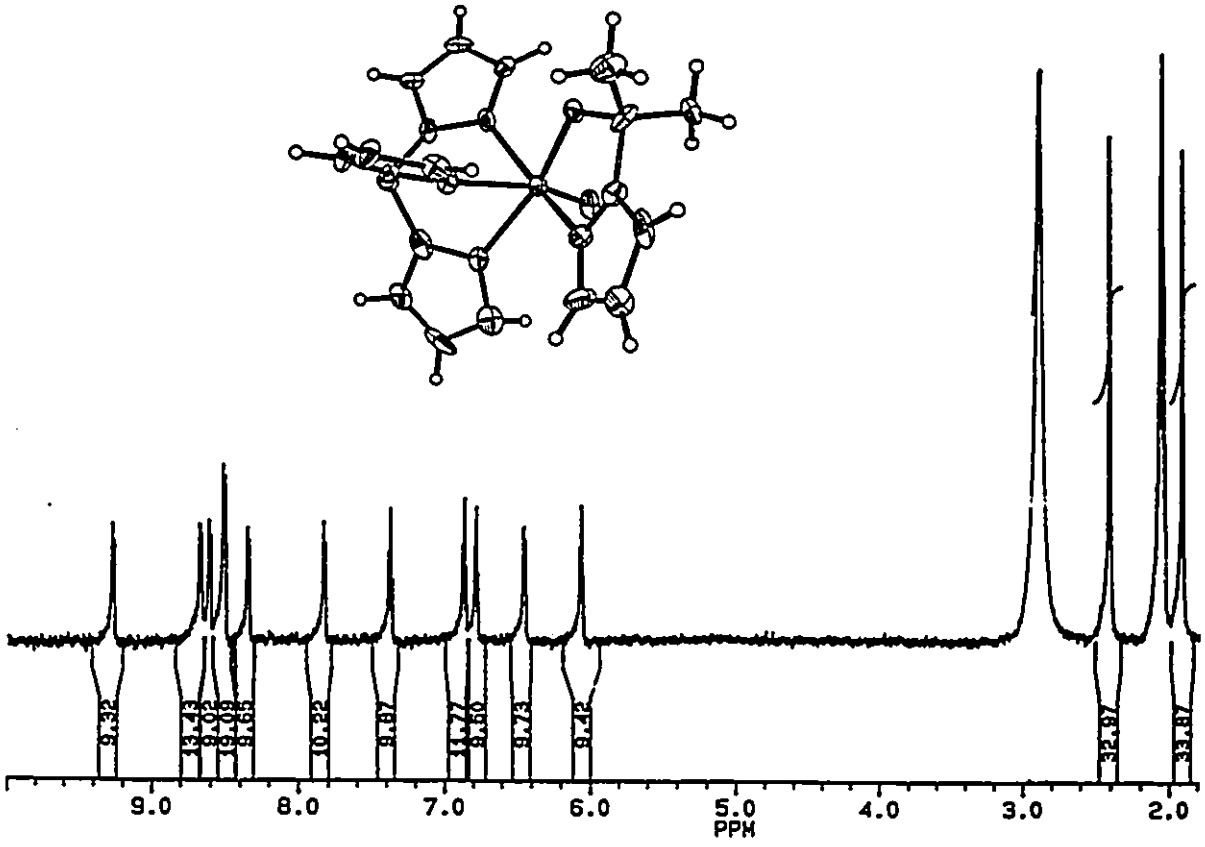

Fig. 5B.3 ^{1}H NMR Spectrum of $ReO(HBpz_3)(pz\text{-}CO(CH_3)_2]^+$ in D_6-Acetone

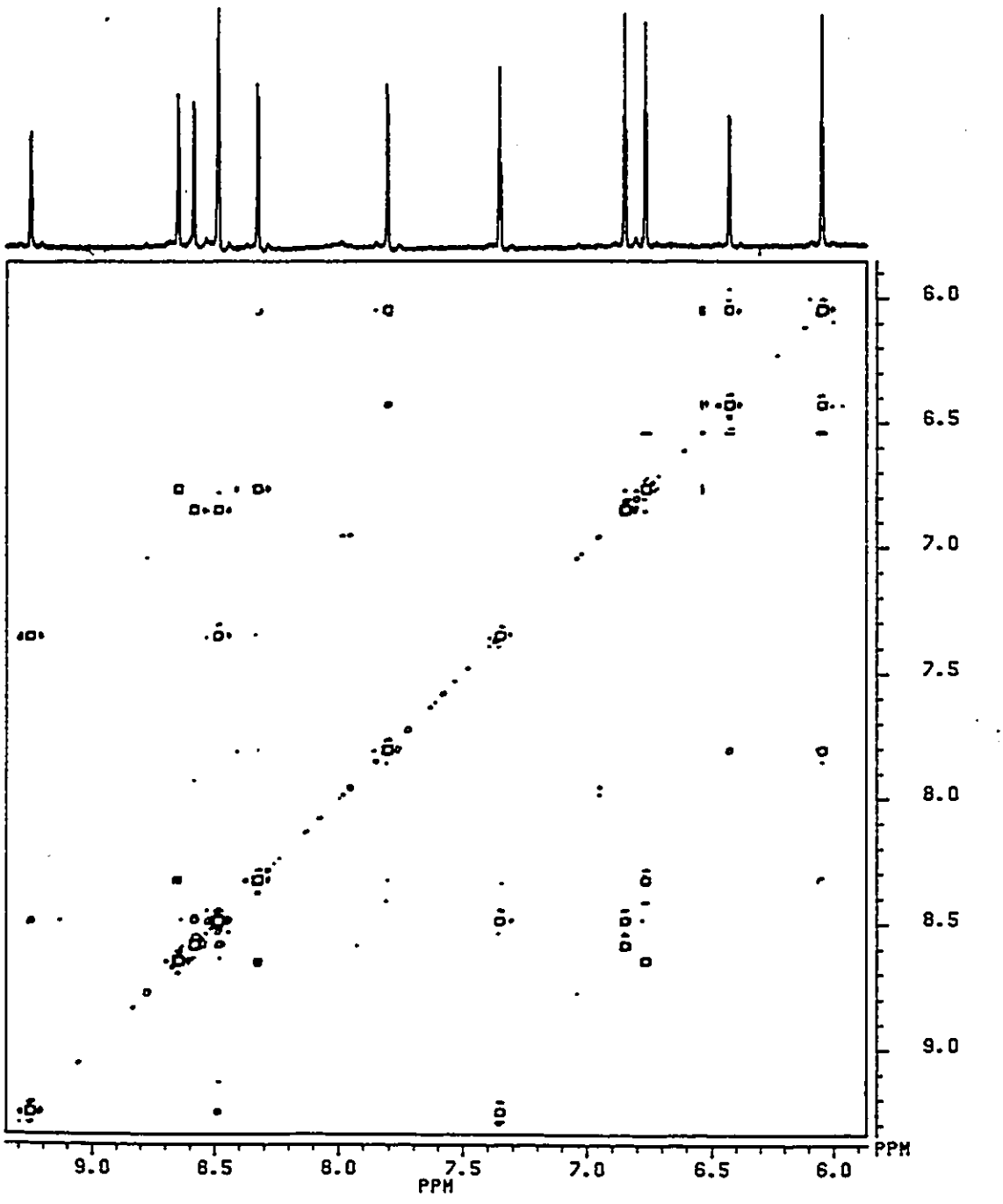

Fig. 5B.4 COSY ^{1}H NMR Spectrum of $ReO(HBpz_3)(pz\text{-}CO(CH_3)_2)^+$ in D_6-Acetone

5.5 Results and Discussion

5.5.1 Preparation

Compound **5A** was obtained relatively easily by a simple ligand substitution reaction. The formation of **5B** was unexpected. It was expected that the Ag^+ would remove Cl^- from the starting material as an AgCl precipitate, and the F^- would replace Cl^-. The reaction involved in obtaining **5B** seems fairly complicated. Chloride ion was indeed removed, but F^- did not coordinate to the rhenium atom. The $HBPz^-$ ligand from some of the starting material molecules was split into pyrazolyl rings by F^- and perhaps formed BF_4^-. Thus the pyrazole reacted with solvent acetone to form a new ligand, which took the positions left by Cl^-. Some Ag^+ was reduced to Ag even though the bottle was covered with a can to avoid possible interference of light. This may imply that the formation of ReO_4^- may involve oxidation by Ag^+, in addition to air. Scheme 1. suggests reactions that are consistent with the observed phenomena.

Scheme 1.

$$ReO(HBpz_3)Cl_2 + 2AgF = 2AgCl + ReO(HBpz_3)^{2+} + 2F^- \quad (1)$$

$$ReO(HBpz_3)Cl_2 + 4AgF + 3H_2O = 2AgCl + 2Ag + ReO_4^- + 6H^+ + 4F^- + HBpz_3^- \quad (2)$$

$$6F^- + 6H^+ + HBpz_3^- = H_2 + 2HF + pz^- + 2Hpz + HBF_4^- \quad (3)$$

$$ReO(HBpz_3)^{2+} + MeCOMe + pz^- + ReO_4^- = ReO(HBpz_3)(pz\text{-}COMe_2)]ReO_4 \quad (4)$$

$$2ReO(HBpz_3)Cl_2 + 6AgF + 3H_2O + MeCOMe = [ReO(HBpz_3)(pz\text{-}COMe_2)]ReO_4 + 4AgCl + 2Ag + H_2 + 2HF + HBF_4 + 2Hpz \quad (5)$$

Equation (1) suggests a very unstable species, $ReO(HBpz_3)^{2+}$, which is four

coordinated. The evidence for this proposal is not solid, even though AgCl precipitates were observed. It was proposed for the convenience of balancing the reaction equations, and with reference to the literature [98]. Perhaps, a five coordinated transition state is more likely to be the case, as suggested by the mass spectra (Fig. 5B.2). When compound **5B** was dissolved in d_6-acetone, an exchanging equilibrium between the coordinated acetone, $CO(CH_3)_2$, and d_6-acetone, $CO(CD_3)_2$, occurred as shown in equation (6):

$$ReO(HBpz_3)(pz\text{-}CO(CH_3)_2]^+ + CO(CD_3)_2 \leftrightharpoons ReO(HBpz_3)(pz\text{-}CO(CD_3)_2]^+ + CO(CH_3)_2 \quad (6)$$

In Fig **5B**.2 The almost identical profile of the isotopic peaks of $ReO(HBpz_3)(pz\text{-}CO(CD_3)_2]^+$, (m/e = 547), $ReO(HBpz_3)(pz\text{-}CO(CH_3)_2]^+$, (m/e = 541), and $[ReO(HBpz_3)(pz)]^+$ (m/e = 483) indicated that the H-D isotopic exchange took place by the exchange of acetone and d_6-acetone as complete molecules. This process suggested a five coordinated intermediate $[ReO(HBpz_3)(pz)]^+$.

Equation (2) was proposed to summarize the redox process. It was suggested by the observation of a silver mirror around the plastic bottle and the perrhenate anion in the product. Equation (3) was suggested by the observation of an etched watch glass which indicates that HF was evolved, $HBPz_3^-$ ligand was split to pyrazoles or pyrazolyl anions, and ^{19}F NMR signal of BF_4^- (-145 ppm). Equation (4) simply assembled all the necessary pieces together, and equation (5) was the balanced overall reaction equation.

Both **5A** and **5B** were fairly stable in air and very soluble in organic solvents. When KHF_2, KCN or KN_3 were used as substitutes for KSCN or AgF in similar substitution reactions with $ReO(HBPz_3)Cl_2$, black precipitates were formed and no pure compounds were obtained.

To investigate the direct addition of pyrazole with acetone, a different starting material, $ReOCl_3(PPh_3)_2$, a yellow, stable and sparely soluble compound, was used. When pyrazole was added, an acetone soluble green compound was formed initially that turned

to the blue compound **5C**. It was confirmed that **5C** contained an acetone-pyrazole condensed ligand.

For CH_3CHO, a blue solution and violet crystals of compound $ReOCl_2(PPh_3)$(pz-COHMe)·0.5CHOCHO **5D** were obtained. Acetaldehyde was found not only condensed with pyrazole to form the new ligand PzOCHMe, but also oxidized to yield glyoxal (CHOCHO) which has a boiling point 51°C and can be prepared by the oxidation of acetaldehyde by nitric or selenious acid. Compound **5D** was not as stable as **5C**. When compound **5D** was dissolved in acetone, it was converted to compound **5C**.

The green compound **5E** was obtained by similar reactions in two different solvents, CS_2 and MeCOEt. The attempted condensation reaction of pyrazole with CS_2 or MeCOEt was unsuccessful. When 3,5-dimethyl-pyrazole was used as a substitute for pyrazole in a very large excess (10:1), and reacted at reflux temperature in NCMe with $ReOCl_3(PPh_3)_2$, compound **5F** was obtained. In **5F**, no condensation had occurred, but two PPh_3 ligands were substituted by two 3,5-dimethyl-pyrazole ligands. This made **5F** different from **5E** not only by the substitution of the pyrazole ligands but also by the coordination environments around rhenium atoms. The formation of the oxygen bridged compounds **5E** and **5F** implied that the O atom may have come from oxygen molecules in the air or water in the solvent.

Investigations of the same reaction in other solvents were also conducted. In DMF, a green solution was formed. In DMSO, a colorless solution and colorless prism-shaped crystals were obtained. These species have not been investigated.

1-hydroxymethyl-3,5-dimethyl-pyrazole is the condensation product of CH_2O and 3,5-dimethyl-pyrazole, and is commercially available. It was used to react with $ReOCl_3(PPh_3)_2$, and the reaction mixture formed a blue solution very rapidly. The blue compound obtained from this reaction was found to be less stable than the compound **5G**,

a compound formed from the direct reaction of $ReOCl_3(PPh_3)_2$ with the bidentate ligand 4-hydroxymethyl-1,5-dimethyl-Imidazole. These two bidentate ligands have the desired geometry already so they can react quickly with the starting material. The C-CH_2OH bond in 4-hydroxymethyl-1,5-dimethyl-Imidazole was more stable than the N-CH_2OH bond in 1-hydroxymethyl-3,5-dimethyl-pyrazole, so the compound formed by the latter ligand was less stable than that of the former.

The advantage of having the desired geometry in the bidentate ligand 4-hydroxymethyl-1,5-dimethyl-Imidazole made the technetium compound **5H** quite stable and easy to prepare. Three ligands were found in the compound, two of which acted as bidentate ligands. The one that acted as a monodentate ligand was stabilized by strong intramolecular hydrogen bond through the free CH_2OH group.

5.5.2 Spectrometric Studies

The IR spectra of **5A** (Fig. 5A.1) and **5B** exhibited absorptions at 3117, 2525 and 982 cm^{-1} for **5A**, and 3139-3090, 2540, and 987, 970 cm^{-1} for (**B**), which were assigned to the C-H, B-H and Re=O stretches, respectively. The strong absorptions at 2059 and 2025 cm^{-1} for **5A** were assigned to the C=N stretches of two NCS^- ligands. The C-H stretches occurred at 3458-3415 cm^{-1} for **5B**. The C-H stretches and absorptions in the range 1500-500 cm^{-1} for **5B** were much more complicated than those of **5A**, and suggested that **5B** had more types of C-H bonds than **5A**, which was confirmed by ^1H NMR and X-ray analysis.

The ^1H NMR spectrum of **5A** is shown in Fig. 5A.2. The molecular geometry of **5A** required that two pyrazolyl rings were trans to two NCS^- ligands and had one pyrazolyl ring trans to a multiply bonded oxygen atom, so the protons in the compound can be grouped into two groups with a 2:1 integration ratio. In each pyrazolyl ring, the third and fifth position protons gave a doublet, the fourth position proton gave a triplet.

The pyrazolyl ring trans to the oxygen atom, which was more loosely coordinated to rhenium than the other two, donated less electron density than the other two rings, therefore, its protons appeared at higher field than those of the other two. In each ring, the third position was the most deshielded because of conjugation of the double bonds in the ring.

The ^{1}H NMR spectrum of **5B** was relatively complicated (Fig. 5B.3). The singlets at 2.398 and 1.899 ppm were assigned to the two methyl groups. In the pyrazolyl region, 12 protons showed up in 11 positions. The relative position of the four fourth position protons were assigned with help of the knowledge of the Re-N bond lengths related to each ring. The COSY experiment (two-dimensional homonuclear shift correlation technique) was used to map out all homonuclear couplings in the NMR spectrum of **5B** as shown in Fig. **5B**.4 Both axes correspond to the proton chemical shift in the same scale. The normal proton spectrum appears along the diagonal while all off-diagonal spots correspond to ^{1}H-^{1}H homonuclear couplings. The spectrum of the aromatic region of **5B** is presented in Fig. **5B**.4.. Therefore, the relative position of these protons could be assigned accordingly. The ^{1}H NMR signal of hydride (B-H) for **5A** was not observed, for **5B** a broad singal was observed at -0.41 ppm. For **5E**, only two distinctive pyrazolyl proton signals were observed, the other one might overlaped with phenyl protons.

The DEI mass spectrum of **5A** showed the parent ion for $ReO(HBPz_3)(NCS)_2$ (m/e, 532) and the characteristic isotopic distribution pattern (m/e 529, 13%; 530, 56%; 531, 33%; 532, 100%; 533, 19%; 534, 10%; 535, 2%;); expected from the formula (m/e 529, 13.40%; 530, 56.25%; 531, 33.08%; 532, 100.00%; 533, 18.71%; 534, 9.99%; 535, 1.51%;). The fragment peaks m/e 474 (M-NCS), m/e 406 (M-pz-NCS-H), were also assigned. The FAB+ mass spectrum of **5C** revealed the parent ion for **5C**, m/e 660, and fragment ions, m/e 625 (M-Cl), m/e 567 (M-Cl-acetone), m/e 460 ([$ReO(PPh_3)$-4H]$^+$. The

FAB+ mass spectrum of **5E** revealed the parent ion for **5E**, m/e 1150, and other fragment ions. The assignments of mass spectra are listed in the appropriate preparation section.

5.5.3 Structural Studies

Compound **5B** has four pyrazolyl rings in its cation structure, this is the highest known number of pyrazolyl rings contained in a rhenium compound to date. Compound **5B** crystallized in chiral space group $P2_12_12_1$. Compounds **5B**, **5C**, **5D**, **5G**, and **5H** had chiral centres at the rhenium atom.

Compounds **5C**, **5D**, and **5G** had the most diversified ligating atoms in their coordination sphere, each with five different types of ligating atoms. Compound **5G** had a structure similar to **5C** and **5D**, except that **5G** contained the 4-hydroxymethyl-1,5-dimethylimidazole ligand. The two Re-Cl bonds in each of these three compounds had significantly different lengths. This observation is discussed in Chapter 7.

Compound **5H** was a technetium compound, and had three 4-hydroxymethyl-1,5-dimethylimidazole ligands in its cation. One of the ligands in **5H** was monodentate, neutral and stabilized by an intramolecular hydrogen bond. The O(6C)-H bond length was 0.85 Å, H···O(6B) hydrogen bond distance was 1.91 Å, and O(6C)···O(6B) distance was 2.71 Å. The three hydrogen bond related atoms, O(6C)-H···O(6B), almost formed a straight line.

The molecules of **5E** and **5F** had two rhenium atoms and a rough 2 fold axis. The structures of compound **5E** and **5F** had bent O=Re-O-Re=O backbones. This contrasted with the linear O=Re-O-Re=O backbones found in compounds $[ReOCl_2py_2]_2O$ [99], $[ReOCl_2(1\text{-MeIm})_2]_2O$ [100], $K_3Na[ReO(CN)_4]_2O{\cdot}2H_2O$ [101], and $[ReOCl_2(3,5\text{-}Me_2HPz)_2]_2(\mu\text{-}O){\cdot}Me_2CO$ [102]. The bent O=Re-O-Re=O backbones in compounds **5E** and **5F** were caused by the bridging coordination of μ-pz or μ-3,5-Me_2pz to the two rhenium atoms in the compound. The arrangements of other ligands (in **5E** they are Cl^-

and PPh_3; in **5F** they are Cl^- and 3,5-Me_2Hpz) around the O=Re-O-Re=O backbones adopted staggered confirmation to minimize crowding.

In contrast to $[ReOCl(3,5\text{-}Me_2HPz)]_2(\mu\text{-}O)(\mu\text{-}3,5\text{-}Me_2Pz)_2$ (**5F**), a nearly linear O=Re-O-Re=O unit was present in $[ReOCl_2(3,5\text{-}Me_2HPz)_2]_2(\mu\text{-}O)\cdot Me_2CO$ prepared by Dahmann and Enemark [102], by reaction of NH_4ReO_4 with concentrated HCl and $K[HB(3,5\text{-}Me_2Pz)_3]$. In their compound, all four 3,5-Me_2HPz ligands acted as monodentate neutral ligands, while in **5F** two of them act as bidentate bridging monoanionic ligands $[\mu\text{-}3,5\text{-}Me_2Pz)]^-$, and two 3,5-$Me_2$HPz ligands act as monodentate neutral ligands. Compound **5F** could be viewed as a new compound formed from Dahmann and Enemark's compound by losing two HCl molecules, so compound **5F** has lower molecular weight but is still a neutral compound. Another remarkable feature of Dahmann and Enemark's compound was that acetone had not condensed with 3,5-Me_2HPz ligand, even though acetone was present in the crystal lattice. This was consistent with the observation that the attempted condensation reaction of 3,5-Me_2HPz and acetone did not occur. This might be caused by the steric effect of the 3,5-dimethyl groups in the ligand. Compound **5F** was found to be quite stable even in a mass spectrometer chamber at high temperature as it gave an intense molecular ion peak.

5.6 Comparison With the Related Research

Rhenium and technetium compounds containing $HBPz_3^-$ are of current interest. Degnan *et al.* [103] reported the syntheses of the high-oxidation state Re(VII) compounds $(pz)ReO_3$ and $(HBPz_3)ReO_3$, and the structure of the latter. They can be prepared easily in high yields by treating a solution of Re_2O_7 in THF with one equivalent of the sodium salts of the ligands, Na(pz) and $Na(HBPz_3)$, respectively. They were reported to be air-stable and the $HBPz_3^-$ compound showed no melting point or decomposition up to 250°C.

Thomas and Davison [104] reported three new methods to prepare $(HBPz_3)ReO_3$: the nitric acid oxidation of $[ReOCl_2(HBPz_3)]$; the thermolysis of $[ReO(eg)(HBPz_3)]$, where eg is ethylene glycolate; and the reaction of NH_4ReO_4 and $Na(HBPz_3)$ in acidified methanol; The technetium analogue, $(HBPz_3)TcO_3$, has also been synthesized.

Degnan *et al.* [105] reported the reduction of $(HBPz_3)ReO_3$ by PPh_3 in the presence of excess Me_3SiX (X = Br, Cl) to give the corresponding Re(V) complexes $[ReOX_2(HBPz_3)]$, the synthesis of $(HBPz_3)ReO(S_2C_6H_4)$, $(HBPz_3)ReO(S_2C_2H_4)$, and the structures of $(HBPz_3)ReO(Cl)(SC_6H_5)$, and $(HBPz_3)ReO(SC_6H_5)_2$. The thiolato derivatives were prepared by ligand substitution reactions of $[ReOCl_2(HBPz_3)]$ with thiols. Duatti *et al.* [106] reported the synthesis of the sulfido complexes $[MSCl_2(HBPz_3)]$ obtained by the reaction of $[MOCl_2(HBPz_3)]$ (M = Tc, Re) with B_2S_3 in dry deoxygenated dichloromethane.

Hamilton *et al.* [107] reported the synthesis of $(HBPz_3)ReH_6$, $(HBPz_3)ReH_4(PPh_3)$ and $\{CH_2(pz)_2\}ReH_7$. $(HBPz_3)ReH_6$ was obtained by treatment of $[ReOCl_2(HBPz_3)]$ with $LiAlH_4$ in THF at 25°C, followed by hydrolysis with H_2O in toluene at 0°C. The compound $(HBPz_3)ReH_4(PPh_3)$ was obtained by treatment of $(HBPz_3)ReCl_2(PPh_3)$ with $LiAlH_4$. Compounds $(HBPz_3)MCl_2(L)$ (M = Re, L = PPh_3; M = Tc, L = PPh_3, $OPPh_3$, and Py) were reported by Abrams *et al.* [108] and the structure of $[TcOCl_2(HBPz_3)]$ was reported by Thomas *et al.* [109].

Recently, Alberto *et al.* [110] reported the preparation and the structure of $(HBPz_3)Tc(CO)_2(PPh_3)$. This compound was reported to be remarkably stable against oxygen and water. Over 90% of the compound was found still present even after it was refluxed in a mixture of 30% H_2O_2 and methanol for 5 hours. Brown and Mayer reported the photolysis of the Re(V)O oxalate complex $(HBpz_3)ReO(C_2O_4)$ and presented evidence that the reactive transient produced on photolysis is the rhenium(III) oxo complex

[(HBpz$_3$)ReO] [98].

The above reports show that the HBPz$_3^-$ ligand can stabilize Tc and Re at high oxidation states as well as the low oxidation state for Tc. In contrast to all the above reports, compound **5B** provided an example of how the HBPz$_3^-$ can somehow split in a reaction and a new ligand can be formed between some of the fragments and the solvent (acetone). The cationic nature of **5B** also makes it different from other compounds.

The mechanism of the formation of the condensed ligand in **5B** was an interesting problem. After the structure of **5B** was determined, it was noticed that similar additions of electrophiles to the pyrazole nitrogen atom had been observed before, for molecules such as CS_2 [111], formaldehyde [112], $(CF_3)CO$ [113], and cyanate anion [114]. Copper-assisted addition of 3(5)-methylpyrazole to acetaldehyde [115], and molybdenum-assisted addition of pyrazole to acetone [116] had also been reported. Most of the authors claimed such condensation reactions were unexpected. In this study, a series of condensation reactions were attempted deliberately, and two of them (**5C** and **5D**) were successful.

5.7 Summary and Suggested Future Work

This part of the work focused on the synthetic and structural aspects of new oxorhenium(V) compounds which contained pyrazole or imidazole ligands. Pyrazole and its derivatives have demonstrated fairly flexible coordination abilities with rhenium. They can either condense with acetone or acetaldehyde to form the new ligands that coordinate simultaneously with the solvent fragments to form the rhenium coordination compounds, or act as a neutral monodentate ligand or a bidentate bridging ligand.

The new compounds **5A**, **5C**, **5D**, **5E**, **5F**, and **5G** were lipophilic and neutral, **5B** and **5H** were lipophilic and monocationic. The potentials for the application of these new compounds as radiopharmaceuticals might be worthy of investigation in the future.

One remarkable feature in this study was the rhenium-facilitated facile condensation of pyrazole with acetone, which was accidentally discovered by the study of the compound $ReO(HBPz_3)(PzOCMe_2)\cdot ReO_4$ (5B). It was confirmed by the designed preparation of the compound $ReOCl_2(PPh_3)(PzOCMe_2)$ (5C), and $ReOCl_2(PPh_3)(PzOCHMe)\cdot 0.5CHOCHO$ (5D). Acetaldehyde, CH_3CHO, not only condensed with pyrazole to form the new ligand PzOCHMe, but was oxidized also to yield glyoxal (CHOCHO).

Tertiary phosphine and related ligands have been employed in controlling reactivity, catalytic, and other properties of transition metal. The asymmetric metal centre as a chiral auxiliary may afford control of the stereochemistry of reactions taking place at organic ligands attached to the metal. The catalytic properties of the systems found in this work might also worthy of study in the future.

CHAPTER 6

SPATIAL STUDIES OF RHENIUM COMPOUND STRUCTURES

6.1 The Non-Bonding Sizes of Ligating Atoms

In a search for a proper set of radii to describe the sizes of ligating atoms in coordination compounds of technetium [10, 11], the conventional van der Waals radii taken from the "Handbook of Chemistry and Physics" [9] were examined, and were found too large to be used to describe the size of ligating atoms in the coordination space. The purpose of this study was to investigate the spatial requirements of the coordination sphere of rhenium compounds, so the van der Waals radii were traced to their sources.

The well known set of *van der Waals radii* of the nonmetallic elements was recommended by Bondi for volume calculations [117]. As noted by Bondi, however, his recommended values for Cl 1.75 Å, Br 1.85 Å, and I 1.97 Å were not in agreement with the shortest non-bonding distances observed in the crystal structures of the very simple diatomic molecules of Cl_2, Br_2, and I_2. The non-bonded interatomic distances of the nearest neighbours vary from 3.34 Å to more than 3.69 Å for Cl_2 [118], from 3.30 Å to 4.10 Å for Br_2 [119], and from 3.54 Å to 4.53 Å for I_2 [120]. If one-half of the shortest intermolecular distance is considered as the van der Waals radii, 1.67 Å, 1.65 Å, and 1.77 Å would be derived for Cl, Br, and I respectively. The set of van der Waals radii given

by Bondi was actually a set of intermolecular non-bonding radii, i.e. the values obtained from the non-bonding distances between atoms of different molecules. It would be wrong to simply use Bondi's van der Waals radii values to describe sizes of ligating atoms or ions in coordination compounds.

Bartell introduced the idea of *Limiting Intramolecular non-bonded radii* of atoms, X, taken as half the X...X distance in the compounds $H_2C{=}CX_2$ [121]. Glidewell extended this work [122]. Again, their radii could not be simply used to describe sizes of ligating atoms in coordination compounds. The bonding interactions between C and X were stronger in their compounds than the bonding interactions between the ligating atoms and the central metal atom in the coordination compounds of transition metals like rhenium, therefore the X...X non-bonding distances were shorter and their radii values were smaller than the real dimensions the ligating atoms occupies in coordination compounds.

Since ligating ions like Cl^-, etc., were often found in the coordination spheres of rhenium compounds, the ionic radii were also examined. Ionic radius refers to the size of the ion like Cl^- in NaCl rather than the size of atom-like Cl in Cl_2, even though their values may not have a big difference, and they are often hard to differentiate. The most recent and well accepted values of ionic radii were the so called "*Effective Ionic Radii*" (EIR) by Shannon and Prewitt [123], and revised by Shannon [124]. The EIR values were based on $r(O^{2-}) = 1.40$ Å, $r(F^-) = 1.33$ Å, and were extracted from the average bonding distance in oxides, halides and chalcogenides. The shortest non-bonding O...O distances in many simple oxides, ranging from 2.15 Å to 3.27 Å, are difficult to reconcile with the EIR value of O^{2-}, however, and the choice of $r(O^{2-}) = 1.40$ Å led to negative EIR values

for C^{4+}, N^{5+}, and H^{+}.

Shannon and Prewitt also derived a set of *Crystal Radii* (CR) based on r(F^{-}) = 1.19 Å and r(O^{2-}) =1.26 Å derived from the work of Fumi and Tosi [125]. The remarkable features of their CR values are that the alkali ions are larger and halogen ions are smaller than the traditional radii by about 0.14 Å, and they agree rather closely with those deduced from the X-ray maps of the electron distribution [126] for NaCl type of alkali halide structures.

The beauty of the approximate additivity of atomic or ionic radii to reproduce certain kinds of bond lengths tends to make people treat atoms or ions as hard spheres. Radii extracted from information on electron density distributions are probably the most accurate in the physical sense. But because atoms or ions are not rigid, an accurate radius in one compound may not be valid in another one. As pointed out by Shannon and Prewitt, if one assumes that the radius of an anion is the distance from the anion nucleus to the minimum in electron density between the anion and a cation, this radius may vary depending on the type of the cation. Again, the ionic radii obtained from simple structures like NaCl type of alkali halide can not be simply used for coordination compounds of rhenium.

So rigid, absolute, and unique radii values for ions or atoms which can be used for any types of interactions do not seem to exist. There was no magic in the numbers given by the previous scholars, but their general ideas, that the bonding distances or non-bonding distances could be used to extract certain types of radii, are still good and are followed in this study.

Table 6.1. Comparison of Different Radii (Å) for Some Nonmetallic Elements

	BD	SN	FT	BG	VR
H	1.20			0.92	1.27(8)
C	1.70			1.25	1.40(6)
N	1.55	1.46	(1.32)	1.14	1.45(8)*
O	1.52	1.40	(1.26)	1.13	1.37(8)*
F	1.47	1.33	1.16	1.08	1.38(7)
Si	2.10			1.55	
P	1.80			1.45	1.74(5)
S	1.80	1.84	(1.70)	1.45	1.70(5)
Cl	1.75	1.81	1.62	1.45	1.69(5)
As	1.85			1.61	1.78(4)
Se	1.90	1.98	(1.84)	1.58	
Br	1.85	1.96	1.76	1.59	1.82(5)
Te	2.06	2.21	(2.07)	1.87	
I	1.98	2.20	1.97	1.86	1.98(5)

BD = Bondi intermolecular van der Waals radii;

SN = Shannon effective ionic radii;

FT = Fumi and Tosi crystal radii, values in bracket are quoted from Shannon's table of

crystal radii;

BG = Bartell and Glidewell limiting intramolecular van der Waals radii;

VR = Virtual Radii, see text in 6.4 and below.

* see detailed analyses below.

The concept of **Virtual Radii** is proposed for the first time in this study. The definitions and procedures are stated below. A set of **Virtual Radii** are derived from *intramolecular* non-bonding distances of ligating atoms or ions of six coordinated rhenium compounds. The values of **Virtual Radii** were found more pertinent to describe the proper size of the ligating atoms in the coordination sphere of rhenium compounds, and other spatial parameters were derived to study the spatial requirements of coordination spheres of these rhenium compounds. Values of different radii are listed in Table 6.1.

6.2 Assumptions

There are two basic assumptions adopted in this study: (1) The limit of a three dimensional coordination space is a solid angle of 4π radians; (2) A ligating atom can be treated as a hard sphere in contact with its neighbours in the coordination polyhedron.

Assumption (1) is not as easy to visualize as that a straight line has an angle of π radians, and a two-dimensional plane has an angle of 2π radians, but it is a result of classical geometry for a three dimensional space. Assumption (2) is not always true, but it is the logical starting point for this study. An objective of this study is to find out to what extent this assumption holds true. The results are expressed in terms of Virtual Radii

(VR) and their standard deviations and Shape Index (SI).

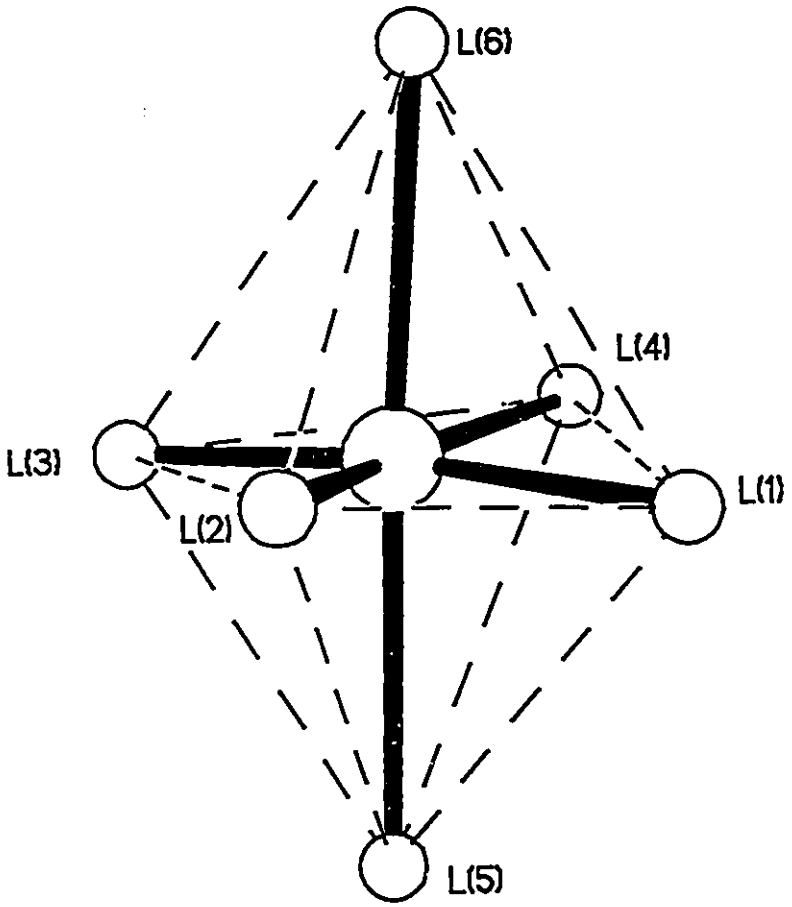

Fig. 6.1 A Typical Distorted Octahedral Coordination.

6.3 Definition of Virtual Radius (VR) and Shape Index (SI) of a Ligating Atom

In a stable structure, it is assumed that all the bonding interactions between central metal and ligating atoms as well as the non-bonding interactions among the ligating atoms reach equilibrium, as shown in Fig. 6.1. In Fig. 6.1 dashed lines represent the non-bonding interactions. The ligating atom numbering schemes are specified as in the following definitions. In an octahedral structure[1], the 6 bond lengths and 12 non-bonded interatomic distances can be used to describe the structure. From the 12 non-bonded interatomic distances, the intramolecular non-bonded radii of ligating atoms have been derived in the following way.

It is assumed that all the 12 non-bonded interatomic distances are the summation of the intramolecular non-bonded radii of related atoms. In other words, it is assumed that all the non-trans ligating atoms are in contact with each other. For example, in the triangle determined by atoms 1, 2 and 5, d12 = r1 + r2; d15 = r1 + r5; d25 = r2 + r5; so r1 could be derived as r1(25) = (d12 + d15 - d25)/2. Since there are four different faces of the octahedron related to one particular atom, for atom 1, three other expressions can be formulated as, r1(45) = (d14+d15-d45)/2; r1(26) = (d12+d16-d26)/2; r1(46) = (d14+d16-d46)/2. The best fitted radius for the ligating atom is obtained by averaging the four values obtained from the four faces. Thus

---

[1] The term octahedral is used in this study to describe any structure in which the ligating atoms form a rough octahedron. True octahedral symmetry is not implied.

$$VR1 = [r1(25)+r1(45)+r1(26)+r1(46)]/4$$

$$= (d12+d14+d15+d16)/4 - (d25+d26+d45+d46)/8 \quad \text{(eq. 6.1)}$$

The radius value obtained in such a way contains the information of 8 equilibrium interaction distances related to the atom in four faces, and therefore gives the best representation of the atom size in four directions. To distinguish the radii obtained in this way from other radii, the name **Virtual Radii (VR)** has been coined and used in this thesis. The purpose of VR is to represent the non-bonding interaction boundaries of ligating atoms in the coordination sphere around the central metal. In this thesis the metal is rhenium.

The **Virtual Radii (VR)**, obtained from real structures, represent the average range of intramolecular interactions of a ligating atom with other ligating atoms at equilibrium in the coordination space in the solid state. Even though the calculation focuses on the intramolecular distances among ligating atoms, other factors affecting the final equilibrium positions of ligating atoms (e.g. metal-ligand bonding interactions, substituent on the ligating atom), may also be represented in the values of VR. It is considered that Virtual Radii incorporate more information than all the previous methods, as shown in expression 6.1. Each VR is extracted from 8 related interactions. This is different from all previous methods used to obtain a radius, and should be expected to be more representative of the real situation.

The **Shape Index (SI)** for a ligating atom is defined as follow:

$$SI(VR1) = \{[VR1-r1(25)]^2 + [VR1-r1(45)]^2 + [VR1-r1(26)]^2 + [VR1-r1(46)]^2\}^{1/2}/2$$

$$= \{[r1(45)+r1(26)+r1(46)-3r1(25)]^2 + [r1(25)+r1(26)+r1(46)-3r1(45)]^2 + [r1(25)+r1(45)+r1(46)-3r1(26)]^2 + [r1(25)+r1(26)+r1(45)-3r1(46)]^2\}^{1/4}/4 \quad \text{(eq. 6.2)}$$

SI measures how good the r values obtained from each of the four faces of the octahedron agree with each other. For perfect octahedral coordination, for example, $ReCl_6^{2-}$, SI would be zero. The smaller the SI the closer the shape of the atom to a sphere. A bigger SI indicates that the different faces give a quite different radius of the atom; the coordination environments around the metal define a shape of the atom quite distorted from the shape of a sphere.

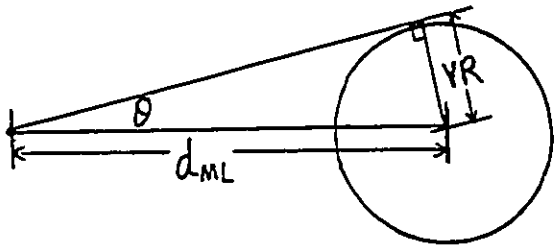

Fig. 6.2 The Relationship of Virtual Radius, Bond Length and Fan Angle of a Ligating Atom

6.4 Definitions of Solid Angle Model

The **Fan Angle (FA)**, θ, is half the angle subtended by a ligating atom. VR is the Virtual Radius of the ligating atom. d_{ML} is the bond length, as shown in eq. 6.3.

The **Solid Angle Factor (SAF)** is ratio of the solid angle of a ligating atom to the solid angle of the whole coordination space (4π), as shown in eq. 6.4.

The **Sum of the Solid Angle Factors (SSAF)** is the occupancy ratio of the coordination space by all the ligating atoms, as shown in eq. 6.5.

$$FA = \theta = \sin^{-1}(VR/d_{ML}) \qquad \text{(eq. 6.3)}$$

$$SAF = \frac{1}{4\pi}\int_0^{\theta}\int_0^{2\pi}\frac{r^2\sin\theta}{r^2}d\theta d\varphi = \frac{1}{2}(1-\cos\theta) \qquad \text{(eq.6.4)}$$

$$SSAF = \sum SAF_i \qquad \text{(eq. 6.5)}$$

In case of a perfect octahedron, the central metal atom is surrounded by six of the same kind of atoms with the same spatial parameters. The SI for each ligating atom is 0. The FA for each ligand is 45°, SAF is 0.1464. The SSAF of the compound is 0.8787. These parameters can be used as standard points to see how far a structure is away from a perfect octahedron.

6.5 Procedures

6.5.1 Data Retrieval

Data for rhenium crystal structures were retrieved from the 1993 version of the Cambridge Structural Database (CSD). Crystal structures that contained the molecular

fragment [$ReL_1L_2L_3L_4L_5L_6$] (L = any ligand, or ligating atom) with a nearly octahedral coordination around rhenium were screened manually and only structures which fulfilled all the following criteria were retained for further analysis: (1) the reported R factor < 0.10; (2) atomic coordinates were included in the CSD; (3) for multiple determinations of the same structure only the most accurate was retained; and (4) there was no disorder for the ligating atom. 707 fragments were obtained from CSD. Some recent rhenium compound structures (82 entries) were retrieved manually from publications based on the same criteria. 22 fragments from 12 rhenium compound structures determined in this study were also included. The final data files contained 811 fragments from 601 references.

6.5.2 Programs

All calculations were performed on PC 286, 386 or 486 computers. A program was written in C language and compiled with Turbo C^{++} to read an input data file, perform the calculations, and then write an output data file as described below. The program is attached in the appendix 6.1. Statistical analysis was conducted with the use of the software STATA [127].

One entry from the input data file and one entry from the output data file are listed here to illustrate the composition of the input and output data. These data files and related reference files are deposited on a magnetic disk.

6.5.3 Input Data File

The input data file was edited manually in the following format as shown in the sample entry. The first line contained the code name of the compound (which can be used

to search the reference and related information, and was the same as CSD if that entry was obtained from CSD); and the oxidation state of rhenium. The second line contained the cell parameters, a, b, c, α, β, and γ. The third line contained the label and coordinates (x, y, z) of the central metal atom. The fourth to the ninth lines contained the labels and coordinates of the six coordinating atoms.

A sample input entry:

```
#blue93  V
12.571  11.557  17.639  90  106.53  90
RE        0.72385   0.84753   0.16873
CL1       0.63034   0.66128   0.14434
CL2       0.73351   0.84507   0.03808
P         0.82254   1.03557   0.18544
N1        0.67516   0.86240   0.27464
O1        0.84519   0.79014   0.22434
O2        0.58132   0.92453   0.13749
```

The input sequence of the ligating atoms always followed the same order so that the three trans-pairs were known to the program. In the above input sample, CL1 and P, CL2 and N1, O1 and O2, were trans-pairs.

The interatomic distance, d, was calculated according to the following general

formula

$$d = [a^2(x_1-x_2)^2 + b^2(y_1-y_2)^2 + c^2(z_1-z_2)^2 - 2ab(x_1-x_2)(y_1-y_2)\cos\gamma$$
$$- 2ac(x_1-x_2)(z_1-z_2)\cos\beta - 2bc(y_1-y_2)(z_1-z_2)\cos\alpha]^{*}$$

Other parameters were calculated according to definitions stated above.

6.5.4 Output Data File

The first line showed the code name of the compound. The second to fourth lines showed the 12 non-bonding distances of the coordination octahedron. The fifth to tenth lines showed the ligating atom label, radius calculated from four different triangles, the average values of the four radii (VR) and the deviation of the four values (SI). The eleventh to sixteenth lines showed the atom label, the value of virtual radii, SI, Re to ligating atom bond length, Fan Angle, Solid Angle Factor, Oxidation state, and code name, for each ligating atom. The last line shows the Sum of the Solid Angle Factors (SSAF), oxidation state and code name of the compound.

A sample output entry:

#blue93

d12=3.330 d14=3.204 d15=3.055 d16=3.100

d23=3.347 d25=3.247 d26=3.080 d34=3.402

d35=2.913 d36=3.178 d45=2.671 d46=2.477

CL1 1.569 1.794 1.675 1.913 1.738 0.129

CL2 1.761 1.655 1.625 1.840 1.720 0.086

P 1.506 1.822 1.722 2.051 1.775 0.196

N1 1.410 1.291 1.351 1.580 1.408 0.108

O1 1.486 1.261 1.407 1.091 1.311 0.151

O2 1.425 1.186 1.456 1.126 1.298 0.144

CL1 1.738 0.129 2.432 45.623 0.150 V #blue93

CL2 1.720 0.086 2.342 47.264 0.161 V #blue93

P 1.775 0.196 2.478 45.765 0.151 V #blue93

N1 1.408 0.108 2.132 41.322 0.124 V #blue93

O1 1.311 0.151 1.696 50.622 0.183 V #blue93

O2 1.298 0.144 1.935 42.143 0.129 V #blue93

0.899 V #blue93

The format of the output data file may be varied for different needs at different stages of analysis.

6.5.5 Statistical Analyses

The unweighted sample mean was defined by $S = \Sigma S_i/n$, where S_i was the ith observation and n was the total number of observations. The sample standard deviation was defined by $\sigma = [\Sigma(S_i - S)^2/(n-1)]^{1/2}$.

Table 6.2 shows the statistics of parameters for different atoms. Table 6.3 shows the statistics of SSAF vs. oxidation state for rhenium compounds. Parameters listed in these two tables correspond to the distributions for nearly octahedral coordinated rhenium compounds. For a symmetrical, normal distribution, 95% of the observations may be

expected to lie within $\pm 2\sigma$ of the mean value.

Table 6.2

Statistics of Geometric Parameters for Ligating Atoms of Six Coordinated Rhenium Compounds

Variable	Obs	Mean	σ	Min	Max
As					
VR	48	1.776	.040	1.670	1.869
SI	48	.130	.048	.031	.234
BL	48	2.543	.043	2.477	2.646
FA	48	44.29	1.19	40.82	45.84
SAF	48	.142	.007	.122	.152
Br					
VR	118	1.817	.054	1.624	1.955
SI	118	.092	.048	0.000	.266
BL	118	2.600	.060	2.432	2.752
FA	118	44.38	1.56	39.79	49.39
SAF	118	.143	.010	.116	.175

C						
	VR	1848	1.403	.057	1.182	1.635
	SI	1848	.086	.056	0.000	.315
	BL	1848	1.958	.085	1.700	2.340
	FA	1848	45.84	2.11	38.21	53.51
	SAF	1848	.152	.013	.107	.203
Cl						
	VR	518	1.686	.051	1.503	1.848
	SI	518	.071	.055	.003	.226
	BL	518	2.396	.068	2.215	2.712
	FA	518	44.79	1.97	38.11	50.41
	SAF	518	.145	.012	.107	.181
F						
	VR	20	1.378	.074	1.292	1.551
	SI	20	.083	.078	.007	.237
	BL	20	2.002	.132	1.789	2.236
	FA	20	43.60	1.92	40.89	48.43
	SAF	20	.138	.012	.122	.168
H						

VR	137	1.274	.077	1.030	1.449
SI	137	.139	.051	.023	.254
BL	137	1.834	.097	1.489	2.103
FA	137	44.06	2.31	37.33	50.02
SAF	137	.141	.014	.102	.179
I					
VR	74	1.977	.052	1.903	2.138
SI	74	.110	.068	.005	.339
BL	74	2.805	.057	2.715	2.952
FA	74	44.85	1.67	41.16	50.49
SAF	74	.146	.010	.124	.182
N					
VR	548	1.454	.077	1.207	1.726
SI	548	.098	.062	.004	.326
BL	548	2.079	.175	1.648	2.456
FA	548	44.78	4.03	33.51	61.06
SAF	548	.146	.026	.083	.258
N, for BL ≤ 1.90 Å					
VR	104	1.361	.051	1.241	1.501

SI	104	.092	.065	.009	.292
BL	104	1.754	.054	1.648	1.895
FA	104	51.11	3.64	44.36	61.06
SAF	104	.187	.025	.142	.258
N, for BL > 1.90 Å					
VR	444	1.476	.065	1.207	1.726
SI	444	.099	.061	.004	.326
BL	444	2.155	.081	1.902	2.456
FA	444	43.30	2.33	33.51	49.64
SAF	444	.136	.014	.083	.176
O					
VR	558	1.373	.082	1.189	1.638
SI	558	.101	.068	.003	.325
BL	558	1.956	.199	1.576	2.465
FA	558	45.26	5.54	35.34	64.46
SAF	558	.150	.036	.092	.284
O, for BL ≤ 1.83 Å					
VR	186	1.333	.064	1.189	1.517
SI	186	.080	.057	.003	.256

BL	186	1.710	.042	1.576	1.802
FA	186	51.49	4.46	43.24	64.46
SAF	186	.190	.031	.136	.284

O, for BL > 1.83 Å

VR	372	1.393	.083	1.191	1.638
SI	372	.111	.070	.003	.325
BL	372	2.080	.115	1.830	2.465
FA	372	42.15	2.63	35.34	49.95
SAF	372	.130	.015	.092	.178

O, for 1.83 Å < BL ≤ 2.05 Å

VR	146	1.338	.065	1.191	1.475
SI	146	.084	.053	.003	.280
BL	146	1.958	.050	1.830	2.049
FA	146	43.17	2.43	38.22	48.02
SAF	146	.136	.014	.107	.166

O, for BL > 2.05 Å

VR	226	1.428	.073	1.243	1.638
SI	226	.129	.074	.006	.325
BL	226	2.158	.066	2.053	2.465

FA	226	41.49	2.55	35.34	49.95
SAF	226	.126	.015	.092	.178

O, for BL ≤ 1.71 Å

VR	108	1.349	.059	1.189	1.517
SI	108	.083	.054	.003	.256
BL	108	1.681	.021	1.576	1.709
FA	108	53.55	3.68	46.00	64.46
SAF	108	.204	.026	.153	.284

O, for BL ≤ 1.68 Å

VR	46	1.357	.060	1.189	1.460
SI	46	.088	.048	.010	.242
BL	46	1.663	.019	1.576	1.680
FA	46	54.87	3.69	46.00	62.24
SAF	46	.213	.026	.153	.267

O, for 1.68 Å < BL ≤ 1.71 Å

VR	62	1.343	.058	1.257	1.517
SI	62	.080	.058	.003	.256
BL	62	1.694	.008	1.681	1.709
FA	62	52.57	3.37	47.73	64.46

SAF	62	.197	.024	.164	.284
P					
VR	618	1.738	.054	1.551	1.907
SI	618	.135	.069	.005	.368
BL	618	2.449	.046	2.335	2.576
FA	618	45.26	1.69	39.51	51.28
SAF	618	.148	.011	.114	.187
S					
VR	169	1.697	.054	1.548	1.843
SI	169	.156	.079	.002	.347
BL	169	2.453	.083	2.239	2.610
FA	169	43.84	2.12	38.48	48.94
SAF	169	.140	.013	.109	.172

6.6 Results

6.6.1 Comparison of Virtual Radii With Other Sets of Radii

As shown in Table 6.1, the VR of H^- is 0.07 Å larger than the van der Waals radius given by Bondi. The VR of I^- is the same as Bondi. All the rest of the VR are smaller (Br 0.03 Å, As 0.07 Å, Cl 0.06 Å, S 0.10 Å, P 0.06 Å, F 0.09 Å, O 0.15 Å, N

0.10 Å, C 0.30 Å) than the corresponding values of Bondi. The VR of N and O atoms are quite close to the Effective Ionic Radii value given by Shannon. The VR of F is 0.05 Å larger than Shannon's value. All the rest of the VR are smaller (S 0.14 Å, Cl 0.12 Å, Br 0.14 Å, I 0.22 Å) than the corresponding value of Shannon. The VR of S and I are essentially the same as the crystal radii given by Fumi and Tosi. All the rest of the VR are larger (N 0.13 Å, O 0.11 Å, F 0.22 Å, Cl 0.07 Å, Br 0.06 Å) than the corresponding value of Fumi and Tosi. All the VR value are larger (H 0.35 Å, C 0.15 Å, N 0.31 Å, O 0.24 Å, F 0.30 Å, P 0.29 Å, S 0.25 Å, Cl 0.24 Å, As 0.17 Å, Br 0.23 Å, I 0.12 Å) than the corresponding *limiting intramolecular van der Waals radii* given by Bartell and Glidewell.

It was expected that VR should be smaller than the corresponding values of Bondi because in the coordination sphere the electron densities of ligating atoms should be more directed towards the central metal than in the cases studied by Bondi. The VR values should be larger than the corresponding values of limiting intramolecular van der Waals radius given by Bartell and Glidewell because the bonding interactions between the central metal and ligating atoms in coordination compounds should be weaker than covalent bonding situations studied by Bartell and Glidewell. In general, the lighter and softer atoms had a larger difference. The position and size of heavier atoms could be determined more precisely than those of lighter atoms. The sizes of softer atoms tend to vary more than the harder atoms.

This set of Virtual Radii provides more pertinent values which could be used in estimating the typical range of the intramolecular atomic distances in the coordination

spheres of rhenium compounds. It was noticed frequently that in literature the non-bonding intramolecular atomic distances were compared or discussed in term of conventional van der Waals radii values. These comparisons could be meaningless, however, from the statistical point of view, since the reliable ranges of van der Waals radii were not discussed.

By use of the set of Virtual Radii, for example, if one wants to compare the non-bonding intramolecular atomic distance between oxygen and chlorine atoms in a rhenium compound, 1.37(8) + 1.69(5) = 3.06(9). This would give a 65% confidence range from 2.97Å to 3.15Å, which makes more sense from the statistical point of view than the use of van der Waals radii, 1.35 + 1.81 = 3.16Å. One could argue that an O..Cl distance of less than 3.00Å could be normal in the coordination sphere, as some examples showed in Chapter 7.

6.6.2. Standard Deviations of Virtual Radii

The final set of the Virtual Radii, obtained from the average of hundreds of related values in different compounds, had standard deviations ranging from 0.04 Å to 0.08 Å, as shown in Table 6.1 and Table 6.2. In general, light atoms had a larger standard deviation ranging from 0.07 to 0.08 Å (H 0.08, N 0.08, O 0.08, F 0.07), and heavy atoms had a smaller standard deviation ranging from 0.04 to 0.05 Å (P 0.05, S 0.05, Cl 0.05, As 0.04, Br 0.05, I 0.05). This might be caused by the fact that the positions of heavy atoms could be more precisely determined by X-ray diffraction method than light atoms, so the boundaries (sizes) of heavy atoms in each structure were defined better than light

atoms. Among the atoms studied, carbon had a intermediate standard deviation of 0.06 Å. This might be caused by the fact that a large number of Re-C fragments were available to be used to obtain a better results than other light atoms.

6.6.3. The Distortion of Atom Shapes

The deviations of the same radius, obtained from four different faces of the octahedron determined by the coordinating atoms, were defined as Shape Index (SI). As shown in Table 6.2, the average SI values ranged from 0.07 Å to 0.16 Å (As 0.13(5), Br 0.09(5), C 0.09(6), Cl 0.07(6), F 0.08(8), H 0.14(5), I 0.11(7), N 0.10(6), O 0.10(7), P 0.14(7), S 0.16(8)). In general the softer atoms had larger SI values than the harder atoms. SI measures to what extent can an atom be viewed as a sphere. The average SI values indicate that the shape of S, P, H, and As atoms were among the most distorted atoms, Cl, F, Br, and C atoms were among the least distorted atoms, and I, N, and O atoms were among the intermediately distorted.

Deviations associated with distortions were much greater than the errors caused by the uncertainty of coordinates. The error caused by the uncertainty of coordinates normally was around the third or second decimal place for a distance or radius (see discussion section below), but the deviations associated with distortion occurred at the second or first decimal place of a radius. Even in the worst situations, the errors associated with the uncertainty of coordinates could be ignored compared to the distortion from face to face in the same compound (individual SI) and from compound to compound (average SI).

The difference between the average SI and the standard deviation of VR for a certain atom is that the former measures the average distortion (shape) of the atom in different compounds and the latter measures the distribution (range) of VRs of the atom in different compounds. The difference between these two parameters could be visualized in a situation where each individual VR of a certain atom is perfectly spherical, i.e. each of them had a SI value equal to 0.000, but each of them had a different VR value, therefore the average SI would be zero, but the standard deviation of VRs would be larger than zero. The results of these studies (Table 6.2) showed that the average SI for each atom was larger than the standard deviation of its VR, especially for those softer atoms. SI introduced another parameter which should be taken into consideration when the non-bonding distance is calculated.

6.6.4 The Total Average of Bond Length, Fan Angle and Solid Angle Factor

6.6.4.1 Bond Length (BL)

The total average bond lengths were obtained. As shown in Table 6.2, the total average bond lengths were Re-As 2.54(4) Å, Re-Br 2.60(6) Å, Re-C 1.96(9) Å, Re-Cl 2.40(7) Å, Re-F 2.00(13) Å, Re-H 1.83(10) Å, Re-I 2.81(6) Å, Re-N 2.08(18) Å, Re-O 1.96(20) Å, Re-P 2.45(5) Å, Re-S 2.45(8) Å. The total average of Re-N and Re-O bond lengths had substantially larger standard deviations than others, and they were grouped into certain subdivisions to conduct a more detailed analysis (section 6.7.5).

6.6.4.2 Fan Angle (FA)

The total average Fan Angle (FA) values and their standard deviations values were

As 44.3(1.2)°, Br 44.4(1.6)°, C 45.8(2.1)°, Cl 44.8(2.0)°, F 43.6(1.9)°, H 44.1(2.3)°, I 44.9(1.7)°, N 44.8(4.0)°, O 45.3(5.5)°, P 45.3(1.7)°, S 43.8(2.1)°. In general, the total average values were quite close to 45°, with some atoms slightly above and some atoms slightly below.

6.6.4.3 Solid Angle Factor (SAF)

The total average Solid Angle Factor (SAF) values and their standard deviations were As 0.142(7), Br 0.143(10), C 0.152(13), Cl 0.145(12), F 0.138(12), H 0.141(14), I 0.146(10), N 0.146(26), O 0.150(36), P 0.148(11), S 0.140(13). Again, the total average SAF values were quite close to 0.1464, the SAF of the ligating atom in a perfect octahedral structure, with some atoms slightly above and some atoms slightly below.

The total average values of FA and SAF for each ligating atom were quite close to the values for a perfect octahedron; therefore, the combinations of different ligating atoms in a real structure might also have a value of the Sum of the Solid Angle Factors (SSAF) quite close to that of a perfect octahedron, even though the sizes and bond lengths of different ligating atoms were varies a great deal.

6.6.5 The Statistics of SSAF Values vs. Oxidation States of Rhenium

The structural data of rhenium compounds were used to provide experimental tests of the basic assumption that the coordination space has a limit of solid angle 4π. Absolute values of structural parameters were used to obtain a quantitative evaluation. The statistics of the Sum of Solid Angle Factors (SSAF) of six coordinated rhenium environments are summarised in Table 6.3. Oxidation State I had the largest number and V had the second

largest number. The standard deviations (σ) were surprisingly small when it is realized that the SSAF value for each fragment was obtained from 15 independent variables.

Table 6.3

Statistics of the Sum of Solid Angle Factors for Six Coordinated Rhenium Atom Environments vs. the Oxidation States of Rhenium

OX	Obs.	Mean	σ	Min	Max
O	64	.886	.006	.880	.900
I	442	.888	.007	.874	.910
II	24	.884	.009	.873	.905
III	37	.882	.006	.874	.898
IV	32	.883	.006	.878	.899
V	171	.899	.011	.879	.938
VI	5	.893	.010	.885	.910
VII	36	.909	.013	.888	.932
Total	811	.8906	.0105	.873	.938

The previous studies for technetium compound [10, 11] gave a standard deviation of 0.065. The principle reason for such a big standard deviation in previous studies might

be that the "normalized van der Waals radii" were incorrect and did not describe the real sizes of ligating atoms. The "normalization" might had introduced some arbitrary errors to the calculations. Technetium compounds studied were not all six coordinated and this might be another reason for a large σ.

According to the statistics law, 95% of the fragments would fall into the $SSAF_{av}$ $\pm 2\sigma$ region, i.e. 0.891 $\pm$ 0.021 (0.870-0.912). This region could be viewed as a quantitative description of the stable region of the coordination sphere of a six coordinated rhenium compound.

The mathematical limit of the solid angle of the coordination space around a central metal is 4π. The solid angle factor of each ligating atom is its solid angle divided by 4π, therefore it is a measurement of the occupancy ratio of the coordination sphere by each ligating atom. The sum of the solid angle factors is the overall (three dimensional) measurement of the occupancy ratio of the coordination sphere by all the ligating atoms around the central metal.

Because of the balance between the bonding interactions and the non-bonding interactions, and the basic 4π limit of the solid angle of the coordination space, it was found that there exists a stable range of the occupancy ratio. This could be visualized physically by assuming that if there were free space around the metal atom, the metal would form some new bonds or attract the ligating atoms closer towards the metal to fill the space. If it were overcrowded around the metal, some bonds would be broken or lengthened to compensate the spatial requirement.

If the ligating atoms were treated as hard spheres and there were no overlaps of

ligating atoms, the SSAF value should not exceed 1.000, and for a perfect octahedron it should be 0.8787. The average SSAF value 0.891 obtained in this study implies that the radii of ligating atoms chosen were correct and no severe overlapping occurred.

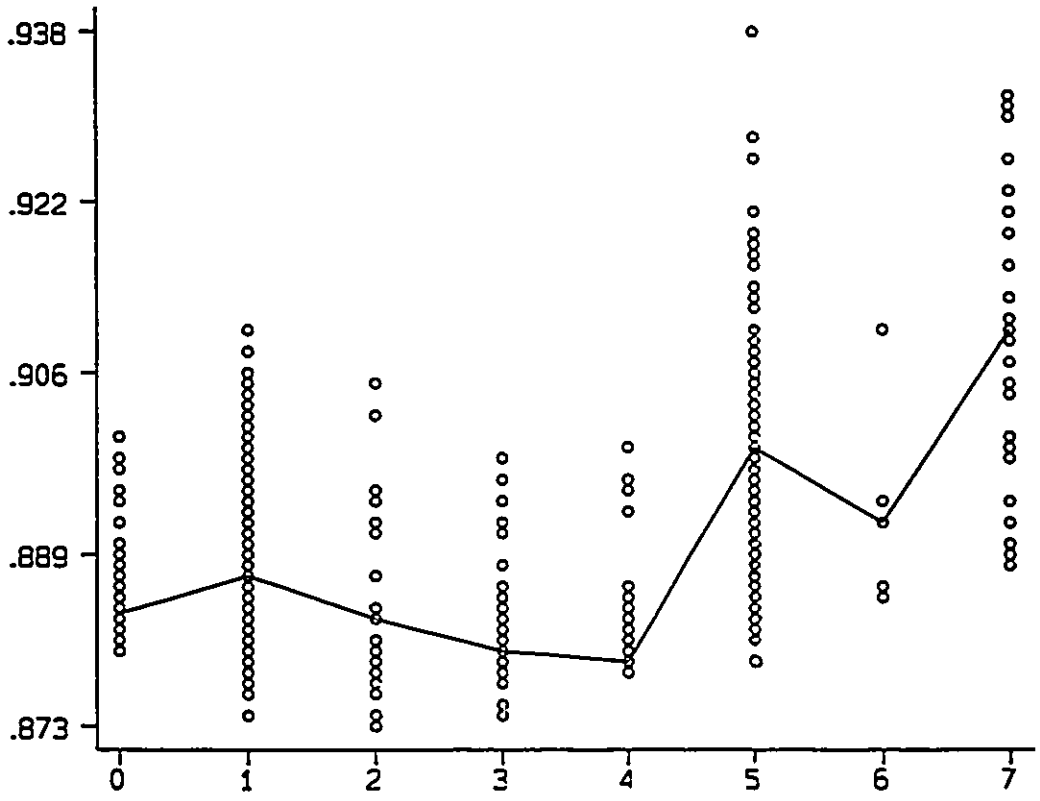

Fig. 6.3 The SSAF Values vs. the Oxidation States of Rhenium

The SSAF value is a index which is related to the size of ligating atoms, bond lengths, and coordination number. The consequence of the existence of a SSAF stable range is that the three parameters related to SSAF have to compensate each other to reach the stable SSAF range. This is consistent with the observation that higher coordination number is usually associated with longer bond lengths or smaller ligating atoms, and lower coordination number is usually associated with shorter bond lengths or larger ligating atoms. A plot of the SSAF data vs. the oxidation state is shown in Fig. 6.3. The general trend indicates that the higher the oxidation state of rhenium the higher the SSAF value of the compound. The reason for this trend might be that the rhenium-ligand bonding interactions were stronger when the oxidation state of rhenium was higher, and stronger bonding interactions caused shorter bond lengths, and perhaps slight overlaps of ligating atoms, and thus produced higher SSAF value.

The steric effect caused by the atom or group of atoms directly coordinated to the metal centre, which was referred to as the first-order steric effect, was usually a matter of more concern than the second-order steric effect caused by the remaining atoms of a coordinating group which are not themselves directly bonded to the metal centre. This was seen from the fact that the metal to ligating atom bond length, for example, Re-P bond length, may vary considerably from compound to compound, but the geometry of the fragments which were not bonded to metal, for example, the phenyl group Ph in PPh_3, varied relatively little. Nevertheless, the overall consideration of the whole ligand, not just the ligating atoms, are important in some cases, and further research could be built upon these studies.

6.6.6 The Statistics of Parameters of Ligating Atoms vs. the Oxidation States of Rhenium

The statistical details for various parameters as a function of the oxidation states of rhenium were summarized in the Appendix Table 6.ox.

In general, the higher the oxidation state of the rhenium atom, the smaller the VR of the atoms; the higher the oxidation state, the shorter the bond length. This general trend was expected as the result of the bonding interactions, i.e. the electronic effects of rhenium-ligating atom bonding interactions. When looking at the general trend, the number of observations in each subgroup should also be taken into consideration. The average value of a subgroup may not be representative if the number of observations is small.

The change of the Fan Angle or Solid Angle Factor as a function of the oxidation state of rhenium did not show a clear general trend. Because these two parameters are related to functions of VR/BL, as shown in their definitions (eq. 6.3 and eq. 6.4), their changing trend as a function of oxidation states of rhenium depended on how large was the influence of the oxidation states on VR and BL, and the consequence was that the variations of FA and SAF with the change of oxidation states were relatively small.

6.7 Discussions

6.7.1 The Transform of Degrees of Freedom in Processing of the Structural Data

In the treatment of each structure, 21 (7X3) coordinates were used. Among them,

there are only 15 independent degrees of freedom (21- 3 orientational degrees of freedom - 3 positional degrees of freedom). In the first stage of the treatment, the 12 edges of the coordination octahedron were obtained, which represented 12 independent degrees of freedom. The three independent degrees of freedom left determined the position of the central metal atom. This process can be viewed as building an octahedral cage with the six ligands first, into which the central metal is placed in a fixed position. This process recovered exactly the same picture as the original data. In the second stage, six Virtual Radii of six ligating atoms were obtained from the 12 edges, and six bond lengths of the ligating atoms were calculated. This counted for 12 independent degrees of freedom. To recover the original picture, another 3 angular degrees of freedom have to be fixed, i.e. there are 3 pairs of ligating atoms in a trans-relationship.

The transform of degrees of freedom can be summarized as the following 3 stages:

1) 7X3 = 21 coordinates - 3 positional - 3 orientational
   = 15 independent degrees of freedom
2) 12 octahedron edges + 3 coordinates of the central metal
3) 6 Virtual Radii + 6 bond lengths
   + 3 trans-pairs of ligating atoms (160-180°)

The analysis of independent degrees of freedom shows that the procedure extracted enough information to recover the original picture, whilst the **virtual radii** introduced some degree of averaging. It is surprising that the SSAF value of each structure fell in such a narrow range, as shown in Table 6.3, considering that 15 independent variables

were used to obtain the value.

6.7.2 Virtual Radii

Atoms exhibit characteristic properties which, in general, vary between relatively narrow limits, and exhibit additive contributions to the whole molecule. Therefore, the molecular properties, such as distances between atoms within a molecule, can be described with the use of certain characteristic atomic properties, such as atomic radii. Conversely, certain molecular properties, such as interatomic distances, can be reduced to extract some characteristic atomic properties, such as atomic radii.

The molecular structure hypothesis of chemistry is that a molecule is a collection of atoms linked by a three-dimensional network of bonds. As mentioned in section 6.1, in previous studies of atomic size, most of the attention has been focused on the metal-ligand bonding interactions, i.e. the bond lengths. For example, Shannon made a substantial effort to extract a set of 'Effective Ionic Radii' which was essentially aimed at defining the typical metal-ligand bond lengths. Knowledge of the metal-ligand bond lengths only is not enough to define the geometry of a coordination compound. The so called non-bonding interactions among ligands are equally important in defining the geometry of the molecule, i.e. the bond angles.

Virtual Radii are different from other radii in that they can be used to describe the typical ligand-ligand non-bonding distances around the central metal atom. The difference between these two aspects of structural parameters (bonding and non-bonding) can be visualized from the above degrees of freedom analysis. With the coordination cages (12

edges of the non-bonding distances) fixed, the central metal still has three independent degrees of freedom (to move along three diagonals of the cage) which need to be fixed to get a definite structure. On the other hand, with the 6 metal-ligand bond lengths fixed, there are still bond angles (and hence non-bonding distances) which need to be fixed in order to get the definite structure. So that the two sets of radii (bonding and non-bonding) represent two unique sets of structural information. Even though they are related, they can not replace each other in recovering the whole picture of the structure.

6.7.3 Errors Associated with the Uncertainty of Coordinates for the Calculations of the Virtual Radii

Without loss of generality, $\sigma_x = \sigma_y = \sigma_z$, where σ_x, σ_y and σ_z are errors of an atom's coordinates along three axes x, y and z. Thus, if atoms 1, 2 and 3 have isotropic errors of their coordinates, σ_1, σ_2 and σ_5, for distances from atom 1 to 2, d12, 1 to 5, d15, 2 to 5, d25, errors can be expressed as

$$\sigma(d12) = [\ \sigma_1^2 + \sigma_2^2\ ]^{1/2}$$

$$\sigma(d15) = [\ \sigma_1^2 + \sigma_5^2\ ]^{1/2}$$

$$\sigma(d25) = [\ \sigma_2^2 + \sigma_5^2\ ]^{1/2}$$

Consideration of the general equation for the error of a sum or difference, i.e. if $y = a \pm b$, $\sigma(y) = [\sigma(a)^2 + \sigma(b)^2]^{1/2}$ leads to the ordinary expression for

$$r1 = (d12 + d15 - d25)/2$$

then

$$\sigma(r1) = [\ \sigma(d12)^2 + \sigma(d15)^2 + \sigma(d25)^2\ ]^{1/2} /2$$

$$= [\ 2(\sigma_1^2 + \sigma_2^2 + \sigma_5^2)\ ]^{1/2} /2$$

Among σ_1, σ_2 and σ_5, suppose the largest value is σ_{max}, which normally would be associated with the lightest atom, then the upper limit of σ(r1) can be estimated as

$$\sigma(r1) \leq (3/2)^{1/2}\sigma_{max}$$

Because the Virtual Radius of VR1 is the average of four such r1 values obtained from four of the triangular faces related to atom 1,

VR1 = (d12+d15+d14+d16)/4-(d25+d26+d45+d46)/8

Similarly, it can be derived that

$$\sigma(VR1) \leq (1/4)^{1/2}(3/2)^{1/2}\sigma_{max} = (3/2)^{1/2}\sigma_{max}/2$$

For the typical light atoms like C, N, O, and F, the σ_{max} can be around 0.0005. For an average cell axis of 10 Å, σ(VR1) ≤ 0.003 Å. For an average cell axis of 20 Å, σ(VR1) ≤ 0.006 Å.

6.7.4 Statistics

It was considered that a sample of bond lengths and other related parameters could be averaged meaningfully if: (1) the sample was unimodally distributed; (2) the sample standard deviation (σ) was reasonably small; (3) there were no conspicuous outlying observations (those which occurred at > 4σ from the mean were eliminated from the sample, other outerliers were inspected carefully); (4) there was no compelling chemical reason for further subdivision of the sample.

Inspection of Table 6.2 shows that, in general, the sample standard deviations involving light atoms are larger than those involving heavier ones. This may be attributed

to the random errors raised from the rather poor location of light atoms in the presence of the heavy transition metals.

Besides the random errors, the larger standard variations of bond lengths and Virtual Radii may also reflect the softness of atoms, i.e. their sensitivity to their chemical and crystal environment. In addition it reflects unresolved chemical information, in the sense of other factors (such as the substituents on the ligating atoms, binding mode of the ligating atom) were not always explicitly taken into account in the tabulation. The analysis of the parameters as a function of the oxidation states of rhenium were conducted, as shown in the Appendix Tables of Chapter 6.

6.7.5 Detailed Analyses of Parameters of Oxygen and Nitrogen

Most of the samples were unimodally distributed, as shown in the Appendix Fig. 6.C, the distribution of Virtual Radii of carbon atoms. In cases of oxygen and nitrogen atoms the initial bond length distributions were clearly not unimodal as shown in the Appendix Figure 6.O and 6.N. They were resolved into their unimodal components based on bond lengths and oxidation states of rhenium, where well defined sub-distributions were observed. It was noted that for oxidation states IV, III, II, I, and O, there was no data available for Re-O bond length less than 1.72 Å. In other words, only the higher oxidation states like V, VI, and VII, which have a stronger bonding interactions, could have a Re-O bond length less than 1.72 Å. Details are summarized in the Appendix Table 6.O and 6.N. Ligating atom substituents may also influence the sub-distribution in some cases. In the longer term, as more structures are determined it will become possible to

derive more precise averages by further subdivision of the distributions.

6.7.6 How Do Structural Parameters Interact?

The definition for the Virtual Radius (eq. 6.1) of an atom in an individual structure dictates that the longer the non-bonding distance between the atom and the four neighbour ligating atoms the larger the Virtual Radius of the atom, and the longer the non-bonding distances between the other four related ligating atoms the smaller the Virtual Radius of the atom. As shown in eq. 6.1 and Fig 6.1, the first four non-bonding distances depend on the five metal to ligating atoms bond lengths and four bond angles related to the atom. The last four distances only depend on the four metal to ligating atoms bond lengths and the bond angles between the four atoms. It is clear that the Virtual Radius did not depend on the metal to the ligating atom bond length alone as it has in previous methods.

The definitions of FA and SAF require that the longer the bond length, the smaller the FA and SAF. If the bond length were imagined to be infinite, then the FA and SAF would became 0, and there would be no interactions between the atom and the central metal. On the other hand, the shorter the bond length, the larger the FA and SAF. But the bond length can not be too short, as there is a minimum length for every type of bond. This implies that only a certain fraction of the coordination sphere could be covered by one ligating atom.

From the definitions, it might be expected that the larger the size of the ligating atom the larger its FA and SAF. This is theoretically true, but in real structures, as shown in Table 6.2, the difference is not that obvious. An iodide ion, I^-, is larger than a hydri

ion H^-, and a Re-I bond length is usually longer than a Re-H bond length. These two parameters, radii and bond lengths, combine to give a new parameter, Solid Angle Factor. In contrast to expectation, Table 6.2 showed that the average values of SAF for I^- and H^- are quite close.

6.7.7 Anomalies Found in the Literature

This study provided a very sensitive tool to detect any unusual arrangement of atoms around a six coordinated central metal atom. For example, errors in some recent publications were found in the process of this study:

1. Wrong labelling: Inorg. Chim. Acta, 212 (1993) 23-29, Re-Cl2, and Re-P2, should be Re-Cl2', and Re-P2'. ibid, 213 (1993) 247-251, Re-P2 should be Re-P2'. ibid, 215 (1994) 159-163. N4 and N1 were bonded to Re, according to the published data, but their atomic numbering scheme in the diagram showed other atoms were bonded to Re.

2. Wrong coordinates: Acta Cryst. C49 (1993) 1424-1426, the coordinates of Cl give an Re-Cl distance of 2.278 Å, rather than the published value of 2.432 Å [128].

3. Wrong symmetry code: Can. J. Chem. 71 (1993) 2070-2077, one of the suggested symmetry codes, 1/4+y, 1/4+x, 1/4-z, should be -1/4+y, 1/4+x, 1/4-z.

4. Wrong bond angle: Inorg. Chim. Acta, 216 (1993) 223-228, the bond angle of N2-Re-N3, 101.2°, should be 173.1°.

These errors were detected because they caused large deviations of certain parameters used in this study away from the systematic trend. Atoms do not exist independently in the compound. It was through the relationships of a ligating atom to its

neighbour atoms and the overall fit of the structure that the errors in the literature were singled out from a large amount of data. The frequent appearance of certain errors for whatever reasons in the publications indicate that it is not trivial to spot an error and eliminate it. It was a real test for this study to be able to detect these errors.

6.8 Summary and Suggested Future Work

In the course of the studies described in this chapter, an extensive and systematic geometric analysis of the structural data of six coordinated rhenium compounds was conducted, to answer the question "What is a typical (ideal, stable) geometry of the coordination environment around the central metal in six coordinated rhenium compounds?" This study provided the set of mean values of Virtual Radii, Shape Index, bond lengths, Fan Angles, Solid Angle Factors, the Sum of Solid Angle Factors for each compound, and their corresponding standard deviations.

Six coordinated structures were chosen for the study because the majority of rhenium compounds are six coordinated, and six coordination is an intermediate coordination number for rhenium compounds. The structural data extracted for six coordination could be used, therefore, as a standard to compare compounds which have a coordination number lower or higher than six. Even though the Virtual Radii are obtained from 6 coordinated rhenium compounds, they could be used to estimate the situations in coordination compounds of other transition metals which are neighbours of rhenium.

Even though it is desirable to compare the same categories of compound, the

general procedures do not require that the central metal must be rhenium, and thus the study could be expanded to investigate other transition metal compounds.

CHAPTER 7

APPLICATIONS OF THE SOLID ANGLE MODEL

Quantitative measures of relative spatial parameters of ligands are useful in a variety of qualitative assessments, such as in the selection of ligands for a trial in a synthetic procedure. Interpretations and predictions of changes in coordination number, rough comparative equilibrium constants or reaction rates provide further examples of qualitative use. In this Chapter some qualitative use of the data provided by the Solid Angle Model is discussed with reference to the structures determined in this work.

For each unique coordination environment of the rhenium atom, the output data from the calculations gave the non-bonding distances, the Virtual Radii, the Shape Index, the parameters for the six ligating atoms, the oxidation state of rhenium, the code name, and the SSAF value of the compound, as described in Chapter 6, and the data are summarized in the Appendix Table 7.1 and 7.2.

7.1 The Extraction of Virtual Radii for Structures Determined in This Work

It can be seen in the Appendix Table 7.1, that in the coordination sphere, it is not uncommon for non-bonding distances between ligating atoms to be below the sum of their conventional van der Waals radii, shown in Table 6.1. For example, the shortest O...O

or C...O distances were around 2.60 Å for those carbonyl compounds (3A to 3E, Chapter 3), the shortest N...O non-bonding distances in compounds 5B to 5G (Chapter 5) were about 2.55 Å. The expected values are 2.77(10) Å and 2.82(11) Å (see Table 6.1).

The Virtual Radius for the same atom varies slightly from compound to compound, depending on its relationships with its neighbouring atoms in the coordination sphere and the overall fit of the structure.

The Shape Index (SI) values for the ligating atoms of carbonyl compounds are in the range of 0.16 to 0.23 Å, average 0.20 Å. The SI values for the ligating atoms of compound 4B are relatively small, in the range of 0.02 to 0.08 Å, average 0.05 Å. The SI values of compounds 5B to 5G are intermediate, in the range of 0.05 to 0.23 Å, average 0.12 Å. Shape Index is clearly related to the extent of the overall distortion of the structure away from the perfect octahedron.

7.2 Rhenium(I) Carbonyl Compounds

In the carbonyl compounds studied in Chapter 3, the bridging O atoms had a SAF of about 0.12, while the C atoms of the carbonyl groups had a SAF of about 0.17-0.18. This difference was caused by the Re-O bridging bonds (average 2.16 Å) which were longer than the Re-C (CO) bonds (average 1.90 Å), even though the two types of atoms were roughly the same size. There were three unique coordination environments of the rhenium atoms in 3A, two in 3B, and four in 3D. All of their SSAF were essentially the same and were close to the value of a perfect octahedron 0.8787.

A recent paper described the structural characterization of three complexes

$[HRe(CO)_4]_n$ (n = 2, 3, 4), in which the rhenium atoms were bridged by the hydride ions [129]. The Re-Re distances (Å) were 2.876 Å, 3.241 Å, and 3.439 Å for n = 2, 3, and 4, respectively. In these compounds, each rhenium atom had essentially an octahedral coordination environment and their bond angles were very close to 90°. In **3D** and **3E**, $K[Re(CO)_3]_n(OH)_{n+1}$, (n = 2, 3), each rhenium atom also had a near octahedral coordination (see Chapter 3, Table 3.2).

None of the carbonyl compounds determined in Chapter 3 had hydride ions in their structures. Even though the hydride ion is small, it has a substantial Solid Angle Factor in the coordination sphere (see Chapter 6. Table 6.2). It is important to notice that the hydride ions took nearly the same segment of the coordination space as OH^- or OR^-, even though H^- is smaller than OH^- or OR^-. The SSAF values of the carbonyl compound structures determined in this study indicated that there was not enough room in the coordination space of rhenium atoms to accommodate other possible ligands even as small as H^-. Their geometries and spectroscopic evidence confirmed that they are not hydride compounds.

7.3 Rhenium Nitrido-cyanide Compounds

7.3.1. Comparison of Structures of $K_2[ReN(CN)_4]\cdot H_2O$ (4A) and $(AsPh_4)_2[ReN(CN)_4(H_2O)]\cdot 5H_2O$ (4B)

As shown in the Appendix Table 7.3, in **4B** the atom N(5) occupied a much larger SAF (0.236) than the O atom (0.105) trans to it. The strong Re≡N bonding interaction caused a short bond (1.655 Å) and a large SAF for N(5). Trans to this, the weak Re-O

(H_2O) interaction caused a long bond (2.463 Å) and a small SAF for O atom. This caused the four CN^- ligands to be bent towards the ligating O (H_2O), as shown in Fig. **4B**.1 and bond angles of **4B** in Table **4B**.1.

In $K_2[ReN(CN)_4]\cdot H_2O$ (**4A**) the space trans to N≡Re was filled by a loosely coordinated nitrido N atom of another **4A** molecule, thus formed a ···N≡Re···N≡Re··· chain structure. Even though the coordination space trans to N≡Re was small, it may play a different role under different conditions. In **4B** the big cation $[AsPh_4]^+$ did not allow the $[ReN(CN)_4]^{2-}$ ions to line up to form a chain structure as in **4A**, so a weakly coordinated H_2O was necessary to fill the space trans to N≡Re. The coordination number of rhenium in **4A** could still be viewed as six. If N≡Re had a length of 1.65 Å, then Re···N would be 2.35 Å (see Chapter 4. where the N≡Re···N separation was determined as 4.005(1) Å), and this would give a FA about 38.9° (VR of N taken as 1.476 Å, see Table 6.2) and a SAF value 0.111 for Re···N quite near the SAF value (0.105) of the weakly bonded O (H_2O) in **4B**. Their SAF's difference, 0.006, is within the standard deviation 0.0105 for the statistics of overall packing of ligating atoms around six coordinated rhenium atoms, as shown in Chapter 6, Table 6.3.

7.3.2. Comparison of $(AsPh_4)_2[TcN(CN)_4(H_2O)]\cdot 5H_2O$ (4B') vs $(AsPh_4)_2[ReN(CN)_4(H_2O)]\cdot 5H_2O$ (4B)

The Tc≡N distance (1.60(1) Å) in **4B'** [74] is significantly shorter than the Re≡N distance (1.655 (4) Å, 5.4σ) in **4B** and the Tc-O distance (2.559 (9) Å) is significantly longer than the Re-O distance (2.463 (3) Å, 10.1σ). It was argued that the strong trans

influence of the Tc≡N system caused the long Tc-O distance [74], but non-bonding repulsions may be equally important in determining the structure. The average N(5)···C distance in the rhenium compound was 2.874 Å (vs. Tc, 2.844 Å), which was significantly shorter than the van der Waals distance 3.25 Å [117] (but in better agreement with the value expected from Virtual Radii, 2.85(10) Å, see Table 6.1). It is normal for distances between atoms bound to a mutual atom to be shorter than the normal van der Waals distance, the difference varying as the strength of the bonds. Thus it was expected the N(5)···C distances for the technetium compound to be slightly smaller than for the rhenium compound since the nitrogen atom was more strongly bound to the technetium atom. (The Bragg-Slater radii of the two metals were identical (Huheey, [130])). A contrasting effect was seen for the O···C distances (ave. Re, 2.990 Å; Tc, 3.038 Å). The van der Waals distance by Bondi was 3.22 Å [117] and Virtual Radii gave a non-bonding distance of 2.77(10) Å (Table 6.1) (or 2.94(8) Å, if VR of H_2O is 1.54(7) Å). In this case the oxygen atom bound to technetium was involved in the weaker bond, so the O···C distances are slightly longer for the technetium compound. Detailed comparison of these two compounds is provided in the Appendix Table 7.3.

7.4 Rhenium Pyrazolyl Compounds

7.4.1 The Bridging Oxo-atoms in $[ReOCl(PPh_3)]_2(\mu\text{-}O)(\mu\text{-}pz)_2\cdot CHCl_3$ (5E) and $[ReOCl(3,5\text{-}Me_2\text{-}HPz)]_2(\mu\text{-}O)(\mu\text{-}3,5\text{-}Me_2\text{-}Pz)_2$ (5F)

In compounds **5E** and **5F**, a nearly octahedral coordination environment around each metal atom was achieved by sharing one coordination atom, i.e. the bridging oxygen.

One advantage of sharing a ligating atom between two different metal atoms is that the spatial requirements of both metal atoms are effectively fulfilled simultaneously. The virtual radius and the SAF values of the bridging oxygen were smaller than the terminal ligating oxygen atoms. This can be explained in this way: since the bridging atom donated more of its electron density to the directional bonding interactions with two metal atoms instead of one metal atom, its non-directional non-bonding interactions with other ligating atoms become smaller.

7.4.2 The Re-Cl Bonds

In compounds **5C**, **5D** and **5G** one Re-Cl bond was substantially longer than the other one. The differences were 0.090(3)Å (2.432(2)-2.342(2)) in **5C**, 0.083(4)Å (2.420(2)-2.337(3)) in **5D**, and 0.050(8)Å (2.410(6)-2.360(6)) in **5G**.

Simplistic observations, such as the above mentioned. 'one Re-Cl bond is much longer than the other one in the same compound', are of little value if they are not rationalized on the basis of the overall structure.

In the coordination octahedron there were three trans-pairs of coordination atoms which could form three planes roughly perpendicular to each other. The sum of the Fan Angles of ligating atoms in these planes could be used to compare the non-bonding interactions in each plane. The sum of FA's (°) for the three planes are shown below:

In $ReOCl_2(PPh_3)(pz\text{-}COMe_2)$ (**5C**):

(1) CL1+CL2+P+N1 = 45.62 + 47.26 + 45.77 + 41.32 = 179.9

(2) CL1+O1+P+O2 = 45.62 + 50.62 + 45.77 + 42.14 = 184.2

(3) CL2+O1+N1+O2 = 47.26 + 50.62 + 41.32 + 42.14 = 181.3

In $ReOCl_2(PPh_3)$(pz-COHMe)·0.5CHOCHO (**5D**):

(1) CL1+CL2+N2+P = 48.17 + 45.03 + 40.61 + 45.27 = 179.1

(2) CL1+O1+N2+O2 = 48.17 + 54.11 + 40.61 + 40.20 = 183.1

(3) CL2+O1+P+O2 = 45.03 + 54.11 + 45.27 + 40.20 = 184.6

In $ReOCl_2(PPh_3)$(4-CH_2O-1,5-Me_2-Im)·$2H_2O$ (**5G**)

(1) CL1+CL2+P+N3A = 45.29 + 48.15 + 45.31 + 40.96 = 179.7

(2) CL1+O1+P+O2 = 45.29 + 51.36 + 45.31 + 41.54 = 183.5

(3) CL2+O1+N3A+O2 = 48.15 + 51.36 + 40.96 + 41.54 = 182.0

The values expected from the results of Chapter 6, Table 6.2:

(1) 44.8(20) + 44.8(20) + 45.3(17) + 43.3(23) = 178(4)

(2) 44.8(20) + 51.5(45) + 45.3(17) + 42.2(26) = 184(6)

(3) 44.8(20) + 51.5(45) + 43.3(23) + 42.2(26) = 182(6)

In the plane (1) that contained CL1 and CL2 atoms the two Cl atoms experienced the same non-bonding interactions. But in the planes that contained only CL1 (2) or CL2 (3) each Cl atom experienced a different non-bonding interactions. In the above three compounds, without exception, as indicated by the sum of FA's in the plane, the Cl atom

trans to the big PPh_3 ligand experienced a larger repulsion from the ligands of that plane than the Cl atom trans to the small N atom. This caused the Cl atom trans to PPh_3 to be further from the rhenium atom than the Cl atom trans to N atom. A longer bond generated a smaller FA to help relieve the repulsion.

In **5C**, the difference of FA(P) - FA(N1) = 4.45 (45.77-41.32) was compensated by the difference of FA(CL2) - FA(CL1) = 1.64 (47.26-45.62), so the difference of the sum of FAs between the two planes (2) and (3) was reduced 4.55 - 1.64 = 2.81. Similarly, in **5D** or **5G**, the difference of FA(P)-FA(N2) = 4.66 (45.27-40.61) or FA(P) - FA(N3A) = 4.35 (45.31-40.96), was compensated by the difference of FA(CL1) - FA(CL2) = 3.14 (48.17-45.03) or FA(CL2) - FA(CL1) = 2.86 (48.15-45.29), so the difference of the sum of FAs between the two planes (2) and (3) got even smaller (4.66 - 3.14 = 1.52 in **5D**, and 4.35 - 2.86 = 1.49 in **5G**). This indicated that each of the above plane tends to have roughly equal non-bonding interactions. The sum of FA values in each plane are quite close to what would be expected from the results of Chapter 6.

In perfect octahedral coordination, each ligating atom experiences the same interactions as other ligands, and the sum of FA's in each plane should be quite close to 180°. In an asymmetric or chiral compound, even though we were comparing two Re-Cl bonds in the same compound, each Cl experienced different non-bonding interactions, so that their bond lengths and angles changed to compensate for the differences. Planes (1), (2), and (3) were named here only for the convenience of discussions. In real structures atoms listed for these planes might not necessarily be in one plane.

After overall consideration of the coordination sphere, the so called "unusual long

Re-Cl bond" could be reasonably explained, and was more or less expected in such situations. In other words, it could be called "unusual" if the two Re-Cl bonds had the same length in such a chiral situation. It was the overall fit within a given set of ligands that determined their Re-Cl bond lengths.

So what is the consequence if one Re-Cl bond was longer than the other Re-Cl bond? Since the longer bond length means a weaker bond, reaction would be expected to occur through breakage of the weaker bond. Thus it is the Cl atom with the longer Re-Cl bond which might be expected to be replaced. Compound **5E**, $[ReOCl(PPh_3)]_2(\mu\text{-}O)(\mu\text{-}pz)_2 \cdot CHCl_3$, could be viewed as a logical product of **5C** or **5D**. The Cl atom trans to PPh_3, which had a longer Re-Cl bond in **5C** or **5D**, was replaced by the smaller N atom of the bridging pyrozolyl ligand in **5E**. The Cl atom cis to PPh_3 which had a shorter Re-Cl bond length in **5C** or **5D** remained in the product **5E**. This was consistent with the observations that the blue compounds **5C** or **5D** were eventually changed to the more stable green compound **5E** in solution.

7.5 Summary and Suggested Future Work

In many cases the determination of a crystal structure was an end in itself, and a crucial element in a research project. Chapters 6 and 7 have indicated some ways in which a broader view and some understanding of the structures can be obtained by study of a collection of structures.

Collections of structures were used to observe the range of geometries adopted by a molecular or submolecular fragment across a wide range of crystal (and/or molecular)

environments, and to examine the bond softness towards perturbation from whatever source. Such studies were of particular utility when molecular flexibility or reactivity were of importance.

In this type of study, the structure-structure correlation methodology can provide some insight into how structural parameters interact. This approach is linked to the desire to be able to engineer molecular structures so as to gain control of reactivity and catalytic properties of the species.

Procedures to obtain Virtual Radii and other structural parameters for six coordinated rhenium compounds were established in this work. Statistical methods were used to extract the typical parameters from a large collection of structural data. Nevertheless there remains much to be learnt about the nature of structural data. This will progress with further understanding of the theory and hypotheses that serve to motivate and rationalize the observation of certain correlations.

REFFERENCE

[1] Allen, F. H.; Bellard, S.; Brice, M. D.; Cartwright, B. A.; Doubleday, A., Higgs, H.; Hummelink, T.; Hummelink-Peters, B. G.; Kennard, O.; Motherwell, W. D. G.; Rogers, J. R.; Watson, D. G. *Acta Cryst.* **1979**, *B35*, 2331.

[2] Magneli, A. *Acta Cryst.* **1956**, *9*, 1038.

[3] Meisel, K. *Z. Anorg. Allg. Chem.* **1932**, *207*, 121.

[4] Cotton, F. A.; Boer, B. G. De; Mester, Z. C. *J. Am. Chem. Soc.* **1973**, *95*, 1159.

[5] Mucker, K. D. S.; Smith, G. S.; Johnson, Q. *Acta Cryst.* **1968**, *24*, 874.

[6] (a) Tolman, C. A. *J. Am. Chem. Soc.* **1970**, *92*, 2956. (b) Tolman, C. A. *Chem. Rev.* **1977**, *77*, 313.

[7] Immirzi, A. and Musco, A. *Inorg. Chim. Acta*, **1977**, *25*, L41.

[8] (a) Bagnall, K.W. and Li Xing-fu, *J. Chem. Soc., Dalton Trans.* **1982**, 1365. (b) Li Xing-fu, Feng Xi-zhang, Xu Ying-ting, Wang Hai-tung, Shi Jie, Liu Li and Sun Peng-nian, *Inorg. Chim. Acta*, **1986**, *116*, 85.

[9] Weast, R. C. ed., "Handbook of Chemistry and Physics", 69th edition, **1988**, CRC Press, Inc., D-188.

[10] Yi Wei, M. Sc. Thesis, Beijing Normal University, Beijing, PRC, **1987**.

[11] (a) Wei, Y.; Liu B.-L.; and Kung, H.F.; *Appl. Radiat. Isot.* **1990**, *41*, 763. (b) Kung, H.F.; Liu, B.-L.; Wei Y.; and Pan, S.; *Appl. Radiat. Isot.* **1990**, *41*,

[12] Cotton, F. A.; Curtis, A.; Robinson, G. *Inorg. Chem.* **1965**, *4*, 1696.

[13] Geilmann, M. and Wrigge. G. *Z. Anorg. Chem.* **1935**, *223*, 144.

[14] Birmingham, A. and Wilkinson, G. *J. Am. Chem. Soc.* **1955**, *77*, 3421.

[15] (a) Abrahams, C.; Ginsberg, K. and Knox. R. *Inorg. Chem.* **1964**, *3*, 558. (b) Franklin, K. J.; Lock, C. J. L.; Sayer, B. G.; Schrobilgen, G. J. *J. Am. Chem. Soc.* **1982**, *104*, 5303.

[16] Hieber, W. H. and Fuchs, A. *Z. Anorg. Chem.* **1941**, *248*, 256.

[17] Hieber, W. H.; Schuh, J. and Fuchs, A. *Z. Anorg. Chem.* **1941**, *248*, 243.

[18] Lock, C. J. L. and Wilkinson, G. *Chem. & Ind.* **1962**, 40.

[19] (a) Cotton, F. A. and Willkinson, G. "Advanced Inorganic Chemistry", 5th. Edn. Interscience-Wiley: New York, **1988**; pp.846-869. (b) Conner, K. A. and Walton, R. A. in "Comprehensive Coordination Chemistry" edited by Willkinson, G., Pergamon Press. 1987, pp.125-213. (c) Holloway, C. E. and Melnik, M. *Reviews in Inorg. Chem.* **1989**, 235. (d) Lebedev, K. B. "The Chemistry of Rhenium", London, Butterworths, **1962**. (e) Druce, J. G. F. "Rhenium", Cambridge University Press, **1948**. (f) Gonser, B. W. (edited), "Rhenium", Elsevier Publishing Company, **1962**. (g) Colton, R. "The Chemistry of Technetium and Rhenium", J. Wiley & Sons Ltd., London, **1965**. (h) Peacok, R. D. "The Chemistry of Technetium and Rhenium", Elsevier Publishing Co., Amsterdam, **1966**. (i) Lock, C. J. L. "Some Coordination Compounds of Rhenium", Ph.D. Thesis, University of London, UK, **1963**. 773.

[20] Abrams, M. J.; Davison, A.; Jones, A. G. *Inorg. Chim. Acta* **1984**, *82*, 125.

[21] Johnson, N. P.; Lock, C. J. L.; Wilkinson, G. *Inorg. Synth.* **1967**, *9*, 145.

[22] Stout, G. H.; Jensen, L. H. "X-Ray Structure Determination - A Practical Guide", 2nd edition, John Wiley & Sons, Inc. **1989.**

[23] Sheldrick, G. M., SIEMENS SHELXTL PC™, RELEASE 4.1, Siemens Analytical X-Ray Instruments, Inc. Madison, **1990.**

[24] Koch, B. and MacGillavry, C. H. "International Tables for X-ray Crystallography", Vol. III. Kynoch Press: Birmingham, England, **1974**; Table 3.2.2B.

[25] Bond, W. L. "International Tables for X-ray Crystallography", Vol. II, Kasper, J. S. and Lonsdale, K. eds., Kynoch Press: Birmingham, England, **1974**; Table 5.3.5B.

[26] Wilson, A. J. C. *Nature*, **1942**, *150*, 151.

[27] Walker, N.; Stuart, D. *Acta Cryst.* **1983**, *A39*, 158.

[28] Cromer, D. T.; Waber, J. T. "International Tables for X-ray Crystallography", Vol. IV. Eds: Ibers, J. A. and Hamilton, W. C., Kynoch Press: Birmingham, England, **1974**; Table 2.2B, pp 99-101.

[29] Cromer, D. T.; Ibers, J. A. "International Tables for X-ray Crystallography", Vol. IV. Eds: Ibers, J. A. and Hamilton, W. C., Kynoch Press: Birmingham, England, **1974**; Table 2.3.1, pp 149-150.

[30] Zachariasen, W. H. *Acta Cryst.* **1952**, *5*, 68.

[31] Sayre, D. *Acta Cryst.* **1952**, *5*, 60.

[32] Patterson, A. L. *Z. Krist.* **1935**, *A90*, 517.

[33] Derome, A. E. "Modern NMR Techniques for Chemistry Research", Pergamon

Press, **1987**.

[34] Martin, M. L.; Delpuech, J-J. and Martin, G. J. "Practical NMR Spectroscopy", Heyden, **1980**.

[35] Davis, R. and Frearon, M. "Mass Spectrometry", Chichester, New York, Wiley, **1987**.

[36] Colthup, N. B.; Daly, L. H. and Wiberley, S. E. "Introduction to Infrared and Raman Spectroscopy", Academic Press: New York, **1964**.

[37] Nakamoto, K. "Infrared and Raman Spectra of Inorganic and Coordination Compounds", 3rd ed., Interscience-Wiley: New York, **1978**.

[38] Hieber, W. H. and Schuster, L. *Z. Anorg. Allgem. Chem.*, **1956**, *285*, 205.

[39] Jayadevan, N. C. Ph. D. Thesis, McMaster University, **1968**.

[40] Gabe, E. J.; Page, Y. Le; Charland J. -P.; Lee, F. L.; White, P. S. *J. Appl. Cryst.* **1989**, *22*, 384.

[41] Horn, E. and Snow, M. R. *Aust. J. Chem.*, **1981**, *34*, 737.

[42] Harrison, W.; Marsh, W. C. and Trotter, J. *J. Chem. Soc. Dalton Trans.*, **1972**, 1009.

[43] Braterman, P. S. *J. Chem. Soc., (A)*, **1968**, 2907.

[44] Herberhold, M. and Suss, G. *Angew. Chem., Int. Ed. Engl.*, **1975**, *14*, 700.

[45] Herberhold, M.; Suss, G.; Ellermann J.; and Gabelein, H. *Chem. Ber.*, **1978**, *111*, 2931.

[46] Nuber, B.; Oberdorfer, F.; and Ziegler, M. L. *Acta Cryst.*, **1981**, *B37*, 2062.

[47] Copp, S. B.; Subramanion, S. and Zaworotko, M. J. *Angew. Chem. Int. Ed. Engl.*

1993, *32*, 706.

[48] (a) Ciani, G.; D'Alfonso, G.; Freni, M.; Romiti, P.; Sironi, A. *J. Organomet. Chem.* **1981**, *220*, C11. (b) Churchill, M. R.; Bird, P. H.; Kaesz, H. D.; Bau, R.; Fontal, B. *J. Am. Chem. Soc.* **1968**, *90*, 7135.

[49] Beringhelli, T.; D'Alfonso, G.; Freni, M.; Ciani, G.; Moret, M.; Sironi, A. *J. Organomet. Chem.* **1988**, *339*, 323.

[50] Beringhelli, T.; Ciani, G.; D'Alfonso, G.; Sironi, A.; Freni, M. *J. Organomet. Chem.* **1982**, *233*, C46.

[51] Huie, B. T.; Kirtley, S. W.; Knobler, C. B.; Kaesz, H. D. *J. Organomet. Chem.* **1981**, *213*, 45.

[52] Abel, E. W.; Crosse, B. C. *J. Chem. Soc. (A).* **1966**, 1141.

[53] Ciani, G.; D'Alfonso, G.; Freni, M.; Romiti, P.; Sironi, A. *J. Organomet. Chem.*, **1981**, *219*, C23.

[54] Cotton, F. A.; Wilkinson, G. "Advanced Inorganic Chemistry", 5th. Edn. Interscience-Wiley: New York, 1988; pp 525-6.

[55] (a) Bruce, D. M. Holloway, J. H.; Russell, D. R. *J. Chem. Soc., Dalton Trans.* **1978**, 1627. (b) Bruce, D. M. Holloway, J. H.; Russell, D. R. *J. Chem. Soc., Dalton Trans.* **1978**, 64. (c) Zalkin, H.; Hopkins, T. E.; Templeton, D.H. *Inorg. Chem.* **1966**, *5*, 1189. (d) Cotton, F. A.; Daniels, L. M. *Acta Cryst.* **1983**, *C39*, 495. (e) Churchill, M. R.; Amoh, K. N. *Inorg. Chem.* **1981**, *20*, 1609. (f) Darst, K. P.; Lenhert, P. G.; Lukehart, C. M.; Warfield, L.T. *J. Organomet. Chem.* **1980**, *195*, 317.

[56] Herrmann, W. A.; Alberto, R.; Bryan, J. C. and Sattelberger, A. P. *Chem. Ber.* **1991**, *124*, 1107.

[57] (a) Marsh, R. E.; Herbstein, F. H. *Acta Cryst.* **1983**, *B39*, 280. (b) Herbstein, F. H.; Marsh, R. E. *Acta Cryst.* **1982**, *B38*, 1051. (c) Marsh, R. E.; Herbstein, F. H. *Acta Cryst.* **1988**, *B44*, 77.

[58] Ciani, G.; Sironi, A. and Albinati, A. *Gazz. Chim. Ital.* **1979**, *109*, 615.

[59] Kolobova, N. E.; Zdanovich, V. I.; Lobanova, I. A.; Andrianov, V. G.; Struchkov, Y. T.; Petrovskii, P. V. Izv. *Akad. Nauk. SSSR, Ser. Khim. (English edition)* **1984**, 871.

[60] Herrmann, W. A.; Mihalios, D.; Öfele, K.; Kiprof, P. and Belmedjahed, F. *Chem. Ber.* **1992**, *125*, 1795.

[61] Nakamoto, K. "Infrared and Raman Spectra of Inorganic and Coordination Compounds", 3rd ed., Interscience-Wiley: New York, **1978**; p 286.

[62] Dehnicke, K. and Strähle, J. *Angew. Chem., Int. Ed. Eng.*, **1981**, *20*, 413.

[63] (a) Clifford, A. F. and Olson, R. R. *Inorg. Synth.*, **1960**, *6*, 167. (b) Chatt, J.; Garforth, J. D.; Johnson, N. P. and Rowe, G. A. *J. Chem. Soc.*, **1964**, 1012. (c) Lock, C. J. L. and Wilkinson, G. *ibid.*, **1964**, 2281.

[64] Davies, W. O.; Johnson, N. P.; Johnson, P. and Graham, A. J. *Chem. Comm.*, **1969**, 736.

[65] Rouschias, G. *Chem. Rev.*, **1974**, *74*, 533.

[66] Britten, J. F.; Lock, C. J. L.; Wei, Yi. *Acta Cryst.* **1993**, *C49*, 1277.

[67] Chatt, J., Falk C. D., Leigh, G. J. & Paske, R. J. *J. Chem. Soc. (A).* **1969**, 2288.

[68] Johnson, N. P. *J. Chem. Soc. (A)*, **1969**, 1843.

[69] Fenn, R. H.; Graham, A. J. and Johnson, N. P. *J. Chem. Soc. (A)*, **1971**, 2880.

[70] Baldas, J.; Colmanet, S. F. and Williams, G. A. *J. Chem. Soc., Chem. Commun.*, **1991**, 954.

[71] (a) Booth, M. R. and Frankiss, S. G. *Spectrochim. Acta*, **1970**, *26A*, 859. (b) Durig, J. R.; Li, Y. S. and Turner, J. B. *Inorg. Chem.*, **1974**, *13*, 1495.

[72] Howard-lock, H. E.; Lock, C. J. L. and Turner, G. *Spectrochim. Acta*, **1982**, *38A*, 1283.

[73] Trop, H. S.; Jones, A. G. and Davison, A. *Inorg. Chem.*, **1980**, *19*, 1993.

[74] Baldas, J.; Boas, J. F.; Colmanet, S. F.; Mackay, M. F. *Inorg. Chim. Acta.* **1990**, *170*, 233.

[75] Liese, W.; Dehnicke, K.; Walker, I. and Straehle, J.; *Z. Naturforsch. Teil B*, **1980**, *35*, 776.

[76] Chatt, J. and Dilworth, J. R. *J. Chem. Soc., Chem. Commun.*, **1974**, 517.

[77] Liese, W.; Dehnicke, K.; Walker, I. and Strähle, J. *Z. Naturforsch. Teil B*, **1979**, *34*, 693.

[78] Doedens, R. J. and Ibers, J. A. *Inorg. Chem.*, **1967**, *6*, 204.

[79] Corfield, P. W. R.; Doedens, R. J. and Ibers, J. A. *Inorg. Chem.* **1967**, *6*, 197.

[80] Forsillini, E.; Casellato, U.; Graziani, R. and Magon, L. *Acta Cryst.* **1982**, *B38*, 3081.

[81] Liese, W.; Dehnicke, K.; Rogers, R. D.; Shakir, R. and Atwood, J. L. *J. Chem. Soc., Dalton Trans.*, **1981**, 1061.

[82] Kafitz, W.; Weller, F. and Dehnicke, K. Z. *Anorg. Allg. Chem.* **1982**, *490*, 175.

[83] Carrondo, M. A. A. de C. T.; Shakir, R. and skapski, A. C. *J. Chem. Soc., Dalton Trans.*, **1978**, 844.

[84] Fletcher, S. R. and Skapski, A. C. *J. Chem. Soc., Dalton Trans.* **1972**, 1079.

[85] Purcell, W.; Damoense, L. J. & Leipoldt, J. G. *Inorg. Chim. Acta*, **1992**, *195*, 217.

[86] Purcell, W.; Potgieter, I. Z.; Damoense, L. J. & Leipolldt, J. S. *Transition Met. Chem.* **1991**, *16*, 473.

[87] Murmann, R. K. and Schlemper, E. O. *Inorg. Chem.*, **1971**, *10*, 2352.

[88] Manoli, J. -M.; Potvin, C.; Bregeault, J. -M. and Griffith, W. P. *J. Chem. Soc., Dalton Trans.*, **1980**, 192.

[89] Shandles, R.; Schlemper, E. O. and Murmann, R. K. *Inorg. Chem.*, **1971**, *10*, 2785.

[90] Lumme, P.O.; Turpeinen, U. and Stasicka, Z. *Acta Cyrst.*, **1991**, *C47*, 501.

[91] Purcell, W.; Roodt, A.; Basson, S. S. and Leipoldt, J. G. *Transition Met. Chem.*, **1990**, *15*, 239.

[92] (a) Roodt, A.; Lisbon, K.; Cutler, C.; Deutsch, E.; Thomas, S. R.; Maxon, H. R.; *J. Nucl. Med.* **1989**, *30*, 732. (b) Bläuenstein, P. *New J. Chem.*, **1990**, *14*, 405.

[93] Egan, J. W.; Haggerty, Jr. B. S.; Rheingold, A. L.; Sendlinger, S. C. and Theopold, K. H. *J. Am. Chem. Soc.* **1990**, *112*, 2445.

[94] Kitajima, N.; Fujisawa, K.; Fujimoto, C.; Moro-oka, Y.; Hashimoto, S.; Kitagawa, T.; Toriumi, K.; Tatsumi, K. and Nakamura, A. *J. Am. Chem. Soc.* **1992**, *114*,

1277.

[95] Armstrong W. H. and Lippard, S. J. *J. Am. Chem. Soc.* **1984**, *106*, 4632.

[96] Kitajima, N.; Fukui, H.; Moro-oka, Y.; Mizutani, Y. and Kitagawa, T. *J. Am. Chem. Soc.* **1990**, *112*, 6402.

[97] Looney, A.; Parkin, G.; Alsfasser, R.; Ruf, M. and Vahrenkamp, H. *Angew. Chem. Int. Ed. Engl.* **1992**, *31*, 92.

[98] Brown, S. N.; Mayer, J. M. *Inorg. Chem.* **1992**, *31*, 4091.

[99] Lock, C. J. L. & Turner, G. *Can. J. Chem.* **1978**, *56*, 179.

[100] Pearson, C. & Beauchamp, A. L. *Acta Cryst.* **1994**, *C50*, 42.

[101] Lumme, P. O.; Turpeinen, U. Stasicka, Z. *Acta Cryst.* **1991**, *C47*, 501.

[102] Dahmann, G. B.; Enemark, J. H. *Inorg. Chem.* **1987**, *26*, 3960.

[103] Degnan, I.; Herrmann, W. A. and Herdtweck, E. *Chem. Ber.*, **1990**, *123*, 1347.

[104] Thomas, J. A. and Davison, A. *Inorg. Chim. Acta*, **1991**, *190*, 231.

[105] Degnan, I.; Behm, J.; Cook, M. R. and Herrmann, W. A. *Inorg. Chem.* **1991**, *30*, 2165.

[106] Duatti, A.; Tisato, F.; Refosco, F.; Mazzi, U. and Nicolini, M. *Inorg. Chem.* **1989**, *28*, 4564.

[107] Hamilton, D. G.; Luo, X.-L. and Crabtree, R. H. *Inorg. Chem.* **1989**, *28*, 3198.

[108] Abrams, M. J.; Davison, A. and Jones, A. G. *Inorg. Chim. Acta*, **1984**, *82*, 125.

[109] Thomas, R. W.; Estes, G. W.; Elder, R. C. and Deutsh, E. *J. Am. Chem. Soc.* **1979**, *101*, 4581.

[110] Alberto, R.; Herrmann, W. A.; Kiprof, P. and Baumgärtner, F. *Inorg. Chem.* **1992**,

31, 895.

[111] Bereman, R. D.; Shields, G. D.; Nalewajek, D. *Inorg. Chem.* **1978**, *17*, 3713.

[112] Hüttel, R.; Jochum, P. *Chem. Ber.* **1952**, *85*, 820.

[113] (a) Mahler, W. S. *U.S. Patent* 3 265 705 (**1966**). (b) Volz, K.; Zalkin A.; Templeton, D. H. *Inorg. Chem.* **1976**, *15*, 1827.

[114] Valach, F.; Kohout, J.; Dunaj-Jurco, M.; Hvastijova, M.; Gazo, J.; *J. Chem. Soc. Dalton Trans.* **1979**, 1867.

[115] Hoedt, R. W. M.; Hulsbergen, F. B.; Verschoor, G. C.; Reedijk, J. *Inorg. Chem.* **1982**, *21*, 2369.

[116] (a) Calhorda, M. J.; Dias, A. R. *J. Organomet. Chem.* **1980**, *197*, 291. (b) Carrondo, M. A. A. F. De C. T.; Domingos, A. M. T. S. *J. Organomet. Chem.* **1983**, *253*, 53.

[117] Bondi, A. *J. Physical Chem.*, **1964**, *68*, 441.

[118] Colin, R. L. *Acta Cryst.*, **1952**, *5*, 431.

[119] Vonnegut, B. and Warren, B. E. *J. Am. Chem. Soc.*, **1936**, *58*, 2459.

[120] Harris, J. *J. Am. Chem. Soc.*, **1928**, *50*, 1583.

[121] Bartell, L. S. *J. Chem. Phys.*, **1960**, *32*, 827.

[122] Glidewell, C. *Inorg. Chim. Acta*, **1975**, *12*, 219., and **1976**, *20*, 113.

[123] Shannon R. D. and Prewitt, C. T. *Acta Cryst.*, **1969**, *B25*, 925.

[124] Shannon, R. D. *Acta Cryst.*, **1976**, *A32*, 751.

[125] (a) Fumi, F. G. and Tosi, M. P. *J. Phys. Chem. Solids*, **1964**, *25*, 31. (b) Tosi, M. P. and Fumi, F. G. *J. Phys. Chem. Solids*, **1964**, *25*, 45. (c) Tosi, M. P. *Solid State*

Physics, **1964**, *16*, 1.

[126] (a) Meisalo, V. and Inkinen, O. *Acta Cryst.*, **1967**, *22*, 58. (b) Schoknecht, *Z. Naturf.*, **1957**, *12a*, 983. (c) Krug, J.; Witte, H. and Wolfel, E. *Z. Phys. Chem.*, **1955**, *4*, 36.

[127] Hamilton, L. C. "Statistics with STATA", Brooks/Cole Publishing Company, Pacific Grove, California, **1990**.

[128] Private communication with Dr. I.D. Brown, Department of Physics, McMaster University, confirmed that there was an error for the coordinates concerned.

[129] Masciochi, N; Sironi, A. and D'Alfonso, G. *J. Am. Chem. Soc.* **1990**, *112*, 9395.

[130] Huheey, J. E. "Inorganic Chemistry", 2nd. Edn., Harper & Row, New York, **1978**, pp. 232-233.

Appendix Table 3.1
Crystallographic Data for Compounds 3D, 3A, 3E, 3C, and 3B

Compound	$K[Re_2(OH)_3(CO)_6]\cdot 2H_2O$ (3D)
Empirical Formula	$C_6 H_7 K O_{11} Re_2$
Color; Habit	Colorless needle
Crystal size (mm)	.21 X .07 X .06
Crystal System	Monoclinic
Space Group	C2/m
Unit Cell Dimensions	$\underline{a}$ = 22.538(5) Å
	$\underline{b}$ = 10.328(3) Å
	$\underline{c}$ = 12.458(3) Å
	$\underline{\beta}$ = 106.68(2)°
Volume	2778(1) $Å^3$
Z	8
Formula weight	666.6
Density(calc.)	3.188 Mg/m^3
Absorption Coefficient	17.764 mm^{-1}
F(000)	2400
Diffractometer Used	Siemens R3m/V
Radiation	AgKα (λ = 0.56086 Å)
Temperature (K)	173
2θ Range	5.4 to 45.1°
Index Ranges	0≤h≤30, 0≤k≤14,
	-17≤l≤16
Reflections Collected	4010
Independent Reflections	3916 (R_{int} =2.81%)
Observed Reflections	3912 ($F \geq 0.0\sigma(F)$)
Absorption Correction	0.928-1.092
Weighting Scheme	$w^{-1} = \sigma^2(F) + 0.0000F^2$
Number of Parameters Refined	218
R Indices (all data)	R =6.27 %, wR =4.38 %
Goodness-of-Fit	1.04
Largest and Mean Δ/σ	0.016, 0.002
Data-to-Parameter Ratio	17.9:1
Largest Difference Peak	2.42 $eÅ^{-3}$
Largest Difference Hole	2.66 $eÅ^{-3}$

$K[Re_3(OMe)_4(CO)_9]$ (3A)	$K[Re_3(OH)_4(CO)_9]$ (3E)
$C_{13}\ H_{12}\ K\ O_{13}\ Re_3$	$C_9\ H_4\ K\ O_{13}\ Re_3$
colourless plate	orange
.17 x .10 x .04	.07 x .08 x .09
Monoclinic	Cubic
P21/n	$Pa\bar{3}$
$\underline{a}$ = 8.838(4) Å	$\underline{a}$ = 14.858(1) Å
$\underline{b}$ = 16.394(8) Å	
$\underline{c}$ = 14.820(7) Å	
$\underline{\beta}$ = 91.95(4)°	
2146(2)	3254(2) $Å^3$
4	8
973.9	917.8
3.014	3.747 Mg/m^3
17.135	22.590 mm^{-1}
1752	3248
Siemens R3m/V	Siemens P4
AgKα (λ = 0.56086 Å)	MoKα (λ = 0.71073 Å)
173	298
3.0 to 45.0	7.0 to 45.0°
-12≤h≤12, 0≤k≤21,	-16≤h≤11, -8≤k≤19,
-20≤l≤20	-8≤l≤19
6722	5875
5756 (R_{int} =4.10%)	1317 (R_{int} =2.11%)
5756 ($F \geq 0.0\sigma(F)$)	1317 ($F \geq 0.0\sigma(F)$)
0.940-1.155	0.862-1.123
$w^{-1} = \sigma^2(F) + 0.0000F^2$	$w^{-1} = \sigma^2(F) + 0.0010F^2$
272	80
R =9.64 %, wR =4.31 %	R =5.93 %, wR =5.64 %
1.01	1.14
0.002, 0.000	0.003, 0.001
21.2:1	16.5:1
3.52 $eÅ^{-3}$	2.14 $eÅ^{-3}$
-4.12 $eÅ^{-3}$	-3.83 $eÅ^{-3}$

$[Re(OH)(CO)_3]_4 \cdot 8H_2O$ (3C)	$Re_4(CO)_{12}(OH)_2(OEt)_2 \cdot 2EtOH$ (3B)
$C_{12}\ H_{20}\ O_{24}\ Re_4$	$C_{20}\ H_{24}\ O_{18}\ Re_4$
colorless tetragnol	colorless plate
.12 x .13 x .13	0.10 x 0.13 x 0.01
Tetragnol	Monoclinic
I_4	C2/c
$\underline{a}$ = 11.377(2) Å	$\underline{a}$ = 17.326(2) Å
	$\underline{b}$ = 9.625(2) Å
$\underline{c}$ = 11.110(3) Å	$\underline{c}$ = 18.071(3) Å
	$\underline{\beta}$ = 92.220(0)°
1438.0(5) Å^3	3011.3(9) Å^3
2	4
1293.1	1297.2
2.986 Mg/m^3	2.861 Mg/m^3
16.874 mm^{-1}	16.103 mm^{-1}
1168	2352
Siemens R3m/V	Siemens P4
AgKα (λ = 0.56086 Å)	MoKα (λ = 0.71073 Å)
173	298
5.6 to 50.0°	5.0 to 45.0°
-17≤h≤17, 0≤k≤17, 0≤l≤16	-1≤h≤20, -11≤k≤11, -21≤l≤21
2824	5701
2496 (R_{int} =2.01%)	2658 (R_{int} =6.32%)
2496 (F ≥ 0.0σ(F))	2658 (F ≥ 0.0σ(F))
0.910-1.113	0.817-1.298
$w^{-1} = \sigma^2(F) + 0.0000F^2$	$w^{-1} = \sigma^2(F) + 0.0000F^2$
91	200
R =3.66 %, wR =2.86 %	R =6.04 %, wR =5.43 %
1.34	1.63
0.014, 0.002	0.035, 0.003
27.4:1	13.3:1
2.18 eÅ^{-3}	1.57 eÅ^{-3}
-3.52 eÅ^{-3}	-1.75 eÅ^{-3}

Appendix Table 3A.2.

Atomic Coordinates ($x10^4$) and Equivalent Isotropic Displacement Coefficients ($Å^2x10^3$) for $K[Re_3(OCH_3)_4(CO)_9]$ (3A)

	x	y	z	U(eq)
Re(1)	316(1)	6001(1)	8235(1)	15(1)
Re(2)	2013(1)	6208(1)	6214(1)	16(1)
Re(3)	-765(1)	7544(1)	6800(1)	15(1)
K	3229(3)	7850(2)	8041(2)	21(1)
O(1)	2469(9)	6234(6)	7647(5)	18(3)
O(2)	1602(9)	7474(5)	6469(5)	14(2)
O(3)	237(9)	7314(5)	8108(5)	15(2)
O(4)	-214(9)	6251(5)	6807(5)	16(2)
O(11)	1360(12)	5772(7)	10200(6)	36(4)
O(12)	-2890(10)	5885(6)	8963(6)	32(3)
O(13)	476(11)	4169(6)	7991(6)	28(3)
O(21)	5291(11)	6243(7)	5613(6)	36(4)
O(22)	2362(12)	4353(6)	6043(6)	33(3)
O(23)	967(11)	6338(6)	4232(6)	32(3)
O(31)	-1249(13)	9375(6)	7030(7)	44(4)
O(32)	-1830(11)	7656(6)	4828(6)	33(3)
O(33)	-4070(10)	7401(6)	7313(7)	36(4)
C(1)	3704(14)	5767(9)	7984(8)	26(4)

C(2)	2141(16)	8047(8)	5832(8)	25(4)
C(3)	-352(15)	7768(9)	8849(8)	28(4)
C(4)	-1388(15)	5712(8)	6390(8)	23(4)
C(11)	978(14)	5876(8)	9454(8)	17(4)
C(12)	-1710(16)	5924(9)	8676(8)	25(4)
C(13)	401(16)	4861(9)	8118(8)	25(4)
C(21)	4045(16)	6247(9)	5855(8)	27(4)
C(22)	2212(14)	5056(9)	6118(9)	25(4)
C(23)	1360(16)	6285(8)	4972(9)	26(4)
C(31)	-1014(15)	8684(8)	6936(9)	22(4)
C(32)	-1468(14)	7613(7)	5573(8)	18(4)
C(33)	-2780(16)	7455(10)	7133(8)	28(4)

Appendix Table 3B.2.

Atomic Coordinates ($x10^4$) and Equivalent Isotropic Displacement Coefficients ($Å^2x10^3$) for $[Re_4(CO)_{12}(OH)_2(EtO)_2]\cdot 2EtOH$ (3B)

	x	y	z	U(eq)
Re(1)	4140(1)	102(1)	6960(1)	36(1)
Re(2)	5528(1)	2548(1)	6694(1)	36(1)
O(1)	4356(5)	2283(9)	7101(5)	36(3)
O(2)	5396(4)	315(8)	6898(4)	32(3)

C(11)	3061(8)	176(17)	7141(9)	51(5)
O(11)	2425(7)	315(15)	7230(8)	80(5)
C(12)	4044(8)	-1863(17)	6895(8)	48(5)
O(12)	3990(7)	-3074(11)	6927(7)	70(5)
C(13)	3856(9)	92(19)	5915(9)	58(6)
O(13)	3700(8)	50(16)	5322(6)	85(6)
C(21)	6609(9)	2542(18)	6431(8)	57(6)
O(21)	7229(6)	2544(17)	6295(8)	89(6)
C(22)	5573(8)	4505(18)	6610(8)	49(5)
O(22)	5586(9)	5658(12)	6563(8)	85(6)
C(23)	5293(8)	2517(17)	5653(8)	49(5)
O(23)	5135(8)	2536(15)	5032(6)	76(5)
O(10)	1591(9)	892(16)	3547(9)	104(7)
C(10)	1886(16)	822(31)	4246(16)	129(13)
C(20)	1664(26)	215(44)	4836(18)	247(31)
C(30)	6262(16)	-1719(29)	6200(14)	337(38)
C(40)	5680(23)	-1015(15)	6685(25)	1021(360)
C(40')	5696(18)	-546(24)	6332(11)	70(11)

The occupancy factor of C(40) is 0.35. The occupancy factor C(40') is 0.65.

Appendix Table 3C.2.

Atomic Coordinates ($x10^4$) and Equivalent Isotropic Displacement Coefficients ($Å^2x10^3$) for $[Re(CO)_3(OH)]_4 \cdot 8H_2O$ (3C)

	x	y	z	U(eq)
Re	372(1)	3558(1)	1378(1)	12(1)
C(1)	1797(7)	2686(7)	1307(11)	17(2)
O(1)	2659(6)	2146(6)	1307(11)	36(2)
C(2)	-418(7)	2094(7)	1289(11)	19(2)
O(2)	-925(6)	1202(6)	1224(8)	32(2)
C(3)	426(7)	3582(8)	-333(6)	18(3)
O(3)	517(6)	3623(6)	-1378(6)	29(2)
O(4)	-1124(4)	4726(6)	1699(5)	16(2)
O(5)	364(5)	1855(5)	4318(5)	25(2)
O(6)	1910(7)	229(6)	3238(6)	31(2)

Appendix Table 3E.2.

Atomic Coordinates ($x10^4$) and Equivalent Isotropic Displacement Coefficients ($Å^2x10^3$) for $KRe_3(CO)_9(OH)_4$ (3E)

	x	y	z	U(eq)
Re	1649(1)	1710(1)	36(1)	22(1)

K(1)	5000	0	0	64(2)
K(2)	0	0	0	63(1)
O(5)	211(5)	1552(5)	269(5)	21(2)
O(4)	1496(5)	1496(5)	1496(5)	21(2)
O(3)	1634(8)	1782(9)	-2034(7)	53(4)
C(2)	2909(9)	1743(11)	-64(8)	35(4)
C(1)	1668(10)	2983(9)	41(10)	34(4)
C(3)	1635(10)	1778(10)	-1235(8)	36(4)
O(2)	3705(7)	1811(8)	-103(8)	47(4)
O(1)	1606(8)	3753(7)	79(7)	45(3)

Appendix Table 3D.2.

Atomic Coordinates ($x10^4$) and Equivalent Isotropic Displacement Coefficients ($Å^2x10^3$) $KRe_2(CO)_6(OH)_3{\cdot}2H_2O$ (3D)

	x	y	z	U(eq)
Re(1)	911(1)	0	3593(1)	18(1)
Re(2)	1690(1)	0	1888(1)	18(1)
Re(3)	3908(1)	0	6082(1)	15(1)
Re(4)	3165(1)	0	7835(1)	16(1)
O(1)	1573(3)	1277(6)	3189(5)	19(2)
O(2)	722(5)	0	1791(8)	33(4)
O(3)	3842(3)	1227(6)	7424(5)	19(2)

O(4)	2939(5)	0	6003(8)	25(3)
C(1A)	320(4)	1251(10)	3702(7)	23(3)
O(1A)	-52(3)	2017(8)	3754(6)	38(3)
C(1B)	1195(7)	0	5201(12)	24(4)
O(1B)	1358(6)	0	6157(8)	38(4)
C(2A)	1659(5)	1261(10)	754(8)	30(3)
O(2A)	1634(4)	2011(8)	70(6)	42(3)
C(2B)	2553(7)	0	2182(10)	24(4)
O(2B)	3095(4)	0	2329(9)	31(4)
C(3A)	3850(4)	1260(10)	4942(7)	22(3)
O(3A)	3795(3)	1987(7)	4218(5)	27(2)
C(3B)	4758(5)	0	6387(10)	15(4)
O(3B)	5311(4)	0	6596(9)	32(4)
C(4A)	2575(4)	1246(10)	7951(8)	25(3)
O(4A)	2188(3)	1974(8)	8008(6)	37(3)
C(4B)	3474(6)	0	9420(11)	21(4)
O(4B)	3657(5)	0	10386(8)	31(3)
K(1)	3965(1)	2094(3)	2042(2)	33(1)
O(11)	2588(7)	2680(14)	4733(12)	30(5)
O(22)	4959(7)	1354(17)	1183(13)	40(6)
O(33)	5101(7)	2394(16)	1181(12)	36(5)
O(44)	4130(14)	5000	1782(19)	170(17)

Appendix Table 4B.
Crystallographic Data for $(AsPh_4)_2[ReN(CN)_4(H_2O)]\cdot 5H_2O$ (4B)

Empirical Formula	$C_{52}\ H_{52}\ As_2\ N_5\ O_6\ Re$
Color; Habit	YELLOW PLATE
Crystal size (mm)	.22 X .21 X .11
Crystal System	Monoclinic
Space Group	$P2_1/n$
Unit Cell Dimension	$\underline{a}$ = 15.330(3) Å
	$\underline{b}$ = 19.808(4) Å
	$\underline{c}$ = 16.915(3) Å
	$\underline{\beta}$ = 101.64(2)°
Volume	5031(2) Å^3
Z	4
Formula weight	1179.0
Density(calc.)	1.557 Mg/m^3
D_m	1.53(1) Mg/m^3
Absorption Coefficient	3.774 mm^{-1}
F(000)	2352
Diffractometer Used	Siemens R3m/V
Radiation	AgKα (λ = 0.56086 Å)
Temperature (K)	167
2θ Range	7 to 40°
Index Ranges	$0 \le h \le 18,\ 0 \le k \le 24$
	$-20 \le l \le 20$
Reflections Collected	10303
Independent Reflections	9615 (R_{int} =5.50%)
Observed Reflections	9615 ($F \ge 0.0\sigma(F)$)
Absorption Correction	0.839-1.124
Weighting Scheme	$w^{-1} = \sigma^2(F) + 0.0000F^2$
Number of Parameters Refined	595
R Indices (all data)	R =5.83 %, wR =3.15 %
Goodness-of-Fit	1.41
Largest and Mean Δ/σ	0.001, 0.000
Data-to-Parameter Ratio	16.2:1
Largest Difference Peak	1.15 eÅ^{-3}
Largest Difference Hole	-1.38 eÅ^{-3}

Appendix Table 4B.2

Atomic Coordinates ($x10^4$) and Equivalent Isotropic Displacement Coefficients ($Å^2x10^3$) for $(AsPh_4)_2[ReN(CN)_4(H_2O)]\cdot 5H_2O$ (4B)

	x	y	z	U(eq)
Re	302(1)	1695(1)	7643(1)	20(1)
As(2)	587(1)	5594(1)	8276(1)	24(1)
As(1)	583(1)	1905(1)	3947(1)	21(1)
O	-932(2)	1648(2)	8375(2)	29(1)
C(1)	1010(3)	1713(3)	8845(3)	25(2)
C(2)	22(3)	2736(3)	7664(3)	26(2)
C(3)	-728(3)	1702(2)	6619(3)	24(2)
C(4)	167(3)	638(3)	7738(3)	26(2)
N(1)	1384(3)	1716(2)	9506(3)	37(2)
N(2)	-185(3)	3293(2)	7584(2)	31(2)
N(3)	-1290(3)	1751(2)	6057(3)	36(2)
N(4)	99(3)	63(2)	7790(3)	35(2)
N(5)	1158(3)	1715(2)	7184(2)	30(1)
O(1)	3242(2)	2039(2)	175(2)	36(1)
O(2)	3690(2)	928(2)	1131(2)	40(1)
O(3)	8827(2)	772(2)	9514(2)	36(1)
O(4)	1847(2)	592(2)	658(2)	38(1)
O(5)	10035(2)	874(2)	942(2)	43(1)
C(1A)	884(3)	1088(2)	4535(3)	22(2)

C(2A)	937(3)	1055(3)	5365(3)	28(2)
C(3A)	1102(3)	432(3)	5752(3)	33(2)
C(4A)	1221(3)	-136(3)	5317(3)	35(2)
C(5A)	1177(3)	-102(3)	4490(3)	33(2)
C(6A)	1001(3)	520(2)	4087(3)	30(2)
C(1B)	1304(3)	1939(2)	3162(3)	25(2)
C(2B)	950(4)	2040(3)	2351(3)	34(2)
C(3B)	1527(4)	2086(3)	1806(3)	45(2)
C(4B)	2442(5)	2045(3)	2108(4)	54(3)
C(5B)	2799(4)	1933(3)	2922(4)	47(2)
C(6B)	2223(3)	1885(2)	3448(3)	33(2)
C(1C)	842(3)	2686(2)	4621(3)	22(2)
C(2C)	1416(3)	3176(2)	4418(3)	27(2)
C(3C)	1618(3)	3738(3)	4920(3)	34(2)
C(4C)	1255(3)	3810(3)	5601(3)	33(2)
C(5C)	673(3)	3317(3)	5784(3)	31(2)
C(6C)	462(3)	2753(2)	5288(3)	28(2)
C(1D)	1064(3)	5563(2)	7325(3)	26(2)
C(2D)	518(3)	5638(3)	6571(3)	31(2)
C(3D)	880(4)	5644(3)	5886(3)	38(2)
C(4D)	1790(3)	5576(3)	5946(3)	34(2)
C(5D)	2342(3)	5505(3)	6698(3)	36(2)
C(6D)	1980(3)	5492(3)	7390(3)	34(2)
C(1E)	1081(3)	4879(2)	8978(3)	24(2)
C(2E)	1333(3)	4995(3)	9801(3)	33(2)

C(3E)	1678(3)	4464(3)	10302(3)	38(2)
C(4E)	1761(3)	3828(3)	9981(3)	37(2)
C(5E)	1501(3)	3715(3)	9158(3)	40(2)
C(6E)	1178(3)	4249(2)	8654(3)	31(2)
C(1F)	875(3)	6437(2)	8829(3)	28(2)
C(2F)	1596(3)	6805(3)	8694(3)	35(2)
C(3F)	1803(4)	7406(3)	9106(3)	42(2)
C(4F)	1284(4)	7633(3)	9633(3)	43(2)
C(5F)	564(4)	7268(3)	9768(4)	49(2)
C(6F)	357(3)	6649(3)	9363(3)	40(2)
C(1G)	-681(3)	5522(2)	7973(3)	22(2)
C(2G)	-1172(3)	6110(3)	7807(3)	32(2)
C(3G)	-2093(3)	6068(3)	7566(3)	33(2)
C(4G)	-2513(3)	5436(3)	7483(3)	30(2)
C(5G)	-2013(3)	4855(3)	7642(3)	33(2)
C(6G)	-1087(3)	4895(3)	7898(3)	28(2)
C(1H)	-646(3)	1906(2)	3420(3)	23(2)
C(2H)	-1171(3)	2454(3)	3519(3)	28(2)
C(3H)	-2062(3)	2452(3)	3130(3)	33(2)
C(4H)	-2406(3)	1913(3)	2651(3)	34(2)
C(5H)	-1869(3)	1370(3)	2552(3)	36(2)
C(6H)	-979(3)	1363(2)	2939(3)	29(2)

Appendix Table 5.1
Crystallographic Data for 5B, 5C, 5D, 5E, 5F, 5G, 5H

Empirical Formula	C_{15} H_{19} B N_8 O_6 Re_2 (5B)
Color; Habit	violet needle
Crystal size (mm)	.03 x .04 x .30
Crystal System	Orthorhombic
Space Group	$P2_12_12_1$
Unit Cell Dimensions	$\underline{a}$ = 7.775(4) Å
	$\underline{b}$ = 15.117(6) Å
	$\underline{c}$ = 19.049(9) Å
Volume	2239(2) $Å^3$
Z	4
Formula weight	790.6
Density(calc.)	2.345 Mg/m^3
Absorption Coefficient	10.851 mm^{-1}
F(000)	1472
Diffractometer Used	Siemens P4
Radiation	MoKα (λ = 0.71073 Å)
Temperature (K)	298
2θ Range	7.0 to 45.0°
Index Ranges	$-1 \leq h \leq 9$, $-1 \leq k \leq 17$
	$-1 \leq l \leq 22$
Reflections Collected	2971
Independent Reflections	2771 (R_{int} =5.97%)
Observed Reflections	2771 ($F \geq 0.0\sigma(F)$)
Absorption Correction	0.856-1.136
Weighting Scheme	$w^{-1} = \sigma^2(F) + 0.0000F^2$
Number of Parameters Refined	290
R Indices (all data)	R =6.27 %, wR =5.69 %
Goodness-of-Fit	1.82
Largest and Mean Δ/σ	0.064, 0.002
Data-to-Parameter Ratio	9.6:1
Largest Difference Peak	2.96 $eÅ^{-3}$
Largest Difference Hole	-2.53 $eÅ^{-3}$

C_{24} H_{24} Cl_2 N_2 O_2 P Re (5C)	C_{24} H_{23} Cl_2 N_2 O_3 P Re (5D)
blue prism	blue prism
0.07 x 0.07 x 0.08	0.02 x 0.03 x 0.07
Monoclinic	Triclinic
$P2_1/c$	$P\bar{1}$
$\underline{a}$ = 12.571(3) Å	$\underline{a}$ = 7.705(2) Å
$\underline{b}$ = 11.557(2) Å	$\underline{b}$ = 8.061(2) Å
$\underline{c}$ = 17.639(4) Å	$\underline{c}$ = 20.245(4) Å
	$\underline{\alpha}$ = 88.34(3)°
$\underline{\beta}$ = 106.53(3)°	$\underline{\beta}$ = 80.23(3)°
	$\underline{\gamma}$ = 85.76(3)°
2456.7(9) $Å^3$	1235.6(5) $Å^3$
4	2
660.5	675.5
1.786 Mg/m^3	1.816 Mg/m^3
5.253 mm^{-1}	5.227 mm^{-1}
1288	658
Siemens P4	Siemens P4
MoKα (λ = 0.71073 Å)	MoKα (λ = 0.71073 Å)
298	298
5.0 to 50.0°	5.0 to 50.0°
$-17 \leq h \leq 16$, $0 \leq k \leq i6$	$-1 \leq h \leq 10$, $-11 \leq k \leq 11$
$0 \leq l \leq 24$	$-28 \leq l \leq 28$
8738	8688
7117 (R_{int} =2.44%)	7194 (R_{int} =4.20%)
7117 ($F \geq 0.0\sigma(F)$)	7194 ($F \geq 0.0\sigma(F)$)
0.808-1.242	0.778-1.316
$w^{-1} = \sigma^2(F) + 0.0000F^2$	$w^{-1} = \sigma^2(F) + 0.0000F^2$
292	288
R =6.88 %, wR =3.91 %	R =9.80 %, wR =9.72 %
1.23	2.81
0.004, 0.000	0.022, 0.003
24.4:1	25.0:1
2.28 $eÅ^{-3}$	2.27 $eÅ^{-3}$
-1.60 $eÅ^{-3}$	-3.05 $eÅ^{-3}$

$C_{43}H_{37}Cl_5N_4O_3P_2Re_2$ (5E)	$C_{20}H_{30}Cl_2N_8O_3Re_2$ (5F)
GREEN NEEDLE	green plate
.12 X .08 X .07	.11 X .21 x .30
Triclinic	Triclinic
$P\bar{1}$	$P\bar{1}$
a = 9.885(2) Å	a = 9.375(2) Å
b = 13.627(3) Å	b = 17.610(4) Å
c = 18.232(4) Å	c = 18.174(4) Å
α = 83.46(3)°	α = 97.84(2)°
β = 76.95(3)°	β = 102.25(2)°
γ = 72.17(3)°	γ = 103.70(2)°
2274.9(8) Å^3	2793(1) Å^3
2	4
1269.4	873.8
1.853 Mg/m^3	2.078 Mg/m^3
5.724 mm^{-1}	8.888 mm^{-1}
1224	1656
Siemens P4	Siemens R3m/V
MoKα (λ = 0.71073 Å)	AgKα (λ = 0.56086 Å)
298	298
5.0 to 50.0°	3.0 to 40.0°
-1 ≤ h ≤ 12, -18 ≤ k ≤ 18	0 ≤ h ≤ 11, -21 ≤ k ≤ 20
-25 ≤ l ≤ 24	-22 ≤ l ≤ 21
11946	11387
10702 (R_{int} =4.54%)	10695 (R_{int} =3.43%)
10702 (F ≥ 0.0σ(F))	10695 (F ≥ 0.0σ(F))
0.712-1.165	0.808-1.239
$w^{-1} = \sigma^2(F) + 0.0000F^2$	$w^{-1} = \sigma^2(F) + 0.0000F^2$
562	631
R =5.82 %, wR =3.86 %	R = 13.35 %, wR =5.50 %
1.22	1.11
0.058, 0.003	0.095, 0.018
19.0:1	16.9:1
1.40 eÅ^{-3}	2.73 eÅ^{-3}
-1.24 eÅ^{-3}	-3.18 eÅ^{-3}

C_{24} H_{24} Cl_2 N_2 O_5 P Re (5G)	C_{18} H_{28} N_6 O_8 Tc_2 (5H)
blue	green plate
.12 x .15 x .17	0.010 X 0.194 X 0.225
Orthorhombic	Triclinic
Pbca	$P\bar{1}$
$\underline{a}$ = 16.804(5) Å	$\underline{a}$ = 7.951(2) Å
$\underline{b}$ = 15.134(4) Å	$\underline{b}$ = 8.992(2) Å
$\underline{c}$ = 23.396(7) Å	$\underline{c}$ = 18.046(4) Å
	$\underline{\alpha}$ = 102.97(3)°
	$\underline{\beta}$ = 97.24(3)°
	$\underline{\gamma}$ = 102.22(3)°
5950(3) $Å^3$	1208.2(5) $Å^3$
8	2
708.5	652.5
1.582 Mg/m^3	1.793 Mg/m^3
4.351 mm^{-1}	1.199 mm^{-1}
2768	656
Siemens R3m/V	Siemens P4
AgKα (λ = 0.56086 Å)	MoKα (λ = 0.71073 Å)
298	298
7.0 to 45.0°	3.0 to 50.0°
$0 \le h \le 20$, $0 \le k \le 18$	$-1 \le h \le 9$, $-10 \le k \le 10$
$-28 \le l \le 0$	$-21 \le l \le 21$
5697	5239
5697 (R_{int} =0.00%)	4240 (R_{int} =4.12%)
5697 ($F \ge 0.0\sigma(F)$)	4240 ($F \ge 0.0\sigma(F)$)
0.833-1.146	0.627-1.408
$w^{-1} = \sigma^2(F) + 0.0012F^2$	$w^{-1} = \sigma^2(F) + 0.0010F^2$
317	308
R =13.72 %, wR =9.18 %	R = 11.72 %, wR =8.93 %
1.23	1.24
.360, 0.015	0.025, 0.007
18.0:1	13.8:1
2.17 $eÅ^{-3}$	1.62 $eÅ^{-3}$
-1.59 $eÅ^{-3}$	-1.82 $eÅ^{-3}$

Appendix Table 5B.2.

Atomic Coordinates ($x10^4$) and Equivalent Isotropic Displacement Coefficients ($Å^2x10^3$) for $[ReO(HBPz_3)(Pz\text{-}(CO)Me_2)][ReO_4]$ (5B)

	x	y	z	U(eq)
Re(1)	2903(1)	2030(1)	7021(1)	26(1)
O	1468(18)	1280(8)	7309(8)	40(4)
B	1505(34)	3945(16)	6401(12)	38(8)
N(1A)	1465(19)	3039(11)	7528(8)	33(5)
N(2A)	835(19)	3735(10)	7149(10)	43(6)
C(3A)	-80(27)	4215(14)	7613(13)	43(8)
C(4A)	-178(36)	3848(16)	8229(15)	69(10)
C(5A)	874(27)	3106(17)	8196(12)	53(8)
N(1B)	1628(21)	2328(9)	6087(8)	33(5)
N(2B)	972(22)	3147(10)	5960(9)	35(5)
C(3B)	225(25)	3113(14)	5300(9)	33(6)
C(4B)	373(30)	2285(14)	5059(11)	44(8)
C(5B)	1287(26)	1794(12)	5538(9)	33(6)
N(1C)	4271(19)	3300(10)	6768(8)	29(5)
N(2C)	3404(22)	3971(10)	6458(7)	33(5)
C(3C)	4568(31)	4542(13)	6255(11)	39(7)
C(4C)	6203(31)	4277(14)	6398(11)	45(7)
C(5C)	5987(27)	3490(14)	6710(12)	43(7)

O(1D)	4564(17)	1411(8)	6465(7)	31(4)
N(1D)	4887(21)	1886(12)	7736(8)	35(5)
N(2D)	6199(22)	1425(11)	7479(8)	36(5)
C(3D)	7486(25)	1363(12)	7934(13)	51(8)
C(4D)	6932(30)	1880(14)	8516(12)	48(7)
C(5D)	5412(34)	2197(17)	8355(10)	55(9)
C(6D)	5957(22)	962(15)	6780(10)	36(6)
C(7D)	5499(33)	33(12)	6881(12)	50(8)
C(8D)	7569(30)	1157(18)	6362(12)	65(10)
Re(2)	1308(2)	1063(1)	9869(1)	79(1)
O(1)	-723(31)	1246(23)	10211(15)	262(27)
O(2)	1124(34)	1115(11)	8968(8)	123(12)
O(3)	1884(38)	22(11)	10092(9)	159(16)
O(4)	2702(44)	1817(17)	10154(14)	435(54)

Appendix Table 5C.2.

Atomic coordinates ($x10^4$) and equivalent isotropic displacement coefficients ($Å^2x10^3$) for $ReOCl_2(PPh_3)(pz\text{-}COMe_2)$ (5C)

	x	y	z	U(eq)
Re	7239(1)	8475(1)	1687(1)	30(1)
O(1)	8452(3)	7901(3)	2243(2)	42(1)
Cl(1)	6303(1)	6613(1)	1443(1)	50(1)

Cl(2)	7335(1)	8451(1)	381(1)	46(1)
P	8225(1)	10356(1)	1854(1)	32(1)
O(2)	5813(3)	9245(3)	1375(2)	31(1)
N(1)	6752(4)	8624(4)	2746(2)	36(1)
N(2)	5793(4)	9192(4)	2668(2)	37(2)
C(3D)	5593(5)	9253(5)	3378(3)	51(2)
C(4D)	6454(6)	8722(5)	3919(3)	55(3)
C(5D)	7149(5)	8324(5)	3505(3)	45(2)
C(6)	5109(4)	9478(5)	1851(3)	39(2)
C(7)	4103(5)	8666(6)	1638(4)	61(3)
C(8)	4785(5)	10756(5)	1800(3)	57(3)
C(1A)	8782(5)	10780(5)	2887(3)	43(2)
C(2A)	9917(6)	10876(6)	3255(4)	65(3)
C(3A)	10283(8)	11123(7)	4062(4)	82(3)
C(4A)	9570(9)	11281(6)	4492(4)	88(4)
C(5A)	8467(9)	11231(6)	4139(4)	78(4)
C(6A)	8063(6)	10983(6)	3336(3)	56(3)
C(1B)	9433(4)	10287(5)	1468(3)	35(2)
C(2B)	9643(5)	11145(5)	991(3)	43(2)
C(3B)	10571(5)	11080(5)	712(3)	47(2)
C(4B)	11282(5)	10163(5)	928(4)	51(2)
C(5B)	11077(5)	9317(6)	1407(4)	59(3)
C(6B)	10137(5)	9363(5)	1666(4)	48(2)

C(1C)	7449(4)	11610(5)	1368(3)	35(2)
C(2C)	6582(5)	11491(5)	693(3)	45(2)
C(3C)	6036(6)	12449(5)	309(4)	53(2)
C(4C)	6361(6)	13541(6)	593(4)	61(3)
C(5C)	7246(6)	13678(5)	1261(4)	61(3)
C(6C)	7777(5)	12709(5)	1652(3)	46(2)

Appendix Table 5D.2.

Atomic coordinates ($x10^4$) and equivalent isotropic displacement coefficients ($Å^2x10^3$) for $ReOCl_2(PPh_3)(pz\text{-}COHMe)\cdot 0.5CHOCHO$ (5D)

	x	y	z	U(eq)
Re	161(1)	1432(1)	2892(1)	25(1)
Cl(1)	296(4)	3776(4)	2185(2)	42(1)
Cl(2)	-1299(5)	3174(5)	3803(2)	48(1)
P	2182(4)	-108(3)	2009(2)	24(1)
O(1)	-1628(11)	633(12)	2723(5)	43(3)
O(2)	2331(9)	1669(8)	3226(4)	24(2)
N(2)	339(15)	-483(13)	3649(5)	37(4)
N(1)	1495(15)	-318(13)	4022(5)	39(4)
C(3)	-670(19)	-1709(17)	3918(8)	46(5)
C(4)	122(32)	-2419(19)	4449(9)	82(9)
C(5)	1410(24)	-1540(20)	4498(8)	59(6)

C(6)	2788(23)	982(22)	3819(9)	67(7)
C(7)	4600(35)	570(29)	3856(12)	109(12)
C(11)	1010(15)	-1123(15)	1434(6)	30(4)
C(12)	-352(16)	-146(16)	1183(7)	35(4)
C(13)	-1243(22)	-932(23)	745(8)	60(6)
C(14)	-754(22)	-2578(21)	553(9)	57(6)
C(15)	512(19)	-3504(18)	805(7)	44(5)
C(16)	1440(17)	-2769(14)	1230(7)	36(4)
C(21)	3561(15)	-1778(14)	2323(6)	28(4)
C(22)	5393(16)	-1759(16)	2194(7)	38(4)
C(23)	6385(18)	-3059(16)	2473(9)	49(6)
C(24)	5559(24)	-4276(19)	2875(8)	56(6)
C(25)	3725(21)	-4293(16)	2990(8)	45(5)
C(26)	2738(17)	-3028(13)	2713(6)	31(4)
C(31)	3686(15)	1250(15)	1482(6)	29(4)
C(32)	3750(21)	1286(19)	788(7)	49(5)
C(33)	4893(23)	2347(21)	394(8)	59(6)
C(34)	5885(23)	3302(22)	693(9)	67(7)
C(35)	5805(23)	3262(21)	1366(9)	67(7)
C(36)	4606(19)	2254(15)	1781(8)	43(5)
C(41)	4209(44)	4651(45)	4885(18)	152(13)
O(41)	4375(54)	3206(50)	5176(22)	297(20)

Appendix Table 5E.2.

Atomic Coordinates ($x10^4$) and Equivalent Isotropic Displacement Coefficients ($Å^2x10^3$) for $[ReOCl(PPh_3)]_2(\mu\text{-}O)(\mu\text{-}pz)_2 \cdot CHCl_3$ (5E)

	x	y	z	U(eq)
Re(1)	3589(1)	7026(1)	2692(1)	38(1)
Re(2)	1179(1)	8569(1)	1647(1)	34(1)
P(1)	2208(1)	5978(1)	3534(1)	35(1)
P(2)	-173(2)	10115(1)	2373(1)	36(1)
Cl(1)	3922(2)	7748(1)	3740(1)	56(1)
Cl(2)	-933(2)	8086(1)	1697(1)	51(1)
O(1)	5165(4)	6059(3)	2561(3)	58(2)
O(2)	1231(4)	9245(3)	806(2)	50(2)
O(3)	1691(3)	7921(3)	2589(2)	31(1)
N(1G)	2317(4)	7076(3)	1304(2)	37(2)
N(2G)	3370(5)	6497(3)	1682(3)	41(2)
N(1H)	3239(5)	8824(3)	1575(3)	42(2)
N(2H)	4171(4)	8224(4)	2028(3)	42(2)
C(1A)	3322(5)	4704(4)	3773(3)	38(2)
C(2A)	2839(7)	3848(5)	3850(4)	55(3)
C(3A)	3625(9)	2913(5)	4124(5)	77(4)
C(4A)	4903(9)	2846(5)	4342(5)	77(3)
C(5A)	5404(8)	3673(7)	4248(5)	83(4)

C(6A)	4637(7)	4609(5)	3969(4)	59(3)
C(1B)	1352(6)	6498(4)	4458(3)	41(2)
C(2B)	1422(6)	5881(5)	5114(3)	48(2)
C(3B)	784(7)	6299(5)	5810(4)	57(3)
C(4B)	73(7)	7351(5)	5848(4)	56(3)
C(5B)	-4(7)	7957(5)	5196(4)	55(2)
C(6B)	639(6)	7550(4)	4501(3)	48(2)
C(1C)	743(5)	5797(4)	3164(3)	39(2)
C(2C)	-696(6)	6264(4)	3469(4)	52(2)
C(3C)	-1788(6)	6156(5)	3144(4)	59(3)
C(4C)	-1442(7)	5586(5)	2533(4)	65(3)
C(5C)	-7(7)	5111(6)	2215(4)	61(3)
C(6C)	1072(6)	5234(5)	2529(3)	49(2)
C(1D)	-1242(5)	9891(4)	3306(3)	37(2)
C(2D)	-2120(7)	9250(5)	3388(3)	55(3)
C(3D)	-3024(8)	9154(6)	4060(4)	65(3)
C(4D)	-3088(7)	9693(5)	4663(4)	59(3)
C(5D)	-2230(7)	10345(5)	4590(3)	57(3)
C(6D)	-1307(7)	10435(4)	3907(3)	50(2)
C(1E)	-1519(6)	11089(4)	1941(3)	43(2)
C(2E)	-2341(8)	11976(5)	2328(4)	64(3)
C(3E)	-3384(9)	12728(5)	2021(4)	81(3)
C(4E)	-3607(8)	12625(5)	1334(4)	68(3)

C(5E)	-2831(8)	11747(5)	932(4)	62(3)
C(6E)	-1772(7)	10991(4)	1251(3)	50(2)
C(1F)	1073(6)	10761(4)	2532(3)	44(2)
C(2F)	1227(8)	11661(5)	2151(3)	59(3)
C(3F)	2352(10)	12045(7)	2219(5)	80(4)
C(4F)	3320(9)	11533(7)	2655(5)	81(4)
C(5F)	3183(7)	10630(6)	3047(4)	65(3)
C(6F)	2072(7)	10242(5)	2996(4)	52(2)
C(3G)	4031(6)	5629(4)	1317(3)	51(2)
C(4G)	3396(7)	5627(5)	715(4)	60(3)
C(5G)	2331(7)	6547(5)	730(3)	50(2)
C(3H)	5319(7)	8593(5)	1901(4)	56(3)
C(4H)	5203(7)	9380(5)	1371(4)	64(3)
C(5H)	3884(7)	9503(5)	1184(4)	54(3)
C(1)	2282(8)	2712(5)	-322(7)	87(6)
C(2)	2336(8)	2982(9)	-290(7)	102(8)
Cl(4)*	1428(8)	1836(6)	165(3)	140(4)
Cl(3)*	1167(11)	3948(5)	-168(7)	234(8)
Cl(5)*	3880(8)	2554(8)	-33(10)	187(8)
Cl(4A)#	757(9)	2971(11)	342(4)	216(8)
Cl(3A)#	2205(10)	4211(9)	-680(5)	212(8)
Cl(5A)#	3781(8)	2569(9)	160(9)	149(6)

* occupancy factor 0.5217, # occupancy factor 0.4783.

Appendix Table 5F.2.

Atomic Coordinates ($x10^4$) and Equivalent Isotropic Displacement Coefficients ($Å^2x10^3$) for $[ReOCl(3,5\text{-}Me_2\text{-}HPz)]_2(\mu\text{-}O)(\mu\text{-}3,5\text{-}Me_2\text{-}Pz)_2$ (5F)

	x	y	z	U(eq)
Re(1)	1786(1)	7424(1)	4990(1)	38(1)
Re(2)	1863(1)	6750(1)	6642(1)	34(1)
Cl(1)	3730(6)	8644(3)	5211(3)	59(2)
Cl(2)	-74(6)	7096(3)	7180(3)	58(2)
O(12)	1894(12)	7611(5)	6068(5)	33(4)
O(1)	1541(13)	7078(6)	4041(6)	48(5)
O(2)	2082(13)	5959(6)	7003(6)	49(5)
N(1A)	216(18)	8121(8)	4928(8)	53(7)
N(2A)	-526(17)	8126(9)	5489(8)	52(7)
C(3A)	-1351(28)	8688(15)	5425(15)	82(12)
C(4A)	-1148(30)	8971(15)	4782(14)	93(14)
C(5A)	-227(27)	8612(12)	4462(12)	65(11)
C(6A)	-2221(25)	8824(14)	6006(14)	101(14)
C(7A)	356(30)	8702(13)	3812(13)	114(17)
N(1B)	113(16)	6404(7)	5025(6)	37(6)
N(2B)	173(16)	6146(7)	5680(7)	37(6)
C(3B)	-1119(20)	5524(10)	5572(10)	39(7)

C(4B)	-1997(21)	5386(11)	4861(12)	58(9)
C(5B)	-1316(21)	5977(11)	4491(10)	48(8)
C(6B)	-1407(22)	5042(9)	6211(11)	73(10)
C(7B)	-1725(22)	6167(12)	3714(10)	77(10)
N(1C)	3442(17)	6858(8)	5365(7)	41(6)
N(2C)	3592(15)	6632(7)	6082(7)	30(5)
C(3C)	4841(19)	6445(10)	6255(11)	45(8)
C(4C)	5568(22)	6490(10)	5669(11)	57(9)
C(5C)	4678(23)	6767(9)	5108(12)	52(9)
C(6C)	5398(24)	6187(11)	7012(11)	77(11)
C(7C)	4950(22)	6972(11)	4368(10)	67(10)
N(1D)	3562(14)	7639(7)	7482(8)	37(6)
N(2D)	4391(16)	8233(8)	7239(8)	51(7)
C(3D)	5422(19)	8778(10)	7821(10)	50(7)
C(4D)	5197(22)	8500(11)	8476(10)	55(9)
C(5D)	4030(23)	7796(11)	8239(10)	51(9)
C(6D)	6474(23)	9502(11)	7690(12)	97(12)
C(7D)	3341(27)	7261(11)	8689(11)	90(12)
Re(3)	3839(1)	3257(1)	9002(1)	35(1)
Re(4)	2618(1)	1286(1)	8971(1)	35(1)
Cl(3)	4697(6)	3477(3)	7894(3)	63(2)
Cl(4)	-51(5)	874(3)	8467(3)	55(2)

O(34)	2661(11)	2162(5)	8489(5)	30(4)
O(3)	4800(15)	4122(6)	9605(7)	59(6)
O(4)	2939(13)	617(6)	9516(6)	47(5)
N(1E)	1828(17)	3519(8)	8503(8)	45(6)
N(2E)	483(16)	2932(9)	8283(8)	53(7)
C(3E)	-641(23)	3181(12)	7923(9)	49(9)
C(4E)	-76(24)	4005(12)	7967(10)	59(10)
C(5E)	1460(26)	4177(11)	8309(9)	55(9)
C(6E)	-2214(22)	2624(13)	7625(11)	80(11)
C(7E)	2628(24)	4955(9)	8449(9)	64(10)
N(1F)	2771(14)	2863(7)	9882(7)	31(5)
N(2F)	2267(14)	2061(7)	9855(7)	34(5)
C(3F)	1519(21)	1986(10)	10385(11)	50(9)
C(4F)	1608(22)	2715(11)	10782(10)	55(9)
C(5F)	2338(18)	3268(11)	10421(10)	42(7)
C(6F)	763(19)	1167(9)	10517(9)	48(8)
C(7F)	2623(22)	4132(9)	10608(11)	70(10)
N(1G)	5486(14)	2666(7)	9295(7)	30(5)
N(2G)	5001(15)	1841(7)	9304(7)	36(6)
C(3G)	6213(19)	1597(9)	9425(9)	35(7)
C(4G)	7536(22)	2216(10)	9518(9)	50(9)
C(5G)	7007(19)	2875(11)	9456(9)	39(7)

C(6G)	6174(21)	739(9)	9453(11)	61(9)
C(7G)	7945(19)	3745(9)	9544(10)	52(8)
N(1H)	2880(15)	698(7)	7946(7)	33(5)
N(2H)	3758(16)	1103(8)	7526(8)	51(7)
C(3H)	3857(22)	639(10)	6865(10)	53(8)
C(4H)	2969(23)	-117(11)	6915(12)	66(10)
C(5H)	2438(22)	-28(10)	7541(10)	47(8)
C(6H)	4779(25)	949(12)	6350(10)	77(12)
C(7H)	1547(27)	-681(10)	7874(10)	84(12)

Appendix Table 5G.2.

Atomic Coordinates ($x10^4$) and Equivalent Isotropic Displacement Coefficients ($Å^2x10^3$) for $ReOCl_2(PPh_3)(4\text{-}CH_2O\text{-}1,5\text{-}Me_2\text{-}Im)\cdot 2H_2O$ (5G)

	x	y	z	U(eq)
Re	637(1)	1873(1)	2262(1)	40(1)
Cl(1)	1003(4)	2554(4)	3156(3)	55(2)
Cl(2)	86(4)	3239(4)	1979(3)	55(2)
P	344(4)	1201(4)	1331(3)	40(2)
O(1)	-154(9)	1311(9)	2532(6)	46(5)
O(2)	1656(8)	2181(8)	1953(5)	36(5)
N(1A)	1942(11)	-410(11)	2758(10)	53(7)

C(2A)	1276(14)	54(15)	2793(11)	48(9)
N(3A)	1388(11)	782(12)	2505(8)	49(8)
C(4A)	2135(14)	811(15)	2307(11)	43(8)
C(5A)	2507(16)	46(16)	2448(10)	46(9)
C(6)	2320(15)	1628(15)	1967(10)	63(11)
C(7)	3326(13)	-284(15)	2305(13)	86(13)
C(8)	2029(16)	-1278(16)	2996(10)	78(12)
C(1B)	865(15)	167(15)	1212(10)	46(9)
C(2B)	674(16)	-596(16)	1562(10)	60(10)
C(3B)	1076(17)	-1386(15)	1539(14)	82(14)
C(4B)	1666(19)	-1455(18)	1152(12)	87(14)
C(5B)	1901(20)	-745(23)	814(14)	123(13)
C(6B)	1468(17)	32(18)	878(12)	77(12)
C(1C)	631(14)	1890(18)	712(8)	52(8)
C(2C)	1128(17)	2618(20)	678(16)	119(16)
C(3C)	1304(20)	3141(28)	210(15)	115(12)
C(4C)	1076(15)	2781(17)	-283(13)	74(13)
C(5C)	553(17)	2116(18)	-351(12)	77(9)
C(6C)	295(17)	1630(16)	177(16)	112(17)
C(1D)	-721(15)	979(15)	1242(10)	48(9)
C(2D)	-1276(15)	1524(15)	1467(11)	56(10)
C(3D)	-2097(16)	1419(19)	1361(13)	78(13)
C(4D)	-2360(19)	741(22)	1060(14)	94(15)
C(5D)	-1816(18)	140(18)	869(11)	68(12)
C(6D)	-981(16)	214(17)	946(10)	61(11)

O(3)	3846(25)	706(28)	857(18)	70
O(4)	4218(24)	1105(23)	1079(15)	70
O(5)	6776(12)	-1798(15)	233(9)	118(7)
O(6)	5419(25)	12(29)	800(15)	80
O(7)	5689(30)	-383(35)	577(18)	80

Appendix Table 5H.2.

Atomic Coordinates ($x10^4$) and Equivalent Isotropic Displacement Coefficients ($Å^2x10^3$) for $[TcO(4\text{-}OCH_2\text{-}1,5\text{-}Me_2\text{-}Im)_2(4\text{-}HOCH_2\text{-}1,5\text{-}Me_2\text{-}Im)]TcO_4$ (5H)

	x	y	z	U(eq)
Tc(1)	2203(1)	1191(1)	3003(1)	35(1)
O	3722(10)	373(8)	2588(4)	48(3)
N(1A)	-1057(12)	-1209(10)	768(4)	43(3)
C(2A)	568(14)	-759(12)	1214(6)	45(4)
N(3A)	455(11)	85(8)	1907(4)	36(3)
C(4A)	-1228(12)	182(11)	1882(5)	36(4)
C(5A)	-2203(12)	-625(11)	1195(5)	35(4)
C(6A)	-1604(13)	1104(12)	2611(6)	47(4)
C(7A)	-4133(14)	-972(14)	868(7)	56(5)
C(8A)	-1455(17)	-2195(15)	-26(6)	69(6)
O(6A)	-2(8)	1708(8)	3163(4)	43(3)
N(1B)	1174(11)	-2772(9)	3979(5)	40(3)
C(2B)	969(13)	-2202(11)	3361(5)	39(4)

N(3B)	1490(11)	-672(9)	3525(4)	39(3)
C(4B)	2085(14)	-191(11)	4325(5)	40(4)
C(5B)	1911(13)	-1466(12)	4615(5)	40(4)
C(6B)	2776(16)	1506(12)	4667(5)	51(4)
C(7B)	2367(16)	-1598(14)	5425(6)	60(5)
C(8B)	806(16)	-4422(12)	3995(7)	55(5)
O(6B)	3207(10)	2304(8)	4072(4)	49(3)
N(1C)	2814(10)	5172(9)	2065(4)	36(3)
C(2C)	2012(13)	3752(11)	2111(5)	35(4)
N(3C)	2954(11)	3298(9)	2654(4)	38(3)
C(4C)	4479(12)	4527(11)	2944(5)	36(4)
C(5C)	4419(13)	5700(11)	2597(6)	40(4)
C(6C)	5982(15)	4481(14)	3526(6)	56(5)
C(7C)	5648(16)	7263(12)	2710(7)	60(5)
C(8C)	2212(14)	6008(13)	1516(6)	52(5)
O(6C)	5763(11)	4981(9)	4310(4)	65(3)
Tc(2)	3083(1)	6024(1)	8825(1)	54(1)
O(21)	4733(13)	7455(10)	8718(6)	85(4)
O(22)	1631(12)	5255(13)	7972(5)	95(5)
O(23)	2098(14)	6872(16)	9525(6)	123(6)
O(24)	3896(17)	4596(14)	9074(6)	115(6)

Appendix 6.1

The Structural Data Processing Program

```
#include <string.h>
#include <stdio.h>
#include <math.h>
#include <conio.h>
#define  N 22

struct DATA {
    char    code [8];    char ox [4];
    float a, b, c, a1, b1, c1;
    char    atom [7] [5];
    float   x [7], y [7], z [7];
    float sas;
    }       line [N], *pline;

void stats() ;
void stats()
 {
   int mm;
   float av, sq, sd ;
   short count = 0;
```

```
    av = 0.0;
    sq = 0.0;

     for(mm=0; mm<N; ++mm){
     av += line[mm].sas;
     ++count ;
     sq += line[mm].sas*line[mm].sas;
                    }
    av = av/count;
    sd = sqrt(((sq - count*av*av)/(count - 1.0)));

printf("\n Average of sas is %.4f, standard deviation is %.4f, total %d",
av,sd,count);
 }

main()
{       FILE *fpnter ;
     float a, b, c, a1, b1, c1;
     short k ;
     short n, m ;
     float x, y, z, dx, dy, dz, X, Y, Z, Xv,Yv,Zv;
     float L[7], L1[6], L2[5], L3[4], L45, L46;
float    r11, r12, r13, r14;
```

```
float   r21, r22, r23, r24;
float   r31, r32, r33, r34;
float   r41, r42, r43, r44;
float   r51, r52, r53, r54;
float   r61, r62, r63, r64;
float dr1,dr2,dr3,dr4;
float sas, r[7], s[7], fa[7], saf[7], vssa,vd;
    if( (fpnter = fopen("mydat.22","r")) == NULL) exit(1) ;
     clrscr();

  for(k=0; k < N; ++k)
    {
     fscanf(fpnter,"%s",line[k].code);
     fscanf(fpnter,"%s",line[k].ox);
     fscanf(fpnter,"%f",&a);  fscanf(fpnter,"%f",&b);
     fscanf(fpnter,"%f",&c);  fscanf(fpnter,"%f",&a1);
     fscanf(fpnter,"%f",&b1);  fscanf(fpnter,"%f",&c1);

        for(m = 0 ; m<7; ++m)
        {
     fscanf(fpnter,"%s",line[k].atom[m]);
     fscanf(fpnter,"%f",&x); line[k].x[m]=x;
     fscanf(fpnter,"%f",&y); line[k].y[m]=y;
```

```
      fscanf(fpnter,"%f",&z); line[k].z[m]=z;
          }
     c1=cos(c1*3.14159265/180);
     a1=cos(a1*3.14159265/180);
     b1=cos(b1*3.14159265/180);
       for(n=2; n<7; ++n)
     {
dx=line[k].x[1]-line[k].x[n];
dy=line[k].y[1]-line[k].y[n]; dz=line[k].z[1]-line[k].z[n];
X=dx*a;Y=dy*b;Z=dz*c;
L1[n]=sqrt(X*X+Y*Y+Z*Z+2*X*Y*c1+2*X*Z*b1+2*Y*Z*a1);
     }
      for(n=3; n<7; ++n)
     {
dx=line[k].x[2]-line[k].x[n];
dy=line[k].y[2]-line[k].y[n]; dz=line[k].z[2]-line[k].z[n];
X=dx*a;Y=dy*b;Z=dz*c;
L2[n]=sqrt(X*X+Y*Y+Z*Z+2*X*Y*c1+2*X*Z*b1+2*Y*Z*a1);
     }

      for(n=4; n<7; ++n)
     {
dx=line[k].x[3]-line[k].x[n];
```

```
dy=line[k].y[3]-line[k].y[n]; dz=line[k].z[3]-line[k].z[n];
X=dx*a;Y=dy*b;Z=dz*c;
L3[n]=sqrt(X*X+Y*Y+Z*Z+2*X*Y*c1+2*X*Z*b1+2*Y*Z*a1);
    }
dx=line[k].x[4]-line[k].x[5];
dy=line[k].y[4]-line[k].y[5]; dz=line[k].z[4]-line[k].z[5];
X=dx*a;Y=dy*b;Z=dz*c;
L45=sqrt(X*X+Y*Y+Z*Z+2*X*Y*c1+2*X*Z*b1+2*Y*Z*a1);
dx=line[k].x[4]-line[k].x[6];
dy=line[k].y[4]-line[k].y[6]; dz=line[k].z[4]-line[k].z[6];
X=dx*a;Y=dy*b;Z=dz*c;
L46=sqrt(X*X+Y*Y+Z*Z+2*X*Y*c1+2*X*Z*b1+2*Y*Z*a1);

r11=0.5*(L1[2]+L1[5]-L2[5]); r12=0.5*(L1[4]+L1[5]-L45);
r13=0.5*(L1[2]+L1[6]-L2[6]); r14=0.5*(L1[4]+L1[6]-L46);
r[1]=0.25*(L1[2]+L1[4]+L1[5]+L1[6])-0.125*(L2[5]+L2[6]+L45+L46);
dr1=(r11-r[1])*(r11-r[1]);dr2=(r12-r[1])*(r12-r[1]);
dr3=(r13-r[1])*(r13-r[1]);dr4=(r14-r[1])*(r14-r[1]);
s[1]=sqrt(0.25*(dr1+dr2+dr3+dr4));

r21=0.5*(L1[2]-L1[5]+L2[5]); r22=0.5*(L1[2]+L2[6]-L1[6]);
r23=0.5*(L2[3]-L3[6]+L2[6]); r24=0.5*(L2[5]+L2[3]-L3[5]);
r[2]=0.25*(L1[2]+L2[3]+L2[5]+L2[6])-0.125*(L3[5]+L3[6]+L1[5]+L1[6]);
```

```
dr1=(r21-r[2])*(r21-r[2]);dr2=(r22-r[2])*(r22-r[2]);
dr3=(r23-r[2])*(r23-r[2]);dr4=(r24-r[2])*(r24-r[2]);
s[2]=sqrt(0.25*(dr1+dr2+dr3+dr4));

r31=0.5*(L2[3]+L3[5]-L2[5]); r32=0.5*(L3[4]+L3[5]-L45);
r33=0.5*(L2[3]+L3[6]-L2[6]); r34=0.5*(L3[4]+L3[6]-L46);
r[3]=0.25*(L2[3]+L3[4]+L3[5]+L3[6])-0.125*(L2[5]+L2[6]+L45+L46);
dr1=(r31-r[3])*(r31-r[3]);dr2=(r32-r[3])*(r32-r[3]);
dr3=(r33-r[3])*(r33-r[3]);dr4=(r34-r[3])*(r34-r[3]);
s[3]=sqrt(0.25*(dr1+dr2+dr3+dr4));

r41=0.5*(L1[4]-L1[5]+L45); r42=0.5*(L1[4]+L46-L1[6]);
r43=0.5*(L3[4]-L3[6]+L46); r44=0.5*(L45+L3[4]-L3[5]);
r[4]=0.25*(L1[4]+L3[4]+L45+L46)-0.125*(L3[5]+L3[6]+L1[5]+L1[6]);
dr1=(r41-r[4])*(r41-r[4]);dr2=(r42-r[4])*(r42-r[4]);
dr3=(r43-r[4])*(r43-r[4]);dr4=(r44-r[4])*(r44-r[4]);
s[4]=sqrt(0.25*(dr1+dr2+dr3+dr4));

r51=0.5*(-L1[2]+L1[5]+L2[5]); r52=0.5*(-L1[4]+L1[5]+L45);
r53=0.5*(L2[5]+L3[5]-L2[3]); r54=0.5*(L3[5]-L3[4]+L45);
r[5]=0.25*(L1[5]+L2[5]+L3[5]+L45)-0.125*(L2[3]+L1[2]+L3[4]+L1[4]);
dr1=(r51-r[5])*(r51-r[5]);dr2=(r52-r[5])*(r52-r[5]);
dr3=(r53-r[5])*(r53-r[5]);dr4=(r54-r[5])*(r54-r[5]);
```

```
s[5]=sqrt(0.25*(dr1+dr2+dr3+dr4));

r61=0.5*(L1[6]-L1[2]+L2[6]); r62=0.5*(-L1[4]+L46+L1[6]);
r63=0.5*(-L2[3]+L3[6]+L2[6]); r64=0.5*(L3[6]+L46-L3[4]);
r[6]=0.25*(L1[6]+L2[6]+L3[6]+L46)-0.125*(L1[2]+L3[4]+L2[3]+L1[4]);
dr1=(r61-r[6])*(r61-r[6]);dr2=(r62-r[6])*(r62-r[6]);
dr3=(r63-r[6])*(r63-r[6]);dr4=(r64-r[6])*(r64-r[6]);
s[6]=sqrt(0.25*(dr1+dr2+dr3+dr4));

printf("%s\n",line[k].code);
printf("d12=%.3f d14=%.3f d15=%.3f d16=%.3f ", L1[2], L1[4], L1[5], L1[6]);
printf("d23=%.3f d25=%.3f\nd26=%.3f ",  L2[3], L2[5], L2[6]);
printf("d34=%.3f d35=%.3f d36=%.3f ",   L3[4], L3[5], L3[6]);
printf("d45=%.3f d46=%.3f\n", L45, L46);
printf("%.3f %.3f %.3f %.3f %.3f  %.3f\n", r11,r12, r13,r14,r[1],s[1]);
printf("%.3f %.3f %.3f %.3f %.3f  %.3f\n", r21,r22, r23,r24,r[2], s[2]);
printf("%.3f %.3f %.3f %.3f %.3f  %.3f\n", r31,r32, r33,r34,r[3],s[3]);
printf("%.3f %.3f %.3f %.3f %.3f  %.3f\n", r41,r42, r43,r44,r[4],s[4]);
printf("%.3f %.3f %.3f %.3f %.3f  %.3f\n", r51,r52, r53,r54,r[5], s[5]);
printf("%.3f %.3f %.3f %.3f %.3f  %.3f\n", r61,r62, r63,r64,r[6],s[6]);

        sas=0;
        X=0;Y=0;Z=0;
```

```
        Xv=0;Yv=0;Zv=0;
        for(n=1; n<7; ++n)
        {
dx=line[k].x[0]-line[k].x[n];
dy=line[k].y[0]-line[k].y[n]; dz=line[k].z[0]-line[k].z[n];
X=dx*a;Y=dy*b;Z=dz*c;
L[n]=sqrt(X*X+Y*Y+Z*Z+2*X*Y*c1+2*X*Z*b1+2*Y*Z*a1);
fa[n]=asin(r[n]/L[n]); saf[n]=(1-cos(fa[n]))/2;
sas += saf[n];
Xv += saf[n]*dx; Yv += saf[n]*dy; Zv += saf[n]*dz;
printf("%s   %.3f %.3f %.3f %.3f %.3f %s %s\n",line[k].atom[n], r[n], s[n], L[n],
fa[n]*180/3.14159, saf[n], line[k].ox, line[k].code);
          }
vssa=sqrt(Xv*Xv+Yv*Yv+Zv*Zv+2*Xv*Yv*c1+2*Xv*Zv*b1+2*Yv*Zv*a1);
vd=sqrt(Xv*Xv*a*a+Yv*Yv*b*b+Zv*Zv*c*c+2*Xv*a*Yv*b*c1+2*Xv*a*Zv*c*b1+2
*Yv*b*Zv*c*a1);
line[k].sas=sas;
  printf("%.3f   %.4f   %.3f %s %s\n", sas, vssa, vd, line[k].ox, line[k].code);
    } printf("\n");
stats();
return;
}
```

Appendix Table 6.3

Statistics of Geometric Data vs. Oxidation States for Six Coordinated Rhenium Compounds

Variable	Obs	Mean	σ	Min	Max
As, ox = I					
VR	18	1.796	.039	1.747	1.869
SI	18	.123	.041	.038	.190
BL	18	2.580	.039	2.498	2.646
FA	18	44.13	1.08	42.20	45.64
SAF	18	.141	.006	.130	.150
As, ox = II					
VR	4	1.777	.033	1.747	1.820
SI	4	.197	.031	.168	.234
BL	4	2.522	.015	2.505	2.536
FA	4	44.79	.91	43.88	45.84
SAF	4	.146	.006	.140	.152
As, ox = III					
VR	16	1.767	.019	1.746	1.805
SI	16	.132	.024	.081	.156

BL	16	2.504	.024	2.477	2.549
FA	16	44.88	.22	44.37	45.50
SAF	16	.146	.001	.143	.150
As, ox = IV					
VR	2	1.702	.001	1.701	1.703
SI	2	.044	.0156	.033	.055
BL	2	2.561	.003	2.559	2.563
FA	2	41.65	.00	41.65	41.65
SAF	2	.126	0.000	.126	.126
As ox = V					
VR	8	1.765	.055	1.670	1.822
SI	8	.133	.069	.031	.207
BL	8	2.546	.008	2.532	2.557
FA	8	43.89	1.75	40.82	45.56
SAF	8	.140	.010	.122	.150
Br, ox = I					
VR	69	1.834	.037	1.761	1.955
SI	69	.109	.052	.000	.266
BL	69	2.641	.030	2.571	2.752
FA	69	44.00	1.05	42.26	47.68

SAF	69	.140	.006	.130	.163
Br, ox = II					
VR	8	1.772	.027	1.738	1.811
SI	8	.053	.015	.027	.070
BL	8	2.513	.009	2.501	2.529
FA	8	44.84	.79	43.82	45.89
SAF	8	.145	.005	.139	.152
Br, ox = III					
VR	5	1.838	.125	1.694	1.951
SI	5	.058	.003	.054	.062
BL	5	2.571	.046	2.526	2.642
FA	5	45.73	3.66	41.62	49.39
SAF	5	.151	.023	.126	.175
Br, ox = IV					
VR	5	1.794	.024	1.762	1.825
SI	5	.0428	.016	.026	.061
BL	5	2.554	.046	2.504	2.601
FA	5	44.62	.65	43.65	45.47
SAF	5	.144	.004	.138	.149

Br, ox = V					
VR	22	1.794	.072	1.624	1.871
SI	22	.081	.027	.021	.118
BL	22	2.533	.036	2.432	2.568
FA	22	45.12	2.03	40.02	48.48
SAF	22	.147	.012	.117	.169
Br, ox = VII					
VR	9	1.788	.031	1.715	1.823
SI	9	.073	.045	.016	.140
BL	9	2.565	.048	2.531	2.680
FA	9	44.23	1.90	39.79	45.97
SAF	9	.142	.011	.116	.152
C, ox = O					
VR	301	1.419	.051	1.242	1.629
SI	301	.066	.051	.007	.315
BL	301	1.994	.084	1.831	2.321
FA	301	45.41	1.61	40.10	49.96
SAF	301	.149	.010	.118	.178
C, ox= I					

VR	1460	1.397	.056	1.182	1.635
SI	1460	.091	.056	.000	.300
BL	1460	1.946	.079	1.700	2.340
FA	1460	45.96	2.14	38.42	52.92
SAF	1460	.153	.013	.108	.199
C, ox = II					
VR	29	1.400	.069	1.303	1.542
SI	29	.127	.073	.018	.271
BL	29	1.935	.101	1.769	2.174
FA	29	46.52	3.04	38.21	53.10
SAF	29	.156	.019	.107	.200
C, ox = III					
VR	7	1.399	.087	1.254	1.479
SI	7	.056	.048	.016	.149
BL	7	2.003	.124	1.775	2.154
FA	7	44.35	1.55	41.23	45.64
SAF	7	.143	.009	.124	.150
C, ox = IV					
VR	1	1.439	.	1.439	1.439
SI	1	.042	.	.042	.042

BL	1	2.142	.	2.142	2.142
FA	1	42.22	.	42.22	42.22
SAF	1	.130	.	.130	.130
C, ox = V					
VR	39	1.474	.035	1.393	1.526
SI	39	.051	.040	.003	.158
BL	39	2.089	.080	1.821	2.193
FA	39	44.96	2.10	42.16	53.26
SAF	39	.146	.014	.129	.201
C, ox = VI					
VR	1	1.461	.	1.461	1.461
SI	1	.008	.	.008	.008
BL	1	2.14	.	2.14	2.14
FA	1	43.05	.	43.05	43.05
SAF	1	.135	.	.135	.135
C, ox = VII					
VR	10	1.453	.028	1.400	1.491
SI	10	.096	.042	.025	.133
BL	10	2.049	.157	1.742	2.160
FA	10	45.62	4.50	41.73	53.51

SAF	10	.151	.029	.127	.203
Cl, ox = I					
VR	71	1.726	.041	1.626	1.846
SI	71	.111	.052	.007	.226
BL	71	2.516	.034	2.417	2.607
FA	71	43.33	1.08	40.67	46.86
SAF	71	.136	.007	.121	.158
Cl, ox = II					
VR	26	1.691	.033	1.629	1.748
SI	26	.139	.070	.013	.220
BL	26	2.423	.041	2.316	2.485
FA	26	44.27	1.05	42.09	45.73
SAF	26	.142	.007	.129	.151
Cl, ox = III					
VR	53	1.682	.044	1.609	1.795
SI	53	.093	.056	.009	.217
BL	53	2.364	.045	2.307	2.502
FA	53	45.37	1.28	41.55	48.44
SAF	53	.149	.008	.126	.168

Cl, ox = IV					
VR	117	1.670	.031	1.555	1.759
SI	117	.033	.029	.003	.164
BL	117	2.346	.025	2.281	2.428
FA	117	45.40	1.36	39.84	49.09
SAF	117	.149	.009	.116	.173
Cl, ox = V					
VR	212	1.686	.059	1.503	1.848
SI	212	.067	.047	.004	.224
BL	212	2.388	.048	2.215	2.633
FA	212	44.99	2.38	38.11	50.41
SAF	212	.147	.015	.107	.181
Cl, ox = VII					
VR	39	1.663	.046	1.560	1.751
SI	39	.063	.051	.006	.165
BL	39	2.394	.072	2.298	2.712
FA	39	44.06	1.99	39.35	46.82
SAF	39	.141	.012	.113	.158
F, ox = I					

VR	7	1.438	.069	1.323	1.551
SI	7	.150	.069	.073	.237
BL	7	2.132	.102	1.973	2.236
FA	7	42.46	1.26	40.89	43.93
SAF	7	.131	.008	.122	.140
F, ox = III					
VR	3	1.417	.074	1.331	1.460
SI	3	.125	.083	.030	.173
BL	3	2.037	.014	2.020	2.045
FA	3	44.12	2.49	41.24	45.56
SAF	3	.141	.015	.124	.150
F, ox = V					
VR	10	1.324	.021	1.292	1.348
SI	10	.024	.009	.007	.038
BL	10	1.900	.070	1.789	2.009
FA	10	44.24	1.95	41.83	48.43
SAF	10	.142	.012	.127	.168
H, ox = O					
VR	1	1.233	.	1.233	1.233
SI	1	.099	.	.099	.099

BL	1	1.695	.	1.695	1.695
FA	1	46.67	.	46.67	46.67
SAF	1	.157	.	.157	.157
H, ox = I					
VR	134	1.277	.076	1.030	1.449
SI	134	.139	.052	.023	.254
BL	134	1.836	.098	1.489	2.103
FA	134	44.14	2.19	37.33	50.02
SAF	134	.141	.013	.102	.179
H, ox = II					
VR	2	1.112	.002	1.110	1.113
SI	2	.176	.056	.136	.215
BL	2	1.823	.003	1.821	1.825
FA	2	37.57	.01	37.56	37.58
SAF	2	.104	.000	.104	.104
I, ox = I					
VR	44	1.986	.056	1.903	2.138
SI	44	.118	.073	.009	.339
BL	44	2.832	.039	2.761	2.917
FA	44	44.57	1.94	41.16	50.49

SAF	44	.144	.012	.124	.182
I, ox = III					
VR	1	1.957	.	1.957	1.957
SI	1	.005	.	.005	.005
BL	1	2.742	.	2.742	2.742
FA	1	45.53	.	45.53	45.53
SAF	1	.150	.	.150	.150
I, ox = IV					
VR	6	1.919	0	1.919	1.919
SI	6	.059	0	.059	.059
BL	6	2.715	0	2.715	2.715
FA	6	44.99	0	44.99	44.99
SAF	6	.146	0	.146	.146
I, ox = V					
VR	15	1.961	.033	1.922	2.036
SI	15	.089	.038	.040	.158
BL	15	2.776	.066	2.719	2.952
FA	15	44.98	1.19	41.18	46.17
SAF	15	.146	.007	.124	.154

I, ox = VII					
VR	4	1.968	.033	1.919	1.987
SI	4	.093	.029	.061	.127
BL	4	2.755	.016	2.736	2.771
FA	4	45.60	.90	44.31	46.42
SAF	4	.150	.006	.142	.155
N, ox = O					
VR	4	1.468	.019	1.444	1.487
SI	4	.173	.094	.060	.261
BL	4	2.189	.032	2.150	2.228
FA	4	42.13	.879	41.35	43.39
SAF	4	.130	.005	.125	.137
N, ox = I					
VR	147	1.492	.072	1.331	1.726
SI	147	.120	.063	.018	.326
BL	147	2.156	.115	1.726	2.407
FA	147	43.90	2.39	38.34	54.67
SAF	147	.140	.015	.108	.211
N, ox = II					
VR	17	1.434	.067	1.320	1.573

SI	17	.085	.079	.018	.230
BL	17	2.017	.168	1.716	2.245
FA	17	45.63	3.45	40.84	52.95
SAF	17	.151	.022	.122	.199
N, ox = III					
VR	28	1.478	.074	1.350	1.641
SI	28	.100	.060	.006	.192
BL	28	2.096	.147	1.708	2.334
FA	28	45.06	2.80	40.46	52.19
SAF	28	.147	.018	.120	.194
N, ox = IV					
VR	21	1.416	.050	1.337	1.540
SI	21	.072	.045	.009	.156
BL	21	2.003	.151	1.731	2.212
FA	21	45.32	3.64	40.66	52.31
SAF	21	.149	.023	.121	.194
N, ox = V					
VR	265	1.449	.073	1.207	1.610
SI	265	.095	.059	.004	.305
BL	265	2.063	.169	1.648	2.360

FA	265	45.01	3.99	33.51	58.07
SAF	265	.147	.025	.083	.236
N, ox = VI					
VR	11	1.449	.055	1.322	1.499
SI	11	.021	.014	.008	.059
BL	11	2.087	.198	1.657	2.456
FA	11	44.41	3.90	36.78	52.93
SAF	11	.144	.024	.100	.199
N, ox = VII					
VR	55	1.384	.068	1.241	1.551
SI	55	.075	.052	.010	.186
BL	55	1.977	.257	1.686	2.434
FA	55	45.68	7.23	36.02	61.06
SAF	55	.153	.046	.096	.258
O, ox = O					
VR	17	1.490	.037	1.411	1.569
SI	17	.099	.052	.034	.233
BL	17	2.165	.028	2.120	2.214
FA	17	43.52	1.58	39.59	46.84
SAF	17	.138	.009	.115	.158

O, ox = I					
VR	127	1.454	.061	1.302	1.590
SI	127	.170	.063	.022	.325
BL	127	2.162	.043	2.055	2.402
FA	127	42.28	2.08	38.41	47.79
SAF	127	.130	.012	.108	.164
O, ox = II					
VR	5	1.425	.039	1.384	1.470
SI	5	.140	.035	.091	.178
BL	5	2.142	.029	2.109	2.169
FA	5	41.71	.857	41.01	42.89
SAF	5	.127	.005	.123	.134
O, ox = III					
VR	17	1.376	.048	1.281	1.428
SI	17	.055	.036	.008	.121
BL	17	1.983	.105	1.720	2.135
FA	17	44.08	2.39	40.41	49.96
SAF	17	.141	.015	.119	.178
O, ox = IV					

VR	20	1.393	.040	1.278	1.447
SI	20	.073	.053	.016	.174
BL	20	2.016	.097	1.795	2.154
FA	20	43.89	2.86	39.18	53.23
SAF	20	.140	.018	.112	.201
O, ox = V					
VR	265	1.333	.069	1.189	1.638
SI	265	.086	.053	.003	.280
BL	265	1.860	.176	1.576	2.463
FA	265	46.59	6.10	36.09	64.46
SAF	265	.158	.040	.096	.284
O, ox = VI					
VR	18	1.351	.053	1.259	1.462
SI	18	.128	.067	.025	.234
BL	18	1.892	.104	1.692	2.084
FA	18	45.89	4.49	38.92	59.78
SAF	18	.153	.030	.111	.248
O, ox = VII					
VR	89	1.349	.055	1.201	1.483
SI	89	.053	.041	.003	.168

BL	89	1.895	.212	1.669	2.465
FA	89	46.49	6.86	35.34	60.41
SAF	89	.158	.043	.092	.253
P, ox = O					
VR	18	1.755	.068	1.638	1.847
SI	18	.092	.054	.018	.188
BL	18	2.434	.047	2.350	2.541
FA	18	46.20	2.49	41.68	49.66
SAF	18	.154	.015	.127	.176
P, ox = I					
VR	319	1.734	.064	1.551	1.907
SI	319	.144	.072	.005	.368
BL	319	2.439	.049	2.335	2.562
FA	319	45.36	2.00	39.51	51.29
SAF	319	.149	.012	.114	.187
P, ox = II					
VR	51	1.721	.033	1.638	1.834
SI	51	.167	.067	.019	.313
BL	51	2.423	.043	2.344	2.517
FA	51	45.25	1.17	42.29	51.17

SAF	51	.148	.007	.130	.186
P, ox = III					
VR	70	1.741	.039	1.597	1.859
SI	70	.150	.048	.025	.291
BL	70	2.460	.027	2.369	2.509
FA	70	45.06	1.19	40.70	49.22
SAF	70	.147	.007	.121	.173
P, ox = IV					
VR	17	1.751	.034	1.669	1.783
SI	17	.085	.040	.030	.139
BL	17	2.491	.018	2.464	2.518
FA	17	44.66	1.03	41.98	45.53
SAF	17	.144	.006	.128	.150
P, ox = V					
VR	142	1.749	.039	1.623	1.836
SI	142	.110	.066	.012	.357
BL	142	2.47	.036	2.406	2.576
FA	142	45.06	1.08	42.31	48.97
SAF	142	.147	.007	.130	.172

P, ox = VII						
	VR	1	1.824	.	1.824	1.824
	SI	1	.148	.	.148	.148
	BL	1	2.453	.	2.453	2.453
	FA	1	48.02	.	48.02	48.02
SAF	1	.166	.	.166	.166	
S, ox = I						
	VR	89	1.716	.053	1.595	1.843
	SI	89	.166	.078	.023	.347
	BL	89	2.497	.048	2.327	2.610
	FA	89	43.45	1.81	40.26	48.75
	SAF	89	.137	.011	.118	.170
S, ox = III						
	VR	19	1.656	.056	1.623	1.822
	SI	19	.159	.037	.083	.221
	BL	19	2.328	.083	2.239	2.565
	FA	19	45.37	1.19	43.20	48.76
	SAF	19	.149	.007	.136	.170
S, ox = IV						
	VR	3	1.704	.011	1.697	1.717

SI	3	.033	.027	.002	.051
BL	3	2.407	.017	2.395	2.427
FA	3	45.07	.11	44.98	45.19
SAF	3	.147	.001	.146	.148
S, ox = V					
VR	38	1.697	.036	1.629	1.755
SI	38	.129	.081	.025	.336
BL	38	2.395	.066	2.280	2.483
FA	38	45.17	1.89	41.26	48.94
SAF	38	.148	.012	.124	.172
S, ox = VII					
VR	7	1.622	.045	1.548	1.683
SI	7	.122	.110	.029	.277
BL	7	2.513	.068	2.423	2.585
FA	7	40.25	2.06	38.48	43.68
SAF	7	.119	.012	.109	.138

Appendix Table 6.O

Detailed Analyses of Parameters of Oxygen Atom in Six Coordinated Rhenium Compounds

Variable	Obs	Mean	σ	Min	Max
O, for ox = V and BL ≤ 1.68 Å					
VR	44	1.356	.060	1.189	1.460
SI	44	.090	.048	.010	.242
BL	44	1.662	.020	1.576	1.680
FA	44	54.85	3.70	46.00	62.24
SAF	44	.213	.026	.153	.267
O, for ox = V and BL ≤ 1.71 Å					
VR	82	1.346	.061	1.189	1.517
SI	82	.094	.053	.004	.256
BL	82	1.676	.021	1.576	1.704
FA	82	53.58	3.86	46.00	64.46
SAF	82	.204	.027	.153	.284
O, for ox = V and BL ≤ 1.83 Å					
VR	135	1.324	.065	1.189	1.517
SI	135	.095	.056	.003	.256
BL	135	1.709	.046	1.576	1.802
FA	135	51.14	4.80	43.24	64.46
SAF	135	.187	.033	.136	.284

O, for ox = V and BL ≤ 2.05 Å					
VR	224	1.325	.066	1.189	1.517
SI	224	.090	.054	.003	.280
BL	224	1.807	.131	1.576	2.040
FA	224	47.81	5.76	38.22	64.46
SAF	224	.166	.038	.107	.284
O, for ox = V and BL > 2.05 Å					
VR	41	1.375	.071	1.258	1.638
SI	41	.068	.046	.006	.249
BL	41	2.146	.096	2.053	2.463
FA	41	39.97	2.77	36.09	49.95
SAF	41	.117	.016	.096	.178
O, for ox = V and 1.68 < BL ≤ 1.71 Å					
VR	38	1.333	.059	1.257	1.517
SI	38	.099	.058	.004	.256
BL	38	1.693	.007	1.682	1.704
FA	38	52.13	3.56	47.73	64.46
SAF	38	.194	.025	.164	.284
O, for ox = V and 1.71Å < BL ≤ 1.83 Å					
VR	53	1.290	.058	1.211	1.480
SI	53	.096	.061	.003	.225
BL	53	1.759	.025	1.711	1.802

FA	53	47.35	3.46	43.24	59.07
SAF	53	.162	.023	.136	.243
O, for ox = V and 1.83Å < BL ≤ 2.05 Å					
VR	89	1.327	.069	1.191	1.475
SI	89	.083	.050	.003	.280
BL	89	1.957	.050	1.847	2.040
FA	89	42.75	2.49	38.22	47.54
SAF	89	.133	.015	.107	.162
O, for ox = VII and BL ≤ 1.71 Å					
VR	24	1.354	.051	1.278	1.478
SI	24	.045	.044	.003	.168
BL	24	1.694	.011	1.669	1.709
FA	24	53.18	2.93	48.71	60.41
SAF	24	.201	.021	.170	.253
O, for ox = VII and BL ≤ 1.68 Å					
VR	2	1.376	.090	1.312	1.439
SI	2	.042	.020	.028	.056
BL	2	1.675	.008	1.669	1.680
FA	2	55.40	5.04	51.83	58.96
SAF	2	.217	.036	.191	.242
O, for ox = VII and 1.71Å < BL ≤ 1.83 Å					
VR	20	1.364	.047	1.292	1.483

SI	20	.028	.020	.007	.103
BL	20	1.728	.022	1.710	1.786
FA	20	52.17	2.67	49.07	59.82
SAF	20	.194	.019	.172	.249
O, for ox = VII and BL ≤ 1.72 Å					
VR	36	1.355	.053	1.278	1.483
SI	36	.041	.039	.003	.168
BL	36	1.701	.013	1.669	1.719
FA	36	52.95	3.06	48.71	60.41
SAF	36	.199	.022	.170	.253
O, for ox = V and BL ≤ 1.72 Å					
VR	86	1.346	.061	1.189	1.517
SI	86	.091	.053	.004	.256
BL	86	1.678	.022	1.576	1.715
FA	86	53.51	3.90	46.00	64.46
SAF	86	.203	.027	.153	.284
O, for ox = VI and BL ≤ 1.72 Å					
VR	2	1.415	.066	1.368	1.462
SI	2	.097	.005	.093	.100
BL	2	1.699	.010	1.692	1.706
FA	2	56.53	4.60	53.28	59.78
SAF	2	.225	.033	.201	.248

Appendix Table 6.N.

Detailed Analyses of Parameters of Nitrogen Atom in Six Coordinated Rhenium Compounds

Variable	Obs	Mean	σ	Min	Max
N, ox = VII and BL ≤ 1.90 Å					
VR	32	1.363	.071	1.241	1.501
SI	32	.098	.054	.017	.186
BL	32	1.772	.056	1.686	1.895
FA	32	50.64	5.08	44.36	61.06
SAF	32	.184	.035	.142	.258
N, ox = VII and BL > 1.90 Å					
VR	23	1.413	.053	1.357	1.551
SI	23	.042	.028	.010	.124
BL	23	2.262	.108	1.902	2.434
FA	23	38.77	2.50	36.02	48.50
SAF	23	.111	.015	.096	.169
N, ox = VI and BL ≤ 1.90 Å					
VR	1	1.322	.	1.322	1.322
SI	1	.015	.	.015	.015
BL	1	1.657	.	1.657	1.657
FA	1	52.93	.	52.93	52.93
SAF	1	.199	.	.199	.199
N, ox = VI and BL > 1.90 Å					

VR	10	1.462	.037	1.401	1.499
SI	10	.022	.015	.008	.059
BL	10	2.130	.145	1.997	2.456
FA	10	43.55	2.83	36.78	45.01
SAF	10	.138	.016	.100	.146
N, ox = V and BL ≤ 1.90 Å					
VR	50	1.359	.044	1.244	1.441
SI	50	.102	.072	.009	.292
BL	50	1.736	.049	1.648	1.868
FA	50	51.62	2.98	44.70	58.07
SAF	50	.190	.020	.145	.236
N, ox = V and BL > 1.90 Å					
VR	215	1.470	.061	1.207	1.610
SI	215	.093	.055	.004	.305
BL	215	2.139	.064	1.904	2.360
FA	215	43.48	2.24	33.51	49.64
SAF	215	.137	.013	.083	.176
N, ox = IV and BL ≤ 1.90 Å					
VR	5	1.369	.021	1.337	1.392
SI	5	.0452	.039	.009	.093
BL	5	1.772	.027	1.731	1.795
FA	5	50.64	1.75	48.19	52.31
SAF	5	.183	.011	.167	.194
N, ox = IV and BL > 1.90 Å					

VR	16	1.431	.048	1.383	1.540
SI	16	.081	.045	.027	.156
BL	16	2.076	.082	1.922	2.212
FA	16	43.66	2.11	40.66	46.01
SAF	16	.139	.013	.121	.153
N, ox = III and BL ≤ 1.90 Å					
VR	3	1.359	.008	1.350	1.365
SI	3	.034	.016	.025	.053
BL	3	1.740	.029	1.708	1.763
FA	3	51.33	.77	50.74	52.20
SAF	3	.188	.005	.184	.194
N, ox = III and BL > 1.90 Å					
VR	25	1.493	.065	1.375	1.641
SI	25	.108	.059	.006	.192
BL	25	2.139	.081	1.992	2.334
FA	25	44.31	1.81	40.46	49.17
SAF	25	.142	.011	.120	.173
N, ox = II and BL ≤ 1.90 Å					
VR	4	1.358	.044	1.320	1.413
SI	4	.080	.101	.018	.230
BL	4	1.753	.040	1.716	1.800
FA	4	50.87	2.67	47.34	52.95
SAF	4	.185	.018	.161	.199
N, ox = II and BL > 1.90 Å					

VR	13	1.457	.055	1.344	1.573
SI	13	.087	.076	.020	.205
BL	13	2.098	.081	1.923	2.245
FA	13	44.02	1.47	40.84	46.78
SAF	13	.140	.009	.122	.158
N, ox = I and BL ≤ 1.90 Å					
VR	9	1.372	.035	1.331	1.431
SI	9	.076	.054	.022	.178
BL	9	1.794	.047	1.726	1.878
FA	9	49.98	2.77	46.85	54.67
SAF	9	.179	.019	.158	.211
N, ox = I and BL > 1.90 Å					
VR	138	1.500	.066	1.347	1.726
SI	138	.123	.062	.018	.326
BL	138	2.180	.070	1.950	2.407
FA	138	43.51	1.75	38.34	49.47
SAF	138	.138	.011	.108	.175
N, ox = O and BL > 1.90 Å					
VR	4	1.468	.019	1.444	1.487
SI	4	.173	.094	.060	.261
BL	4	2.189	.032	2.150	2.228
FA	4	42.13	.88	41.35	43.39
SAF	4	.130	.005	.125	.137

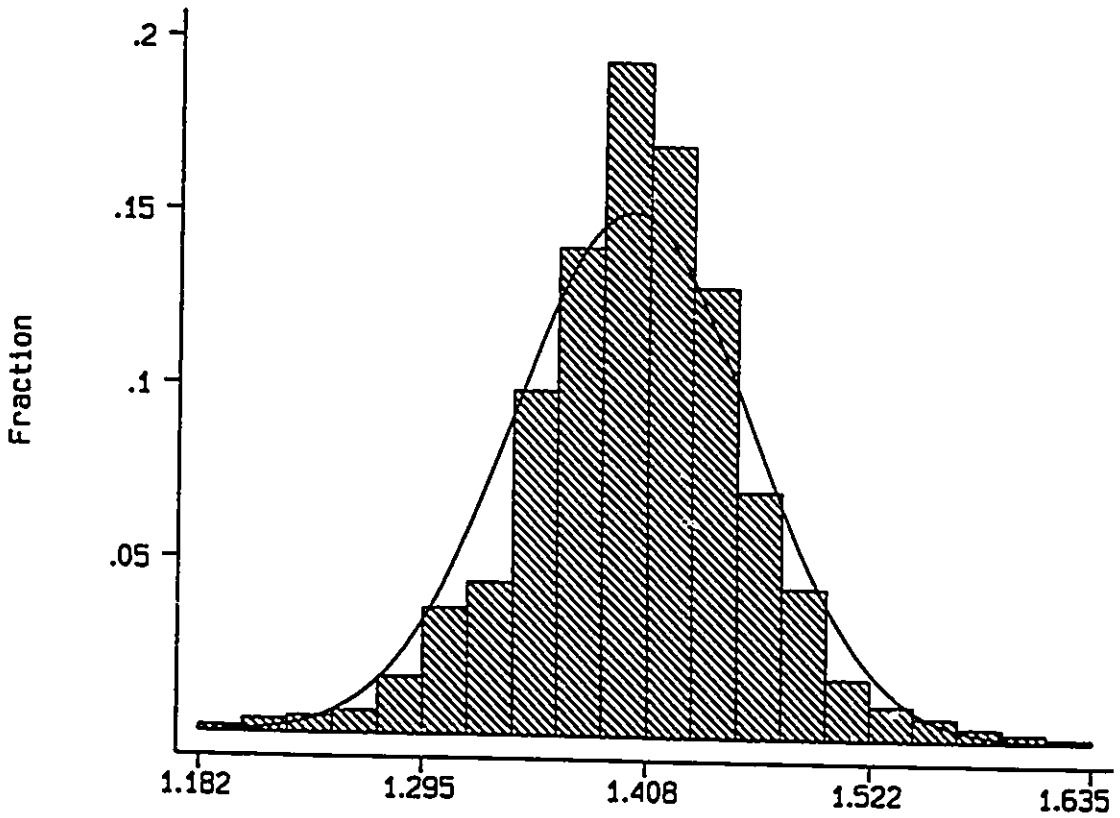

The Appendix Fig. 6.C1

The Normal Distribution of the Virtual Radii of Carbon Atoms.

Number of Observation 1848, Mean 1.403 Å, Standard Deviation 0.057.

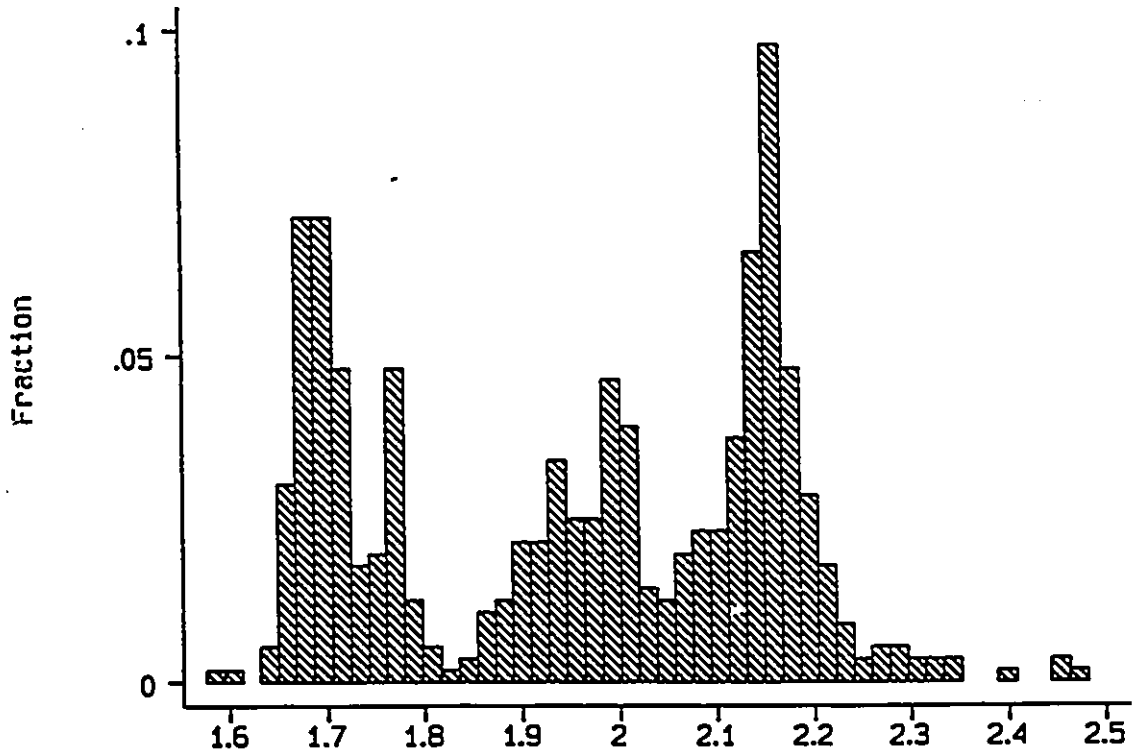

The Appendix Fig. 6.O1

The Non-unimodal Distribution of Re-O Bond Lengths

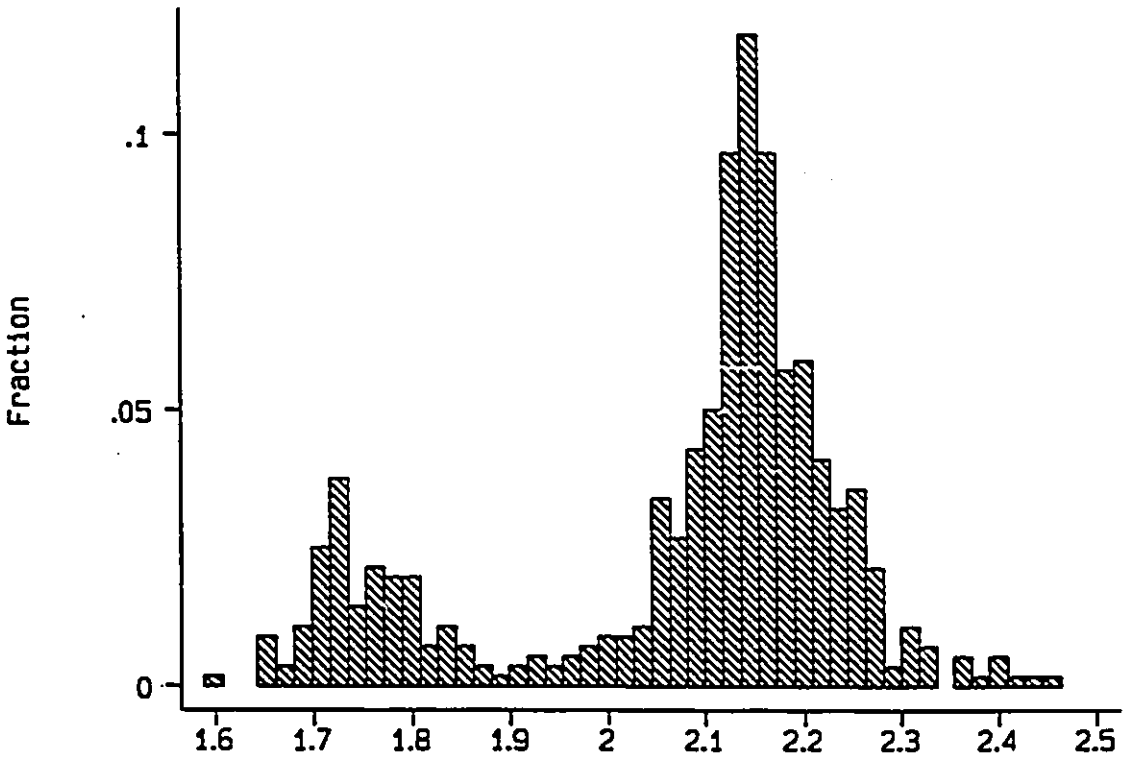

The Appendix Fig. 6.N1

The Non-unimodal Distribution of Re-N Bond Lengths

Appendix Table 7.1

The Non-bonding Distances, Virtual Radii (VR) and Shape Index (SI) of Ligating Atoms for Structures Determined in This Study

	R1	R2	R3	R4	VR	SI
NUJOI-4 $[Re(CO)_3(OH)]_4 \cdot 8H_2O$ (3C)						
d12=3.118 d14=2.651 d15=2.604 d16=3.135 d23=2.593 d25=3.122						
d26=2.593 d34=3.068 d35=3.074 d36=2.650 d45=2.602 d46=3.144						
C2	1.300	1.326	1.830	1.321	1.444	0.223
O4B	1.818	1.289	1.268	1.321	1.424	0.228
O4A	1.273	1.770	1.325	1.287	1.414	0.207
C3	1.324	1.330	1.781	1.298	1.434	0.201
C1	1.304	1.278	1.801	1.304	1.422	0.219
O4	1.305	1.814	1.325	1.363	1.452	0.210
TriPa-3 $KRe_3(CO)_9(OH)_4$ (3E)						
d12=2.572 d14=3.095 d15=2.609 d16=3.108 d23=3.148 d25=2.612						
d26=3.004 d34=2.642 d35=3.102 d36=2.642 d45=3.053 d46=2.760						
C3	1.285	1.326	1.338	1.721	1.417	0.177
C2	1.287	1.234	1.755	1.329	1.401	0.207
O4	1.819	1.345	1.393	1.262	1.455	0.215

O5	1.770	1.374	1.380	1.297	1.455	0.185
C1	1.324	1.283	1.283	1.756	1.412	0.200
O5A	1.770	1.386	1.249	1.380	1.446	0.195

Y2P21n1 $K[Re_3(\mu_2\text{-}OCH_3)_3(\mu_3\text{-}OCH_3)(CO)_9]$ (3A)

d12=2.620 d14=3.032 d15=3.156 d16=2.640 d23=3.144 d25=2.995

d26=2.754 d34=2.623 d35=2.607 d36=3.081 d45=2.703 d46=2.997

O4	1.390	1.742	1.253	1.337	1.430	0.187
O3	1.230	1.367	1.408	1.766	1.443	0.198
C11	1.378	1.264	1.736	1.354	1.433	0.180
C13	1.289	1.694	1.269	1.359	1.403	0.171
C12	1.766	1.413	1.229	1.343	1.438	0.200
O1	1.387	1.303	1.346	1.728	1.441	0.168

Y2P21n2 $K[Re_3(\mu_2\text{-}OCH_3)_3(\mu_3\text{-}OCH_3)(CO)_9]$ (3A)

d12=2.628 d14=3.110 d15=2.956 d16=2.771 d23=3.102 d25=3.097

d26=2.640 d34=2.574 d35=2.725 d36=2.979 d45=2.672 d46=3.040

O2	1.243	1.697	1.379	1.420	1.435	0.165
O4	1.384	1.248	1.382	1.737	1.438	0.181
C22	1.365	1.314	1.721	1.256	1.414	0.181
C21	1.413	1.690	1.318	1.260	1.420	0.165
C23	1.712	1.258	1.360	1.411	1.436	0.169

O1	1.391	1.350	1.258	1.723	1.431	0.175

Y2P21n3 $K[Re_3(\mu_2\text{-}OCH_3)_3(\mu_3\text{-}OCH_3)(CO)_9]$ (3A)

d12=2.572 d14=3.141 d15=2.697 d16=3.024 d23=3.057 d25=2.634

d26=2.998 d34=2.628 d35=3.069 d36=2.620 d45=2.988 d46=2.760

C31	1.317	1.425	1.299	1.702	1.436	0.161
C33	1.254	1.273	1.718	1.311	1.389	0.191
O4	1.746	1.354	1.339	1.243	1.421	0.193
O2	1.716	1.439	1.384	1.273	1.453	0.163
C32	1.380	1.272	1.323	1.715	1.422	0.173
O3	1.725	1.322	1.280	1.376	1.426	0.176

Y7C2c1 $[Re_4(CO)_{12}(OH)_2(EtO)_2]\cdot 2EtOH$ (3B)

d12=2.602 d14=3.135 d15=2.637 d16=3.149 d23=3.103 d25=2.638

d26=3.157 d34=2.625 d35=3.013 d36=2.646 d45=3.122 d46=2.596

C1B	1.300	1.325	1.297	1.844	1.442	0.232
C1C	1.302	1.305	1.807	1.364	1.444	0.211
O1	1.739	1.258	1.296	1.337	1.408	0.193
O2A	1.810	1.292	1.288	1.367	1.439	0.217
C1A	1.337	1.312	1.274	1.755	1.419	0.195
O2	1.851	1.305	1.350	1.308	1.454	0.230

Y7C2c2 $[Re_4(CO)_{12}(OH)_2(EtO)_2]\cdot 2EtOH$ (3B)

d12=3.133 d14=2.589 d15=2.646 d16=3.140 d23=2.625 d25=3.092

d26=2.595 d34=3.181 d35=3.131 d36=2.619 d45=2.625 d46=3.136

O1	1.343	1.305	1.839	1.297	1.446	0.228
C2C	1.789	1.294	1.300	1.293	1.419	0.214
C2A	1.332	1.844	1.325	1.333	1.458	0.223
O1A	1.285	1.292	1.849	1.338	1.441	0.236
O2	1.302	1.341	1.799	1.288	1.433	0.213
C2B	1.301	1.843	1.295	1.287	1.432	0.238

YDC2m1 $KRe_2(CO)_6(OH)_3\cdot 2H_2O$ (3D)

d12=2.632 d14=3.065 d15=2.582 d16=3.070 d23=3.158 d25=2.632

d26=3.158 d34=2.556 d35=3.070 d36=2.638 d45=3.065 d46=2.556

C1A	1.291	1.291	1.272	1.790	1.411	0.219
C1B	1.341	1.360	1.840	1.360	1.475	0.210
O1C	1.798	1.280	1.319	1.319	1.429	0.214
O2	1.774	1.276	1.237	1.276	1.391	0.222
C1AA	1.291	1.291	1.272	1.790	1.411	0.219
O1	1.798	1.280	1.319	1.319	1.429	0.214

YDIC2m2 $KRe_2(CO)_6(OH)_3\cdot 2H_2O$ (3D)

d12=2.638 d14=3.096 d15=2.556 d16=3.127 d23=3.096 d25=2.556

d26=3.127 d34=2.604 d35=3.065 d36=2.619 d45=3.065 d46=2.619

O1	1.319	1.293	1.319	1.802	1.433	0.213
O1C	1.319	1.319	1.802	1.293	1.433	0.213
C2AA	1.803	1.302	1.294	1.302	1.425	0.218
C2A	1.803	1.294	1.302	1.302	1.425	0.218
O2	1.237	1.262	1.262	1.763	1.381	0.221
C2B	1.808	1.325	1.325	1.317	1.444	0.211

YDIC2m3 $KRe_2(CO)_6(OH)_3{\cdot}2H_2O$ (3D)

d12=2.535 d14=3.097 d15=2.612 d16=3.011 d23=3.097 d25=2.612

d26=3.011 d34=2.602 d35=3.036 d36=2.648 d45=3.036 d46=2.648

O3	1.268	1.336	1.268	1.730	1.400	0.192
O3C	1.268	1.268	1.730	1.336	1.400	0.192
C3AA	1.761	1.301	1.367	1.301	1.432	0.191
C3A	1.761	1.367	1.301	1.301	1.432	0.191
O4	1.344	1.276	1.276	1.735	1.408	0.191
C3B	1.743	1.281	1.281	1.346	1.413	0.193

YDIC2m4 $KRe_2(CO)_6(OH)_3{\cdot}2H_2O$ (3D)

d12=2.612 d14=3.108 d15=2.535 d16=3.109 d23=3.059 d25=2.612

d26=3.059 d34=2.643 d35=3.109 d36=2.574 d45=3.108 d46=2.643

O3	1.268	1.268	1.331	1.787	1.413	0.217

O4	1.344	1.281	1.772	1.281	1.420	0.205
C4AA	1.779	1.322	1.287	1.287	1.419	0.208
C4B	1.840	1.321	1.356	1.321	1.459	0.220
O3C	1.268	1.268	1.331	1.787	1.413	0.217
C4A	1.778	1.322	1.287	1.287	1.419	0.208

GREEN1 $[ReOCl(PPh_3)]_2(\mu\text{-}O)(\mu\text{-}pz)_2\cdot CHCl_3$ (5E)

d12=3.085 d14=3.439 d15=3.104 d16=3.314 d23=2.876 d25=2.936

d26=2.573 d34=3.378 d35=2.547 d36=2.602 d45=3.084 d46=2.962

CL1	1.627	1.730	1.914	1.896	1.791	0.119
N2H	1.459	1.172	1.423	1.633	1.422	0.165
N2G	1.243	1.420	1.453	1.509	1.406	0.099
P1	1.709	1.543	1.869	1.958	1.770	0.158
O1	1.478	1.375	1.304	1.126	1.321	0.128
O3	1.401	1.419	1.149	1.093	1.265	0.146

GREEN2 $[ReOCl(PPh_3)]_2(\mu\text{-}O)(\mu\text{-}pz)_2\cdot CHCl_3$ (5E)

d12=3.035 d14=3.492 d15=3.103 d16=3.299 d23=2.923 d25=2.933

d26=2.592 d34=3.364 d35=2.571 d36=2.574 d45=3.077 d46=3.028

CL2	1.602	1.759	1.871	1.881	1.778	0.112
N1G	1.432	1.164	1.470	1.642	1.427	0.172
N1H	1.280	1.429	1.452	1.455	1.404	0.072

P2	1.733	1.611	1.909	1.935	1.797	0.133
O2	1.501	1.344	1.291	1.142	1.320	0.128
O3	1.428	1.418	1.121	1.119	1.272	0.151

Yviolet $[ReO(HBPz_3)(Pz\text{-}(CO)Me_2)][ReO_4]$ (5B)

d12=2.952 d14=3.205 d15=2.692 d16=2.648 d23=2.767 d25=2.819

d26=2.840 d34=2.537 d35=2.902 d36=2.921 d45=2.926 d46=2.862

N1A	1.412	1.485	1.380	1.495	1.443	0.049
N1B	1.540	1.573	1.343	1.342	1.449	0.107
O1D	1.424	1.256	1.423	1.298	1.350	0.075
N1D	1.720	1.710	1.239	1.281	1.487	0.228
O	1.279	1.207	1.477	1.646	1.402	0.172
N1C	1.268	1.153	1.497	1.623	1.385	0.185

blue $ReOCl_2(PPh_3)(pz\text{-}COMe_2)$ (5C)

d12=3.330 d14=3.204 d15=3.055 d16=3.100 d23=3.347 d25=3.247

d26=3.080 d34=3.402 d35=2.913 d36=3.178 d45=2.671 d46=2.477

CL1	1.569	1.794	1.675	1.913	1.738	0.129
CL2	1.761	1.655	1.625	1.840	1.720	0.086
P	1.506	1.822	1.722	2.051	1.775	0.196
N1	1.410	1.291	1.351	1.580	1.408	0.108
O1	1.486	1.261	1.407	1.091	1.311	0.151

O2	1.425	1.186	1.456	1.126	1.298	0.144

YIAG1 [$ReOCl(3,5\text{-}Me_2\text{-}HPz)]_2(\mu\text{-}O)(\mu\text{-}3,5\text{-}Me_2\text{-}Pz)_2$ (5F)

d12=3.149 d14=3.111 d15=3.021 d16=3.194 d23=2.938 d25=2.594

d26=2.807 d34=3.033 d35=2.604 d36=2.691 d45=2.714 d46=2.938

CL1	1.788	1.709	1.768	1.684	1.737	0.042
N1C	1.361	1.381	1.527	1.464	1.433	0.066
N1B	1.473	1.462	1.411	1.393	1.435	0.034
N1A	1.402	1.428	1.640	1.572	1.510	0.099
O12	1.233	1.312	1.130	1.142	1.204	0.074
O1	1.426	1.511	1.281	1.298	1.379	0.095

YIAG2 [$ReOCl(3,5\text{-}Me_2\text{-}HPz)]_2(\mu\text{-}O)(\mu\text{-}3,5\text{-}Me_2\text{-}Pz)_2$ (5F)

d12=3.030 d14=3.012 d15=2.786 d16=2.608 d23=3.086 d25=3.086

d26=3.009 d34=2.904 d35=2.877 d36=2.697 d45=2.637 d46=2.608

N2B	1.365	1.580	1.315	1.507	1.442	0.107
CL2	1.665	1.715	1.699	1.648	1.682	0.027
N1d	1.438	1.572	1.388	1.497	1.474	0.069
N2C	1.432	1.506	1.407	1.333	1.419	0.062
O2	1.421	1.206	1.438	1.305	1.343	0.094
O12	1.294	1.102	1.310	1.200	1.226	0.083

YIAG3 [ReOCl(3,5-Me_2-HPz)]$_2$(μ-O)(μ-3,5-Me_2-Pz)$_2$ (5F)

d12=3.132 d14=3.125 d15=3.105 d16=3.135 d23=2.955 d25=2.683

d26=2.924 d34=3.034 d35=2.631 d36=2.738 d45=2.614 d46=2.801

CL3	1.777	1.808	1.671	1.730	1.747	0.052
N1E	1.355	1.460	1.570	1.503	1.472	0.078
N1F	1.451	1.525	1.385	1.486	1.462	0.052
N1G	1.317	1.395	1.548	1.509	1.442	0.092
O34	1.328	1.297	1.179	1.105	1.227	0.090
O3	1.464	1.406	1.354	1.253	1.369	0.078

YIAG4 [ReOCl(3,5-Me_2-HPz)]$_2$(μ-O)(μ-3,5-Me_2-Pz)$_2$ (5F)

d12=3.158 d14=3.088 d15=2.968 d16=3.205 d23=2.960 d25=2.704

d26=2.866 d34=3.029 d35=2.600 d36=2.666 d45=2.608 d46=2.783

CL4	1.711	1.724	1.748	1.755	1.735	0.018
N1H	1.447	1.410	1.580	1.532	1.492	0.067
N2G	1.428	1.510	1.380	1.456	1.443	0.047
N2F	1.364	1.333	1.573	1.518	1.447	0.101
O34	1.257	1.244	1.172	1.090	1.191	0.067
O4	1.456	1.450	1.286	1.210	1.351	0.106

YIBL $ReOCl_2(PPh_3)$(pz-COHMe)·0.5CHOCHO (5D)

d12=3.334 d14=3.359 d15=3.110 d16=3.210 d23=3.123 d25=3.098

d26=3.022 d34=3.394 d35=2.682 d36=2.453 d45=3.059 d46=2.914

CL1	1.673	1.705	1.761	1.827	1.741	0.059
CL2	1.661	1.573	1.846	1.770	1.712	0.104
N2	1.353	1.508	1.277	1.466	1.401	0.091
P	1.654	1.532	1.928	1.886	1.750	0.163
O1	1.437	1.405	1.329	1.174	1.336	0.102
O2	1.449	1.383	1.176	0.987	1.249	0.182

AGIMPbcaV $ReOCl_2(PPh_3)(4\text{-}CH_2O\text{-}1,5\text{-}Me_2\text{-}Im)\cdot 2H_2O$ (5G)

d12=3.322 d14=3.151 d15=3.074 d16=3.073 d23=3.463 d25=3.217

d26=3.086 d34=3.319 d35=2.936 d36=3.029 d45=2.712 d46=2.521

CL1	1.589	1.757	1.654	1.852	1.713	0.100
CL2	1.733	1.668	1.760	1.872	1.758	0.074
P	1.591	1.77	1.703	1.914	1.745	0.117
N3A	1.394	1.299	1.406	1.548	1.412	0.089
O1	1.485	1.317	1.345	1.164	1.328	0.114
O2	1.419	1.222	1.326	1.115	1.270	0.113

Appendix Table 7.2

The Spatial Parameters for Structures Determined in This Study

	VR	SI	BL	FA	SAF
$[Re(CO)_3(OH)]_4 \cdot 8H_2O$ (3C)	0.885	I NUJOI-4			
C2	1.444	0.223	1.896	49.637	0.176
O4B	1.424	0.228	2.174	40.911	0.122
O4A	1.414	0.207	2.165	40.763	0.121
C3	1.434	0.201	1.900	48.992	0.172
C1	1.422	0.219	1.902	48.369	0.168
O4	1.452	0.210	2.193	41.466	0.125
$KRe_3(CO)_9(OH)_4$ (3E)	0.884	I TriPa-3			
C3	1.417	0.177	1.891	48.559	0.169
C2	1.401	0.207	1.878	48.268	0.167
O4	1.455	0.215	2.205	41.284	0.124
O5	1.455	0.185	2.178	41.929	0.128
C1	1.412	0.200	1.893	48.230	0.167
O5A	1.446	0.195	2.161	42.003	0.128
$K[Re_3(\mu_2\text{-}OCH_3)_3(\mu_3\text{-}OCH_3)(CO)_9]$ (3A)	0.884	I Y2P21n1			
O4	1.430	0.187	2.190	40.787	0.121
O3	1.443	0.198	2.162	41.856	0.128

C11	1.433	0.180	1.892	49.231	0.173
C13	1.403	0.171	1.879	48.308	0.167
C12	1.438	0.200	1.932	48.094	0.166
O1	1.441	0.168	2.153	42.003	0.128

$K[Re_3(\mu_2\text{-}OCH_3)_3(\mu_3\text{-}OCH_3)(CO)_9]$ (3A) 0.884 I Y2P21n2

O2	1.435	0.165	2.144	42.022	0.129
O4	1.438	0.181	2.184	41.185	0.124
C22	1.414	0.181	1.901	48.037	0.166
C21	1.420	0.165	1.892	48.669	0.170
C23	1.436	0.169	1.915	48.561	0.169
O1	1.431	0.175	2.148	41.771	0.127

$K[Re_3(\mu_2\text{-}OCH_3)_3(\mu_3\text{-}OCH_3)(CO)_9]$ (3A) 0.885 I Y2P21n3

C31	1.436	0.161	1.894	49.289	0.174
C33	1.389	0.191	1.870	47.974	0.165
O4	1.421	0.193	2.174	40.799	0.121
O2	1.453	0.163	2.168	42.098	0.129
C32	1.422	0.173	1.905	48.303	0.167
O3	1.426	0.176	2.136	41.872	0.128

$[Re_4(CO)_{12}(OH)_2(EtO)_2]\cdot 2EtOH$ (3B) 0.884 I Y7C2c1

C1B	1.442	0.232	1.895	49.538	0.176
C1C	1.444	0.211	1.927	48.571	0.169
O1	1.408	0.193	2.150	40.893	0.122

O2A	1.439	0.217	2.184	41.223	0.124
C1A	1.419	0.195	1.900	48.325	0.168
O2	1.454	0.230	2.193	41.519	0.126

$[Re_4(CO)_{12}(OH)_2(EtO)_2]\cdot 2EtOH$ (3B) 0.884 I Y7C2c2

C1	1.446	0.228	2.200	1.090	0.123
C2C	1.419	0.214	1.898	48.394	0.168
C2A	1.458	0.223	1.938	48.794	0.171
O1A	1.441	0.236	2.182	41.333	0.125
O2	1.433	0.213	2.193	40.788	0.121
C2B	1.432	0.238	1.877	49.704	0.177

$KRe_2(CO)_6(OH)_3\cdot 2H_2O$ (3D) 0.884 I YDC2m1

C1A	1.411	0.219	1.888	48.374	0.168
C1B	1.475	0.210	1.920	50.208	0.180
O1C	1.429	0.214	2.157	41.490	0.125
O2	1.391	0.222	2.161	40.047	0.117
C1AA	1.411	0.219	1.888	48.374	0.168
O1	1.429	0.214	2.157	41.490	0.125

$KRe_2(CO)_6(OH)_3\cdot 2H_2O$ (3D) 0.884 I YDIC2m2

O1	1.433	0.213	2.164	41.475	0.125
O1C	1.433	0.213	2.164	41.475	0.125
C2AA	1.425	0.218	1.908	48.325	0.168
C2A	1.425	0.218	1.908	48.326	0.168

O2	1.381	0.221	2.149	39.988	0.117
C2B	1.444	0.211	1.872	50.448	0.182

$KRe_2(CO)_6(OH)_3{\cdot}2H_2O$ (3D) 0.886 I YDIC2m3

O3	1.400	0.192	2.137	40.940	0.122
O3C	1.400	0.192	2.137	40.940	0.122
C3AA	1.432	0.191	1.902	48.849	0.171
C3A	1.432	0.191	1.902	48.849	0.171
O4	1.408	0.191	2.161	40.651	0.121
C3B	1.413	0.193	1.842	50.088	0.179

$KRe_2(CO)_6(OH)_3{\cdot}2H_2O$ (3D) 0.886 I YDIC2m4

O3	1.413	0.217	2.155	40.972	0.122
O4	1.420	0.205	2.191	40.379	0.119
C4AA	1.419	0.208	1.887	48.770	0.170
C4B	1.459	0.220	1.896	50.345	0.181
O3C	1.413	0.217	2.155	40.973	0.122
C4A	1.419	0.208	1.886	48.769	0.170

$[ReOCl(PPh_3)]_2(\mu\text{-}O)(\mu\text{-}pz)_2{\cdot}CHCl_3$ (5E) 0.896 V GREEN1

CL1	1.791	0.119	2.375	48.967	0.172
N2H	1.422	0.165	2.067	43.449	0.137
N2G	1.406	0.099	2.129	41.347	0.125
P1	1.770	0.158	2.451	46.224	0.154
O1	1.321	0.128	1.694	51.233	0.187

O3	1.265	0.146	1.936	40.814	0.122

$[ReOCl(PPh_3)]_2(\mu\text{-}O)(\mu\text{-}pz)_2\cdot CHCl_3$ (5E) 0.896 V GREEN2

CL2	1.778	0.112	2.355	49.039	0.172
N1G	1.427	0.172	2.090	43.061	0.135
N1H	1.404	0.072	2.140	41.004	0.123
P2	1.797	0.133	2.467	46.761	0.157
O2	1.320	0.128	1.696	51.082	0.186
O3	1.272	0.151	1.938	41.004	0.123

$[ReO(HBPz_3)(Pz\text{-}(CO)Me_2)][ReO_4]$ (5B) 0.902 V Yviolet

N1A	1.443	0.049	2.124	42.794	0.133
N1B	1.449	0.107	2.086	44.010	0.140
O1D	1.350	0.075	1.914	44.880	0.146
N1D	1.487	0.228	2.069	45.946	0.152
O	1.402	0.172	1.683	56.449	0.224
N1C	1.385	0.185	2.247	38.071	0.106

$ReOCl_2(PPh_3)(pz\text{-}COMe_2)$ (5C) 0.899 V blue

CL1	1.738	0.129	2.432	45.623	0.150
CL2	1.720	0.086	2.342	47.264	0.161
P	1.775	0.196	2.478	45.765	0.151
N1	1.408	0.108	2.132	41.322	0.124
O1	1.311	0.151	1.696	50.622	0.183
O2	1.298	0.144	1.935	42.143	0.129

[ReOCl(3,5-Me_2-HPz)]$_2$(μ-O)(μ-3,5-Me_2-Pz)$_2$ (5F) 0.897 V YIAG1

CL1	1.737	0.042	2.387	46.692	0.157
N1C	1.433	0.066	2.083	43.477	0.137
N1B	1.435	0.034	2.105	42.952	0.134
N1A	1.510	0.099	2.123	45.350	0.149
O12	1.204	0.074	1.919	38.874	0.111
O1	1.379	0.095	1.695	54.425	0.209

[ReOCl(3,5-Me_2-HPz)]$_2$(μ-O)(μ-3,5-Me_2-Pz)$_2$ (5F) 0.897 V YIAG2

N2B	1.442	0.107	2.054	44.580	0.144
CL2	1.682	0.027	2.272	47.756	0.164
N1d	1.474	0.069	2.110	44.293	0.142
N2C	1.419	0.062	2.122	41.970	0.128
O2	1.343	0.094	1.654	54.249	0.208
O12	1.226	0.083	1.953	38.889	0.111

[ReOCl(3,5-Me_2-HPz)]$_2$(μ-O)(μ-3,5-Me_2-Pz)$_2$ (5F) 0.898 V YIAG3

CL3	1.747	0.052	2.367	47.541	0.162
N1E	1.472	0.078	2.096	44.618	0.144
N1F	1.462	0.052	2.168	42.407	0.131
N1G	1.442	0.092	2.076	43.995	0.140
O34	1.227	0.090	1.967	38.614	0.109
O3	1.369	0.078	1.676	54.760	0.211

[ReOCl(3,5-Me_2-HPz)]$_2$(μ-O)(μ-3,5-Me_2-Pz)$_2$ (5F) 0.896 V YIAG4

CL4	1.735	0.018	2.369	47.067	0.159
N1H	1.492	0.067	2.095	45.410	0.149
N2G	1.443	0.047	2.131	42.634	0.132
N2F	1.447	0.101	2.095	43.681	0.138
O34	1.191	0.067	1.872	39.509	0.114
O4	1.351	0.106	1.680	53.490	0.203

$ReOCl_2(PPh_3)$(pz-COHMe)·0.5CHOCHO (5D) 0.907 V YIBL

CL1	1.741	0.059	2.337	48.173	0.167
CL2	1.712	0.104	2.420	45.027	0.147
N2	1.401	0.091	2.153	40.607	0.120
P	1.750	0.163	2.463	45.272	0.148
O1	1.336	0.102	1.649	54.113	0.207
O2	1.249	0.182	1.935	40.197	0.118

$ReOCl_2(PPh_3)(4\text{-}CH_2O\text{-}1,5\text{-}Me_2\text{-}Im)\cdot 2H_2O$ (5G) 0.899 V AGIMPbcaV

CL1	1.713	0.100	2.410	45.289	0.148
CL2	1.758	0.074	2.360	48.151	0.166
P	1.745	0.117	2.454	45.311	0.148
N3A	1.412	0.089	2.154	40.960	0.122
O1	1.328	0.114	1.700	51.362	0.188
O2	1.270	0.113	1.916	41.538	0.126

Appendix Table 7.3

Comparison of the Nonbonding Distances, Virtual Rdaii (VR), Shape Index (SI) and Spatial Parameters of $(AsPh_4)_2[ReN(CN)_4(H_2O)]\cdot 5H_2O$ (4B) and $(AsPh_4)_2[TcN(CN)_4(H_2O)]\cdot 5H_2O$ (4B')

$(AsPh_4)_2[ReN(CN)_4(H_2O)]\cdot 5H_2O$ (4B)

d12=3.028 d14=2.956 d15=2.864 d16=2.924 d23=2.796 d25=2.891

d26=2.990 d34=2.977 d35=2.857 d36=3.051 d45=2.884 d46=2.955

	R1	R2	R3	R4	VR	SI
C1	1.501	1.468	1.481	1.462	1.478	0.015
C2	1.527	1.547	1.368	1.415	1.464	0.075
C3	1.381	1.475	1.428	1.536	1.455	0.057
C4	1.488	1.493	1.441	1.502	1.481	0.024
N5	1.364	1.396	1.476	1.382	1.404	0.043
O	1.443	1.462	1.622	1.514	1.510	0.070

$(AsPh_4)_2[TcN(CN)_4(H_2O)]\cdot 5H_2O$ (4B')

d12=2.998 d14=2.814 d15=2.861 d16=3.039 d23=2.953 d25=2.852

d26=2.967 d34=2.992 d35=2.837 d36=3.008 d45=2.826 d46=3.137

	R1	R2	R3	R4	VR	SI
C1	1.503	1.424	1.535	1.358	1.455	0.069
C2	1.495	1.463	1.456	1.484	1.474	0.016

C3	1.469	1.501	1.497	1.431	1.475	0.028
C4	1.389	1.456	1.560	1.490	1.474	0.062
N5	1.358	1.437	1.368	1.336	1.375	0.038
O1	1.504	1.681	1.512	1.577	1.569	0.071

$(AsPh_4)_2[ReN(CN)_4(H_2O)]\cdot 5H_2O$ (**4B**) SSAF = 0.909

	VR	SI	BL	FA	SAF
C1	1.478	0.015	2.102	44.684	0.144
C2	1.464	0.075	2.108	43.995	0.140
C3	1.455	0.057	2.096	43.968	0.140
C4	1.481	0.024	2.114	44.469	0.143
N5	1.404	0.043	1.655	58.070	0.236
O	1.510	0.070	2.463	37.823	0.105

$(AsPh_4)_2[TcN(CN)_4(H_2O)]\cdot 5H_2O$ (**4B'**) SSAF = 0.917

	VR	SI	BL	FA	SAF
C1	1.455	0.069	2.113	43.533	0.138
C2	1.474	0.016	2.110	44.315	0.142
C3	1.475	0.028	2.093	44.791	0.145
C4	1.474	0.062	2.113	44.229	0.142
N5	1.375	0.038	1.596	59.441	0.246
O1	1.569	0.071	2.559	37.803	0.105